Epigenetic programming by prenatal stress in female serotonin transporter deficient mice

Epigenetische Programmierung durch Pränatalstress in weiblichen Serotonintransporter-defizienten Mäusen

Doctoral thesis for a doctoral degree
at the Graduate School of Life Sciences,
Julius-Maximilians-Universität Würzburg,
Section Neuroscience

Submitted by

Karla-Gerlinde Schraut

from Timişoara, România

Würzburg, 2015

Submitted on: .....

Members of the Promotionskomitee:

Chairperson:	Prof. Dr. Thomas Dandekar
Primary Supervisor:	Prof. Dr. Klaus-Peter Lesch
Supervisor (Second):	Prof. Dr. Charlotte Förster
Supervisor (Third):	Dr. Daniel van den Hove

Date of Public Defense: .....

Date of Receipt of Certificates: .....

Table of Contents

Abbreviations

	µ	micro-
	11ß-HSD-2	11ß-hydroxysteroid dehydrogenase 2
	5-HIAA	5-hydroxyindole acetic acid
	5-hmC	5-hydroxymethylcytosine
#	5-Ht	5-hydroxytryptamine (serotonin)
	5-HtR	5-hydroxytryptamine (serotonin) receptor
	5-HTT	5-hydroxytryptamine (serotonin) transporter, encoded by SLC6A4
	5-Htt+/-	heterozygous for the serotonin transporter gene
	5-HTTLPR	5-HTT linked polymorphic region
	5-mC	5-methylcytosine
	AA	arachidonic acid
	ACTH	Adrenocorticotrophic hormone
	ADHD	attention deficit hyperactivity disorder
A	Amy	amygdala
	ANOVA	analysis of variance
	as-	antisense
	AVP	arginine-8-vasopressin
	B6	C57BL/6 mice
	BBB	blood brain barrier
	Bdnf	brain derived neurotrophic factor
B	biDNA	bisulfite DNA
	Bm	base mean expression
	bp	base
	C	control
	C	cytosine
	CA1	Cornu Ammonis area 1
	CA2	Cornu Ammonis area 2
	CA3	Cornu Ammonis area 3
C	Cacna1c	alpha 1C subunit calcium channel, voltage dependent, gamma
	Cadm3	cell adhesion molecule 3
	Cadm4	cell adhesion molecule 4
	Camk2a	II alpha calcium/calmodulin-dependent protein kinase
	cDNA	complementary DNA
	CGI	CpG island

	Chr	chromosome
	Cldn11	claudin 11
	Cnp	2',3'-cyclic nucleotide 3' phosphodiesterase
	CNS	central nervous system
	Cntn2	contactin 2
	CORT	corticosterone
	Crfr2	corticotropin releasing hormone receptor 2
	CRH	corticotrophin releasing hormone
	CRHR1	CRH receptor type 1
	Cryab	crystallin, alpha B
	CSF	cerebrospinal fluid
	Cspg4	chondroitin sulfate proteoglycan 4
	Ctcf	CCCTC-binding factor
D	DAVID	database for Annotations, Visualization and Integrated Discovery
	DEG	differentially expressed genes
	DEPS	differentially expressed probesets
	DG	Dentate gyrus
	dir.	direction
	Dnmt	DNA methyl transferase
	Dnmt	DNA methyltransferase
	DRN	dorsal raphe nucleus
E	E	embryonal day
	ECS	electroconvulsive stimulation
	E-effect	environment effect
	EPM	elevated plus maze
	ESC	embryonic stemm cell
	ex	exon
	EZM	elevated zero maze
F	f	female
	Fa2h	fatty acid 2-hydroxylase
	FC	fold change
	FST	rorced swim test
	Fzd	rrizzled homolog
G	G	guanine
	g	gram
	Gal3st1	galactose-3-O-sulfotransferase 1
	Gdi2	Gdp dissociation inhibitor 2

	GDP	guanosine diphosphate
	GDP	guanosine diphosphate
	G-effect	genotype effect
	Gfap	glial fibrillary acidic protein
	Gh	growth hormone
	Gja	gap junction protein, alpha 1
	GO	gene ontology
	GPC	glial precursor cell
	GR	glucocorticoid receptor, encoded by *Nr3c1*
	Gsn	gelsolin
	GxE-effect	gene-environment-interaction effect
H	h	hour
	H19	H19, imprinted maternally expressed transcript
	H2	histone 2
	H3	histone 3
	H4	histone 4
	HCP	high-CpG promoters
	HDAC	histone-deacetylase
	Hip	hippocampus
	HMT	Histone methyltransferase
	HPA	hypothalamus-pituitary-adrenal
	hsa	homo sapiens
	Hz	Herz
I	ICP	intermediate-CpG promoters
	IGF2	insulin-like growth factor 2
K	K	lysine
	k	kilo
	kDa	kilo Dalton
	KEGG	Kyoto Encyclopedia of Genes and Genomes
	KW	Kruskal-Wallis test
L	l	long
	l	liter
	LCP	low-CpG promoters
	LIMMA	Linear models for microarray analysis
	Lpar1	lysophosphatidic acid receptor 1

	m	male
	m	milli-
	MA	micro array
	Mag	myelin-associated glycoprotein
	Mal	myelin and lymphocyte protein, T cell differentiation protein
	MAOA	monoamine oxidase A
	MBD	methyl-CpG-binding domain
	Mbp	myelin basic protein
	MDD	major depression disorder
	MDMA	3,4-methylene-N-dioxymethamphetamine (Ecstasy)
	MECP2	methyl CpG binding protein 2
	MeDIP	methyl DNA immunoprecipitation
	min	minute
	miRNA	microRNA
M	MMC	Modulated Modalarity Cluster
	Mobp	myelin-associated oligodendrocytic basic protein
	Mog	myelin oligodendrocyte glycoprotein
	mol	mole
	MP	mammalian phenotypes
	MR	mineralocorticoid receptor
	mRNA	messenger RNA
	mSIN3A	transcriptional regulator, SIN3A (yeast)
	mmu	mus musculus
	MWU	Mann-Whitney-U test
	MYC	v-myc avian myelocytomatosis viral oncogene homolog
	Myrf	myelin regulatory factor
	n	number of animals/pools/samples
	nm	nanometer
	Ncam1	Neural cell adhesion molecule 1
	NCBI	National Center for Biotechnology Information
	ncRNA	non-coding RNA
	Necl1	nectin-like 1, official name Cadm3
	Necl4	nectin-like 4, official name Cadm4
N	neo	neomycin
	NG2	neural/glial antigen 2, encoded by *Cspg4*
	Ngf1a	nerve growth factor
	Nkx2-2	NK2 homeobox 2
	Nkx2-6	NK2 homeobox 6
	Nos1	nitrit oxide synthase 1, neuronal
	NPC	neural progenitor cells

	Nr3c1	nuclear receptor subfamily 3, group C, member 1 (encodes GR)
	Ntrk2	neurotrophic tyrosine kinase, receptor type 2
O	OCT3	organic cation transporter 3, encoded by *Slc22a3*
	OCT4	octamer binding transcription factor 4, encoded by *POU5F1*
	OL	oligodendrocyte
	Olig1	oligodendrocyte transcription factor 1
	Olig2	oligodendrocyte transcription factor 2
	ON	over night
	OPC	oligodendrocyte progenitor cell
	ORT	object regocnition task
P	P	post-natal day
	PAR	predictive adaptive response
	PCR	Polymerase chain reaction
	Plp1	proteolipid protein (myelin) 1
	POU5F1	POU class 5 homeobox 1
	PS	Prenatal stress
	PST	Porsolt swim test
	PVN	paraventricular nucleus
R	r	correlation coefficient
	RFU	raw fluorescent units
	rpm	rounds per minute
	RT	room temperature
	RT-qPCR	Reverse transcription quantitative real-time PCR
S	s	short
	SAM	sympathetic-adreno-medullary
	sec	second
	Slc22a3	solute carrier family 22 (organic cation transporter), member 3 (encodes OCT3)
	SLC6A4	Solute carrier family 6, member 4 (encodes 5-HTT)
	Snip1	Smad nuclear interacting protein 1
	SNP	single nucleotide polymorphisms
	SNRI	serotonin and norepinephrine reuptake inhibitors
	Sox10	SRY (sex determining region Y)-box 10
	SSRI	selective serotonin reuptake inhibitors
	SUV39H1	suppressor of variegation 3-9 homolog 1 (Drosophila)
T	T	thymine

T	TCA	tricyclic antidepressants
	Tet	ten–eleven translocation
	TF	transcription factor
	TPH	tryptophan hydroxylase
	Trf	transferrin
	Trp	tryptophan
U	U	uracil
	U	units
	UDP	Uridine diphosphate
	Ugt8a	UDP galactosyltransferase 8A
	UHRF	ubiquitin-like, containing PHD and RING finger domain
W	WT	wild type
X	Xaf1	XIAP associated factor 1
Y	Yy1	Yin Yang 1
Z	ZBTB38	zinc finger and BTB domain containing 38
	ZBTB4	zinc finger and BTB domain containing 4

Summary

Early life stress, including exposure to prenatal stress (PS), has been shown to affect the developing brain and induce severe effects on emotional health in later life, concomitant with an increased risk for psychopathology. However, some individuals are more vulnerable to early-life stress, while others adapt successfully, i.e. they are resilient and do not succumb to adversity. The molecular substrates promoting resilience in some individuals and vulnerability in other individuals are as yet poorly investigated. A polymorphism in the serotonin transporter gene (5-HTT/SLC6A4) has been suggested to play a modulatory role in mediating the effects of early-life adversity on psychopathology, thereby rendering carriers of the lower-expressing short (s)-allele more vulnerable to developmental adversity, while long (l)-allele carriers are relatively resilient. The molecular mechanisms underlying this gene x environment interaction (GxE) are not well understood, however, epigenetic mechanisms such as DNA methylation and histone modifications have been discussed to contribute as they are at the interface of environment and the genome. Moreover, developmental epigenetic programming has also been postulated to underlie differential vulnerability/resilience independent of genetic variation.

The present work comprises two projects investigating the effects of prenatal maternal restraint stress in 5-HTT deficient mice. In the first study, we examined to which extent previously observed changes in behavior and hippocampal gene expression of female *5-Htt+/-* prenatally stressed (PS) offspring were associated with changes in DNA methylation patterns. Additionally, we investigated the expression of genes involved in myelination in hippocampus and amygdala of those animals using RT-qPCR. The genome-wide hippocampal DNA methylation screening was performed using methylated-DNA immunoprecipitation (MeDIP) on Affymetrix GeneChip® Mouse Promoter 1.0R arrays. In order to correlate individual gene-specific DNA methylation, mRNA expression and behavior, we used hippocampal DNA from the same mice as assessed before. *5-Htt* genotype, PS and their interaction differentially affected the DNA methylation signature of numerous genes, a part of which were also differentially expressed. More specifically, we identified a differentially methylated region in the *Myelin basic protein* (*Mbp*) gene, which was associated with *Mbp* expression in a *5-Htt-*, PS- and *5-Htt* x PS-dependent manner. Subsequent fine-mapping linked the methylation status of two specific CpG sites in this region to *Mbp* expression and anxiety-related behavior. We furthermore found that not only the expression of *Mbp* but of large gene set associated

with myelination was affected by a 5-Htt x PS interaction in a brain-region specific manner. In conclusion, hippocampal DNA methylation patterns and expression profiles of female PS *5-Htt+/-* mice suggest that distinct molecular mechanisms, some of which are associated with changes in gene promoter methylation, and processes associated with myelination contribute to the behavioral effects of the *5-Htt* genotype, PS exposure, and their interaction.

In the second study, we aimed at investing the molecular substrates underlying resilience to PS. For this purpose, we exposed *5-Htt+/+* dams to the same restraint stress paradigm and investigated the effects of PS on depression- and anxiety-like behavior and corticosterone (CORT) secretion at baseline and after acute restraint stress in female *5-Htt+/+* and *5-Htt+/-* offspring. We found that PS affected the offspring's social behavior in a negative manner. When specifically examining those PS animals, we grouped the PS offspring of each genotype into a social, resilient and an unsocial, vulnerable group. While anxiety-like behavior in the EPM was reduced in unsocial, but not social, PS *5-Htt+/+* animals when compared to controls, this pattern could not be found in animals of the other genotype, indicating that social anxiety and state anxiety in the EPM were independent of each other. We then assessed genome-wide hippocampal gene expression profiles using mRNA sequencing in order to identify pathways and gene ontology (GO) terms enriched due to *5-Htt* genotype (G), PS exposure (E) and their interaction (GxE) as well as enriched in social, but not unsocial, PS offspring, and vice versa. Numerous genes were affected by *5-Htt* genotype, PS and most of all a GxE-interaction. Enrichment analysis using enrichr identified that the genotype affected mitochondrial respiration, while GxE-interaction-affected processes associated primarily with myelination and chromatin remodeling. We furthermore found that *5-Htt+/-* mice showed profound expression changes of numerous genes in a genomic region located 10 mio kb upstream of the *5-Htt* locus on the same chromosome. When looking at social vs. unsocial mice, we found that a much higher number of genes was regulated in *5-Htt+/-* animals than in *5-Htt+/+* animals, reflecting the impact of GxE-interaction. Double the number of genes was regulated in social PS vs. control mice when compared to unsocial PS vs. control in both genotypes, suggesting that the successful adaption to PS might have required more active processes from the social group than the reaction to PS from the unsocial group. This notion is supported by the up-regulation of mitochondrial respiration in social, but not in unsocial, PS *5-Htt+/-* mice when compared to controls, as those animals might have been able to raise energy resources the unsocial group was not. Next to this, processes associated with myelination seemed to be down-regulated in social *5-Htt+/-* mice, but not in unsocial animals, when compared to controls. Taken

together, PS exposure affected sociability and anxiety-like behavior dependent on the *5-Htt* genotype in female offspring. Processes associated with myelination and epigenetic mechanisms involved in chromatin remodeling seemed be affected in a GxE-dependent manner in the hippocampus of these offspring. Our transcriptome data furthermore suggest that mitochondrial respiration and, with this, energy metabolism might be altered in *5-Htt*+/- offspring when compared to *5-Htt*+/+ offspring. Moreover, myelination and mitochondrial respiration might contribute to resilience towards PS exposure in *5-Htt*+/- offspring, possibly by affecting brain connectivity and energy capabilities.

Zusammenfassung

Frühes Stresserleben wie zum Beispiel in Form von pränatalem Stress (PS) kann sich auf die Entwicklung des Gehirns auswirken und einen gravierenden Einfluss auf die emotionale Gesundheit im Erwachsenenaltern ausüben, was mit einem erhöhten Risiko für eine Psychopathologie einhergeht. Manche Individuen sind jedoch frühem Stresserleben gegenüber vulnerabler, während andere Individuen sich erfolgreich anpassen, d.h. resilient sind, und widrigen Umständen nicht erliegen. Die molekularen Substrate, die Resilienz in manchen und Vulnerabilität in anderen Individuen bedingen, sind bisher nur unzureichend erforscht. Ein Polymorphismus im Serotonintransportergen (5-HTT/SLC6A4) soll eine modulierende Rolle in der Vermittlung der Effekte von frühem Stresserleben auf die Entwicklung einer Psychopathologie spielen, wobei Träger des niedrig-exprimierenden kurzen (s-) Allels empfänglicher gegenüber Stresserlebnissen während der Entwicklung sind, während Träger des langen (l-) Allels als resilienter gelten. Die molekularen Mechanismen, die dieser Gen-Umwelt-Interaktion zu Grunde liegen, sind noch nicht aufgeklärt. Epigenetische Mechanismen wie DNA-Methylierung und Histonmodifikationen könnten jedoch dazu beitragen, da sie an der Schnittfläche zwischen Genom und Umwelt liegen. Des Weiteren wird vermutet, dass epigenetische Programmierung während der Entwicklung unabhängig von genetischer Varianz zur Ausbildung von Resilienz bzw. Vulnerabilität beiträgt.

Die vorliegende Arbeit umfasst zwei Projekte, in denen die Auswirkungen von pränatalem „maternal restraint“ Stress in 5-HTT defizienten Mäusen behandelt werden. In der ersten Studie wurde untersucht, in ob und in welchem Maß zuvor beobachtete Veränderungen im Verhalten und in der hippocampalen Genexpression in weiblichen PS Mäusen mit Veränderungen in DNA-Methylierungsmustern einhergingen. Des Weiteren untersuchten wir mittels RT-qPCR die Expression von Genen, die mit Myelinisierung im Zusammenhang stehen, im Hippocampus und in der Amygdala dieser Tiere. Ein genomweites hippocampales DNA-Methylierungsscreening wurde durchgeführt indem methylierte DNA mit Hilfe der Methyl-DNA-Immunoprezipitation angereichert und auf Affymetrix GeneChip® Mouse Promoter 1.0R Arrays aufgetragen wurde. Um individuelle genspezifische DNA-Methylierung, mRNA-Expression und Verhalten miteinander korrelieren zu können, wurde hippocampale DNA derselben Mäuse, die zuvor getestet wurden, dafür eingesetzt. Der *5-Htt* Genotyp, PS und ihre Interaktion veränderten die DNA-Methylierung von zahlreichen Genen, wovon ein Teil auch differentiell exprimiert war. Um genau zu sein, identifizierten wir eine differentiell methylierte Region im *Myelin*

basic protein (*Mbp*) Gen, was mit *Mbp* Expressionsveränderungen auf Grund eines *5-Htt*-, PS und eines *5-Htt* x PS-Effekts einherging war. Eine anschließende genauere Untersuchung dieser Region zeigte eine Assoziation zwischen dem Methylierungsstatus zweier spezifischer CpG-Stellen mit der *Mbp* Expression und Angst-ähnlichem Verhalten. Es zeigte sich weiterhin, dass nicht nur die Expression von *Mbp* sondern eines ganzes Satzes an Genen, die mit Myelinisierung im Zusammenhang stehen, durch eine *5-Htt* x PS-Interaktion in einer Gehirnregionen-spezifischen Weise verändert war. Zusammenfassend weisen die hippocampalen DNA-Methylierungsmuster und Genexpressionprofile der weiblichen PS *5-Htt*+/- Mäuse darauf hin, dass eindeutige molekulare Mechanismen, wovon einige mit Veränderungen in der Promotermethylierung einhergingen, und Prozesse, die mit Myelinisierung im Zusammenhang stehen, zu den Verhaltenseffekten des *5-Htt* Genotyps, PS-Exposition und ihrer Interaktion beitragen.

Die zweite Studie hatte zum Ziel, molekulare Substrate, die einer Resilienz gegenüber PS zu Grunde liegen, zu erforschen. Zu diesem Zweck wandten wir das gleiche „restrainst stress" Paradigma wie zuvor auf schwangere *5-Htt*+/+ Weibchen an und untersuchten die PS-Effekte auf Depressions- und Angst-ähnliches Verhalten sowie auf die Corticosteronausschüttung im Grundzustand und nach akutem „restraint stress" im weiblichen *5-Htt*+/+ und *5-Htt*+/- Nachwuchs. Wir stellten fest, dass sich PS negativ auf das Sozialverhalten auswirkte. Als wir die PS Tiere genauer untersuchten, teilten wir den PS Nachwuchs jeden Genotyps in je eine soziale, resiliente und eine unsoziale, vulnerable Gruppe ein. Während das Angst-ähnliche Verhalten im EPM in unsozialen, aber nicht sozialen, *5-Htt*+/+ PS Tieren im Vergleich zu Kontrolltieren verringert war, konnte man diesen Effekt im anderen untersuchten Genotyp nicht finden, was darauf hinweist, dass soziale Ängstlichkeit und die sogenannte „state anxiety", wie in potentiell angsteinflößenden Situationen zu Tage tritt, unabhängig voneinander funktionierende Prozesse sind. Wir erstellten anschließend mittels mRNA-Sequenzierung genomweite hippocampale Genexpressionsprofile um Netzwerke und Gene Ontology (GO) Terms zu identifizieren, die auf Grund des *5-Htt* Genotyps (G), der PS-Exposition (E) oder einer Interaktion (GxE) sowie in sozialem, aber nicht in unsozialem, PS Nachwuchs und umgekehrt angereichert waren. Die Expression zahlreicher Gene war durch den *5-Htt* Genotyp, der PS-Exposition und vor allem einer GxE-Interaktion verändert. Durch eine Anreicherungsanalyse mittels enrichr stellten wir fest, dass die mitochondriale Atmungskette vom Genotyp beeinflusst wurde, wohingegen sich die GxE-Interaktion vor allem auf Prozesse, die mit Myelinisierung und Chromatinumgestaltung in Verbindung standen, auswirkte. Darüber hinaus fanden wir in *5-Htt*+/- Mäusen höchst signifikante Expressionsveränderungen zahlreicher Gene, die in einer genomischen Region 10 mio kb

in 5‘ Richtung des *5-Htt* Lokus auf dem gleichen Chromosom lagen. Als wir soziale und unsoziale PS Mäuse verglichen, zeigte sich, dass eine deutlich höhere Anzahl an Genen in *5-Htt*+/- Mäusen als in *5-Htt*+/+ Mäusen reguliert war, was die Auswirkungen der GxE-Interaktion widerspiegelt. In beiden Genotypen war die doppelte Anzahl an Genen in sozialen PS vs. Kontroll-Tieren im Vergleich zu unsozialen PS vs. Kontroll-Tieren verändert, was darauf hinweist, dass eine erfolgreiche Anpassung an PS den sozialen Tieren möglicherweise mehr aktive Prozesse abverlangte als die Reaktion auf PS in der unsozialen Gruppe. Diese Vorstellung wird durch eine Steigerung der mitochondrialen Atmungskette auf mRNA-Ebene in sozialen, aber nicht in unsozialen, *5-Htt*+/- Mäusen im Vergleich zu Kontrollmäusen unterstützt, da diese Tiere in der Lage gewesen sein könnten, Energieressourcen zu mobilisieren, die den unsozialen Tieren nicht zur Verfügung standen. Des Weiteren schienen Prozesse, die mit Myelinisierung im Zusammenhang stehen, in sozialen, aber nicht in unsozialen, PS *5-Htt*+/- Mäusen im Vergleich zu Kontrollmäusen herunterreguliert zu sein. Zusammengefasst wirkte sich die PS-Exposition auf das Sozial- und Angst-ähnliche Verhalten abhängig vom *5-Htt* Genotyp im weiblichen Nachwuchs aus. Prozesse, die mit Myelinisierung im Zusammenhang stehen, und epigenetische Mechanismen, die in der Chromatinumgestaltung beteiligt sind, schienen von einer GxE-Interaktion im Hippocampus dieser Tiere beeinflusst zu sein. Unsere Transkriptomdaten gaben des weiteren Hinweise darauf, dass die mitochondriale Atmungskette, und damit vermutlich auch der Energiemetabolismus, in *5-Htt*+/- Tieren im Vergleich zu *5-Htt*+/+ Tieren verändert sein könnte. Ferner könnten Veränderungen in der Myelinisierung sowie in der mitochondrialen Atmungskette zur Resilienzentwicklung gegenüber PS in *5-Htt*+/- Mäusen beitragen, möglicherweise durch Veränderungen in der Gehirnkonnektivität und in den zu mobilisierenden Energieressourcen.

1. General introduction

1.1. Variation in the serotonin transporter gene – from mice and men

1.1.1. Anatomy and function of the serotonergic system

Nowadays society celebrates the neurotransmitter serotonin as "the happiness hormone" (Glückshormon in German) that is needed for chocolate to give you a blissful moment. The name serotonin (5-hydroxytryptamine [5-HT]), however, originates from "serum" and "tone", attributed to its vasoconstrictive character. In fact, 95% of the 5-HT is located outside the central nervous system (CNS) (Berger *et al.* 2009). Peripheral 5-HT is mainly produced and stored by the enterochromaffin cells of the gut mucosa, where it regulates gut motility, but also by serotonergic neurons innervating the myenteric plexus. Thrombocytes furthermore store 5-HT from the blood stream, where it is involved in thrombocyte aggregation and vasoconstriction. In addition, in the pineal gland, 5-HT is also used as a precursor of the circadian rhythm hormone melatonin. The remaining 5% of 5-HT is produced in the CNS, more specifically by serotonergic neurons that are clustered in discrete cells groups, the raphe nuclei, which are located in the brain stem (Fig. 1.1-1, B1-B9). On the basis of their projection fields, the raphe nuclei can be classified into two distinct groups: the caudal raphe complex (Fig. 1.1-1, B1 – B3) located in the medulla oblongata and the caudal pons, and the rostral raphe complex (Fig. 1.1-1, B5 – B9) comprising the median (B5 + B8) and dorsal raphe nuclei (B6 + 7) of the rostral pons. Caudal raphe neurons send descending projections to the motor and autonomic systems in the anterior and dorsal horn of the spinal cord where they, amongst other things, control locomotor activity and inhibit nociception (Kriegebaum *et al.* 2010). The

rostral raphe nuclei on the other hand project mainly to the regions of the forebrain and the diencephalon, including the cortex, striatum, hippocampus, septum, amygdala, thalamus, hypothalamus, and olfactory bulb. The medial raphe nucleus (B7) and the dorsal raphe nucleus (B8) are furthermore reciprocally connected with each other. Next to this, afferent projections reach the raphe nuclei from regions of the forebrain, e.g. the prefrontal cortex (PFC), hypothalamus, amygdala, locus coeruleus, ventral tegmental area and bed nucleus of the stria terminalis (BNST) (Gobbi 2005).

In line with the numerous reciprocal connections that the raphe 5-HT system has with other regions of the CNS, 5-HT neurotransmission modulates a wide variety of processes regulating brain function and behavior. For example, 5-HT It is involved in the regulation of the circadian rhythm, thermoregulation, food intake, cognition, affective, social and sexual behavior (Kriegebaum *et al.* 2010). As such, a dysfunctional serotonergic system is associated with e.g. sleep and eating disorders, anxiety, depression, migraine and aggression.

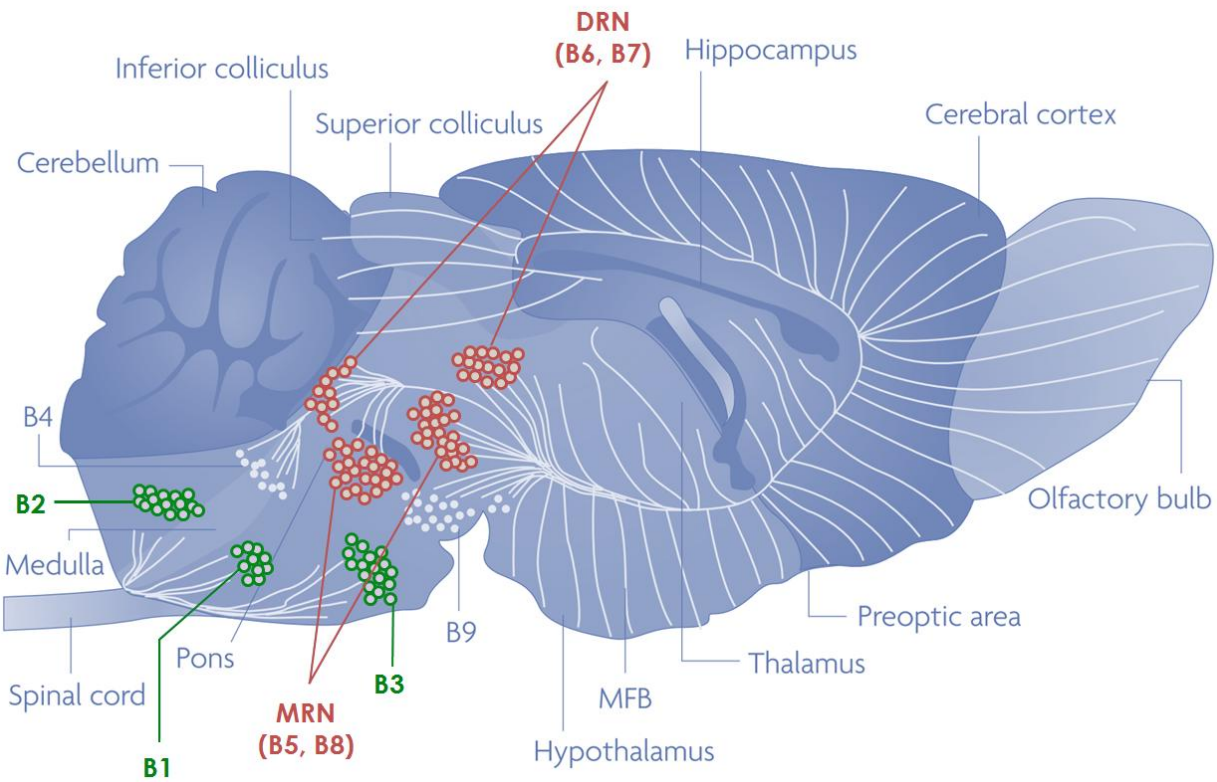

Figure 1.1-1 Scheme of the raphe nuclei and their projections. The caudal raphe B1-3 (green) are located in the medulla oblongata. The rostral raphe complex (dark red) comprises the median (B5 + B8) and dorsal raphe nuclei (B6 + 7) of the rostral pons. Modified from Murphy and Lesch 2008.

1.1.2. 5-HT synthesis and metabolism

The indolamine 5-HT belongs to family of the monoamines, like the catecholamines adrenalin, noradrenalin and dopamine. Most of the central 5-HT is synthesized in the soma of serotonergic neurons and to a lesser extent in dendrites and axons. Starting point is the essential amino acid L-tryptophan (Trp), which, in the rate limiting step of 5-HT synthesis, is hydroxylated to 5-hydroxytryptophan (5-HTP) by tryptophan hydroxylase (TPH). The TPH1 isoform fulfills this function in the periphery and the pineal gland, while TPH2 does so in the CNS (Gutknecht *et al.* 2009). Finally, 5-HTP is decarboxylated to 5-Ht. In contrast to 5-HT, both L-tryptophan and 5-HTP are able to pass the blood-brain barrier (BBB). As a result, 5-HT production can be supported by increasing the peripheral availability of those precursors.

Upon its synthesis, 5-HT is stored in intracellular vesicles that are located either at the synapse, the soma or along the axon. Upon release into the synaptic cleft, 5-HT exerts its effects by binding to its numerous pre- and postsynaptic receptors (5-HT_{1-7}), thereby initiating specific intracellular signaling pathways (5-HT_{1-2}, 5-HT_{4-7}) or, in one case, activating a cation channel (5-HT_3). The presynaptic 5-HT_{1A}, 5-HT_{1B} and 5-HT_{1D} receptors convey autoinhibition, whereas the 5-HT transporter (5-HTT) terminates serotonergic neurotransmission by re-uptake of 5-HT into the presynaptic neuron thereby depleting most of the 5-HT from the synaptic cleft (Zhou *et al.* 1998). A small portion of the recovered 5-HT is repacked into new vesicles, while most 5-HT is degraded to 5-hydroxyindole acetaldehyde by monoamine oxidases (MAO) A (during early development) and B. 5-hydroxyindolacetaldehyd is finally degraded into 5-hydroxyindole acetic acid (5-HIAA) by aldehyde dehydrogenase.

1.1.3. Dysfunction of the serotonergic system in psychiatric disorders

The serotonergic system is implicated in a wide range of psychiatric disorders, such as depression, anxiety, panic disorder (PD), obsessive compulsive disorder (OCD), autism, impulsivity and aggression. Already in 1967, Schildkraut and Kety suggested a possible relationship between biogenic amines, in particular norepinephrine but also serotonin, and affective states (Schildkraut and Kety 1967). By now, several studies have found alterations in serotonergic system function to be associated with various disorders. For example, some, but not all, studies found a decrease in 5-HIAA concentrations in the cerebrospinal fluid (CSF) and blood of depressed patients (Coppen *et al.* 1972; Asberg and Traskman 1981; Delgado *et al.* 1990; Meltzer 1990). 5-HIAA levels were found to be increased in the brain of suicide victims (Stanley *et al.* 1986; Arranz *et al.* 1997) and in

suicide attempters (Lester 1995; Chatzittofis *et al.* 2013) or correlated with suicide attempts in other studies (Brown *et al.* 1982). Furthermore, TRP depletion causes aggravation of symptoms in depressive patients (Delgado *et al.* 1990; Merens and van der Does 2007) and lowers mood in healthy male volunteers (Young *et al.* 1985). Next to this, 5-HTT is targeted by different classes of pharmacological antidepressants such as selective 5-HT reuptake inhibitors (SSRIs; e.g. fluoxetine/Prozac), selective 5-HT and norepinephrine reuptake inhibitors (SNRIs; e.g. venlafaxine) and tricyclic antidepressants (TCAs; e.g. imipramine) (Torres *et al.* 2003). In addition, several substances of abuse such as cocaine (inhibition) and amphetamines (substrates), e.g. 3,4-methylene-N-dioxymethamphet-amine (MDMA, Ecstasy), also operate on the 5-HTT.

1.1.4. Genetic variation in the *5-HTT* gene

As described above, the 5-HTT is a pivotal player of homeostasis of serotonergic neurotransmission as it controls extracellular (synaptic) 5-HT concentrations, terminates 5-HT signaling and contributes to maintaining intracellular 5-HT storage (Torres *et al.* 2003). Its central role for the serotonergic system and for mood disorders is furthermore underlined by successful pharmacological manipulation in antidepressant therapies.

In the CNS, 5-HTT expression is restricted to the raphe nuclei and the axons of the serotonergic neurons (Blakely *et al.* 1994). The human 35 kb long Solute carrier family 6, member 4 (*SLC6A4*; synonymous: *5-HTT*, *SERT,* 17q.12.2) gene comprises of 15 exons and a number of non-coding regulatory regions. Like all monoamine transporters, the 5-HTT protein contains 12 transmembrane α-helix domains (Rudnick 2011; Koldso *et al.* 2013). The re-uptake of 5-HT is mediated by the symport of Na^+ and Cl^- and export of K^+.

In humans, 5-HTT expression underlies a complex regulation involving regulatory polymorphisms in the promoter region of the 5-HTT gene, alternative splicing and post-transcriptional and –translational modifications (Collier *et al.* 1996; Lesch *et al.* 1996; Hu *et al.* 2006; Murphy and Lesch 2008). Transcriptional activity has been shown to be regulated by the serotonin-transporter-gene-linked-polymorphic region (*5-HTT*LPR) in the 5' UTR, a variety of single nucleotide polymorphisms (SNPs) and, as suggested recently, by means of the degree of DNA methylation at a 5' CpG island within the *5-HTT* gene promoter region (Nikolova *et al.* 2014; Wankerl *et al.* 2014).

Regarding the 5-HTTLPR, the long (l) and short (s)-alleles of the 5-HTTLPR are associated with high and low 5-HTT protein levels, respectively (Fig. 1.1-2). This leads to an altered 5-HT homeostasis: The rate of 5-HT reuptake is two times higher in cells homozygous for the l-allele when compared to cells carrying one or two s-alleles (Lesch *et al.* 1996). The s-allele is associated with increased anxiety- and depression-related personality traits (Collier *et al.* 1996; Lesch *et al.* 1996; Hu *et al.* 2006) and, moreover, after experiencing psychosocial adversity, s-allele carriers are at a higher risk of developing a depressive disorder (Caspi *et al.* 2003). Although not replicated by all studies, there is accumulating evidence suggesting that the s-allele is associated with increased sensitivity to negative stimuli, but also to positive ones (for review see Homberg and Lesch 2011; Homberg and van den Hove 2012). For s-allele carriers, it is suggested that the evolutionary disadvantageous increased stress sensitivity could have been evened out by advantages regarding cognitive functions, e.g. better performance regarding memory and attention and higher cognitive flexibility.

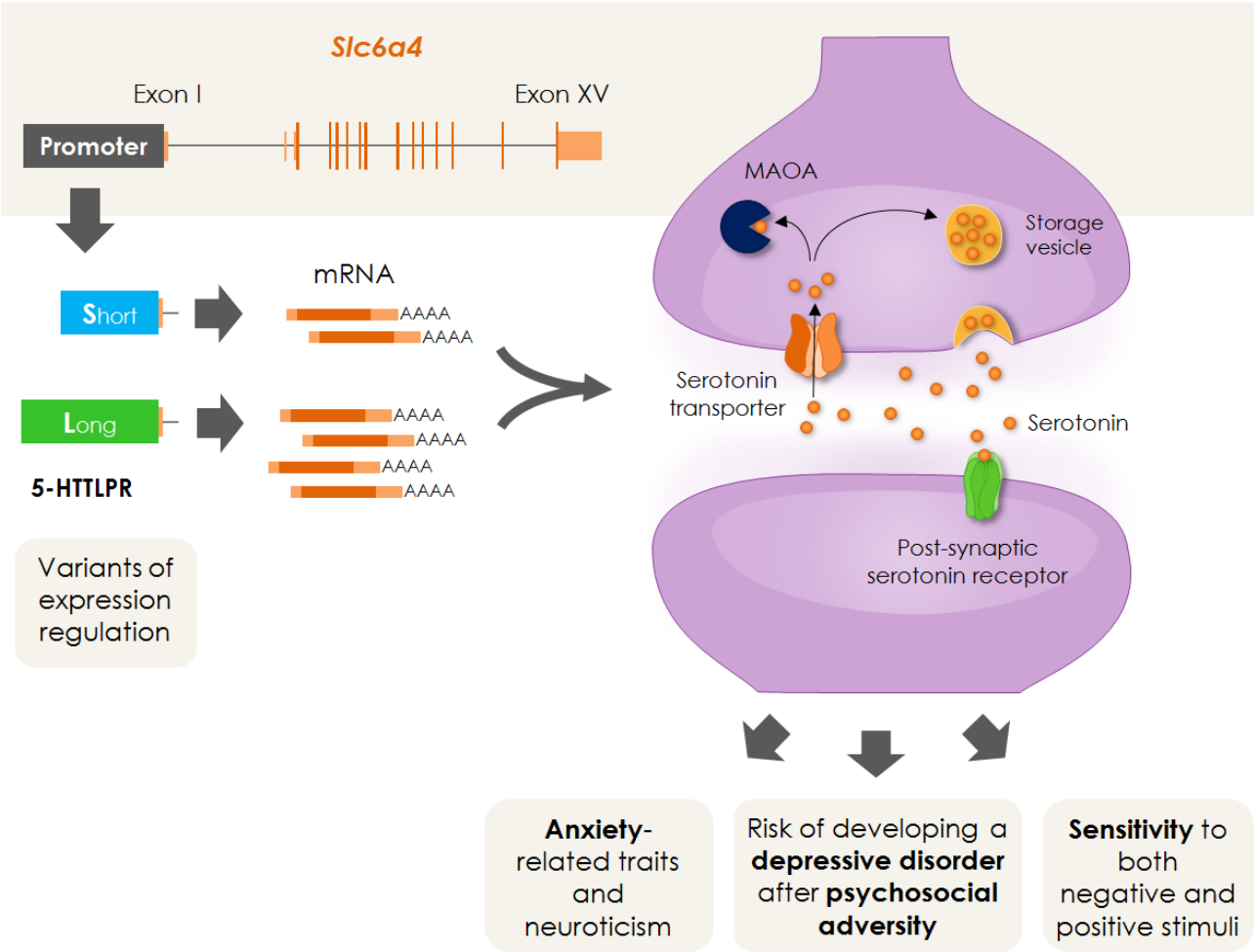

Figure 1.1-2 Differential expression of the 5-HTT due to a polymorphism in the *5-HTT (Slc6a4)* promoter. Adapted from Canli and Lesch, Nat Neurosci 10, 1103-1109 (2007).

1.1.5. 5-HTT deficient mice

Characterization of the 5-HTT deficient mouse. As mice are not endowed by nature with polymorphisms in the *5-Htt* gene, a genetically engineered C57BL/6J mouse deficient in 5-HTT has been created in our lab in order to study the role of 5-HTT in mood and anxiety disorders in more detail (Bengel *et al.* 1998). A 1.1 kb genomic region of the murine *5-Htt* comprising exon 2 and flanking genomic sequences was replaced by a 1.8 kb PGK neomycin (*neo*)-polyA expression cassette. Exon 2 contains the translation start codon and several sites for posttranslational modifications (Bengel *et al.* 1998). In addition, it also encodes the first transmembrane domain that harbors two amino acids presumably involved in substrate interaction, i.e. Asp98 and Tyr95 (Koldso *et al.* 2013)(ensemble.org). The disrupted gene is transcribed into a *5-Htt* mRNA that is spliced between exon1 and 3, resulting in the formation of a dysfunctional N-terminally truncated protein that is not functionally incorporated into the plasma membrane and can only be detected in the endoplasmatic reticulum of the soma and dendrites of serotonergic neurons, but not in the axons (Ravary *et al.* 2001). In *5-Htt-/-* mice, 5-HTT binding sites and 5-HT reuptake are absent, while 5-HT brain tissue concentrations are, except for the frontal cortex, reduced by 60-80% and 5-HT synthesis is increased in the brain stem, frontal cortex, hippocampus and striatum in *5-Htt-/-* mice, particularly in females (Bengel *et al.* 1998; Kim *et al.* 2005). Interestingly, mice heterozygous for the *5-Htt* do not necessarily show a gene dose-effect regarding all the findings described for the KO animals. As expected, *5-Htt+/-* mice show a reduction in 5-Htt density of approximately 50%. 5-HT uptake in synaptosomes prepared from brain stem and cortex as well as 5-HT synthesis and concentrations in the brain stem, frontal cortex, hippocampus and striatum are, however, comparable to *5-Htt+/+* mice, indicating that a single functional 5-Htt allele might be sufficient to maintain a certain degree of 5-HT homeostasis in serotonergic cells (Mathews *et al.* 2004; Kim *et al.* 2005). Despite these findings, extraneuronal 5-HT concentrations are increased in a gene dose-dependent manner in striatum and frontal cortex of both *5-Htt+/-* and *5-Htt-/-* mice (Mathews *et al.* 2004). Adaptive changes in 5-HT autoreceptors in response to increased extracellular 5-HT concentrations were detected in both heterozygous and KO mice, although it is not yet fully understood to what extend this translates into functional autoinhibition (Araragi *et al.* 2013). 5-Ht_{1A} receptor protein levels are decreased in a gene dose-dependent manner in the dorsal raphe nucleus, whereas only female *5-Htt-/-* animals show a significant decrease in several amygdala and hypothalamus nuclei, the septum and the medial raphe nucleus (Fabre *et al.* 2000; Li *et al.* 2000). 5-Ht_{1B} receptor density is increased in the substantia nigra. Araragi and colleagues showed, however, that despite marked desensitization of the 5-Ht_{1A} autoreceptors, autoinhibition of 5-HT

neurons is unaltered in *5-Htt-/-* mice (Araragi *et al.* 2013). Next to this, it was suggested that increased expression of the Organic cation transporter 3 (*Slc22a3*, encodes OCT3) in the hippocampus of *5-Htt+/-* and *5-Htt-/-* mice might represents an adaptive mechanism to clear the elevated extracellular 5-HT levels, thereby supporting 5-HT homeostasis in the hippocampus (Schmitt *et al.* 2003; Baganz *et al.* 2008). OCT3 is preferably expressed in neurons and transports 5-HT with a low affinity.

Behavioral phenotype. Generally, both female and male *5-Htt-/-*, but not *5-Htt+/-*, mice have been characterized as more anxious when tested under naïve conditions in a variety of anxiety-related behavioral task, including the elevated plus maze (EPM), the light-dark box and the open field test (Holmes *et al.* 2003; Heiming *et al.* 2009; Kloke *et al.* 2013), although not all studies could replicate this finding. *5-Htt-/-* mice furthermore show reduced home cage activity (Holmes *et al.* 2002; Lewejohann *et al.* 2010). Both *5-Htt+/-* and *5-Htt-/-* mice have reduced basal corticosterone (CORT) levels, although CORT increase in reaction to stress does not seem to be affected (Lanfumey *et al.* 2000; Van den Hove *et al.* 2011). Both *5-Htt-/-* and *5-Htt+/-* males behave less aggressive in the resident intruder test (Holmes *et al.* 2002) and a group housing paradigm (Lewejohann *et al.* 2010). Also, when facing an unknown *5-Htt+/+* male of equal social status, *5-Htt-/-* animals are less likely to obtain dominance (Lewejohann *et al.* 2010), in contrast to *5-Htt+/-* males. Male *5-Htt-/-* mice show, however, also increased socio-positive behavior in group housing, while no differences regarding social exploration were detected between all genotypes (Lewejohann *et al.* 2010). Interestingly, also the maternal 5-Htt genotype seems to affect various behavioral phenotypes in offspring, independent of an offspring's own genotype (Jones *et al.* 2010), adding to the complexity of 5-HT system function regulation.

1.2. Prenatal stress

"Stress may be defined as a threat, real or implied, to the psychological or physiological integrity of an individual.'' (McEwen 2000).

Stress plays a major role in the etiology of mental disorders, although research is still struggling to understand the intricate relationship between stress, genetic susceptibility, disease and resilience. When looking at the impact of stress throughout the life span, the brain seems to be most vulnerable to stress during early life and in old age (Lupien *et al.* 2009). Early life stress is of particular interest as it seems to shape the physiology of the stress reaction in adulthood and with it, the risk for developing a mental disorder.

1.2.1. Early environment might shape adult phenotypes

First observations that intrauterine conditions may have long-lasting consequences on the future child's physiology and metabolism were made when analyzing subjects born during periods of famine in World War II. For example, Dorner and colleagues studied the offspring of mothers that were pregnant during the German famine. The subjects exposed to undernourishment during intrauterine growth were more likely to be obese or have diabetes type II compared to subjects born after the famine (Dorner 1973; Dorner *et al.* 1985). Similar devastating effects of malnourishment on the offspring's metabolism were observed in subjects born during the Dutch Hunger winter. Roseboom and colleagues found an increased rate of coronary heart disease and glucose intolerance, altered blood coagulation and more obesity in women after exposure to famine in early gestation compared to those not exposed to the famine (Roseboom *et al.* 2006). Exposure during mid gestation was associated with obstructive airways disease and microalbuminuria, whereas exposure during late gestation was associated with glucose intolerance. This shows that changes in the intrauterine environment affect the outcome differently depending on which systems, regions and functions undergo a critical developmental period. Barker later proposed what is now called the "developmental origins of adult health and disease" (DOHaD) hypothesis, suggesting that the offspring's immanent plasticity enables it to adapt to its pre- or perinatal environment thereby permanently reprogramming its physiology and metabolism. Although often indicative of adaptive capacity, several diseases in adulthood could originate from this developmental programming (Barker 1997). As such, the "predictive adaptive response" (PAR) hypothesis states that the fetus anticipates the future environment and adapts it physiology accordingly, thereby enhancing survival (Gluckman and Hanson 2004). In

fact, the above described metabolic changes might have increased the offspring's short-term chances of survival would they have lived in an environment with low food availability. The environment changed, however, but the programmed metabolic changes turned out to persist. This is called the "mismatch hypothesis", where disease arises from the mismatch between the (predicted) environment to which offspring adapt during early life and the (actual) environment that the offspring is exposed to later in life.

1.2.2. What do we know about the effects of prenatal stress?

Human studies. The effects of maternal stress during pregnancy on the offspring's physiological and behavioral outcome as well its risk to develop mental disorders such as depression and anxiety disorders has been intensively studied over the past decades. Several issues such as the long time span between the stress experience and the measured outcome, the difficulty to assess the timing and intensity of the perceived stress, the interaction between PS and other negative or positive (or both) experiences in later life, the social environment, other environmental influences as well as the interaction of PS with the genetic heterogeneity of humans increase the difficulty to study the effects of PS in adult offspring. Stressors analyzed in humans are typically more of emotional than physical nature and include sustained situations of interpersonal tension, e.g. familiar/marital conflicts (Stott 1973) and conflicts at work, loss of the marital partner (Huttunen and Niskanen 1978), job loss (Schneiderman *et al.* 2005), disease, e.g. anxiety and depression disorder (Buss *et al.* 2010; Loomans *et al.* 2011; Winsper *et al.* 2015), as well as catastrophes, e.g. war time (Meijer 1985) and earthquakes (Watson *et al.* 1999). Especially the role of maternal depression and anxiety as PSors should not be neglected as e.g. 10-16% of pregnant women in a recent US study fulfilled the criteria for major depressive disorder diagnosis (Marcus 2009) and 15.6% and 13% of pregnant woman showed anxiety-symptoms in a Swedish and an English cohort (Heron *et al.* 2004; Rubertsson *et al.* 2014). Maternal depression has been suggested to lead to alterations in the maternal hypothalamus-pituitary-adrenal (HPA) axis and maternal uterine blood flow, which in turn may contribute to preterm delivery, low birth weight and pre-eclampsia (Teixeira *et al.* 1999). Maternal stress was in general linked to preterm birth, low birth weight and a smaller head circumference (corrected for birth weight) (Hedegaard *et al.* 1993; Copper *et al.* 1996; Torche 2011; Oyarzo *et al.* 2012) as well as increased basal HPA axis activity in the offspring at an age of 6 months (Lyons-Ruth *et al.* 2000), 5 years (Gutteling *et al.* 2005) and 10 years (O'Connor *et al.* 2005). Moreover, PS was associated with reduced gray matter volume (Buss *et al.* 2010), reduced attention and concentration (Gutteling *et al.* 2006), impulsivity (Van den Bergh *et al.* 2005), increased

risk for attention deficit hyperactivity disorder (ADHD) (Li *et al.* 2010; Class *et al.* 2014) and for several psychiatric disorders such as schizophrenia (Huttunen and Niskanen 1978; van Os and Selten 1998; Malaspina *et al.* 2008) borderline personality disorder (Schwarze *et al.* 2013; Winsper *et al.* 2015) and anxiety (Van den Bergh and Marcoen 2004) and depression (Watson *et al.* 1999).

Animal studies. Animal studies have analyzed the effects of PS during different stages of pregnancy and linked PS to changes in behavior, physiology, metabolism and brain morphology (reviewed in Beydoun and Saftlas 2008; Weinstock 2008). Different types of PS protocols are established using stressors of different intensity, ranging from chronic restraint stress over adverse odors and unpredictable stress with different stressors to bystander stress, in which not the pregnant dam but the cage mate is stressed. When translating the results of PS studies in animals to the human situation, one should be aware of the differences in pre- and postnatal brain development of the different species (see for example review by Lupien *et al.* 2009). As rats and mice give birth to rather immature pups, prenatal brain growth and neuroendocrine development in those rodents is delayed when comparing it to the development in humans and non-human primates. The rodent brain of a 10-14 day old pup is comparable to the ad-term human brain in regard to its development. Thus PS during for example the third trimester in mice, rats and men does not necessarily affect the same processes and developing brain regions. The hippocampus grows in the first two years of a toddler, whereas prefrontal cortex and amygdala development stretches into the second and third decade respectively (Giedd *et al.* 1996). In contrast, development of both the rodent hippocampus and amygdala expands into adulthood (Chareyron *et al.* 2012). While the major part of neurogenesis takes place in the second trimester in humans, in rats it starts in the second but reaches its peak in the third trimester. Synaptogenesis stretches from the third trimester of pregnancy to childhood in humans, whereas it starts only after birth in rats. Myelination in humans starts already towards the end of pregnancy, while in rodents it starts only during the second and third postnatal week (reviewed nicely by Schuurmans and Kurrasch 2013)

Intrauterine stress exposure in animals was described to lead to a range of behavioral alteration in the offspring, among them decreased response inhibition and lowered behavioral restraint in Rhesus monkeys (Schneider 2001), deficits in learning and memory (Hayashi *et al.* 1998; Gué *et al.* 2004), increased anxiety-like behavior (Estanislau and Morato 2005; Barros *et al.* 2006; Zagron and Weinstock 2006; Laloux *et al.* 2012) and increased depression-like behavior in rodents (Secoli and Teixeira 1998; Morley-Fletcher *et*

al. 2003; Van den Hove *et al.* 2011). While it is not yet completely understood how maternal stress induces the above described effects, PS exposure has been linked to reduced or increased birth weight and increased pre-weaning mortality (Cabrera *et al.* 1999; Mueller and Bale 2006), delayed motor development (Patin *et al.* 2004; Burlet *et al.* 2005), increased blood pressure (Igosheva *et al.* 2004), increased cortisol levels (Coe *et al.* 2003) and altered HPA axis function (see review by Weinstock 2008), altered immune response (Coe *et al.* 2002; Llorente *et al.* 2002; Stefanski *et al.* 2005), hyperglycemia and glucose intolerance (in aged rats, (Lesage *et al.* 2004)). Morphological changes associated with PS include decreased neurogenesis in the dentate gyrus of rhesus monkeys (Coe *et al.* 2003) and rats (Lemaire *et al.* 2000), reduced brain cell proliferation in various brain regions in P1 rat pups (Van den Hove *et al.* 2006), decreased synaptic density in the rat hippocampus (Hayashi *et al.* 1998), reduced number of neurons and glia cells in the amygdala in rats (Kraszpulski *et al.* 2006) as well as alterations in dendritic branching, length and arborization in neurons of the nucleus accumbens (Muhammad *et al.* 2012), and altered synaptic connectivity, spine density and dendritic complexity (Barros *et al.* 2006; Murmu *et al.* 2006). Part of the difficulty to create a working concept of PS is caused by the differences in stressor types, timing and intensity of the stress, interspecies differences and the different time points in analyzing the outcome and outcome measures in the different studies. Also, some changes are only transient or only apparent under certain conditions, while others are lasting. Nevertheless, a few key ideas have emerged. Although malnutrition and hypoxia induced by reduced placental circulation have been suggested as contributing factors mediating the effects of PS (see review by Huizink *et al.* 2004), recent research focused especially on the mis-programming of the fetal HPA axis by PS and the role of epigenetic mechanisms in this process (see section 1.3 "Epigenetics") (reviewed by Weinstock 2008; Lupien *et al.* 2009; Harris and Seckl 2011; Reynolds *et al.* 2013; Xiong and Zhang 2013). Other studies analyzed PS and its interaction with later life experiences in the context of the mismatch hypothesis by experimentally creating different life histories (Kloke *et al.* 2013). Another focus of recent research is to broaden the understanding the molecular base of resilience.

Interaction of 5-Htt genotype and stress. Recent studies involving 5-HTT deficient mice aimed to test the hypothesis that central 5-HTT deficiency is a vulnerability factor when it comes to coping with adversity and the subsequent risk to develop a depression disorder. *5-Htt-/-,* and to a lesser extend *5-Htt+/-,* mice were indeed often shown to be more vulnerable towards different forms of stress than wild types. For example, when repeatedly exposed to the forced swim test, *5-Htt-/-* mice show increased depression-like

behavior when compared to *5-Htt+/+* littermates (Wellman *et al.* 2007). While Carroll and colleagues replicated the anxious phenotype of control *5-Htt-/-* mice and found that repeated exposure to the FST increased depression-like behavior in those animals, early life stress by means of repeated foot shocks did not modify this behavior (Carroll *et al.* 2007). Carola et al found that poor maternal care increases anxiety-like and some parameters of depressive-like behavior as well as hippocampal *Bdnf* expression in male *5-Htt+/-* mice but not in *5-Htt+/+* mice when compared to controls experiencing high maternal care (Carola *et al.* 2008). A study by Jansen et al could not replicate the anxious phenotype of naïve *5-Htt-/-* animals in the EPM. Those animals showed, however, increased anxiety after repeated negative social encounters when compared to 5-Htt+/+ mice (Jansen *et al.* 2010). In the same study, repeated negative social encounters, but not positive, let to increased CORT levels in *5-Htt+/-* mice, but not in 5-Htt+/+ or *5-Htt-/-* mice. Bartolomucci and colleagues furthermore found that male *5-Htt+/-* mice show increased avoidance of an unfamiliar male and decreased 5-HT turnover in the frontal cortex when compared to 5-Htt+/+ mice and 5-Htt+/- controls after three weeks of psychosocial stress exposure (Bartolomucci *et al.* 2010). Recently, our group found that while *5-Htt+/-* mice had a better memory and were a little bit less anxious than *5-Htt+/+* litter mates, they also showed increased depressive-like behavior when exposed to PS (Van den Hove *et al.* 2011). The study by Kloke and associates on the other hand, where 5-HTT deficient mice were exposed to early life stress in the form of an aversive olfactory cue during the lactation phase, did not find main convincing evidence for a modulation of anxiety-like behavior in *5-Htt+/-* and *5-Htt-/-* mice by this form of stress (Kloke *et al.* 2013). Taken together, these findings show that 5-HTT deficient mice represent a suitable model system to study the effects of early life stress on the background of an altered serotonergic system.

1.2.3. The HPA axis

Organisms strive for the maintenance of stability, also known as homeostasis. When a stressor challenges this homeostatic state, the organisms reacts in order to adapt to the acute stress by activating stress hormone systems that initiate physiological and behavioral reactions, finally re-establishing a (possibly new) homeostatic state. McEwen coined the term "allostasis", literally traduced as "maintaining homeostasis through change", for this process and "allostatic load" for "the price the body pays for being forced to adapt to adverse psychosocial or physical situations" (McEwen 2000). The normal allostatic stress response follows the pattern of initiation by a stressor, continues for an adequate time interval followed by termination of the stress response by negative

feedback. Allostatic load refers to an inadequate, that is exaggerated or insufficient, stress response and its consequences, which ultimately will build up and wear the body up ("wear and tear"). While in the short run stress hormones have a protective role and are even essential for survival, excessive and/or long-term dysregulation of the stress systems can have dire long-term consequences.

When the brain detects a stressor, it engages two basic hormonal systems that mediate the stress response, the fast acting sympathetic-adreno-medullary (SAM) axis and the relatively slowly acting HPA axis (Fig.1.2-1). The function and long-term regulation of the HPA axis by environmental factors has been the subject of numerous studies. Signals from cortex, hippocampus and amygdale initiate the stress response by activating the hypothalamic paraventricular nucleus (PVN) (Lupien et al. 2009), which reacts by setting free corticotropin-releasing hormone (CRH) and the anti-diuretic hormone arginine-8-vasopressin (AVP) (Vale et al. 1981). This triggers the subsequent production and secretion of adrenocorticotropic hormone (ACTH) from the adenohypophysis, the anterior part of the pituitary gland, by binding to the CRH receptor type 1 (CRHR1) and AVP type 1b receptor, respectively (Whitnall 1989; Aguilera and Rabadan-Diehl 2000). ACTH reaches the adrenals through the blood circulation, where it leads to the production and secretion of glucocorticoids from the adrenal cortex. The main glucocorticoid in humans is cortisol, whereas in rodents it is CORT. Glucocorticoid secretion enhances the effects of catecholamines and raises the physical resources needed for the stress reaction, e.g. increased availability of energy by inducing gluconeogenesis and lipo- and proteinolysis, and inhibition of unnecessary energy consuming functions including immunological and inflammatory processes (Dallman et al. 1994). Glucocorticoid secretion follows, however, also a diurnal cycle, with high morning and low evening cortisol in humans and the other way in rodents. Additionally, glucorticoids are released in a pulsatile ultradian fashion with varying amplitudes, reaching a peak in release about every 1-2 h (Walker et al. 2012). The effects of glucocorticoids in the brain are transmitted by nuclear receptors, the mineralcorticoidreceptor (MR) and the glucocorticoid receptor (GR), that both act as transcription factors on gene expression or by non-classical pathways. While central MR expression is restricted to the PVN and some hippocampal regions, the GR is expressed all over the brain. The MR binds glucocorticoids with a 10-fold higher affinity than the GR, indicating a preferred activation of the MR at basal glucocorticoid concentrations and an additional occupancy of the GR only in case of elevated concentrations as reached by the peaks of the diurnal cortisol cycle and during stress (Reul and de Kloet 1985). It was suggested that the MR plays a role in maintaining basal HPA axis activity and

mediating mainly the *permissive* effects of GCs, whereas the GR is involved in terminating the stress response, i.e. mediating mainly the *suppressive* effects of GCs.

After the stressor has vanished, GR binding engages several negative feedback loops, returning the HPA axis to a set point of homeostasis (reviewed by Xiong and Zhang 2013). GR activation directly inhibits secretion of ACTH from the pituitary gland and of CRH and AVP from the hypothalamus, in addition to the negative feedback loops comprising the hippocampus, the frontal cortex and the raphe nuclei (reviewed in Lupien *et al.* 2009; Vincent and Jacobson 2014). The described reaction cascade is strongly inhibited in new born rodents, which exhibit an approximately 10 day long period of stress hypo-

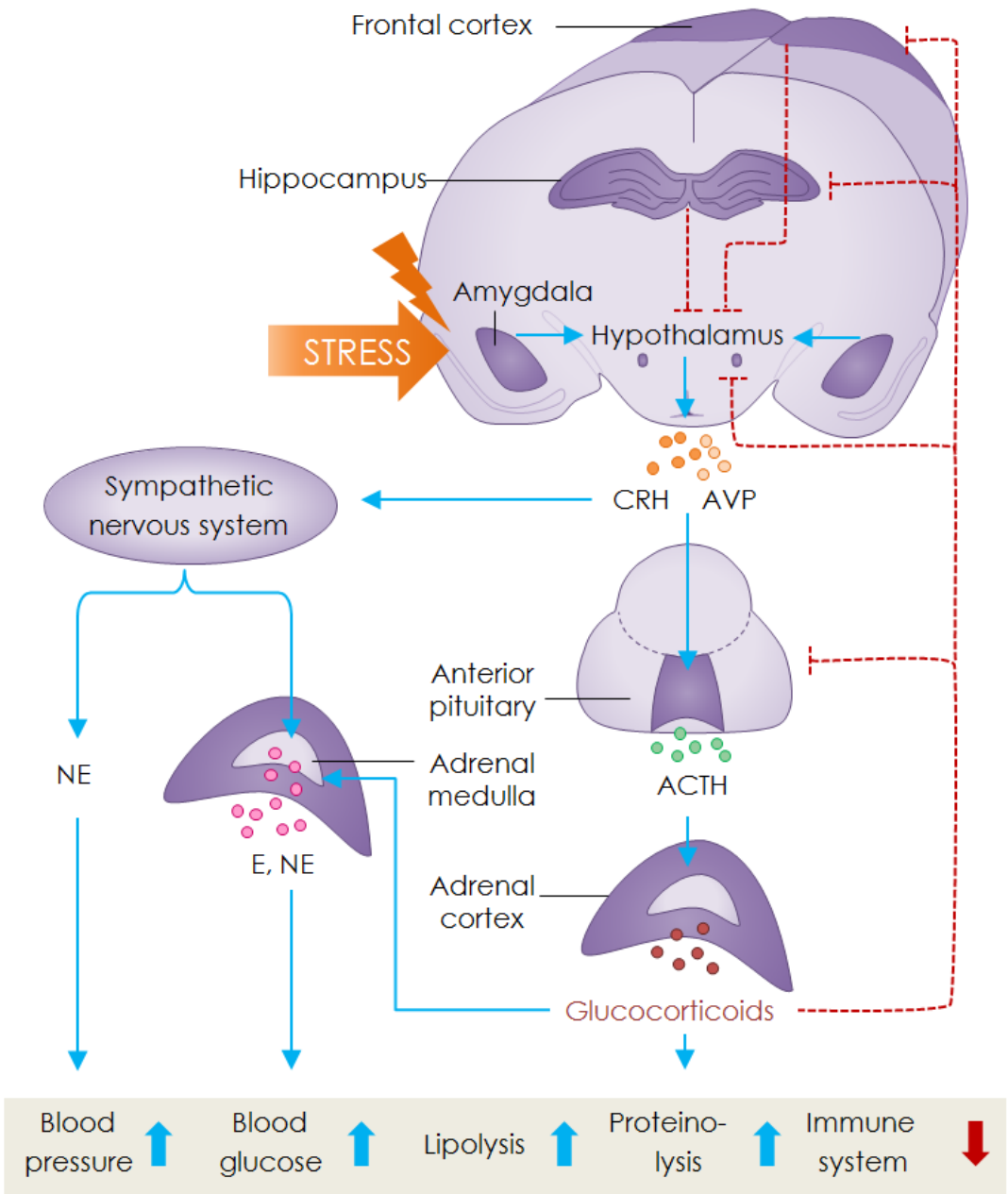

Figure 1.2-1 Scheme of the hypothalamo-pituitary-adrenal axis. Adapted from (Lupien *et al.* 2009). CRH = corticotropin releasing hormone, AVP = arginine vasopressin, ACTH = Adrenocorticotropic hormone, E = epinephrine, NE = Norepinephrine.

responsiveness (SHRP) during their first two weeks of life. During the SHRP, mild stressors produce only an attenuated CORT response in pups (Schapiro 1962; Sapolsky and Meaney 1986; Levine 2001). The main mechanisms contributing to this phenomenon is a strongly diminished adrenal CORT release to rising ACTH levels, which leads to a reduced translation of the brain's stress response into CORT levels (Rosenfeld *et al.* 1991; Okimoto *et al.* 2002). Additionally, regulation of many of the above-mentioned components of the HPA-axis has been suggested to be involved in this phenomenon (reviewed in Daskalakis *et al.* 2013). The SHRP is maintained by caregiving of the dam, e.g. by licking and grooming and giving milk. Interestingly, human toddlers have been suggested to go through a similar period between the first and second year of life (reviewed in Gunnar and Quevedo 2007).

1.2.4. Stress hormones during pregnancy

The HPA axis is regulated differently in pregnant women. Additional CRH is secreted in increasing amounts by the primate placenta during pregnancy, thus maternal plasma CRH increases gradually (Petraglia *et al.* 1996; McLean and Smith 1999; Weinstock 2005). Not only CRH but also catecholamines and glucocorticoids from the maternal circulation can reach the fetal brain. In addition to the effects of maternal glucocorticoids on the fetal brain, the human fetus expresses CRH type 1 receptor from mid-gestation on and CRH can trigger this way the release of glucocorticoids from the fetal adrenals. The right level of glucocorticoids, however, is essential for normal brain development of the fetus and thus, extremely elevated or lowered stress hormone levels should be avoided. Indeed, mechanisms sheltering the fetus from exaggerated CRH levels exist. On the one hand, CRH is bound and inactivated by CRH-binding protein (CRH-BP). CRH-BP lever, however, fall towards the end of pregnancy, thereby increasing CRH levels. On the other hand, the primate placenta expresses an enzyme, 11ß-hydroxysteroid dehydrogenase (11ß-HSD)-2, that catalyzes about 80% of the cortisol to an inactive form (White *et al.* 1997; Weinstock 2008). Although cortisol levels are around 13 times lower in the fetus than the mother due to this mechanisms, there is still a linear relationship between maternal and fetal cortisol levels (Gitau *et al.* 1998).

Next to the continuously increasing cortisol levels during gestation, pregnant women still show an additional increase in stress hormones of individual magnitude when experiencing stress, although the stress response in general is dampened during pregnancy (de Weerth and Buitelaar 2005). Women reporting high levels of perceived stress during pregnancy show elevated levels of plasma CRH and ACTH during the last

trimester (Wadhwa *et al.* 1996). Additionally, maternal trait anxiety was found to be negatively correlated with placental 11ß-HSD-2 expression, further increasing cortisol levels in those women (O'Donnell *et al.* 2012). An increase in CORT was also detected in rat dams and fetus after maternal stress exposure (Dauprat *et al.* 1984; Cadet *et al.* 1986). Moreover, elevated CRH levels at 16-20, 18-20 and 28-30 weeks of gestation have been associated with pre-term delivery, and at 33 weeks additionally with smaller birth weight (McLean *et al.* 1995; Hobel *et al.* 1999; Wadhwa *et al.* 2004). Taken together, in times of maternal stress, maternal stress hormones are elevated. Exaggerated levels of CRH and glucocorticoids have the chance to reach the fetal brain, where they are thought to affect the development of the fetal HPA axis. The necessary fetal receptors are already expressed during gestation and the HPA axis is already responsive in mid gestation, illustrating a possible point of action. Both MR and GR are expressed in the fetal hippocampus from the 24th week of gestation in humans (Noorlander *et al.* 2006). In rats, GR can be detected from around E12-13 in the hippocampus, hypothalamus and pituitary, whereas MR is expressed from E15.5 onwards in the rat hippocampus (Cintra *et al.* 1993; Kitraki *et al.* 1996; Diaz *et al.* 1998). In the mouse, GR can be detected in the pituitary from E12, at intermediate levels in periventricular neuroepithelial CNS regions, low-intermediate levels in hippocampus and cerebellum and at very low levels also in the majority of other CNS regions (Speirs *et al.* 2004), while MR is expressed from E13.5 in hippocampus, rhinencephalon, hypothalamus and pituitary (Brown *et al.* 1996). Indeed there are findings hinting towards a programming role of maternal stress hormones on the HPA axis of the offspring. For example, 17 months old infants exposed to high levels of cortisol *in utero* showed higher baseline cortisol values and a blunted response to acute separation stress (O'Connor *et al.* 2013). Waking levels of plasma cortisol in 10-year-old children correlated with their mother's anxiety level in pregnancy (O'Connor *et al.* 2005). Another study linked prenatal exposure to maternal anxiety at 12–22 weeks with a high, flattened cortisol day-time profile in the adolescent offspring, and in females even with depressive symptoms (Van den Bergh *et al.* 2007).

1.3. Epigenetics

1.3.1. DNA methylation and the epigenome

There is evidence that epigenetic mechanisms are involved in fetal programming in response to changes in the intrauterine and early environment (reviewed in e.g. Tsankova *et al.* 2007). The epigenome forms a sort of dynamic cellular memory that is thought to transmit the effects of the environment to the molecular level, i.e. the DNA, thereby leading to long-lasting changes in gene expression, physiology and behavior. To which extend this kind of programming is reversible by later experiences or by drug treatment is the subject of many recent studies. There is accumulating evidence that the epigenome is more plastic than previously anticipated (Guo *et al.* 2011), and may be normalized in response to e.g. behavioral and pharmacological therapy. If this is sufficient to counteract changes at the functional (e.g. behavioral) level remains to be

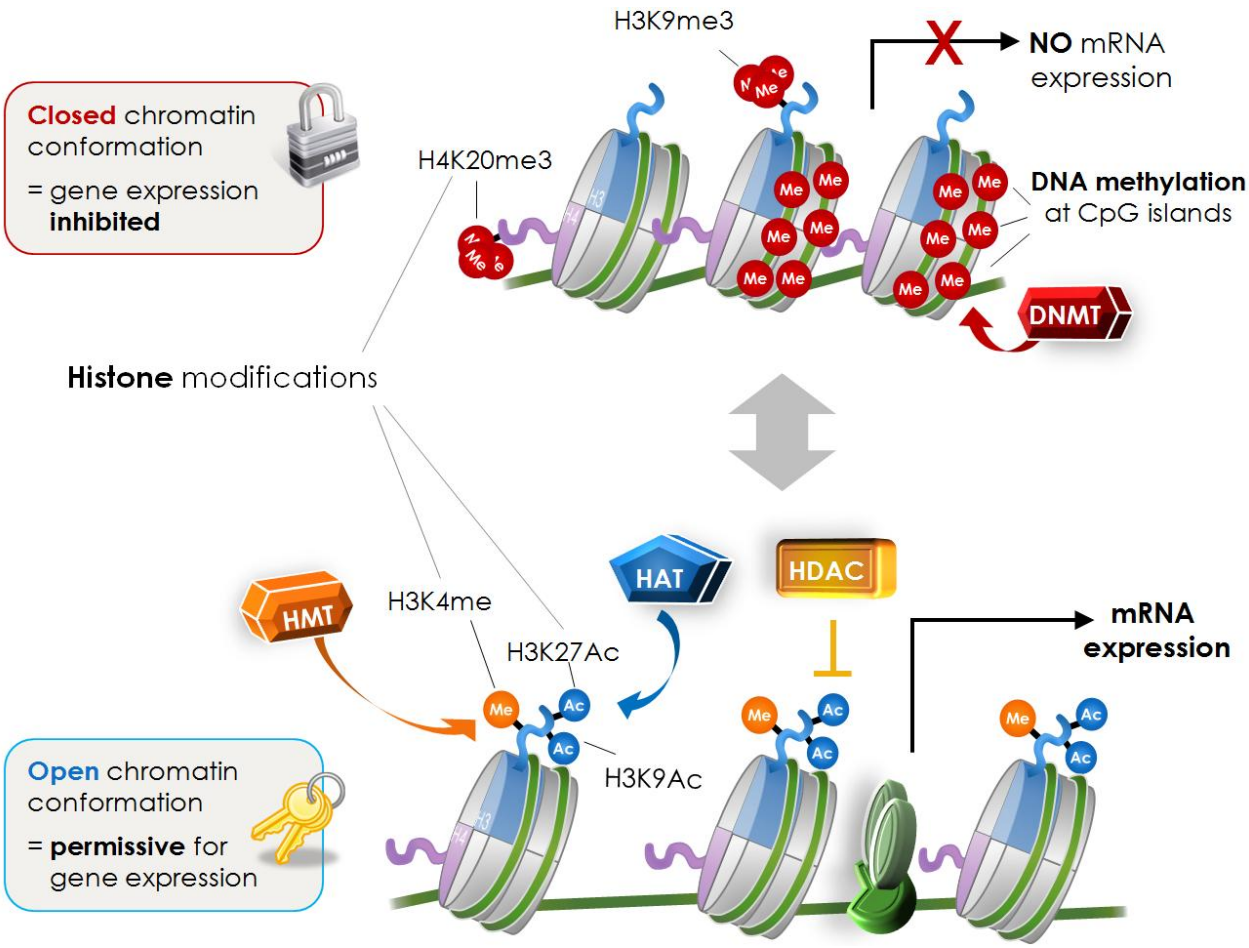

Figure 1.3-1 Histone modifications and DNA methylation regulate gene expression by affecting chromatin conformation. H3 = histone 3, H4 = histone 4, K = lysine, me = methylation, me3 = triple methylation, Ac = acetylation, DNMT = DNA methyltransferase, HMT = histone methyltransferase, HAT = histone acetyltransferase, HDAC = histone deacetylase.

studied.

Epigenetic mechanisms can be defined as modifications that lead to changes in gene expression that are (1) self-sustaining in the absence of the original signal that initiated the change, (2) not associated with a modification of the DNA sequence itself and (3) heritable from mother to daughter cell (Dulac 2010). Epigenetic mechanisms comprise DNA methylation, various post-translational modifications at histone N-terminal tails and non-coding RNAs (ncRNAs). Those mechanisms interact with each other and define how dense or accessible the chromatin is packed (Fig. 1.3-1). The basic chromatin element is a nucleosome consisting of DNA wrapped around a core histone octamer comprising the histone proteins H2A, H2B, H3 and H4. An open chromatin state with a low number of nucleosomes is permissive for transcription (euchromatin), whereas a closed, condensed chromatin conformation displaying a high nucleosome density does not allow for the initiation of transcription (heterochromatin).

Genomic distribution of DNA methylation in mammals. DNA methylation is the most stable and long-lasting epigenetic modification. We speak of DNA methylation when one of the DNA bases is covalently modified by the addition of a methyl moiety (-CH3). In mammals, the only methylated base is cytosine and it usually is only methylated in a 5'cytosine-guanin-3' dinucleotide, a so called "CpG site" (the p standing for phosphate). Next to this, a lower degree of DNA methylation can be found outside of the CpG context, e.g. in CpAs, CpTs and CpCs (as illustrated in the pyrosequencing results of mir137) (Guo *et al.* 2013). In the mammalian genome, the frequency of CpG sites is four to five times lower than to be expected by chance (Bird 1980). This is due to an evolutionary loss of CpGs: A methylated C can spontaneously deaminate, which leads to the false pairing of T and G and stochastically to the replacement of C by T. Regions enriched for CpG sites, that is by arbitrary definition regions of more than 300bp or 1000bp and 55% C/G-content, are termed CpG islands (CGIs) and are highly conserved between humans and mice (Illingworth *et al.* 2010). CGIs are predominantly unmethylated (Bird 2002), whereas regions of lower CpG density are more often found to be methylated, indicating that CGIs are protected from methylation. Approximately 50% of the CpG islands are associated with promoters of protein coding genes, whereas the other CpG islands are located in gene bodies (the transcribed region past the first exon, (Brenet *et al.* 2011)), in promoter sequences of regulatory RNAs and outside of genes (Illingworth *et al.* 2008). About 56% (Antequera and Bird 1993) to 70% (Saxonov *et al.* 2006) of human genes harbor CGIs in their promoters. If promoter CGIs are methylated, this is associated with gene silencing, but rarely in a tissue-specific manner. CGI

methylation in gene bodies, on the other hand, is associated with expressed genes in dividing cells (Hellman and Chess 2007; Ball *et al.* 2009) but not in nondividing or slowly dividing cells as found in the brain (Aran *et al.* 2011; Guo *et al.* 2011; Guo *et al.* 2011; Xie *et al.* 2012), and partially with tissue-specific gene expression (Rakyan *et al.* 2004; Eckhardt *et al.* 2006; Meissner *et al.* 2008; Illingworth *et al.* 2010; Maunakea *et al.* 2010). DNA methylation outside of CGIs is thought to be more dynamic and also partially involved in regulation of tissue specific expression (Jones 2012). Especially so called "shore" regions, that is regions of lower CpG density located up to 2 kb from a CGI, were found to display conserved tissue-specific methylation patterns (Irizarry *et al.* 2009). It is moreover discussed if gene body methylation could influence splicing, e.g. by allowing or inhibiting CCCTC-binding factor (zinc finger protein) (CTCF) binding, which in turn affects RNA polymerase II kinetics and the inclusion of otherwise skipped exons (Lyko *et al.* 2010; Shukla *et al.* 2011; Jones 2012).

1.3.2. Functional molecular mechanisms of DNA methylation and demethylation

In mammals, methylation of DNA is mediated by DNA methyltransferases (DNMTs) that create a covalent bond between a methyl moiety and the 5th carbon of the cytosine creating 5-mC. There are two distinct forms of DNA methylation, *de novo* DNA methylation by DNMT3A and B, and maintenance of DNA methylation patterns after cell division by DNMT1. A CpG site is a palindrome, that is, the CpG-motif repeats itself on the complementary DNA strand, and methylation occurs uniformly on both of the opposing CpG sites. This allows for the "maintenance" DNMT1 to copy DNA methylation patterns in a semi-conservative manner after cell division. Thus, DNA methylation constitutes a form of cellular memory. We speak of *de novo* DNA methylation, on the other hand, when the methyl group is added to a completely unmethylated CpG site. DNA demethylation can either occur passively, that is by lacking maintenance DNA methylation after cell division, or actively, involving enzymatic degradation of 5-mC. The degradation of 5-mC to C is not direct though, but requires several steps in which 5-mC is modified into intermediates. Those intermediates finally trigger the base excision repair pathway which replaces them by cytosine (Cortellino *et al.* 2011; He *et al.* 2011). Several demethylation mechanism have been shown to exist, one of them involving hydroxylation of the 5-mC methyl moiety by ten–eleven translocation (Tet) enzymes, thereby creating 5-hydroxymethylcytosine (5-hmC) (Tahiliani *et al.* 2009; Ito *et al.* 2010). 5-hmC levels in the adult brain range between 0.3% and 0.7% and are thus tenfold lower than the average 5-mC levels (Kriaucionis and Heintz 2009; Globisch *et al.* 2010). Whether 5-hmC has

functions besides being an intermediate metabolite in the demethylation pathway is still under debate. It is known, however, that the "readers" of 5-mC, proteins recognizing and binding to 5-mC, among them the Methyl-CpG-binding domain (MBD) proteins like methyl CpG binding protein 2 (MECP2), have a much lower affinity for 5-hmC, at least indicating that 5-hmC has not the same effect on gene expression as 5-mC (Valinluck *et al.* 2004).

DNA methylation can exert its effects on gene expression by interacting with the chromatin machinery or by inhibiting the binding of transcription factors. Both types of interaction are based on the methyl moiety first attracting or repelling DNA binding proteins that are sensitive to methylation from the major groove. For example, binding of CTCF, an insulator protein that affects DNA folding and consequently the interaction of e.g. enhancers and promoters, is sensitive to DNA methylation. This mechanism has for example been found to contribute to expression regulation at the imprinted IGF2/H19 locus. It was furthermore shown that DNA methylation can affect gene expression by preventing binding of a few transcription factors that are sensitive to the methylation status of CpG sites, e.g. MYC and OCT4.

Next to this, methylated CpGs are recognized by methyl-CpG-binding proteins and recruit repressor complexes to methylated promoter regions, which is associated with silencing of the adjacent gene's expression. Three protein families recognize and bind to methylated DNA: MBDs including MBD1-4 and methyl CpG binding protein 2 (MECP2) (Kimura and Shiota 2003; Sarraf and Stancheva 2004), ubiquitin-like, containing PHD and RING finger domain (UHRF) proteins (Hashimoto *et al.* 2008; Hashimoto *et al.* 2009) and zinc-finger proteins comprising Kaiso, ZBTB4 and ZBTB38 (Prokhortchouk *et al.* 2001; Filion *et al.* 2006). For example, MECP2 binding induces a reduction of activating acetylation marks by recruiting histone deactylases (HDACs) and promotes the repressive histone mark H3K9 by recruiting histone methyltransferases (HMTs) (Jones *et al.* 1998; Nan *et al.* 1998; Fuks *et al.* 2003). Not all classes are associated with gene silencing though, MECP2 and the UHRF proteins play a role in maintaining DNA methylation by targeting DNMT1 to hemimethylated DNA. Interestingly, MBDs have a higher expression in the brain when compared to other tissues and ZBTB4 and 38 are also highly expressed in the brain (Amir *et al.* 1999; Moore *et al.* 2013). Next to MBDs, DNMTs are also known to interact with histone modifying enzymes. Dnmt1 and Dnmt3a can bind to the HMT SUV39H1, which results in methylation on H3K9 and subsequent transcriptional repression (Fuks *et al.* 2003). Dnmt1 and Dnmt3b can induce a more condensed chromatin conformation by recruiting HDACs that remove acetyl groups from histone tails (Fuks *et al.* 2000; Geiman

et al. 2004). The interaction of epigenetic mechanisms is often bidirectional with histone modifications having the capacity to induce a certain DNA methylation state. For example, the active histone mark H3K4me3 prevents DNA methylation by impairing binding of DNMT3A, DNMT3B and their regulatory factor DNMT3L to the H3 histone tail (Ooi *et al.* 2007; Zhang *et al.* 2010). DNMT3L can only bind and recruit DNMT3A if there is a nucleosome with an unmethylated H3K4, leading to *de novo* methylation. This indicates that this kind of *de novo* methylation can only occur if a nucleosome is already present, i.e. if there is already a condensed chromatin state (Ooi *et al.* 2007; Hu *et al.* 2009). As indicated by these results, the causal relationship of DNA methylation and gene expression is not entirely clear yet. Although DNA methylation can recruit histone-modifying enzymes, it was recently suggested that DNA methylation does not *induce* but follows gene silencing, e.g. if chromatin remodeling represses transcription and DNA methylation *secures* the chromatin conformation state and thus gene silencing (the "lock" model of DNA methylation) (Jones 2012). Additional evidence for this theory comes from an early experiment showing that DNA methylation of *Hprt1* on the inactivated X chromosome follows inactivation of the chromosome (Lock *et al.* 1987).

1.3.3. DNA methylation patterns across the lifespan

DNA methylation patterns during development. DNA methylation patterns are tightly regulated during development. They mediate genomic imprinting, that is methylation in a parent-of-origin manner, silencing of the additional X chromosome in female cells (Wolf *et al.* 1984), silencing of retrotansposons, establishment and maintenance of tissue- or cell type-specific gene expression (Bruniquel and Schwartz 2003) and possibly even contribute to the maintenance of the chromosomal number (Ehrlich *et al.* 2003; Gaudet *et al.* 2003). The majority of DNA methylation is lost and created *de novo* during early embryogenesis (Mayer *et al.* 2000). This is necessary as DNA methylation is involved in the regulation of gene expression and embryonic stem cells need to express different genes than oocytes and sperm cells. The paternal DNA methylation is actively erased during the first hours after fertilization (Mayer *et al.* 2000), whereas the maternal methylome is passively lost during the first cleavage divisions due to the absence of maintenance methylation. DNA methylation patterns are established *de novo* by the DNMTs 3A and B at the stage of implantation. An exception are methylation patterns of imprinted regions, which are established during gametogenesis and are protected from reprogramming during embryogenesis. Imprinted genes are methylated and expressed in a parent-of-origin fashion, that is only one, either the maternal or paternal allele, is expressed. *IGF2* for example is expressed only from the paternal allele, whereas the adjacent *H19* is only

expressed from the maternal allele. How essential the correct establishment and maintenance of normal methylation patterns is for embryonic development, is demonstrated by the embryonic lethality of mice lacking DNMT3b or DNMT1. Although DNA methylation patterns are heritable from mother to daughter cell, there is obviously a need for plasticity during cell lineage differentiation, e.g. when multipotent neural progenitor cells (NPCs) sequentially switch to neurogenesis and then to astrogliogenesis, which seem to be excluding each other (Fan *et al.* 2005). An orchestrated change in DNA promoter methylation of the astrocyte marker glial fibrillary acidic protein (*Gfap*) has been shown to be involved in these steps of differentiation. First, the *Gfap* promoter becomes methylated at E11.5 when neurogenesis begins, possibly in order to suppress astrogliogenesis, and is then demethylated at E14.5, which coincides with astrocyte differentiation. The promoter is remethylated after birth when *Gfap* expression decreases (Teter *et al.* 1996; Fan *et al.* 2005).

DNA methylation and environmental stimuli. It is not well understood, however, how environmental factors affect DNA methylation patterns during development and in adult organism. The focus of many studies lay especially on epigenetic programming of HPA axis function, as (in-)adequate regulation of the HPA axis is associated with the extent of stress responsivity and subsequently the risk of developing a psychopathology. The Meaney group for example reported that rat pups exposed to different amounts of maternal care not only show differences in stress responsivity in adulthood but also show corresponding differences in hippocampal *GR* expression, DNA methylation levels and H3K9 acetylation levels at the *GR* promoter (Weaver *et al.* 2007). Those epigenetic changes enable binding of the transcription factor nerve growth factor 1 (*Ngf1a*), which in turn enhances *GR* expression. These changes are initiated by the different levels of tactile stimulation provided by the mother and the pathway activated by the 5-HT_7R. Deducting from these findings in rodents, McGowan and colleagues analyzed *GR* expression and promoter DNA methylation level in the hippocampus of suicide completers with a history of childhood abuse and found decreased *GR* expression and increased *GR* gene promoter methylation when compared to suicide completers without a history of childhood abuse (McGowan *et al.* 2009). In another study, male mice exposed to early PS showed increased CORT levels in response to acute stress, increased CRF levels in the amygdala, decreased GR levels in the hippocampus and corresponding changes in DNA methylation (Mueller and Bale 2008). These studies on the impact of early life stress on epigenetic programming of the HPA axis demonstrate that the early environment can leave an epigenetic mark that finally leads to long lasting changes in gene expression, HPA axis function and behavior. Recent work also

addressed the question to what extent early life traumata lead to changes in epigenetic marks and to what extent those are heritable across generations. Franklin and colleagues for example found that early life stress in the form of maternal separation combined with unpredictable maternal stress leads to differences in social recognition and depressive-like behavior in the following F1, F2 and F3 generations when compared to offspring from control groups (Franklin *et al.* 2010). F2 animals additionally showed impaired fear conditioning learning and increased social interaction after social defeat. Interestingly, they also detected small changes in *Crfr2* and *Mecp2* promoter methylation in the sperm of the F1 and the brain of the F2 generation (Franklin *et al.* 2010).

DNA methylation in the adult brain. Recent studies show furthermore that DNA methylation in the *adult* brain is more dynamic and thus plastic than previously anticipated. The adult brain comprises mostly postmitotic neurons and glia cells. Surprisingly, and in contrast to other differentiated tissues, both *Dnmt1* and *Dnmt3a* are still expressed in postmitotic neurons, indicating a special role for DNA methylation in the adult brain (Goto *et al.* 1994; Inano *et al.* 2000; Moore *et al.* 2013). Although this notion awaits a more detailed exploration, it is already known that changes in DNA methylation in the adult brain occur in response to neuronal and physical activity and contribute for example to learning and memory formation (Martinowich *et al.* 2003; Lubin *et al.* 2008; Guo *et al.* 2011). Martinowich and colleagues have shown that increased *Bdnf* expression in depolarized murine postmitotic neurons is associated *in vitro* with reduced DNA methylation in the *Bdnf* IV promoter and involves dissociation of a MECP2-HDAC-mSIN3A repressor complex from the promoter (Martinowich *et al.* 2003). Guo and colleagues moreover analyzed genome-wide DNA methylation changes in dentate granule neurons of adult mice after electroconvulsive stimulation (ECS) and found DNA methylation changes in 1.4% of the analyzed CpG sites 4h after ECS, of which some lasted for at least 24 h (Guo *et al.* 2011). Interestingly, the affected CpG sites were enriched in low-CpG density regions but not in CGIs, which fits with the notion that DNA methylation of low-CpG density regions but rarely of promoter CGIs is associated with cell differentiation and tissue-specific gene expression (Meissner *et al.* 2008). Lubin and coworkers found that contextual fear learning in rats is associated with decreased *Bdnf* DNA methylation and increased expression of several Bdnf transcripts in the hippocampus. When memory formation was however prevented by applying a NMDA receptor blocker to the rats, the changes in *Bdnf* DNA methylation and expression were also precluded (Lubin *et al.* 2008). Loss of function experiments show that in contrast to the developmental functions described above, the two DNMTs have overlapping

functions in the adult brain. Double KO, but not single KO, of *Dnmt1* and *Dnmt3a* leads to an observable phenotype including reduced DNA methylation and deficits in synaptic plasticity, learning and memory in double KO mice (Feng *et al.* 2010). Taken together, these result raises the question if the plasticity of DNA methylation patterns in adulthood can be exploited for therapy, e.g. by experience or drug intervention.

2. Project 1 – The effects of *5-Htt* genotype and PS on hippocampal gene expression and DNA methylation

2.1. Introduction

This thesis comprises work on two PS studies. The first study will be presented in chapter 2, the second study in chapter 3. In the first study, pregnant *5-Htt+/-* mice were exposed to a restraint stress paradigm combining restrain, bright light and water exposure three times a day during the last trimester (Fig. 2.1-1). The adult male and female offspring underwent behavioral testing in order to assess cognition, anxiety- and depressive-like behavior (Van den Hove and Jakob *et al.* 2011). The hippocampi of the same female offspring subsequently underwent genome-wide gene expression and promoter DNA methylation screening in order to investigate the molecular mechanisms underlying the observed behavioral phenotype (Schraut *et al.* 2014). The expression of a set of myelination-associated genes that emerged from the expression screenings was followed up using RT-qPCR. A differentially methylated region in the *Mbp* gene was fine-mapped using pyrosequencing of bisulfite-treated DNA and the methylation levels of single CpG sites were correlated with anxiety-like behavior in the EPM.

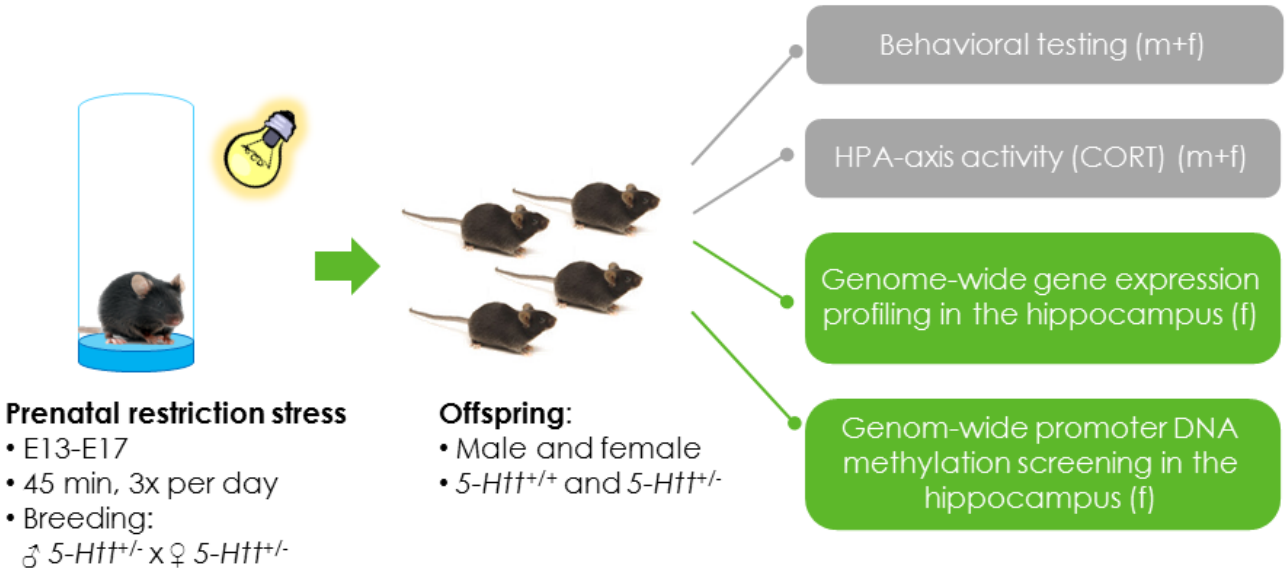

Figure 2.1-1 Experimental setup of the first PS study.

2.2. Methods and Materials

2.2.1. Animals and ethics

Breeding and behavioral studies were performed in collaboration with Daniel van den Hove and Valentina Wiescholleck from the Maastricht University. The study was approved by the Animal Ethics Board of Maastricht University, The Netherlands (Permit number: OE 2007-109), and all efforts were made to minimize suffering. Behavioral testing was described in detail by S. Jakob in her thesis (Jakob 2012) and in (Van den Hove *et al.* 2011). Mice were single housed in individually ventilated cages. Temperature was set to 21±1°C, light-dark cycle was 12h/12h with lights on from 7 am. Male and female *5-Htt+/-* mice [B6.129(Cg)-Slc6a4tm1Kpl/J] (Bengel *et al.* 1998) were used for breeding. Standard rodent chow and water were available *ad libitum*.

Prenatal restraint stress exposure

For determination of pregnancy, the vaginal-plug-method was used. Pregnant females (n=15) were stressed for 45 min each day, E13 through E17, by restraining them in a 25 cm-high glass cylinder filled up to a height of 5 mm with water (RT) whilst exposing them to bright light (adapted from Behan *et al.* 2011). PS was applied between 8 am and 10 am, 12 am and 2 pm, and 4 and 6 pm. Control females (=unstressed group, n=14) were left undisturbed in their home cages. Maternal weight was determined at E0, E12 and E17. Litters were left undisturbed from birth to P5 in order to avoid cannibalism and pup mortality was monitored from P5 onwards. Genotyping was performed using polymerase chain reaction (PCR) with DNA-fragments of 225 bp size corresponding to the *5-Htt+/+*, 272 bp size to the *5-Htt-/-* and one of each to the *5-Htt+/-* genotype. After weaning (P25), offspring were individually housed under a reversed day-night cycle (12 h light/12 h dark cycle; lights on from 19.00 h) in ventilated cages (TouchSLIMLine, Techniplast, Italy) in order to prevent the establishment of a hierarchy. Only two pups per litter/genotype/sex were used for the subsequent experiments to avoid litter effects (Chapman and Stern 1979) and litters with less than five animals were excluded.

2.2.2. Behavioral testing

Offspring were tested from the age of 2 months (P60) (n=10-14/group). First, memory abilities were assessed in the object recognition task (ORT). Next, we analyzed anxiety- and depression-like behavior using the elevated zero maze (EZM) and forced swim task

(FST), respectively. Tests were performed in the dark phase (between 9.00 and 17.00 h for the ORT and between 9.00 and 13.00 h for the other tasks). Males and females were always tested separately. One week after behavioral testing, plasma CORT secretion was examined at baseline and after acute stress. One week later, mice were sacrificed and brains removed. Additionally, the adrenals were removed and weighted. All tissue and blood samples were immediately placed on dry ice and stored at -80°C for future experiments.

Object recognition task (ORT)

Memory in the ORT was assessed as described by Sik and coworkers (Sik *et al.* 2003). Two objects were placed symmetrically 5 cm away from the wall of a circular area of 43 cm diameter (D) illuminated by approximately 20 lux. The four objects used were a) a brass cone (D 6 cm, height (h) 3.8 cm), b) a transparent glass bottle (D 2.7 cm, h 8.5 cm), c) a metal cuboid (2.5 cm × 5 cm × 7.5 cm) with two holes (D 1.5 cm), and d) a truncated pyramid made of aluminum (4.5 cm × 4.5 cm × 8.5 cm). Three copies per object were available. In the first week, animals were allowed to explore the empty arena twice a day for 5 min each time. Each testing session comprised of two trials (T1, T2) of 5 min each. During T1, the mouse was presented with two randomly employed identical objects in the arena and was then replaced in the home cage. After a set delay interval (2, 3 or 4 h) mice were presented in T2 with two different objects, a familiar one and a new one. Exploration time during the trials, which was defined as the time spent directing the nose to the object at a distance of no more than 2 cm and/or touching the object with the nose, was recorded manually on a personal computer. Objects were cleaned with 70% ethanol between trials to avoid olfactory cues. Each delay interval was tested once in each animal with a resting period of two days between the sessions. The order of testing was determined randomly. A relative discrimination index (RDI) ([time spent on new object in T2 - time spent on familiar object in T2]/total exploration time during T2) was determined for all animals.

Elevated zero maze (EZM)

Anxiety-like behavior was measured in the EZM (Shepherd *et al.* 1994). The test was conducted on a circular black plastic maze made transparent for infrared light (D 50 cm, pathway width 5 cm) placed 10 cm above floor level. The runway consisted of 2 opposite open and 2 opposite closed parts lined by 50 cm high walls. A 5 mm high rim lined the open parts to prevent mice from falling. A mouse was placed into the middle of one of the open parts, facing the outside of the maze and then explored the arena for 5

min. Distance travelled and % of time spent in the open parts of the maze was determined under low light conditions (20 lux) by use of an infrared video tracking system (Ethovision Pro, Noldus, Wageningen, The Netherlands; van Donkelaar *et al.* 2010). The maze was cleaned with 70% ethanol between trials in order to avoid the presence of olfactory cues.

Forced swim test (FST)

The FST is used to determine behavioral despair in rodents (Borsini and Meli 1988; van Donkelaar *et al.* 2010). Animals were individually placed in a transparent Perspex cylinder (40 cm tall; 19 cm in diameter; filled to a height of 15 cm with water of 31°C; (van Donkelaar *et al.* 2010)). Distance moved, an indicator of mobility of the mice, was measured during a 5 min session using a computerized video tracking system (Ethovision Pro, Noldus, The Netherlands).

CORT response to acute restraint stress

A blood sample was taken from the saphenous vein of the tested offspring at the age of 3 months (P90) in order to determine basal CORT levels. Mice were then subjected to 20 min of restraint stress (identical to the PS procedure applied to the dams) and immediately following thereafter a second blood sample was taken (stress-induced CORT level). A third blood sample was taken after a 40 min recovery period ('recovery' CORT level), which the animals spent in their home-cage. Blood collection, sample preparation and determination of plasma CORT levels were performed as previously described (Van den Hove *et al.* 2006). All blood samples were taken between 10:30 - 13:00 h.

2.2.3. Gene expression analysis

RNA extraction

RNA was extracted from hippocampus, amygdala, prefrontal cortex and striatum of female and male mice. For this, the left part of each tissue was homogenized using 500 µl PegGOLD RNAPure (Peglab, Erlangen, Germany) and metal beads for 3 min at 20 Hz in a Tissue Lyser (Qiagen, Hilden, Germany)). 100 µl chloroform was then added and samples were centrifuged for 5 min at 4° C and 12.000 x g. The water phase subsequently mixed with 250 µl ethanol. From here, the RNeasy Mini kit (Qiagen, Hilden, Germany) was

employed as instructed by the manufacturer. RNA-quality was analyzed using Experion (Bio-Rad, Munich, Germany).

Transcriptome analysis using GeneChip® Mouse Genome 430 2.0 Arrays

For transcriptome analysis using GeneChip® Mouse Genome 430 2.0 Arrays (Affymetrix, Santa Clara, CA), 2-4 hippocampus RNA samples from the female offspring were pooled based on their performance in the FST, thereby creating 3 pools per group. RNA integrity and comparability were assured prior to hybridization using the BioAnalyzer (Agilent Technologies, Palo Alto, CA). All samples yielded RNA integrity numbers (RIN) between 8.3 and 8.6, indicative of high quality RNA. cDNA synthesis for the array, library preparation and the actual microarray analysis were performed by the Interdisciplinary Centre for Clinical Research (IZKF) at the University of Wuerzburg. Generation of double-stranded cDNA, preparation and labelling of cRNA, hybridization to GeneChip® Arrays and washing were performed according to the standard Affymetrix protocol. Array were subsequently scanned using a GeneChip® Scanner 3000 (Affymetrix, Santa Clara, CA). Data analysis was performed using R and different packages from the Bioconductor project (www.bioconductor.org). Probe sets were summarized using the PLIER algorithm and the resulting signal intensities were normalized by variance stabilization normalization (VSN) (Huber et al. 2002). The signal intensity from a specific probeset is referred to as the expression of the associated gene from here onwards. Quality and comparability of all data sets were tested by density plot, RNA degradation plot and correspondence analysis. All data is MIAME compliant. The raw data has been deposited in the Gene Expression Omnibus (GEO) (accession number: GSE26025).

Gene expression analysis using RT-qPCR

Reverse transcription quantitative real-time PCR (RT-qPCR) was utilized to verify the gene expression array results and to analyze specific isoforms of genes of interest, such as *Mbp* or *Plp1*. The RT-qPCR reactions were performed in a 384-well format on the CFX384™ Real-Time PCR Detection System (Bio-Rad).

We used 500 ng RNA per sample for cDNA synthesis, which was performed using the iScript™ kit (Bio-Rad) according to the manufacturer´s instructions. We used the same RNA as for the gene expression array. cDNA was diluted 1:5 with 1xTE and stored at -20°C. We used either Metabion primers designed by ourselves using Primer 3 (Koressaar and Remm 2007; Untergasser *et al.* 2012) or QuantiTect Primer Assays (Qiagen) (see Table 2.2-1 for sequences). Primers were intron-spanning wherever possible and specificity and

product size checked on an agarose gel. All RT-qPCR reactions were performed in triplicate. No-template reverse-transcription controls were checked. A no template control as well as five interrun calibration samples were used in each run. Mean efficiencies were calculated using LinReg (Ruijter *et al.* 2009) on non-baseline corrected raw fluorescence data obtained from the cycler. Normalization, interrun calibration (where applicable) and calculation of relative expression values were performed using the qBase+ software (Biogazelle, Zwijnaarde, Belgium). For normalization *CCCTC-binding factor (Ctcf)*, *guanosine diphosphate (GDP) dissociation inhibitor 2 (Gdi2)* and *Smad nuclear interacting protein 1 (Snip1)* were used. Reference gene stability was very high (M<0.110).

Table 2.2-1. Primer sequences used in RT-qPCR.
Bp = PCR product size in bp.

Gene	RT-qPCR Primer	Sequence	bp
Mbp	RT_Mbp_F	CTCCCTGCCCCAGAAGTC	95
	RT_Mbp_R	GAGGTGGTGTTCGAGGTGTC	
Mbp	RT_Mbp_ex1/3_F	ACAGAGACACGGGCATCCT	90
	RT_Mbp_ex1/3_R	TGTGTGAGTCCTTGCCAGAG	
Mbp	RT_Mbp_ex1/2_F	ACAGAGACACGGGCATCCT	89
	RT_Mbp_ex1/2_R	CCAGGGTACCTTGCCAGAG	
Plp1	RT_Plp1_F	AGGCCAACATCAAGCTCATT	82
	RT_Plp1_R	CAAACACCAGGAGCCATACA	
Mag	RT_Mag_F	TTCTCAGGGGGAGACAACC	123
	RT_Mag_R	ACTCTCCTGGGGCTCTCAGT	
Mog	RT_Mog_F	CTGGCAGGACAGTTTCTTGA	113
	RT_Mog_R	AAAGAGGCCAATGGGAAATC	
Sox10	RT_Sox10_F	ATGTCAGATGGGAACCCAGA	88
	RT_Sox10_R	CGGACTGCAGCTCTGTCTTT	
Ctcf	RT_Ctcf_F	ACACCCATGTGAAAAATCCTG	105
	RT_Ctcf_R	CAGAGCAAAGAAAATGTTGATGAG	
Gdi2	RT_Gdi2_F	GTCAGAATTGGTTGGTTCTGTTC	126
	RT_Gdi2_R	AGCTCTTGGATCACACAATCG	
Snip1	RT_Snip1_F	CGTGGCTTCTACCAACAGG	129
	RT_Snip1_R	CAAAGCTAAAGAAAAAGACCAGATG	

2.2.4. DNA methylation analysis

DNA from the right hippocampus of the female offspring was analyzed for 5-methyl-cytosine (5-mC) and 5-hydroxymethyl-cytosine (5-hmC) using methyl-DNA immunoprecipitation (MeDIP) and pyrosequencing. Genomic DNA from the same animals (n=36 in total) as used for the gene expression array study was used here so that we could directly compare the relation of DNA methylation and expression of specific gene later on.

DNA extraction

Genomic DNA was isolated using phenol/chloroform/isoamyl alcohol extraction (house protocol developed by Gabriela Ortega). All centrifugation steps were performed at 14 000 g. The frozen tissue was homogenized with one inert stainless steel bead (Qiagen) in 300µl 0.5%-SDS extraction buffer using the TissueLyser (Qiagen)(25 Hz, 60 sec, 4°C). We then added 200 µl 0.5%-SDS extraction buffer and 50 µl 20mg/µl-proteinase K and incubated the samples at 55°C overnight. Samples were subsequently incubated for 1 h with 50 µl 10mg/µl-RNAse A at 37°C and then mixed with 700 µl of phenol/chloroform/isoamyl alcohol solution (25:24:1). Phases were separated using MaXtract high density tubes (Qiagen) by centrifuging the samples for 5 min at RT. The aqueous phase was then mixed with 700 µl phenol/isoamyl alcohol (24:1) and phases were again separated as described above. The DNA was precipitated by incubating the samples for 10 min with 50 µl sodium acetate and 1000 µl ice-cold ethanol (95-100%) at -20°C, followed by 20 min centrifugation at 4°C. In order to remove salt residues, the DNA pellet was washed with 500 µl cold 80%-ethanol using the same conditions as for the precipitation. Finally, the pellet was air-dried at RT for 5 to 30 min and resuspended in 50 µl 1xTE. DNA was stored at -80°C for further use.

Analysis of 5-mC using Methyl-DNA immunoprecipitation

Methyl-DNA immunoprecipitation (MeDIP). We used MeDIP to enrich methylated DNA from the hippocampus samples of the female offspring. MeDIP was performed using the same design as for the gene expression array, i.e. we pooled the DNAs of 2 to 4 single animals creating 3 pools per group. IP samples were worked in duplicate, untreated input controls single.

As MeDIP requires DNA fragments of 300±200 bp, DNA was first sheared using Biorupter™ UCD-200 (Diagenode, Liège, Belgium). Shearing conditions were low power, 20 KHz, 30 s ON alternated by 30 s OFF, performed three times for 5 min. Shearing was performed in

technical duplicates and efficiency was controlled on the Bioanalyzer 2100 (Agilent, Santa Clara, California, USA). MeDIP was performed using the MagMeDIP kit (Diagenode) as described in the manufacturer's instructions. In brief, DNA was precipitated using a monoclonal murine antibody against 5-methyl-cytosine and magnetic beads. We used 1000ng of sheared gDNA for each IP and 100ng for each input control. The genomic DNA was spiked with completely methylated (positive control) and completely unmethylated (negative control) DNA from *Arabidopsis thaliana*. MeDIP DNA was then purified using the IPure Kit (Diagenode), with slight modifications, according to the manual. IP duplicates were then pooled. Isolated DNA was stored at -20°C. (Note: Concentrations of the isolated MeDIP DNA could not be determined with the Nanodrop as they were too low, as expected from literature.)

MeDIP-on-chip. The GeneChip Mouse Promoter 1.0R Array (Affymetrix) used in this study is comprised of over 4.6 million 25-mer probes tiled to interrogate over 28,000 mouse promoter regions with an average resolution of 35bp. Promoter regions cover approximately 6 kb upstream through 2.5 kb downstream of the transcription start sites. DNA amplification, labeling, hybridization and the bioinformatic analysis of the tiling array were performed by Margarete Göbel and Claus-Jürgen Scholz at the Interdisciplinary Centre for Clinical Research (IZKF) (University of Wuerzburg). In brief, MeDIP DNA samples were amplified with a two-step whole genome amplification protocol using the GenomePlex Kit (Sigma, St. Louis, Missouri, USA). 7.5 µg of amplified DNA were fragmented and labeled with the GeneChip 10K Xba Assay kit (Affymetrix). Fragment size of 100±100bp was verified on the Bioanalyzer (Agilent). IP and input samples were then hybridized to separate GeneChip ® Mouse Promoter 1.0R Arrays using the GeneChip® Expression Wash, Stain and Scan Kit (Affymetrix, Santa Clara, USA) as described in the manuals. Finally, arrays were scanned with the GeneChip® Scanner 3000 (Affymetrix).

Bioinformatic analysis of the array data was performed by Claus-Jürgen Scholz. Affymetrix quality metrics and visual inspection of overall microarray signals confirmed high-quality readout from the hybridized samples. Genomic locations of the array probes were adjusted to the *Mus musculus* NCBI assembly version 37.1 (MMv37). The probe signals from corresponding MeDIP and input samples were subsequently subjected to within-sample pairwise loess normalization and calculation of MeDIP-input signal log2 ratios (SLRs). Quantile normalization was employed to ensure a common signal distribution between samples. A sliding-window approach was applied to determine SLR medians in successive genomic regions of 300 bp width in order to decrease the noise in the experiment readout. The SLRs were free from biases introduced by varying probe GC

content and particular probe sequence compositions (data not shown), thus confirming successful data normalization. A correspondence analysis was performed to detect possible outliers. The samples and/or SLRs were free from outliers. For each sample, genomic regions enriched by MeDIP were detected by the CMARRT algorithm (Kuan *et al.* 2008). In brief, CMARRT tests for increased signal content correcting for signal autocorrelation in considered genomic regions instead of applying a fixed threshold to all SLRs. This method has the advantage of a higher sensitivity and specificity of the detected enriched regions. For CMARRT modeling, a typical DNA fragment length of 300 bp was assumed (due to sonication). Moreover, enriched regions were required to cover at least five consecutive array probes and display an enrichment statistic with a false discovery rate (FDR)<0.05. Only detected regions that were consistently found within each analysis group were kept in the analysis. With the present (=1) and absent (=0) calls for MeDIP enrichment, effect directions were determined as previously described (Van den Hove and Jakob *et al.* 2011). In brief:

- Genotype (G) effect directions (d) were calculated by
  Gd = ((5-Htt+/- C + 5-Htt+/- PS) – (5-Htt+/+ C + 5-Htt+/+ PS)) * 0.5

- Environment (E) effect directions:
  Ed = ((5-Htt+/+ PS + 5-Htt+/- PS) – (5-Htt+/+ C + 5-Htt+/- C)) * 0.5

- Interaction (GxE) effect directions:
  GxEd = ((5-Htt+/- PS – 5-Htt+/- C) - (5-Htt+/+ PS – 5-Htt+/+ C)) * 0.5

Effect directions for regions with inconclusive effect size, i.e. with absolute values less than 1, were set to zero. Data from probes localized inside the regions defined by CMARRT and of all samples of the same group were summarized to determine the median SLR per region and group in order to obtain log2 fold changes (logFCs), which are quantifying the change of microarray signal for each effect described above. With these, we calculated "raw" logFCs (RlogFC) according to the aforementioned formulas. For a few regions, RlogFCs and effect (Eff) directions were not consistent, i.e. negative dEff and positive RlogFC or *vice versa*. Thus, RlogFCs were corrected according to the following formula in order to determine the logFC for each region and effect.

$$logFC_{Eff} = RlogFC_{Eff} * \begin{cases} 1, if\ d_{Eff} * RlogFC_{Eff} > 0 \\ 0, if\ d_{Eff} * RlogFC_{Eff} < 0 \end{cases}$$

Hence, whenever the direction of RlogFC and of effect are not the same, the logFC is set to zero. Consequently, regions with non-zero logFC for the G, E or GxE effect display a conclusive effect direction concordant with the observed median signal change.
Analysis of Affymetrix tiling arrays was performed with R v2.15 along with the Bioconductor package Starr (Zacher *et al.* 2010). The package ChIPpeakAnno (Zhu *et al.* 2010) was used for the annotation of enriched regions.

The overlap between differentially methylated genes and differentially expressed genes was determined using MS Access.

MeDIP-qPCR. We used the MeDIP-DNA that was applied to the promoter array for MeDIP-qPCR. MeDIP-qPCR was performed using IQ™ SYBR® Green Supermix (BioRad) on the CFX384™ Real-Time PCR Detection System (Bio-Rad). Initially, before forwarding the DNA for promoter array hybridization, we performed an initial quality control by analyzing if we would find enrichment were methylation was expected and *vice versa* using MeDIP-qPCR. We tested for enrichment of the spiked *Arabidopsis* control methylated and unmethylated DNAs as well as enrichment at loci that are known to be methylated (*Testis specific H2B, Tsh2B,* only not methylated in sperm) or unmethylated (*glyceraldehyde-3-phosphate dehydrogenase, Gapdh*). qPCR was performed as described in the Diagenode MeDIP manual. As expected, no enrichment was found for the unmethylated *Arabidopsis* DNA and for the *Gapdh* locus and positive enrichment was found for the methylated *Arabidopsis* and the *Tsh2b* locus, which was, however, lower than for the spiked control.

We also used MeDIP-qPCR in order to validate the promoter array findings for specific gene *loci*.

Table 2.2-2. Primers used for MeDIP-qPCR.
Bp = PCR product size in bp.

Primer	Sequence	bp	Genomic location
MeDIP Mbp forward	TGGCTAGTGCTTGTTCCTGA	119	chr18: 82694078-82694196
MeDIP Mbp reverse	GTGCATGTGTGAGGGTGACT		

Analysis of 5-mC and 5-hmC using Pyrosequencing

Pyrosequencing of PCR products amplified from sodium-bisulphite treated DNA was used to validate and fine-map the MeDIP promoter array results. Sodium-bisulfite treatment is

commonly used on DNA to convert the epigenetic information of DNA methylation into sequence information, which can then be easily "read", e.g. by sequencing.

Sodium-bisulfite treatment of genomic DNA and biDNA-PCR. Bisulfite conversion was performed using the EZ DNA Methylation-Gold™ Kit (Zymo Research, Irvine, California, USA) similar to the manufacturer's instructions. In brief, we converted 800 ng DNA/reaction using a regular cycler and the following cycling protocol: 10 min at 98°C and 4h at 53°C. Samples were purified using Zymo-Spin columns and eluded in 65 µl of nuclease-free water. Bisulfite DNA (biDNA) was stored at -20°C for further use. PCR amplification was performed according to our house protocol using HotStarTaq® Plus DNA polymerase (Qiagen) and 3 µl biDNA template/rct in a standard PCR-cycler (5 min 20 s at 94°C, 30 s at the primers' annealing temperature, 72°C for 4 min).

Pyrosequencing of biDNA PCR products. The amplicons of interest were amplified from biDNA using biotinylated primers designed with the PyroMark® Assay Design 2.0 software (Qiagen). 10µl of the biotinylated PCR product was then bound to Streptavidin Sepharose High Performance beads (34 µm, GE Healthcare, Freiburg, Germany) and isolated using the PyroMark® Q96 Vacuum Workstation (Qiagen) according to the manufacturer's instructions. The PCR templates were sequenced on the PyroMark® Q96 MD (Biotage, now Qiagen) using the PyroMark® Gold Q96 CDT Reagents kit (Qiagen) and sequencing primers designed with the PyroMark® Assay Design 2.0 software. Pyrosequencing results were analyzed with the PyroMark® CpG software (Qiagen). For each amplicon, an unmethylated, a 50%-methylated and an 100%-methylated control as well as a no-template control were carried along. If the methylation levels of the controls are not identified correctly, this could indicate a bias in PCR amplification of biDNA, contamination or incomplete bisulfite conversion and thus a flaw in the obtained data. To control for conversion efficiencies of unmethylated cytosines, bisulfite conversion controls were used in the sequencing assays wherever possible.

Table 2.2-3. Primer sequences used for pyrosequencing.
Mod. = modification on the primer, Bp = PCR product size in bp.

Primer	Mod.	Primer sequence	Bp	Genomic location
Pyrosequencing Bisulfite-PCR Primer				
PP-Mbp-A-F		AGTATTTAGGGTAAGGTATGGTATAGA	250	chr18: 82693519-82693769
PP-Mbp-A-Rb	Biotin	ATTCAACCTCTAACATAACAAAATATCA		
PP-Mbp-B-F		GAGGTTGAATTTAGGAGTTGAATATATG	214	chr18: 82693760-82693972
PP-Mbp-B-Rb	Biotin	AAAAAAAATACTCACAAAAACCTCTTATA		
PP-Mbp-C-F		TTTGATTGAAGGTAGAATAATGTAGAAG	193	chr18: 82694026-82694219
PP-Mbp-C-Rb	Biotin	ACTCACCAACACCAATATAAATTATACA		
Pyrosequencing Sequencing Primer				
Seq-Mbp-A-CG3		GTATTGTGTTTAGGATGG		
Seq-Mbp-A-CG4		ATATTTATATATATAGAGGAGTAT		
Seq-Mbp-A-CG5-6		GGTATTAAAGGGAAGGTATAA		
Seq-Mbp-B-CG7		ATGTTTAAGTGATTGTTTTATTAT		
Seq-Mbp-B-CG8		GAGTTGTGGTATTAGTTTTAA		
Seq-Mbp-B-CG9		GATAGTAGTTTTTGTGTAATATTG		
Seq-Mbp-C-CG10		AGGTAGAATAATGTAGAAGTT		
Seq-Mbp-C-CG11-13		TTTTTGAGGTTTGGGAT		
Seq-Mbp-C-CG14-15		GTGGTATGAAGGTATTTTAG		

2.2.5. Statistics

Statistics on behavioral, RT-qPCR, MeDIP-qPCR and pyrosequencing data were performed using IBM SPSS Statistics (IBM Deutschland GmbH, Ehningen, Germany). Data were tested for normal distribution and homogeneity of variance. 2-factorial ANOVAs or Kruskal-Wallis tests were performed to test for overall main effects (genotype effects, PS effects, GxE interaction) in more than two groups. Kruskal-Wallis tests were followed up with Mann-Whitney tests. T-tests or Mann-Whitney-U tests were performed for two groups. Correlations were either calculated with Spearman's or Pearson's correlation coefficient. P-values smaller than 0.05 were considered significant.

2.3. Results

Our group performed a prenatal restraint stress experiment on *5-Htt+/-* mice to study the effects of *5-Htt* genotype, PS and most of all, interaction effects of genotype and PS on behavior, and gene expression and DNA methylation in the hippocampus in these animals. The behavioral testing, genome-wide expression profiling of the hippocampus and the DNA methylation promoter array were performed in collaboration with Sissi Jakob and Daniel van den Hove (Van den Hove and Jakob *et al.* 2011). The work on gene expression and DNA methylation assessed by MeDIP-qPCR and pyrosequencing presented here is based on those previous findings.

Jakob and van den Hove found that *5-Htt+/-* offspring displayed adaptive capacity but were also more vulnerable to the PS exposure when compared to WT offspring. In brief, on the one hand, 5-Htt+/- animals showed enhanced memory performance and reduced anxiety as compared to WT offspring. On the other hand, *5-Htt+/-* mice exposed to PS showed increased depressive-like behavior, an effect that tended to be more pronounced in the female offspring. This encouraged us to study the molecular mechanisms underlying the observed behavioral changes in the female offspring. We analyzed genome-wide gene expression in the hippocampus of the female offspring using Affymetrix GeneChip® Mouse Genome 430 2.0 Arrays and found that *5-Htt* genotype, PS and their interaction differentially affected the expression of numerous genes and related pathways. Both the *5-Htt* genotype and PS exposure regulated the *mitogen activated protein kinase (Mapk)* and neurotrophin signaling pathways, whereas their interaction interestingly did not affect those pathways but rather modulated cytokine and Wnt signaling. The aim of the work presented here was to elucidate the details of the found gene expression patterns and analyze if differences in DNA methylation might underlie the observed gene expression changes.

2.3.1. Expression of myelin-associated genes

The gene expression array study revealed that gene expression patterns in the female offspring's hippocampus were affected by *5-Htt* genotype, PS and an interaction of both (Van den Hove and Jakob *et al.* 2011). In addition to the pathways identified using DAVID, we found that a considerable number of genes involved in myelination were affected in a GxE-interactive manner. Figure 2.3-1 shows the expression patterns of numerous genes associated with myelin and oligodendrocyte (OL) development and migration as detected using gene expression arrays. Notably, the expression of the

majority of those genes follows the same pattern: While expression was up-regulated in *5-Htt+/+* animals after PS exposure, this was not the case for *5-Htt+/-* animals. Some genes, however, diverge from this pattern (lower panel of Fig. 2.3-1). Genes showing a significant interaction effect or a trend for include the myelin proteins *Myelin basic protein* (*Mbp*, all isoforms detected), *Myelin-associated glycoprotein* (*Mag*), *Myelin oligodendrocyte glycoprotein* (*Mog*), *Myelin-associated oligodendrocytic basic protein* (*Mobp*, several isoforms detected), and *2',3'-cyclic nucleotide 3' phosphodiesterase (Cnp)* as well as the transcription factors (TFs) *Myelin regulatory factor* (*Myrf*) and *NK6 homeobox 2* (*Nkx6-2*). The closely related TF *NK2 homeobox 2 (Nkx2-2)* shows no significant effect but the expression pattern resembles the one of *Nkx6-2*. Other myelin-related genes showing differential GxE interaction affected expression or a trend for were *Lysophosphatidic acid receptor 1* (*Lpar1*, also known as *Edg2*), *Transferrin* (*Trf*), encoding a protein suggested to promote oligodendrocyte maturation, *Crystalline, alpha B* (*Cryab*), the *UDP galactosyltransferase 8A (Ugt8a)*, an enzyme involved in the key step of the biosynthesis of galactocerebrosides of the myelin membrane, *Claudin 11* (*Cldn11*, also known as *OSP*, *oligodendrocyte specific protein*) and *Gelsolin (Gsn)*. The expression changes for *Myelin and lymphocyte protein, T cell differentiation protein* (*Mal*) did not reach statistical significance but also echo the myelin proteins' expression pattern. On the other hand, expression patterns for *Proteolipid protein (myelin)1* (*Plp1*), the gene encoding the major intrinsic myelin protein, diverged from the expression patterns of the other myelin proteins. *Plp1* expression was tested with three probesets (lower panel of Fig. 2.3-1), of which 1451718_at and 1425467_a_at cover both the *Plp1* splice variant encoding the myelin major protein PLP1 and the one encoding the more in early development involved DM20 protein. The expression of the 1425468_at *Plp1* probeset that covers only the PLP1-coding transcript resembles more the myelin proteins' expression patterns and shows a trend for an interaction. *Yin Yang 1* transcription factor (*Yy1*), a TF reported to be involved in myelination, showed reduced expression only in *5-Htt+/-* animals after PS exposure when compared to C animals, but not in *5-Htt+/+* mice. An important TF for OL differentiation is *Oligodendrocyte transcription factor (Olig2)*, which was not significantly changed in our sample. The three probesets on our array testing for expression of *SRY (sex determining region Y)-box 10 (Sox10)*, a TF involved in myelination, gave ambiguous results (two probe sets shown in Fig. 2.3-1), Interestingly, the *Phosphatase and tensin homolog (Pten,* lower panel of Fig. 2.3-1), a known negative regulator of myelin formation, also shows a trend for a GxE interaction, however with an expression pattern that is exactly opposite to the myelin proteins' expression. The same pattern was observed for *Neural cell adhesion molecule 1 (Ncam1)*.

Expression of genes associated with myelin and oligodendrocytes

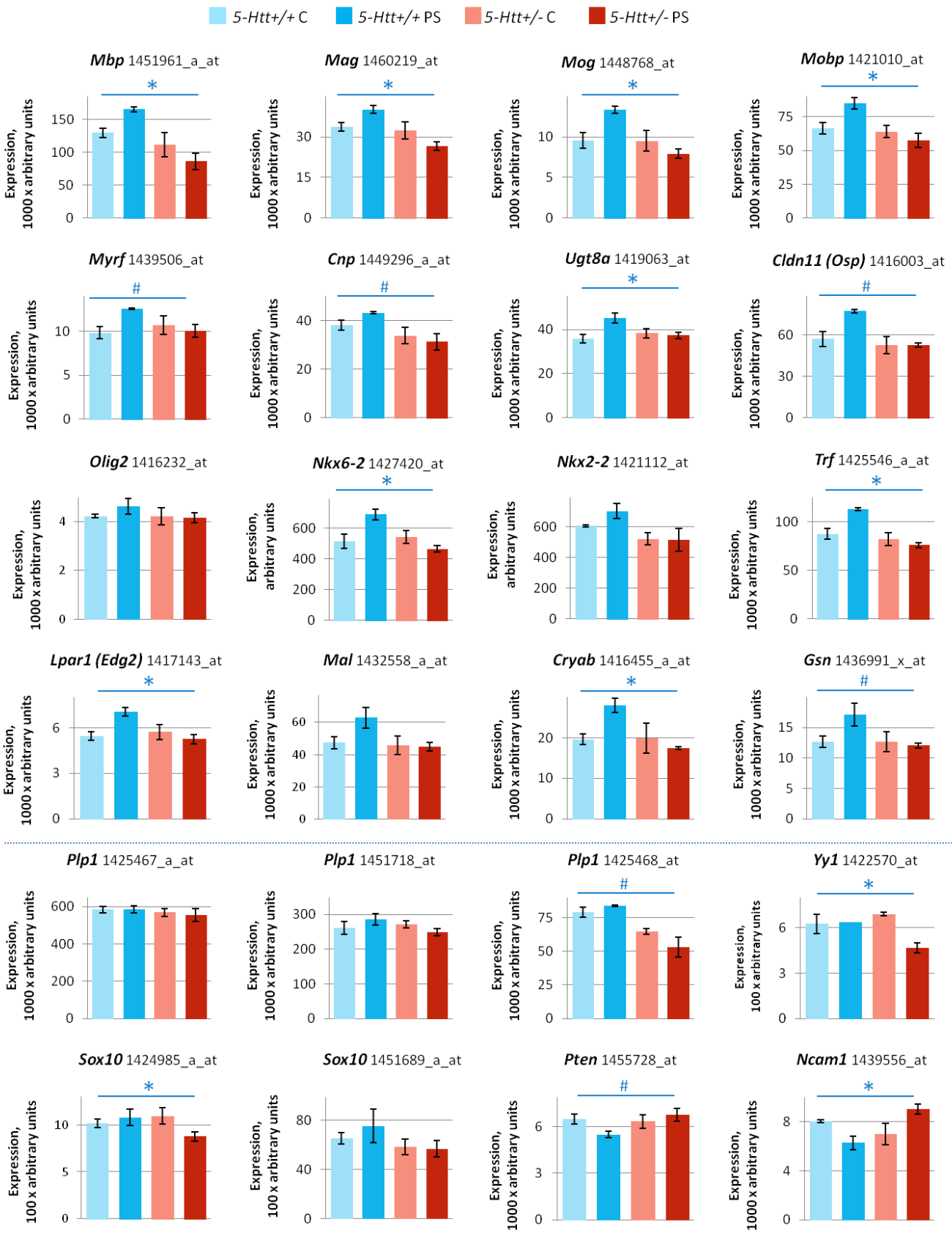

Figure 2.3-1. Expression of genes associated with myelin or oligodendrocytes in the hippocampus of female *5-Htt*+/- or *5-Htt*+/+ mice, exposed to PS or not (control). Expression measured using Affymetrix 430 2.0 GeneChip arrays (7-10 animal per group, 2-4 hippocampi pooled per array, 2-3 arrays used per group). *Mbp* = myelin basic protein, *Mag* = myelin-associated glycoprotein, *Mog* = myelin oligodendrocyte glycoprotein, *Mobp* = myelin-associated oligodendrocytic basic protein, *Myrf* = myelin regulatory factor, Cnp = 2',3'-cyclic nucleotide 3' phosphodiesterase, *Ugt8a* = UDP galactosyltransferase 8A, *Cldn11* = claudin 11, *Olig2* = oligodendrocyte transcription factor 2, *Nkx6-2* = NK6 homeobox 2, *Nkx2-2* = NK2 homeobox 2, *Trf* = transferrin, *Lpar1* = lysophosphatidic acid receptor 1, *Mal* = myelin and lymphocyte protein, T cell differentiation protein; *Cryab* = crystallin, *Gsn* = gelsolin, alpha B, *Plp1* = proteolipid protein (myelin) 1, *Yy1* = Yin Yang 1 transcription factor, *Sox10* = SRY (sex determining region Y)-box 10, *Pten* = phosphatase and tensin homolog, *Ncam1* = neural cell adhesion molecule 1. Bars represent mean values, error bars SEM. *p<0.05, #p<0.1.

A Modulated Modularity Cluster analysis (MMC) (Stone and Ayroles 2009) using a subset of the gene expression micro array data comprised of genes from myelin- and OL associated annotations identified several clusters of highly correlated genes (Fig. 2.3-2). Five clusters listing *Mbp* have been identified. The four clusters with an average correlation of r<0.05 have been listed in Table 2.3-1 (the whole clustering analysis is shown in Appendix Table 2). Module 5, the first larger cluster, comprises 15 highly correlating genes (r=0.73), among them the previously discussed *Mbp, Mobp, Mag, Tspan2, Pten, Mal, Ugt8a* and *Plp1*. Module 11, the second cluster listing *Mbp*, contains amongst others *Mal, Mobp, Myrf, Tspan2, Nkx6-2, Bcl1* and *Pten*.

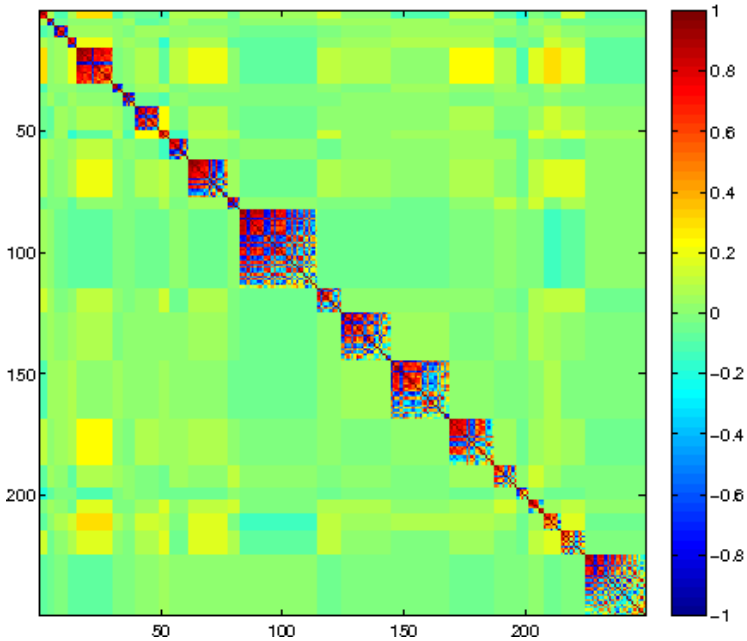

Figure 2.3-2. Modulated Modalarity Cluster (MMC) analysis of myelin-associated genes differentially expressed due to *5-Htt* x PS interaction in the hippocampus of female *5-Htt*+/+ and *5-Htt*+/- mice exposed to PS or not (controls). Gene expression data were obtained using Affymetrix 430 2.0 GeneChips. 7-10 animals per group. Hippocampus RNA from 2-4 animals was pooled per array, 2-3 arrays were analyzed per group. A total of 11 arrays was analyzed. Red and blue color indicate a high correlation and anti-correlation, respectively, between the genes' expression, whereas green indicated no correlation.

Table 2.3-1. Clusters containing *Mbp* identified by Modulated Modalarity Cluster (MMC) analysis of myelin-associated genes, differentially expressed due to *5-Htt* x PS interaction in the hippocampus of female *5-Htt*+/+ and *5-Htt*+/- mice exposed to PS or not (controls). Gene expression data were obtained using Affymetrix 430 2.0 GeneChips. Hippocampus RNA from 2-4 animals was pooled per array, 2-3 arrays were analyzed per group. A total of 11 arrays was analyzed. Av. Correl. = avarage correlation of the whole cluster, Correl. = correlation of the respective gene with the rest of the cluster, Entry Idx. = entry index. Appendix Table 2 shows all clusters identified by MMC anylsis.

Module	Affy ID	Entry Idx.	Av. Correl.	Correl.	Gene symb.
5	1451961_a_at	212	0.727	0.835	Mbp
	1426960_a_at	94	0.727	0.822	Fa2h
	1450088_a_at	195	0.727	0.813	Mobp
	1460219_at	246	0.727	0.765	Mag
	1421010_at	36	0.727	0.753	Mobp
	1424567_at	67	0.727	0.753	Tspan2
	1454722_at	224	0.727	0.745	Pten
	1432558_a_at	126	0.727	0.725	Mal
	1419064_a_at	25	0.727	0.724	Ugt8a
	1425467_a_at	80	0.727	0.709	Plp1
	1454078_a_at	220	0.727	0.691	Gal3st1
	1417551_at	13	0.727	0.687	Cln3
	1435166_at	139	0.727	0.662	Cntn2
	1422833_at	55	0.727	0.641	Foxa2
	1422068_at	46	0.727	0.584	Pou3f1
11	1435165_at	138	0.620	0.765	Cntn2
	1417275_at	9	0.620	0.745	Mal
	1419646_a_at	31	0.620	0.722	Mbp
	1433785_at	129	0.620	0.721	Mobp
	1439506_at	159	0.620	0.686	Myrf
	1424568_at	68	0.620	0.671	Tspan2
	1427420_at	99	0.620	0.671	Nkx6-2
	1417133_at	8	0.620	0.633	Pmp22
	1418663_at	19	0.620	0.620	Mpdz
	1416999_at	6	0.620	0.616	Smpd2
	1440770_at	163	0.620	0.614	Bcl2
	1422686_s_at	50	0.620	0.593	Exoc4
	1450655_at	201	0.620	0.536	Pten
	1444418_at	176	0.620	0.451	Itpr2
	1459020_at	241	0.620	0.449	Amigo1
	1416635_at	4	0.620	0.426	Smpdl3a
16	1422779_at	53	0.503	0.665	Smpd3
	1421841_at	43	0.503	0.625	Fgfr3
	1456010_x_at	231	0.503	0.612	Hes5

	1425264_s_at	77	0.503	0.611	Mbp
	1429735_at	113	0.503	0.598	Qk
	1427682_a_at	101	0.503	0.591	Egr2
	1455252_at	227	0.503	0.579	Tsc1
	1417839_at	16	0.503	0.577	Cldn5
	1449278_at	191	0.503	0.553	Eif2ak3
	1449024_a_at	189	0.503	0.552	Hexa
	1427683_at	102	0.503	0.545	Egr2
	1423146_at	60	0.503	0.497	Hes5
	1451888_a_at	211	0.503	0.496	Tenm4
	1429318_a_at	108	0.503	0.494	Qk
	1438699_at	157	0.503	0.478	Srd5a1
	1437122_at	151	0.503	0.478	Bcl2
	1446974_at	180	0.503	0.467	Pikfyve
	1429736_at	114	0.503	0.442	Qk
	1448781_at	186	0.503	0.417	Nab1
	1442256_at	170	0.503	0.416	Prkcd
	1441361_at	166	0.503	0.379	Mpdz
	1457687_at	238	0.503	0.348	Bcl2
	1423504_at	66	0.503	0.338	Jam3
	1418782_at	21	0.503	0.313	Rxrg
17	1423102_a_at	59	0.502	0.658	Rnf10
	1423221_at	61	0.502	0.630	Tubb4a
	1449942_a_at	193	0.502	0.624	Ilk
	1427481_a_at	100	0.502	0.624	Atp1a3
	1417930_at	17	0.502	0.592	Nab2
	1417456_at	12	0.502	0.580	Gnpat
	1448807_at	187	0.502	0.572	Hrh3
	1422553_at	47	0.502	0.556	Pten
	1417558_at	14	0.502	0.544	Fyn
	1430651_s_at	119	0.502	0.519	Zfp191
	1429531_at	112	0.502	0.505	Smpd4
	1447811_s_at	181	0.502	0.499	Amigo1
	1454649_at	222	0.502	0.489	Srd5a1
	1448945_at	188	0.502	0.467	Pllp
	1423292_a_at	64	0.502	0.391	Prx
	1453730_at	217	0.502	0.386	Samd8
	1434402_at	133	0.502	0.361	Samd8
	1425263_a_at	76	0.502	0.334	Mbp
	1424833_at	69	0.502	0.198	Itpr2

2.3.2. Gene expression of major myelin proteins and transcription factors in hippocampus and amygdala assessed by RT-qPCR

The intriguing changes in expression of myelin-associated genes revealed by the GeneChip array prompted us to look more closely at several genes of which the probesets on the expression array either recognized different splice variants or gave ambiguous/contradictory results. Thus, we analyzed the expression of several of the above presented genes in the hippocampus of the female offspring using RT-qPCR in order to pin the effects observed in the array on specific isoforms (*Mbp*, *Plp1*), to gain a clearer picture of the expression pattern (*Plp 1*, *Olig2*, *Sox10*) and to simply validate the array results (*Mbp*, *Mag*, *Mog*, *Mobp*). We furthermore analyzed those genes with RT-qPCR in the amygdala, a brain region involved in anxiety and emotion regulation.

Figure 2.3-3 depicts a scheme of the *Golli-Mbp* locus and its various transcripts. There are three kind of transcripts transcribed from this locus: The *Golli-Mbp* transcripts (green), that include three additional 5' exons compared to "classic" *Mbp* transcripts, the *Mbp* splice variants lacking exonII (exII) (orange)and the *Mbp* transcripts containing exII (violet). The probeset 1451961_a_at recognizes a multitude of transcripts derived from the *Golli-Mbp* locus including a long *Golli* transcript as well as all *Mbp* variants, as indicated with an arrow in Fig. 2.3-3. We thus determined the expression levels of the *Golli* transcripts (Fig. 2.3-3, "*Golli-Mbp*"), the *Mbp* variants containing exII (Fig. 2.3-3 "*Mbp* w *ExII*") and *Mbp* variants lacking exII (Fig. 2.3-3 "*Mbp* w/o ExII") with RT-qPCR. The discrimination of *Mbp* splice variants with and without exII is of importance as exII encodes a nuclear translocation signal. Subsequently, MBP proteins with this translocation signal have a different cellular localization and have been suspected to play a different role from MBPs lacking this signal, which are basic myelin proteins (Harauz and Boggs 2013). The expression data presented in Fig. 2.3-3 depict a complex regulation of expression. We first validated the signal of *Mbp* probeset 1451961_a_at (Fig. 2.3-3 "*Mbp* all", middle part) in the hippocampus and found a GxE interaction (two-way ANOVA p=0.034). When looking at the splice variants with and without exII, they show the same pattern as *Mbp all,* with an increase in expression in *5-Htt*+/+ mice after PS exposure but not in *5-Htt*+/- mice. More precisely, we found an effect of GxE interaction and of PS exposure for *Mbp* lacking exII (2-way-ANOVA p=0.017 and p=0.021). We furthermore found an increase in expression of *Mbp* transcripts containing exon II in PS mice when compared to C mice (Mann–Whitney U P = 0.009). Moreover, *Golli* expression was also affected by a GxE interaction (two-way ANOVA p=0.017). In contrast to the *Mbp* mRNAs, its expression was

increased in *5-Htt+/-* animals after PS exposure (t-test p=0.02) but not in *5-Htt+/+* (p=0.630).

When looking at the amygdala (Fig. 2.3-3, lower part), we found again a GxE interaction for all *Mbp* transcripts (*Mbp* all and *Mbp* w ExII: 2-way-ANOVA, p=0.002, *Mbp* w/o ExII: KW p=0.010). The expression pattern, however, was the inverted picture of the on in the hippocampus. All *Mbp* transcripts were increased in *5-Htt+/-* mice after PS exposure but not in *5-Htt+/+* mice (Mbp *all* and Mbp w ExII: p<0.001 for *5-Htt+/-* C vs. PS and p>0.9 *5-Htt+/+* C vs. PS, respectively, Mbp w/o ExII MWU: p=0.002 and p=0.606, respectively). *Golli* was not differentially expressed in the amygdala.

We next analyzed the expression of three other major myelin proteins, *Plp1*, *Mog* and *Mag*, and two transcription factors expressed in OLs, *Sox10* and *Olig2*, using RT-qPCR in hippocampus and amygdala (Fig. 2.3-4). In both tissues, the expression of *Plp1*, *Mog* and *Mag* mimicked the GxE-affected expression pattern found for *Mbp*, whereas Sox10 and Olig2 showed a somewhat deviating pattern. In detail, we found in the hippocampus an effect of GxE interaction for *Mog* and a trend for *Mag* (Fig. 2.3-4, A, 2-way ANOVA p=0.035 and p=0.064), which was due to an up-regulation of expression in *5-Htt+/+* animals after PS that was not detected in *5-Htt+/-* animals. Moreover, we found an effect of genotype for *Mog* and *Mag* (2-way ANOVA p=0.049 and p=0.021) and a trend for a PS effect for *Mog* (p=0.072). We furthermore found a PS effect for *Sox10* (2-way ANOVA p=0.011), i.e. an increase in PS animals compared to controls. Although *Plp1* expression shows the same pattern as *Mbp*, *Mog* and *Mag*, the differences in expression did not reach statistical significance. In the amygdala (Fig. 2.3-4, B), the expression of *Plp1*, *Mog* and *Mag* was affected in a GxE interactive manner (2-way-ANOVA, p=0.004, p=0.009, p=0.020), i.e. increased expression of those genes after PS exposure in *5-Htt+/-*, but not in *5-Htt+/+* animals. Moreover, we found a PS effect on *Plp1* and *Mog* expression (2-way-ANOVA, p=0.022 and p=0.034) as well as a genotype effect on *Olig2* expression (2-way-ANOVA, p=0.033).

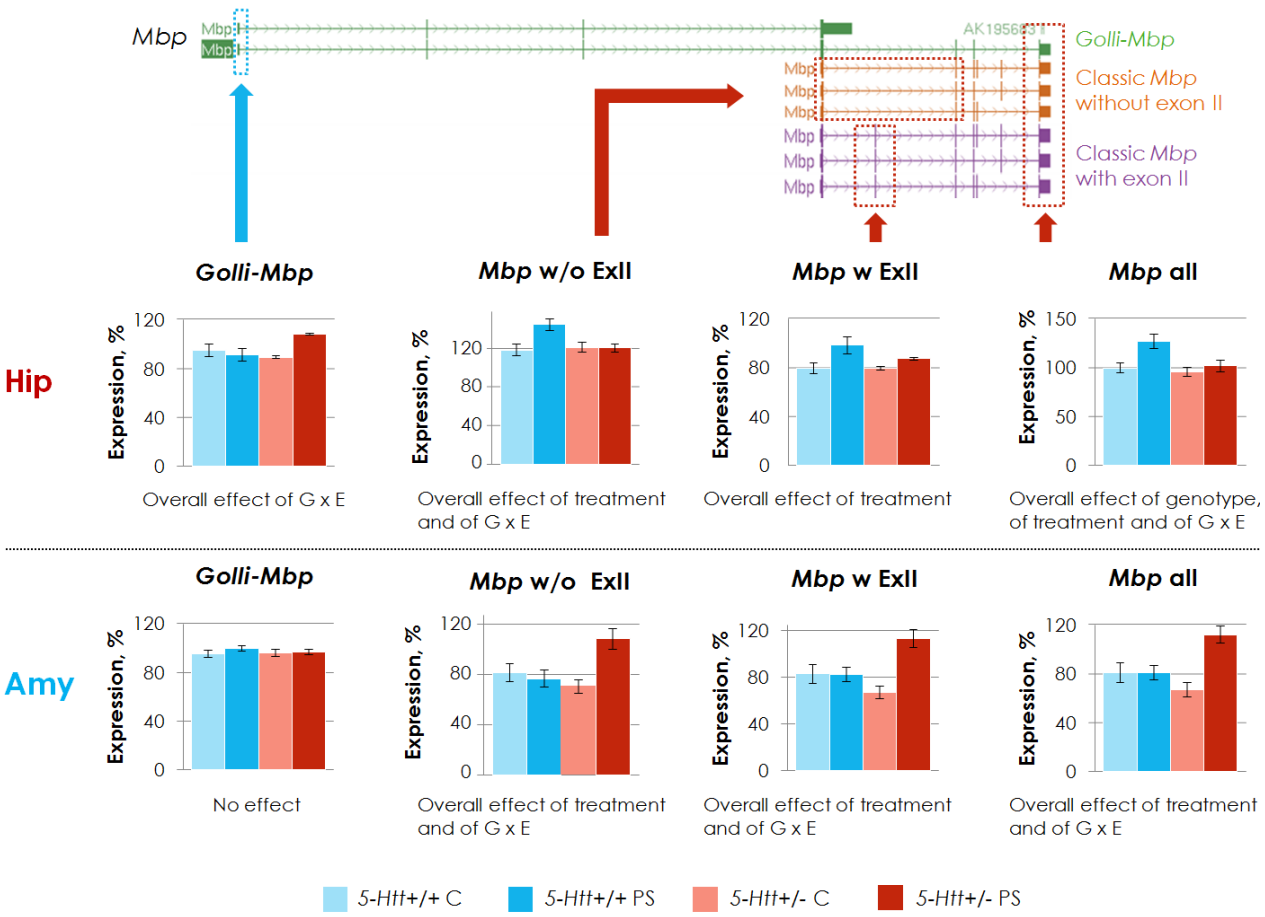

Figure 2.3-3. Expression of the different *Golli-Mbp* splice variants in the hippocampus and amygdala of female *5-Htt+/-* or *5-Htt+/+* mice, exposed to PS or not (control). Expression measured by RT-qPCR (n=7-10 per group). *Golli* = Gene of oligodendrocyte lineage, *Mbp* = *myelin basic protein*, w = with, w/o = without, Ex = exon. Bars represent mean values, error bars SEM. 2-way-ANOVA for overall effects.

As Figure 2.3-5 shows, the expression of *Mbp w/o exII, Mag, Mog* and *Sox10* was highly correlated with each other within the hippocampus (Spearman correlation, 0.673<r<0.952, p<0.0001, Bonferroni-corrected). We found a comparably high correlation between *Mbp w/o exII, Mag, Mog, Plp1* and *Sox10* expression in the amygdala (Figure 2.3-5, 0.641<r<0.976, p<0.0012, Bonferroni-corrected). Notably, *Mbp w/o exII, Mag,* and *Mog* expression reached almost a correlation of 1.0 in the hippocampus, whereas *Plp1* expression did not correlate that well with those genes, while in the amygdala, *Mbp w/o exII, Mag, Mog* and *Plp1* show the same extremely high degree of correlation. Interestingly, *Olig2* expression shows the highest correlation with *Sox10* expression in the hippocampus, whereas this was not found for the amygdala.

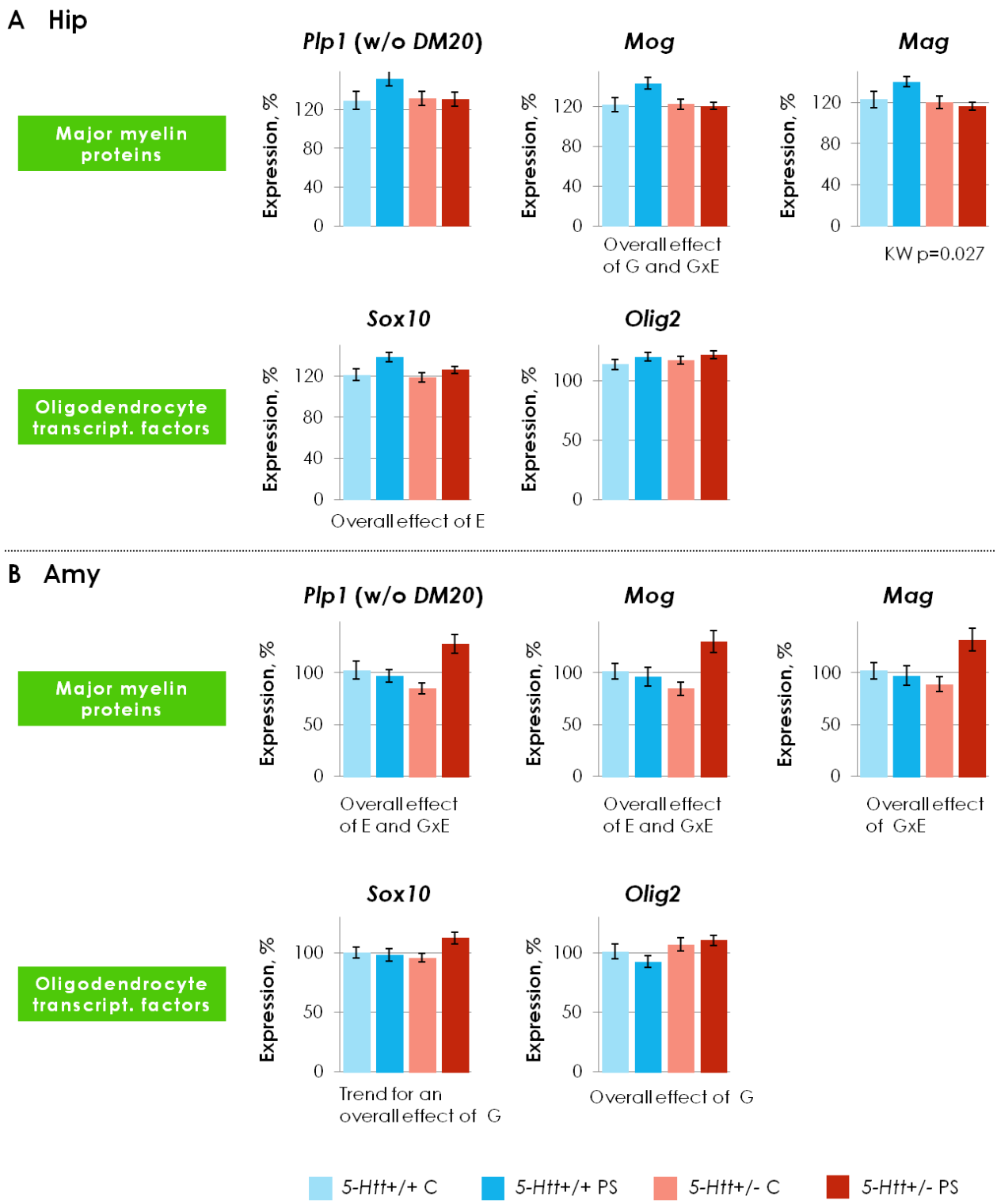

Figure 2.3-4. Expression of genes encoding major myelin proteins and transcription factors expressed in oligodendrocytes in the hippocampus and amygdala of female *5-Htt+/-* or *5-Htt+/+* mice, exposed to PS or not (control). Expression measured by RT-qPCR (n=7-10 per group). *Plp1* = proteolipid protein (myelin) 1, *Mog* = myelin oligodendrocyte glycoprotein, *Mag* = myelin-associated glycoprotein, *Sox10* = SRY (sex determining region Y)-box 10, *Olig2* = oligodendrocyte transcription factor 2, w/o = without. Bars represent mean values, error bars SEM. 2-way-ANOVA or Kruskal-Wallis test (KW) for overall effects.

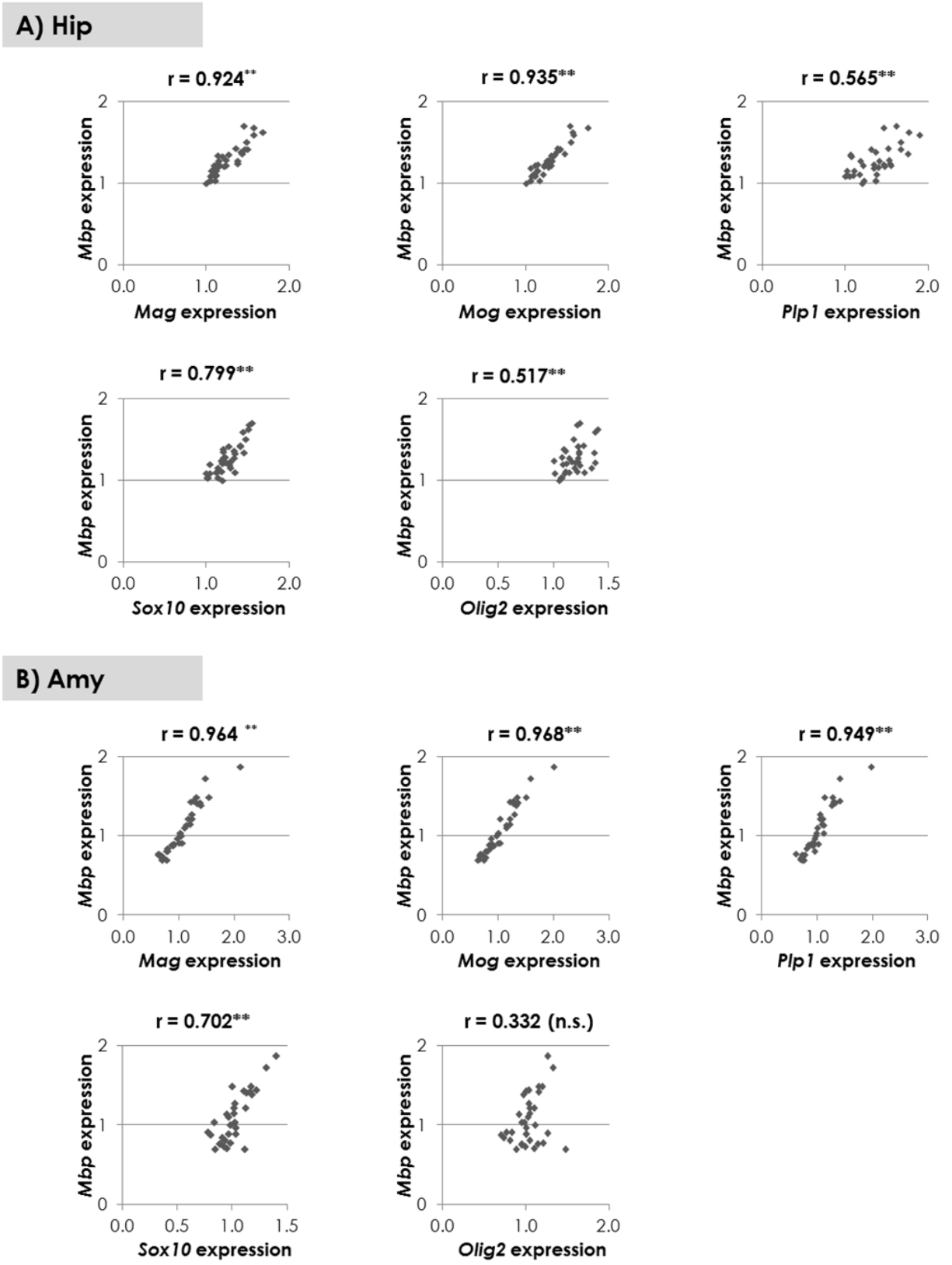

Figure 2.3-5 Correlation of expression of genes encoding major myelin proteins and oligodendrocyte-transcription factors in the hippocampus and amygdala of female *5-Htt*+/- or *5-Htt*+/+ mice, exposed to PS or not (control). Expression assessed by RT-qPCR (n=7-10 per group). *Mbp* = myelin basic protein transcript lacking exII, *Plp1* = proteolipid protein (myelin) 1, *Mog* = myelin oligodendrocyte glycoprotein, *Mag* = myelin-associated glycoprotein, *Sox10* = SRY (sex determining region Y)-box 10, *Olig2* = oligodendrocyte transcription factor 2. r = Spearman correlation coefficient. **p<0.01, n.s. = not significant.

2.3.3. DNA methylation

We next engaged in clarifying the role of DNA methylation as a possible mediator for the above described effects of *5-Htt* genotype, PS and their interaction on gene expression. We raised the following questions: Does 5-Htt genotype, PS or their interaction have an effect on DNA methylation in the adult hippocampus? And if yes, are those changes in DNA methylation associated with the observed changes in gene expression? To tackle these questions, we assessed genome-wide DNA methylation in promoter regions in the hippocampus of the female offspring by applying DNA enriched for 5-mC to a tiling array and determined differentially methylated regions (DMRs) (Schraut *et al*. 2014). We then investigated to which extent the genes harboring a DMR also displayed changes in their expression. A DMR in the *Mbp* gene was furthermore fine-mapped using pyrosequencing.

Genome-wide promoter DNA methylation

We analyzed genome-wide promoter DNA methylation by first enriching 5-mC using methyl-DNA immunoprecipitation (MeDIP) and then applying the enriched MeDIP-DNA to an Affymetrix GeneChip Mouse Promoter 1.0R tiling array. The calculation of effects was based on the same comparisons as for the gene expression array data (G-, E- and GxE-effects). The subsequent identification of DMRs revealed that the methylation status of two to four hundred genomic regions was significantly modified by either the *5-Htt*+/- genotype, PS exposure or their interaction (Fig. 2.3-6; see Appendix Table 1 for an overview of all genes significantly affected by G, E and GxE, respectively). More specifically, 235 DMRs, which correspond to 254 genes, were differentially methylated in *5-Htt*+/- when compared to WT mice, with 40.9% of the DMRs showing a decreased and 59.1% displaying an increased degree of methylation in *5-Htt*+/- mice (Fig. 2.3-6, A). PS exposure affected 323 DMRs, involving 347 genes. Methylation was increased in the majority, 81.7%, of the DMRs PS mice compared to controls whereas merely 18.3% of the DMRs showed a decrease in methylation (Fig. 2.3-6, B). Finally, a *5-Htt* x PS interaction affected the DNA methylation status of 218 genomic regions involving 245 genes.

Functional Annotation Clustering

A Functional Annotation Clustering was performed using DAVID (Huang *et al.* 2007) to determine which groups of functionally similar annotation terms were found to be enriched in our DMR lists. An enrichment score of 1.3 or higher is considered enriched. As shown in Table 2.3-2 A), only two clusters have been found to be enriched for the DMRs

associated with genotype effects, i.e. one with annotations associated with ribosomal proteins and one cluster containing ion/cation binding annotation terms. Five annotation clusters were identified to be enriched due to PS exposure (Table 2.3-2, B), the most enriched among them was the WD repeat terms cluster containing *PAK1 interacting protein 1 (Pak1ip1)* and *striatin, calmodulin binding protein 3 (Strn3,* also known as *Sg2na)*. Another five clusters were found to be enriched in the DMR list associated with 5-Htt x PS interaction (Table 2.3-2, C). Interestingly, two clusters harbored cytoskeleton annotation terms. The largest cluster contained EGF-associated terms. Of note, less clusters and lower enrichment scores were detected for the DMRs affected by genotype than for clusters identified for the PS and GxE DMR lists.

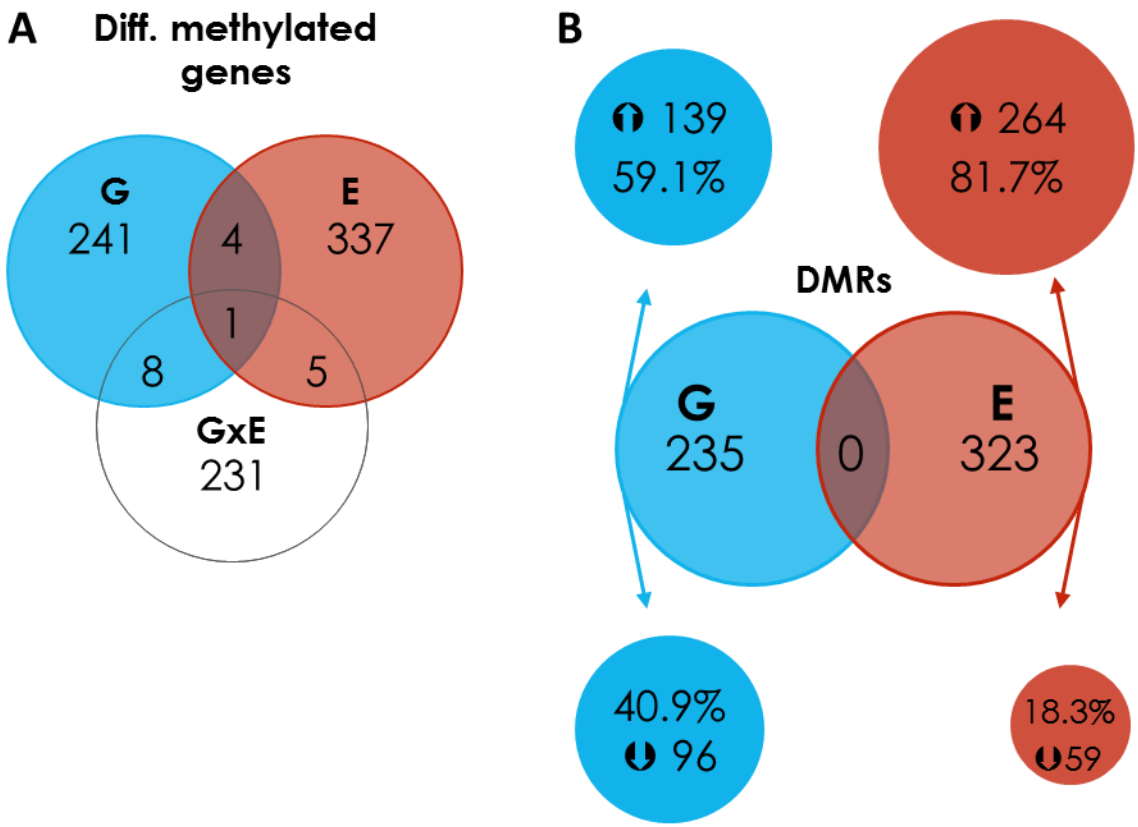

Figure 2.3-6 Number of differentially methylated genes. Number of genes with DNA methylation status levels significantly altered by genotype (G; i.e. *5-Htt+/-* vs *5-Htt+/+*), the environment (E; i.e. prenatal stressed versus control mice) or an interaction of both (GxE) in the hippocampus of female mice. DNA methylation analysis was performed by enriching methylated DNA from the hippocampus using methyl-DNA immunoprecipitation (MeDIP) and applying MeDIP DNA to Affymetrix Mouse Promoter 1.0R arrays. 6-10 animals per group, 2-4 hippocampi were pooled per array, 2-3 pools per group were analyzed.

a

Table 2.3-2 Functional annotation clustering of differentially methylated genes. Functional annotation clustering of differentially methylated genes affected by genotype (G; i.e. *5-Htt+/-* vs *5-Htt+/+*), the environment (E; i.e. prenatal stressed versus control mice) or by an interaction of both (GxE) in the hippocampus of female mice. DNA methylation analysis was performed by enriching methylated DNA from the hippocampus using methyl-DNA immunoprecipitation (MeDIP) and applying MeDIP DNA to Affymetrix Mouse Promoter 1.0R arrays. 6-10 animals per group, 2-4 hippocampi were pooled per array, 2-3 pools per group were analyzed.

Cluster	Score	Category	Enrichment Term	# of Genes	% of Genes	p	FE
A) G-effects: *5-Htt+/+* vs. *5-Htt+/-*							
1	1,37	SP_PIR_KEYWORDS	ribosomal protein	8	2,87	0,01	3,67
		GOTERM_CC_FAT	GO:0005840~ribosome	8	2,87	0,01	3,52
		GOTERM_MF_FAT	GO:0003735~structural constituent of ribosome	7	2,51	0,01	3,83
		GOTERM_CC_FAT	GO:0030529~ribonucleoprotein complex	11	3,94	0,05	2,01
		GOTERM_BP_FAT	GO:0006412~translation	8	2,87	0,09	2,10
		GOTERM_MF_FAT	GO:0005198~structural molecule activity	10	3,58	0,09	1,83
		SP_PIR_KEYWORDS	ribonucleoprotein	6	2,15	0,23	1,83
		KEGG_PATHWAY	mmu03010:Ribosome	3	1,08	0,30	2,72
2	1,34	GOTERM_MF_FAT	GO:0043167~ion binding	61	21,86	0,02	1,28
		GOTERM_MF_FAT	GO:0043169~cation binding	60	21,51	0,02	1,27
		GOTERM_MF_FAT	GO:0046872~metal ion binding	59	21,15	0,03	1,26
		SP_PIR_KEYWORDS	zinc-finger	23	8,24	0,04	1,55
		GOTERM_MF_FAT	GO:0008270~zinc ion binding	34	12,19	0,06	1,33
		SP_PIR_KEYWORDS	metal-binding	42	15,05	0,08	1,27
		GOTERM_MF_FAT	GO:0046914~transition metal ion binding	40	14,34	0,08	1,27
		SP_PIR_KEYWORDS	zinc	30	10,75	0,12	1,29
B) E-effects: Controls vs. Prenatal stress							
1	2,06	INTERPRO	IPR019775:WD40 repeat, conserved site	13	3,24	0,00	2,94
		SP_PIR_KEYWORDS	wd repeat	13	3,24	0,00	2,84

		UP_SEQ_FEATURE	repeat:WD 3	12	2,99	0,00	2,87
		UP_SEQ_FEATURE	repeat:WD 1	12	2,99	0,00	2,82
		UP_SEQ_FEATURE	repeat:WD 2	12	2,99	0,00	2,82
		INTERPRO	IPR017986:WD40 repeat, region	11	2,74	0,01	2,82
		UP_SEQ_FEATURE	repeat:WD 4	11	2,74	0,01	2,79
		UP_SEQ_FEATURE	repeat:WD 6	9	2,24	0,01	3,09
		UP_SEQ_FEATURE	repeat:WD 5	10	2,49	0,01	2,73
		INTERPRO	IPR019782:WD40 repeat 2	10	2,49	0,01	2,73
		INTERPRO	IPR001680:WD40 repeat	11	2,74	0,01	2,48
		INTERPRO	IPR019781:WD40 repeat, subgroup	10	2,49	0,02	2,49
		UP_SEQ_FEATURE	repeat:WD 7	7	1,75	0,02	3,12
		SMART	SM00320:WD40	11	2,74	0,04	2,07
		INTERPRO	IPR015943:WD40/YVTN repeat-like	10	2,49	0,08	1,92
2	1,77	SP_PIR_KEYWORDS	sh3 domain	10	2,49	0,01	2,81
		INTERPRO	IPR001452:Src homology-3 domain	10	2,49	0,01	2,77
		SMART	SM00326:SH3	10	2,49	0,03	2,31
		UP_SEQ_FEATURE	domain:SH3	8	2,00	0,03	2,71
3	1,72	GOTERM_CC_FAT	GO:0030017~sarcomere	6	1,50	0,01	4,38
		GOTERM_CC_FAT	GO:0031674~I band	5	1,25	0,01	5,51
		GOTERM_CC_FAT	GO:0044449~contractile fiber part	6	1,50	0,02	4,08
		GOTERM_CC_FAT	GO:0030016~myofibril	6	1,50	0,02	3,85
		GOTERM_CC_FAT	GO:0043292~contractile fiber	6	1,50	0,02	3,69
		GOTERM_CC_FAT	GO:0030018~Z disc	4	1,00	0,04	5,08
4	1,47	SP_PIR_KEYWORDS	tpr repeat	9	2,24	0,00	3,66
		INTERPRO	IPR011990:Tetratricopeptide-like helical	9	2,24	0,00	3,51
		UP_SEQ_FEATURE	repeat:TPR 3	8	2,00	0,01	3,75
		UP_SEQ_FEATURE	repeat:TPR 1	8	2,00	0,01	3,40
		UP_SEQ_FEATURE	repeat:TPR 2	8	2,00	0,01	3,40

		INTERPRO	IPR013026:Tetratricopeptide region	7	1,75	0,01	3,59
		UP_SEQ_FEATURE	repeat:TPR 5	5	1,25	0,02	4,53
		UP_SEQ_FEATURE	repeat:TPR 10	3	0,75	0,03	11,05
		UP_SEQ_FEATURE	repeat:TPR 9	3	0,75	0,06	7,53
		UP_SEQ_FEATURE	repeat:TPR 4	5	1,25	0,06	3,37
		UP_SEQ_FEATURE	repeat:TPR 6	4	1,00	0,08	4,02
		INTERPRO	IPR019734:Tetratricopeptide repeat	5	1,25	0,12	2,61
		UP_SEQ_FEATURE	repeat:TPR 8	3	0,75	0,15	4,36
		SMART	SM00028:TPR	5	1,25	0,19	2,18
		INTERPRO	IPR001440:Tetratricopeptide TPR-1	4	1,00	0,22	2,46
		UP_SEQ_FEATURE	repeat:TPR 7	3	0,75	0,22	3,38
5	1,31	INTERPRO	IPR001849:Pleckstrin homology	11	2,74	0,01	2,46
		SMART	SM00233:PH	11	2,74	0,04	2,06
		INTERPRO	IPR011993:Pleckstrin homology-type	10	2,49	0,06	2,02
		UP_SEQ_FEATURE	domain:PH	7	1,75	0,16	1,91
C) GxE-effects: *5-Htt* x PS interaction							
1	2,14	GOTERM_CC_FAT	GO:0043232~intracellular non-membrane-bounded organelle	38	13,43	0,00	1,63
		GOTERM_CC_FAT	GO:0043228~non-membrane-bounded organelle	38	13,43	0,00	1,63
		GOTERM_CC_FAT	GO:0005856~cytoskeleton	25	8,83	0,00	1,83
		GOTERM_CC_FAT	GO:0044430~cytoskeletal part	18	6,36	0,01	1,91
		GOTERM_CC_FAT	GO:0015630~microtubule cytoskeleton	10	3,53	0,09	1,83
2	1,74	SP_PIR_KEYWORDS	hydroxylation	6	2,12	0,00	7,79
		INTERPRO	IPR008160:Collagen triple helix repeat	4	1,41	0,08	4,06
		SP_PIR_KEYWORDS	collagen	4	1,41	0,08	3,95
3	1,72	GOTERM_MF_FAT	GO:0030246~carbohydrate binding	11	3,89	0,01	2,81
		GOTERM_MF_FAT	GO:0005529~sugar binding	8	2,83	0,01	3,58
		SP_PIR_KEYWORDS	Lectin	7	2,47	0,02	3,48

		UP_SEQ_FEATURE	domain:Ricin B-type lectin	3	1,06	0,03	10,71
		INTERPRO	IPR000772:Ricin B lectin	3	1,06	0,04	8,81
		SMART	SM00458:RICIN	3	1,06	0,05	8,15
4	1,71	GOTERM_BP_FAT	GO:0030029~actin filament-based process	8	2,83	0,01	3,57
		GOTERM_BP_FAT	GO:0030036~actin cytoskeleton organization	7	2,47	0,02	3,33
		GOTERM_BP_FAT	GO:0007010~cytoskeleton organization	9	3,18	0,06	2,17
5	1,69	INTERPRO	IPR006209:EGF	8	2,83	0,00	5,14
		INTERPRO	IPR000152:EGF-type aspartate/asparagine hydroxylation	6	2,12	0,01	5,25
		INTERPRO	IPR000742:EGF-like, type 3	8	2,83	0,01	3,31
		INTERPRO	IPR006210:EGF-like	8	2,83	0,01	3,24
		SMART	SM00181:EGF	8	2,83	0,02	3,00
		SP_PIR_KEYWORDS	egf-like domain	8	2,83	0,02	2,99
		INTERPRO	IPR001881:EGF-like calcium-binding	5	1,77	0,02	4,52
		INTERPRO	IPR018097:EGF-like calcium-binding, conserved site	5	1,77	0,03	4,37
		SMART	SM00179:EGF_CA	5	1,77	0,03	4,18
		INTERPRO	IPR013032:EGF-like region, conserved site	9	3,18	0,04	2,39
		INTERPRO	IPR013091:EGF calcium-binding	4	1,41	0,05	4,77
		UP_SEQ_FEATURE	domain:EGF-like 2	4	1,41	0,08	3,98
		UP_SEQ_FEATURE	domain:EGF-like 1	4	1,41	0,15	2,96

Differential DNA methylation associated with changes in gene expression

In the next step, we examined to which extent the changes that we previously found in gene expression in the hippocampus of the same animals (Van den Hove and Jakob *et al.* 2011) were associated with the DMRs. For this, we compared the DMR data with the hippocampal gene expression profiles and found a modest overlap between DMRs and gene expression changes (Fig. 2.3-7). 25 genes were both differentially methylated and expressed ($p<0.05$) in *5-Htt+/-* compared to WT offspring (Table 2.3-3, A). These 25 genes corresponded to 26 DMRs, half of which showed up-regulation and half down-regulation of methylation. *E2F transcription factor 3 (E2f3)*, *kinesin family member 13A (Kif13a)*, *low density lipoprotein receptor class A domain containing 3 (Ldlrad3)*, *Fibroblast growth factor receptor 4 (Fgfr4)* and *bone morphogenic protein receptor 1b (Bmpr1b)* were among the differentially methylated/expressed genes. When looking at the 35 genes of which DNA methylation and expression were differentially affected by PS (Table 2.3-3, B), we see the majority, i.e. 28 genes, showing decreased methylation, as observed when looking only at DMRs. The histone acetyltransferase *K[lysine] acetyltransferase 2A (Kat2a)*, *nitric oxide synthase 1 (Nos1)*, *calsyntenin 2 (Clstn2)*, *Musashi homolog 1 (Msi1)* and *four jointed box 1 (Fjx1)* were among those differentially methylated and expressed genes. Additionally, we detected a DMR about 10 kb upstream of Mir124-2. As our RNA extract did not contain miRNAs, we cannot say if this DMR was associated with a change in miRNA expression. We found moreover 23 differentially methylated/expressed genes that were affected in a *5-Htt* x PS fashion (Table 2.3-3, C). Among those genes were *ankyrin 3, epithelial (Ank3)*, *calcineurin binding protein 1 (Cabin1)*, *myelin basic protein (Mbp)*, *phospholipase A2, group V (Pla2g5)* and the guanine nucleotide exchange factor *pleckstrin and Sec7 domain containing 3 (Psd3)*.

At this point it should be also be noted that 60% and 63% of the differentially methylated/expressed genes that were affected by a G and E effect, respectively, followed the "canonical anticorrelation" of promoter methylation and gene expression, i.e. an increase in promoter methylation levels and a decrease in gene expression or vice versa. This leaves approximately 40% of differentially methylated/expressed genes that showed an "atypical" pattern.

Figure 2.3-7 Number of differentially methylated and expressed genes. Genes of which both DNA methylation status and gene expression level were significantly altered by genotype (G; i.e. *5-Htt+/-* vs *5-Htt+/+*), the environment (E; i.e. prenatal stressed versus control mice) or an interaction of both (GxE) in the hippocampus of female mice. DNA methylation analysis was performed by enriching methylated DNA from the hippocampus using methyl-DNA immunoprecipitation (MeDIP) and applying MeDIP DNA to Affymetrix Mouse Promoter 1.0R arrays. Gene expression was analyzed using Affymetrix 430 2.0 GeneChip arrays. For both DNA methylation and gene expression analysis, 6-10 animals per group were used, 2-4 hippocampi were pooled per array, 2-3 pools per group were analyzed.

Table 2.3-3 Differentially methylated and expressed genes. Genes of which both DNA methylation status and gene expression level were significantly altered by genotype (G; i.e. *5-Htt+/-* vs *5-Htt+/+*), the environment (E; i.e. prenatal stressed versus control mice) or by an interactive manner (GxE) in the hippocampus of female mice. DNA methylation analysis was performed by enriching methylated DNA from the hippocampus using methyl-DNA immunoprecipitation (MeDIP) and applying MeDIP DNA to Affymetrix Mouse Promoter 1.0R arrays. Gene expression was analyzed using Affymetrix 430 2.0 GeneChip arrays. For both DNA methylation and gene expression analysis, 6-10 animals per group were used, 2-4 hippocampi were pooled per array, 2-3 pools per group were analyzed. FC=fold change, D = directin of change, indicated with arrows.

		Methylation					Expression		
Symbol	**Gene name**	**chr**	**start**	**end**	**FC**	**D**	**FC**	**D**	**Affy ID**
A) G-effects: *5-Htt+/+* vs. *5-Htt+/-*									
Bbx	bobby sox homolog (Drosophila)	16	50435836	50436363	1.58	↑	1.26	↑	1430820_a_at
Ldlrad3	low density lipoprotein receptor class A domain containing 3	2	102029692	102029893	1.28	↑	1.12	↓	1438666_at
Bcl2l11 // Acoxl	BCL2-like 11 (apoptosis facilitator) // acyl-Coenzyme A oxidase-like	2	127946767	127947010	1.26	↑	1.11	↓	1456005_a_at
Bcl2l11 // Acoxl	BCL2-like 11 (apoptosis facilitator) // acyl-Coenzyme A oxidase-like	2	127946767	127947010	1.26	↑	1.35	↑	1456006_at
Kif13a	kinesin family member 13A	13	47028519	47029667	1.23	↓	1.12	↓	1451890_at
Spsb1	splA/ryaNodine receptor domain and SOCS box containing 1	4	149331144	149332126	1.23	↑	1.19	↓	1428472_at
Fank1 // Dhx32	fibronectin type 3 and ankyrin repeat domains 1 // DEAH(Asp-Glu-Ala-His) box polypeptide 32	7	140975216	140978199	1.19	↓	1.17	↓	1447495_at
Dhx32 // Fank	DEAH (Asp-Glu-Ala-His) box polypeptide 32 // fibronectin type 3 and ankyrin repeat domains 1	7	140975216	140978199	1.19	↓	1.19	↓	1420427_a_at
Fgfr4	fibroblast growth factor receptor 4	13	55249814	55250054	1.17	↑	1.15	↓	1427845_at
Fgfr4	fibroblast growth factor receptor 4	13	55249814	55250054	1.17	↑	1.26	↓	1427776_a_at
E2f3	E2F transcription factor 3	13	30080878	30081078	1.17	↓	1.14	↑	1427462_at
Ttn	titin	2	76823368	76823897	1.17	↓	1.21	↑	1427446_s_at
Nr5a1	nuclear receptor subfamily 5, group A, member 1	2	38568797	38569145	1.15	↓	1.17	↓	1421730_at
BC030307	cDNA sequence BC030307	10	86175833	86176109	1.14	↑	1.15	↑	1441409_at
Bmpr1b	bone morphogenetic protein receptor, type 1B	3	141593558	141593900	1.14	↑	1.19	↓	1422872_at
C030046E11Rik	RIKEN cDNA C030046E11 gene	19	29654132	29654407	1.14	↓	1.14	↑	1431023_at
Cybrd1	cytochrome b reductase 1	2	70957388	70957814	1.12	↓	1.13	↑	1425040_at

Fabp6	fatty acid binding protein 6, ileal (gastrotropin)	11	43418691	43419752	1.10 ↑	1.27 ↓	1450682_at
Akap6 // n-R5s58	A kinase (PRKA) anchor protein 6 // nuclearencoded rRNA 5S 58	12	53980545	53980725	1.09 ↓	1.14 ↑	1440859_at
Krt23	keratin 23	11	99352405	99352894	1.07 ↓	1.21 ↓	1418213_at
Nr5a1	nuclear receptor subfamily 5, group A, member 1	2	38569234	38569481	1.07 ↓	1.17 ↓	1421730_at
Lgr5	leucine rich repeat containing G protein coupled receptor 5	10	115028742	115029312	1.05 ↑	1.13 ↑	1444519_at
Mttp	microsomal triglyceride transfer protein	3	137796736	137797014	1.04 ↑	1.25 ↑	1419399_at
Tmem100	transmembrane protein 100	11	89896819	89897137	1.03 ↓	1.22 ↑	1446625_at
Pdlim4	PDZ and LIM domain 4	11	53883752	53883994	1.02 ↑	1.21 ↓	1417928_at
Pla2g5 // Pla2g2a	phospholipase A2, group V // phospholipaseA2, group IIA (platelets, synovial fluid)	4	138390529	138390886	1.02 ↑	1.59 ↓	1417814_at
Kcnj5	potassium inwardly-rectifying channel, subfamily J, member 5	9	32130003	32130278	1.01 ↑	1.18 ↑	1421762_at
0610040J01Rik	RIKEN cDNA 0610040J01 gene	5	64268747	64268986	1.01 ↓	1.12 ↓	1424404_at
B) E-effects: Controls vs. Prenatal stress							
Ddx46	DEAD (Asp-Glu-Ala-Asp) box polypeptide 46	13	55749228	55749440	1.33 ↑	1.16 ↓	1424569_at
Kcnh3	potassium voltage-gated channel, subfamily H (eag-related), member 3	15	99050982	99051487	1.31 ↑	1.11 ↓	1459107_at
Tlr12	toll-like receptor 12	4	128291909	128292687	1.31 ↑	1.10 ↓	1437931_at
Ropn1l // Gm6361	ropporin 1-like // predictedgene 6361	15	31378527	31378689	1.26 ↑	1.15 ↓	1423959_at
Tmtc1	transmembrane and tetratricopeptide repeat containing 2 // Smallnucleolar RNA SNORA17	10	104626225	104626657	1.25 ↓	1.14 ↑	1441033_at
Fjx1	four jointed box 1 (Drosophila	2	102295770	102296667	1.23 ↑	1.20 ↓	1450728_at
Fjx1	four jointed box 1 (Drosophila)	2	102295770	102296667	1.23 ↑	1.17 ↓	1422733_at
Cdc73	cell division cycle 73, Paf1/RNA polymerase II complex component, homolog (S. cerevisiae)	1	144990530	144990925	1.23 ↓	1.15 ↑	1427972_at
Sox6	SRY-box containing gene 6	7	123171580	123171989	1.23 ↓	1.14 ↑	1427677_a_at
Bcl10 // Ddah1	B cell leukemia/lymphoma 10 // dimethylarginine dimethylamiNohydrolase 1	3	145538088	145538612	1.21 ↓	1.18 ↑	1443524_x_at
Mettl7a1	methyltransferase like 7A1	15	100131133	100131965	1.21 ↑	1.16 ↑	1434151_at
Mettl7a1	methyltransferase like 7A1	15	100131133	100131965	1.21 ↑	1.13 ↑	1454858_x_at
Prkab1 // Cit	protein kinase, AMP-activated, beta 1 Non-catalytic subunit // citron	5	116457782	116458147	1.20 ↑	1.13 ↓	1424119_at

BC051628 BC006779	// cDNA sequence BC051628 // cDNA sequence BC006779	2	180964456	180964941	1.19 ↓	1.11 ↑	1431758_at
Pnlip	pancreatic lipase	19	58744425	58744760	1.17 ↑	1.25 ↑	1433431_at
Zfp64	zinc finger protein 64	2	168808365	168808848	1.16 ↑	1.21 ↑	1456431_at
Zfp64	zinc finger protein 64	2	168808365	168808848	1.16 ↑	1.12 ↓	1451696_at
Xpot	exportin, tRNA (nuclear export receptor for tRNAs)	10	121044448	121044882	1.16 ↑	1.13 ↑	1441681_at
Nr2c1 // Ndufa12	nuclear receptor subfamily 2, group C, member 1 // NADHdehydrogenase (ubiquinone) 1 alpha subcomplex, 12	10	93657585	93657974	1.14 ↑	1.19 ↓	1449157_at
Mast4 // Cd179	microtubule associated serine/threonine kinase family member 4 // CD180antigen	13	103564348	103564628	1.14 ↓	1.14 ↑	1459387_at
Clstn2	calsyntenin 2	9	97936180	97936420	1.12 ↑	1.19 ↓	1422158_at
Cldn18	claudin 18	9	99617339	99617897	1.12 ↑	1.19 ↑	1425445_a_at
Map3k1	mitogen-activated protein kinase kinase kinase 1	13	112601065	112601546	1.12 ↑	1.24 ↑	1443540_at
Akap13	A kinase (PRKA) anchor protein 13	7	82870878	82871179	1.11 ↑	1.10 ↓	1433722_at
Kdm6b // Dnahc2	KDM1 lysine (K)-specific demethylase 6B // dynein, axonemal, heavy chain 2	11	69290421	69290898	1.11 ↑	1.26 ↑	1440346_at
Kdm6b // Dnahc2	KDM1 lysine (K)-specific demethylase 6B // dynein, axonemal, heavy chain 2	11	69290421	69290898	1.11 ↑	1.14 ↑	1456610_at
Kat2a // Dhx58	K(lysine) acetyltransferase 2A //DEXH(Asp-Glu-X-His) box polypeptide 58	11	100566819	100567318	1.10 ↑	1.15 ↓	1422972_s_at
Prok2	prokineticin 2	6	99674161	99674602	1.10 ↑	1.15 ↑	1451952_at
Ptpn21	protein tyrosine phosphatase, Non-receptor type 21	12	99923550	99923778	1.09 ↑	1.15 ↑	1419055_a_at
Rad9b	RAD9 homolog B (S. cerevisiae)	5	122803144	122803311	1.09 ↑	1.18 ↓	1425800_at
Mcm3	minichromosome maintenance deficient 3 (S. cerevisiae)	1	20807895	20808068	1.09 ↑	1.17 ↑	1420029_at
Msi1	Musashi homolog 1(Drosophila)	5	115873837	115874905	1.08 ↑	1.24 ↑	1444306_at
Stt3b	STT3, subunit of the oligosaccharyltransferase complex, homolog B (S. cerevisiae)	9	115162948	115163232	1.08 ↑	1.22 ↑	1431541_at
Dna2 // Slc25a16	DNA replication helicase 2 homolog (yeast) // solute carrier family 25 (mitochondrial carrier, Graves disease autoantigen), member 16	10	62407000	62407211	1.08 ↑	1.25 ↑	1457909_at
Slc30a1 1700034H15Rik	// solute carrier family 30 (zinc transporter), member 1 // RIKENcDNA 1700034H15 gene	1	193732789	193733167	1.08 ↑	1.15 ↓	1436164_at

Nos1	nitric oxide synthase 1, neuronal	5	118312626	118312968	1.07 ↑	1.20 ↓	1438483_at
Prss23 // 1700019G06Rik	protease, serine, 23 // RIKENcDNA 1700019G06 gene	7	96658688	96659035	1.07 ↓	1.17 ↓	1446560_at
Chaf1b // Morc3	chromatin assembly factor 1, subunit B (p60) // microrchidia 3	16	93865780	93866055	1.07 ↑	1.24 ↑	1431275_at
Gja1	gap junction protein, alpha 1	10	56216896	56217111	1.04 ↑	1.42 ↓	1415801_at
C) GxE-effects: *5-Htt* x PS interaction							
2010001K21Rik	RIKEN cDNA 2010001K21 gene	13	47102005	47102256	- -	- -	1447576_at
5430421N21Rik	RIKEN cDNA 5430421N21 gene	15	101325243	101325528	- -	- -	1427118_at
Ank3	ankyrin 3, epithelial	10	68991227	68992000	- -	- -	1447259_at
Atp10b	ATPase, class V, type 10B	11	42964973	42965240	- -	- -	1444911_at
Cabin1	calcineurin binding protein 1	10	75229253	75229611	- -	- -	1437794_at
Cage1	cancer antigen 1	13	38127687	38128016	- -	- -	1434810_a_at
Chrna9	cholinergic receptor, nicotinic, alpha polypeptide 9	5	66361850	66362047	- -	- -	1447214_at
Chrna9	cholinergic receptor, nicotinic, alpha polypeptide 9	5	66362494	66362774	- -	- -	1447214_at
Clpb // Phox2a	ClpB caseinolytic peptidase B homolog (E. coli) // paired-likehomeobox 2a	7	108938653	108939395	- -	- -	1454168_a_at
Dppa3	developmental pluripotency-associated 3	6	122594236	122594653	- -	- -	1424295_at
F10 // Proz	coagulation factor X // proteinZ, vitamin K-dependent plasma glycoprotein	8	13055218	13055381	- -	- -	1449305_at
Fam135a // 1110058L19Rik	family with sequence similarity 135, member A // RIKENcDNA 1110058L19 gene	1	24034551	24034832	- -	- -	1453122_at
Fam170a	family with sequence similarity 170, member A	18	50438458	50438693	- -	- -	1456560_at
Foxj1 // Rnf157	forkhead box J1 // ring finger protein 157	11	116218086	116218410	- -	- -	1425291_at
Glra1	glycine receptor, alpha 1 subunit	11	55418779	55418960	- -	- -	1422277_at
Heatr1 // Lgals8	HEAT repeat containing 1 // lectin,galactose binding, soluble 8	13	12520880	12521218	- -	- -	1452419_at
Mbp // Rpl21-ps8	myelin basic protein // ribosomalprotein L21, pseudogene 8	18	82693616	82694069	- -	- -	1451961_a_at
Parp14	poly (ADP-ribose) polymerase family, member 14	16	35858088	35858439	- -	- -	1451564_at
Pim1	proviral integration site 1	17	29656335	29656796	- -	- -	1423006_at
Pla2g5 // Pla2g2a	phospholipase A2, group V // phospholipaseA2, group IIA (platelets, synovial fluid)	4	138382101	138382425	- -	- -	1417814_at

Psd3	pleckstrin and Sec7 domain containing 3	8	70220885	70221160	-	-	-	-	-	1418749_at
Tcof1	Treacher Collins Franceschetti syndrome 1, homolog	18	61013037	61013345	-	-	-	-	-	1423600_a_at
Uevld	UEV and lactate/malate dehyrogenase domains	7	54224905	54225077	-	-	-	-	-	1421785_at
Wdr66	WD repeat domain 66	5	123745990	123746262	-	-	-	-	-	1447215_at

DNA methylation of an intronic sequence of the Mbp gene

We next engaged in validating and fine-mapping the DMR found in the Mbp gene using MeDIP-qPCR and pyrosequencing. Five consecutive primer sets covering the DMR and a smaller flanking region (Chr. 18, 82,693,122 – 82,694,510) in a non-overlapping manner were analyzed in order to assess 5-mC enrichment in the Mbp DMR using qPCR. The same pooled MeDIP DNA as applied for the promoter arrays was used. Primer set 1 was excluded due to overlap with the ubiquitous ribosomal protein L21, pseudogene 8. The remaining four primer sets yielded the same DNA methylation pattern with a slight decrease in 5-mC levels in *5-Htt+/+* animals after PS and an increase in 5-mC levels in *5-Htt+/-* animals after PS exposure, as shown in Figure 2.3-8 representatively for primer pair 3 and 4. The highest enrichment was found for Primer pairs 2, 3 and 4, indicating that the signal originated in the middle of this region. Although statistically not detectable due to the small sample size, it is clear that the enrichment patterns of all four primer pairs show a GxE effect. Furthermore, DNA methylation levels at the analyzed *Mbp* region were higher in *5-Htt+/-* when compared to *5-Htt+/+* animals (KW p=0.046, MWU p=0.004).

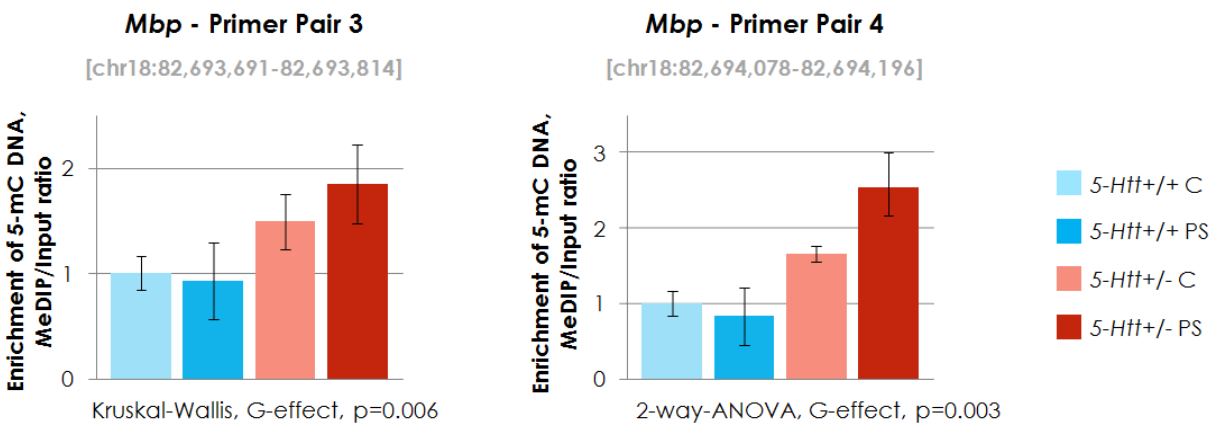

Figure 2.3-8 Enrichment of 5-mC at the *Mbp* locus in the hippocampus of female *5-Htt+/-* or *5-Htt+/+* mice, exposed to PS or not (control). Methylated DNA was enriched by methyl-DNA immunoprecipitation (MeDIP). Enrichment was analyzed by MeDIP qPCR. 6-10 animals per group, 2-4 hippocampi were pooled, 2-3 pools per group were analyzed. 5 neighboring DNA stretches at the *Mbp* locus were investigated, all showing the same enrichment pattern but with different intensity. Primer pair 3 and 4 showed the highest enrichment. Bars represent means, error bars SEM.

After having validated the promoter array signal with MeDIP-qPCR, we moved on to fine-mapping the *Mbp* DMR using pyrosequencing, a technique with a better resolution than the array screening approach. Pyrosequencing analyzes amplicons of bisulfite-treated DNA, yielding signals for 5-mC and 5-hmC with single base resolution. Here we aimed to clarify if all CpG sites within the *Mbp* DMR would be changed due to a GxE interaction or if the screening signal emerged from specific CpG sites. 13 consecutive CpG sites within the region of interest (Chr18, 82,693,582- 82,694175) were chosen for pyrosequencing (Fig. 2.3-9). Figure 2.3-9 A) shows the percentage of unconverted, hence methylated, cytosines, at CpG sites 3 through 15. As assumed from the MeDIP-qPCR results, the *Mbp* DMR showed an overall high degree of methylation, i.e. 70-90%. While methylation levels at most CpG sites did not vary, methylation was modestly increased in *5-Htt*+/- mice when compared to *5-Htt*+/+ animals (two-way ANOVA p=0.031 and p=0.019, respectively) at CpG sites 14 and 15 (Fig. 2.3-9, B), a finding matching the MeDIP-qPCR data. Furthermore, the methylation pattern at CpG site 14 matched the observed pattern of the promoter array and, additionally showed a trend towards a *5-Htt* x PS interaction effect (two-way ANOVA p=0.066). In regard to *Mbp* mRNA expression, Spearman correlation analysis revealed a significant negative correlation of methylation status at CpG site 14 and 15 with *Mbp* expression (r=-0.412, p=0.012 and r=-0426, p=0.010, respectively). Noteworthy, when looking for associations with the behavioral data, methylation status at CpG site 14 correlated with the time spent in the open arms of and distance moved in the elevated zero maze (EZM) (Spearman correlation, r=0.396, p=0.020 and r=0.345, p=0.046, respectively). Moreover, individual *Mbp* expression levels obtained by RT-qPCR correlated with time spent in the open arms of and distance moved in the EZM (Spearman correlation, r=-0.452, p=0.007 and r=-0.358, p=0.037, respectively). We furthermore analyzed the 5'-flanking region of the *Mir137* gene that did not harbor a DMR in our analysis (Fig. 2.3-10) as a negative control and confirmed that there were no changes in DNA methylation levels in this region.

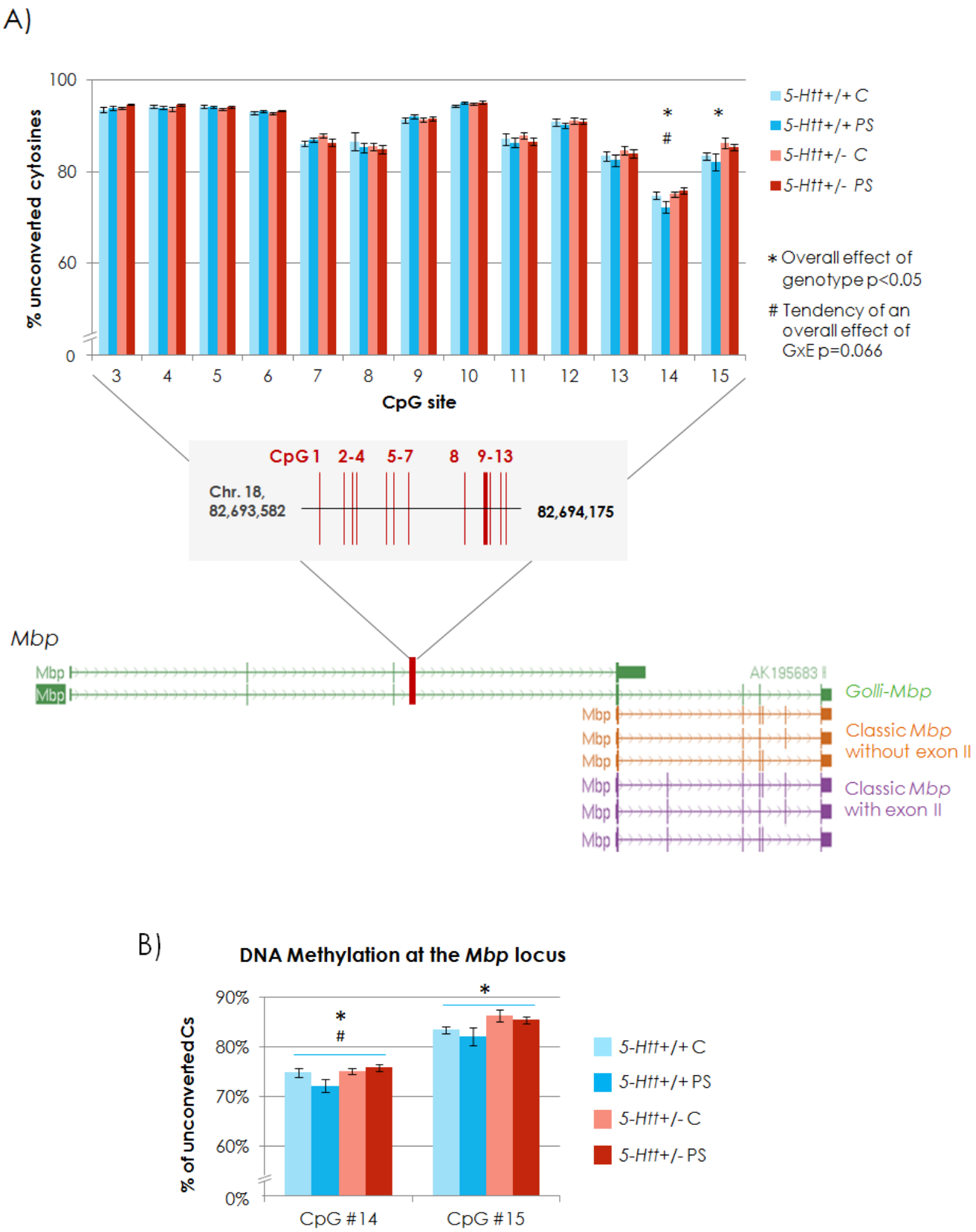

Figure 2.3-9 Cumulative levels of 5-mC and 5-hmC at the *Mbp* locus in the hippocampus of female *5-Htt+/-* or *5-Htt+/+* mice, exposed to PS or not (control). DNA methylation levels were analyzed using pyrosequencing on bisulfite-converted DNA. Bars represent means, error bars SEM. N=7-10 animals per group. *p<0.05, #p<0.1. A) All analyzed CpG sites. B) Detail on CpG sites 14 and 15.

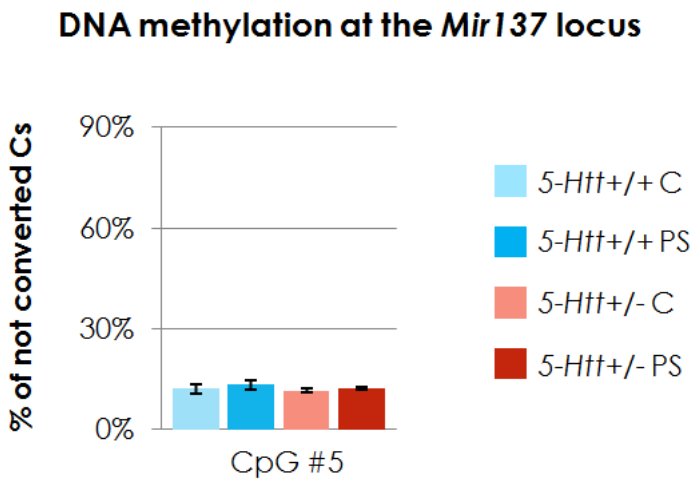

Figure 2.3-10 Cumulative levels of 5-mC and 5-hmC at the *Mir137* locus in the hippocampus of female *5-Htt+/-* or *5-Htt+/+* mice, exposed to PS or not (control). DNA methylation levels were analyzed using pyrosequencing on bisulfite-converted DNA. Bars represent means, error bars SEM. N=7-10 animals per group. No significant differences in DNA methylation levels observed.

2.4. Discussion

The work presented here demonstrates that exposure of female *5-Htt+/-* mice to PS in form of maternal restraint during E13 through E17 leads to alterations in the expression of myelin-associated genes in hippocampus and amygdala of the adult animals. Next to this, the *5-Htt* genotype, PS exposure and their interaction affected the DNA methylation levels in hundreds of genomic regions. Especially PS was associated with increased methylation levels in the DMRs. Furthermore, methylation levels at a specific CpG site in the *Mbp* gene was negatively associated with *Mbp* expression and positively with anxiety-like behavior in the EZM.

2.4.1. Effects of 5-Htt genotype and PS on DNA methylation

The promoter array analysis of enriched methylated hippocampus DNA revealed a few hundred regions affected by the *5-Htt* genotype, PS exposure and an interaction of both.

Changes in DNA methylation can be a way for an organism of translating present environmental information into specific long-term self-perpetuating changes in gene expression. However, when measuring DNA methylation in a heterogeneous tissue as the hippocampus, changes in DNA methylation levels could also reflect an altered ratio of different cell types, each with its own cell type-specific DNA methylation finger print. Although DNA regions that are methylated in a tissue- or cell type-defining way are predominantly found in so called shore regions, i.e. regions at the margins of CpG islands, it is very well possible that our promoter array picked some of them up. This entanglement of PS-response and cell type-specific DNA methylation patterns should always kept in mind when interpreting our DMR findings.

5-mC levels were found to by increased in ~60% and decreased in ~40% of the DMRs when comparing *5-Htt+/-* to *5-Htt+/+* mice. As of yet it is not known how the *5-Htt* genotype affects DNA methylation, however, generally speaking, human s-allele carriers and 5-HTT deficient mice seem to be more sensitive to both adverse and positive factors in early life environment. This might reflect a higher plasticity in response to changes in environment. One might speculate that altered levels of 5-HT in the developing brain and the resulting adaptive changes may have an effect on the extent to which environmental variation is perceived and translated into long-ranging changes in brain function and behavior. One could also very well imagine epigenetic mechanisms being involved in this process. PS, on the other hand, led to an increase in the majority of the DMRs, 80% to be precise. As no changes in DNMT expression were detected in the

hippocampus of the adult mice, this increase in methylation levels could be the result of a temporary increase in DNMTs during development. Interestingly, Mychasiuk and coworkers detected an increase in global DNA methylation in the hippocampus of young female rat offspring in a mild PS as well as in a bystander PS paradigm. In the bystander PS paradigm the dam is not stressed directly, but indirectly, by stressing the cage mate of the pregnant dam.

Functional Annotation Clustering using DAVID (Huang *et al.* 2007) detected only two functional annotation clusters enriched due to *5-Htt* genotype effects, one containing ribosome associated annotations and one with ion binding terms. The most enriched among the five clusters identified for the DMRs affected by PS were a cluster of WD repeat terms and one with SH3 domain terms, which contains *Pak1ip1, Strn3* and *Pacsin2* among others. *Pak1ip1* is involved in the p53-dependent regulation of cell growth and proliferation in response to stressors (Yu *et al.* 2011). STRN3 is a Ca^{2+}-calmodulin binding protein that is mainly expressed in the brain, cerebellum, muscle and lung (Castets *et al.* 2000). In the hippocampus, *Strn3* is expressed in pyramidal and granular cells (Castets *et al.* 2000). *Pacsin2*, a member of the protein kinase C and casein kinase substrate-in-neurons family, is involved in linking the actin cytoskeleton with vesicle formation by regulating tubulin polymerization. Next to this, five enriched clusters were identified for a GxE effect, two of which harbored cytoskeleton-associated terms and one EGF-associated cluster. The EGF cluster comprises two genes, *Notch3* and *Fat1,* which are of particular interest as they are expressed in the ventricular zones during prenatal mouse development and thus have been suggested to play a role in CNS development (Cox *et al.* 2000; Irvin *et al.* 2001). Their expression in the ventricular zones during development makes them an interesting target for DNA methylation changes induced by PS. NOTCH3 is a protein of the Notch family, which plays a key role in neuronal development. Of note, *Notch3* was found to be essential for OL development in zebrafish and a mutation in Notch3 was associated with lower numbers of OLs accompanied by decreased *Mbp* expression (Zaucker *et al.* 2013). *Fat1* encodes a protein of the cadherin family (Cox *et al.* 2000). Next to this, variation in *FAT1* has been associated with bipolar disorder (Light *et al.* 2007; Abou Jamra *et al.* 2008).

2.4.2. Genes affected both on expression and DNA methylation level

When comparing the genes associated with DMRs with the gene expression profiles assessed before (Van den Hove and Jakob *et al.* 2011), there was a modest overlap, i.e. 24, 30 and 16 genes were affected regarding both DNA methylation and expression by

G, E and GxE, respectively. The reasons underlying this unexpectedly small overlap between DNA methylation and expression will be discussed further down. Several genes of interest will be discussed below.

We identified increased methylation levels in the first intron of the *bone morphogenetic protein receptor, type 1B* (*Bmpr1b*), accompanied by decreased *Bmpr1b* mRNA expression in *5-Htt+/-* mice compared to WT controls. The class I *Bmp receptor* genes are involved in BMP signaling. BMPs are tightly temporospatially regulated secreted growth factors with a multitude of functions in the development of the nervous system (Bond *et al.* 2012). For example, BMPs are involved in neurogenesis and astrogliogenesis during forebrain development as well as in neurite outgrowth from immature neurons (Bond *et al.* 2012). In the adult brain, BMP signaling moreover plays a pivotal role in the maintenance of the adult neural stem cell niches in the subventricular and subgranular zones. Mice deficient for both the functionally redundant *Bmpr1b* and *Bmpr1a* develop smaller DG when compared to wild type mice, indicating impaired granule cell production during DG development, and a reduced neuronal progenitor pool in the DG (Caronia *et al.* 2010). Behaviorally, these mice are characterized by decreased anxiety-like behavior in the EPM when compared to WT controls (Caronia *et al.* 2010).

Next to this, we detected increased methylation at a DMR located upstream of the *Calsyntenin-2 (Clstn2) and K(lysine) acetyltransferase 2A* (*Kat2a*) gene in PS mice when compared to controls. The sparsely studied *Clstn2* is one of three calsyntenin genes encoding post-synaptic proteins. In the hippocampus, *Clnst2* is found in the granular cell layer of the DG, in pyramidal cells of the CA2 and CA3 region, as well in a subset of interneurons in the CA1 pyramidal cell layer (Hintsch *et al.* 2002). The effects of stress exposure on *Clnst2* have not yet been studied.

Moreover, the tiling array identified a DMR spreading over several exons and introns of the *Kat2a* gene. The increase in 5-mC levels in this DMR in PS mice compared to C mice was associated with decreased Kat2a expression. *Kat2a* was identified as the histone acetyltransferase with the highest expression in the CA1 region of the hippocampus in mice (Stilling *et al.* 2014), underlining its role in hippocampal processes. The acetyltransferase is recruited by several DNA binding factors such as myc (McMahon *et al.* 2000; Kenneth *et al.* 2007), E2F (Lang *et al.* 2001) and p53 (Candau *et al.* 1997), thereby affecting chromatin structure. KAT2A targets lysine residues of histone 3 and 4, thereby promoting transcriptional activation (Grant *et al.* 1997; Ciurciu *et al.* 2006). Thus not surprising, *Kat2a* plays a critical role for embryonic development and brain growth (Xu *et al.* 2000). Furthermore, *Kat2a* KO mice show impaired hippocampal synaptic

plasticity and hippocampus-dependent memory consolidation (Stilling *et al.* 2014). A loss-of-function of *Kat2a* leads to impaired stem cell proliferation in the mouse cortex (Martinez-Cerdeno *et al.* 2012).

We furthermore noted that the secretory phospholipase A2, group V (*Pla2g5*) gene was regulated in a G and a GxE fashion on both expression and methylation level. PLA2G5 is a protein of the phospholipase A2 family, the key enzymes in the activation of the arachidonic acid (AA) cascade (Balboa *et al.* 1996; Shinohara *et al.* 1999). Prostaglandines and leukotrienes, which are mediators of inflammation and associated with allergic reactions, are synthesized from AA. A role of AA and is metabolites in neurotransmitter release, cerebral blood flow regulation and inflammatory processes, which are also involved in multiple-sclerosis and Alzheimer's disease (reviewed in Cho 2000; Sun *et al.* 2010), has been reported. Furthermore*, Ankyrin 3, epithelial* (*Ank3*, also known as *Ankyrin-G*), *calcineurin binding protein 1* (*Cabin1*) and *pleckstrin and Sec7 domain containing 3* (*Psd3*, also known as *EFA6D*) were also regulated in a GxE fashion in our study. In the brain, ANK3 is localized in the axonal segments and at the nodes of Ranvier, where is contributes in the localization of voltage-gated sodium and potassium channels, transmembrane adhesion molecules and the spectrin membrane skeleton (Kordeli *et al.* 1995; Jenkins and Bennett 2001; Pan *et al.* 2006). Although not part of the myelin sheath but of the internodes, *Ank3* is another gene linking the GxE effects to myelination. ANK3 was identified as a candidate gene for bipolar disorder in several studies suggested (Schulze *et al.* 2009; Smith *et al.* 2009; Rueckert *et al.* 2013). Although expressed throughout the brain, *Psd3* is not very well characterized. Its highest expression is found in olfactory bulb, cerebral cortex, hippocampal pyramidal cell layer and cerebellar granule cell layer (Sakagami *et al.* 2006). PSD3 is a guanine nucleotide exchange factor for the small GTPase ARF6 (Sakagami *et al.* 2006), a regulator of membrane trafficking and of the actin cytoskeleton. ARF6 is moreover involved in neuronal functions including spine density and maintenance (Miyazaki *et al.* 2005; Choi *et al.* 2006), neurite formation (Hernandez-Deviez *et al.* 2002; Hernandez-Deviez *et al.* 2004), endo- and exocytosis of synaptic vesicles (Galas *et al.* 1997; Krauss *et al.* 2003) as well as receptor internalization (Delaney *et al.* 2002).

2.4.3. 5-Htt genotype dependent changes in expression of myelin-associated genes and in Mbp methylation induced by PS

In the present study, we revealed a highly consistent pattern of expression changes in the expression of the most prominent myelin-associated genes, both in hippocampus

and amygdala. More precisely, PS increased the expression of myelin-associated genes in the hippocampus of female 5-Htt+/+ offspring, but not in 5-Htt+/-, whereas expression of those genes in the amygdala was increased in female 5-Htt+/-, but not in 5-Htt+/+ offspring. *Mbp* is of special interest as promoter array analysis identified a DMR at the *Mbp* locus that was regulated in a *5-Htt* x PS fashion. Subsequent pyrosequencing identified differential effects of the *5-Htt* genotype on DNA methylation at two out of 13 analyzed CpG sites and a tendency for a GxE interaction effect at CpG site 14. Of note, we found a negative correlation between methylation levels at CpG site 14 and 15, and *Mbp* expression and anxiety-like behavior in the EZM, possibly implying a functional methylation of *Mbp*. Supportive data come from Föcking and colleagues, who exposed WT mice to the very same PS paradigm and found an increase in hippocampal MBP protein levels in the adult animals (Focking *et al.* 2014), a finding matching our RT-qPCR results on *Mbp* expression in the hippocampus.

The *Golli-Mbp* locus gives rise to two different groups of transcripts, as illustrated in Figure 2.3-3, the "classical" *Mbp* transcripts encoding MBP proteins and the only later discovered *Golli-Mbp* transcripts that comprise a couple of additional exons at the 5' end and result in GOLLI proteins. While *Mbp* is expressed in myelinating cells, that is OLs and Schwann cells, Golli-Mbp is additionally expressed in neuronal cells (Landry *et al.* 1996; Landry *et al.* 1997; Landry *et al.* 1998). The expression of the several *Mbp* and *Golli* splice variants is subject to complex developmental regulation, followed by post-translational modifications yielding MBP proteins from 14 to 21.5 kD in size (for a detailed review see Harauz and Boggs 2013). There are two *Mbp* transcript groups that differ in splicing of exonII, which encodes a nuclear trafficking signal. A transcript without exonII encodes the 18.5 kD classic MBP that is essential for CNS myelin formation. The 18.5 kD MBP forms the myelin major dense line and is, next to PLP1, the main structural component of myelin in the mature brain (Readhead and Hood 1990; Pedraza *et al.* 2001; Harauz and Boggs 2013). It prevents proteins of the paranodal loops to diffuse into the compact myelin by acting as a kind of "molecular sieve" (Aggarwal *et al.* 2011). A mouse model with a deletion in *Mbp* and subsequent unstructured brain myelin, the shiverer mouse, shows early-onset generalized tremors and seizures, symptoms that become worse with aging, as well as a shortened lifespan (Dupouey *et al.* 1979; Privat *et al.* 1979). MBP is discussed, however, to cover also other functions different from myelin formation. Seen from a biochemical view, MBPs are intrinsically disordered proteins (IDPs) (Hill *et al.* 2002; Harauz *et al.* 2004), implicating a certain structural flexibility and thus a wide range of interaction partners. That is why Golli-MBPs have been suggested as regulators of the cytoskeleton (Boggs *et al.* 2005; Bamm *et al.* 2011; Smith *et al.* 2012) and

of voltage-gated Ca2+ channels (Paez *et al.* 2009; Paez *et al.* 2009; Paez *et al.* 2011; Smith *et al.* 2011). Furthermore, IDPs have been discussed to function as interaction hubs, a role that has also been suggested for MBP due to its cellular plenitude (Dagliyan *et al.* 2011; Dogan *et al.* 2012; Ganguly *et al.* 2012; Harauz and Boggs 2013).

The expression of both *Mbp* transcripts containing and lacking exon II was increased in the hippocampus of *5-Htt*+/+ mice after PS, but not in *5-Htt*+/- mice. In the amygdala, on the other hand, *Mbp* expression was increased in *5-Htt*+/- mice after PS but not in *5-Htt*+/+. Furthermore, the expression of other major myelin-protein coding genes was changed in the same pattern as *Mbp*, both in hippocampus and amygdala.

Mbp exon II encodes a nuclear trafficking signal, implicating a function different from the one of a myelin structural protein for the nuclear localized 21.5 kD MBP proteins. The 21.5 kD MBP has been suggested to play a role in OL differentiation and to be involved in early myelination (Harauz and Boggs 2013; Ozgen *et al.* 2014). Interestingly, expression of *Mbp* exII in a co-culture of N2a neuronal cells and N19-OLs facilitates neurite outgrowth and branching of neuronal cells (Smith *et al.* 2013).

An association, without investigating a causal relationship, of myelination and anxiety-like behavior in rodents has been previously reported in a few studies. Kikusui and coworkers found decreased levels of two out of four analyzed MBP isoforms in brain homogenates of 5 weeks old early weaned male outbred IRC mice when, in which they also found increased anxiety-like behavior (Kikusui *et al.* 2007). This finding could not be replicated in Wistar rats exposed to an early weaning paradigm (Kodama *et al.* 2008). FYN is a protein-tyrosine kinase involved in the post-translational regulation of MBP. Fyn deficient mice have decreased MBP levels in the forebrain (Lu *et al.* 2005) and are characterized by increased anxiety-like behavior in the EPM when compared to wt mice (Miyakawa *et al.* 1996). Increased deposition of abnormally composed myelin in adult male rats resulting from intracranial apotransferrin injection into the three days-old pups was associated with anxiolytic behavior in the EPM, when comparing the adult injected rats to control rats (Viola *et al.* 2001). In this context it is most interesting that in the hippocampus it is mostly GABAergic fibers that are myelinated whereas cholinergic fibers are not (Gartner *et al.* 2001). It was thus suggested that myelination might affect anxiety-like behavior by influencing GABAergic transmission (Gartner *et al.* 2001; Kikusui *et al.* 2007). In line with this hypothesis, we found a modest but significant negative correlation between anxiety-like behavior in the EZM and total *Mbp* expression. This correlation was, however, not found for the expression other myelin-associated genes. We did not analyze the protein levels of any myelin proteins though, which might be more informative in this regard.

Furthermore, the role of the hippocampus in innate anxiety has been subject of several studies, demonstrating in particular the regulatory function of the ventral hippocampus on the exploration time of the open arms in the EPM (Trent and Menard 2010; McEown and Treit 2013; Zhang *et al.* 2014). For example, in rats, injection of TPA023, a GABA a2 agonist, into the ventral hippocampus has anxiolytic effects on behavior in the EPM (McEown and Treit 2013). Next to this, changes in MBP expression and myelination were found to be associated with schizophrenic disorders, major depressive disorder and bipolar disorders (Chambers and Perrone-Bizzozero 2004; Le-Niculescu *et al.* 2007; Le-Niculescu *et al.* 2009; Parlapani *et al.* 2009; Sibille *et al.* 2009; Ayalew *et al.* 2012; Edgar and Sibille 2012; Matthews *et al.* 2012; Mosebach *et al.* 2013; Hercher *et al.* 2014).

Although rather speculative, the changes in DNA methylation at CpG sites 14 and 15 could affect *Mbp* expression by interacting with transcription factors involved in *Mbp* expression. Transcription factor binding site analysis of the DMR using JASPAR (Bryne *et al.* 2008) identified a putative SOX 10 binding site a few bases upstream of CpG site 14. SOX10 is Sry-related high mobility-box transcriptional regulator and is involved in the differentiation of neural crest precursors into myelin-producing cells, i.e. Schwann cells and OLs, as well as melanocytes (Britsch *et al.* 2001). It is not only expressed in oligodendrocyte progenitor cells (OPCs) but is also required for terminal differentiation of OLs in mice (Stolt *et al.* 2002). Moreover, *Mbp* and *Plp1* expression are both under the control of SOX10 (Stolt *et al.* 2002). As it has been shown that SOX10 binds to three binding sites in the proximal promoter region of *Mbp* in Neuro2a mouse cells (Stolt *et al.* 2002), it might be of interest to investigate the DNA methylation levels in this region in our samples. Intriguingly, SOX10 cooperates with the epigenetic machinery, i.e. the chromatin remodeling enzymes SWI/SNF, in order to induce the expression of *Mbp* (Marathe *et al.* 2013).

PS could have had an impact on the expression myelin-associated genes in the hippocampus and amygdala of the adult mice by affecting OL development. As MBP expression in mature OLs starts around P10 in the murine hippocampus (Savaskan *et al.* 1999), it is unlikely that PS directly affected mature OLs, but PS could have interfered with different stages of OL development, i.e. OL progenitor migration from the ventricular zone, proliferation of immature OLs in the target tissues or reprogramming of (future) gene expression by changes in DNA methylation. Indeed, murine NG2-positive OPCs express the GR and the GR-cofactors SRC1 and p300 *in vivo* (Matsusue *et al.* 2014). Furthermore, several studies linked changes in myelination to stress exposure. Xu and colleagues for example exposed Sprague-Dawley rats to PS and found disturbed myelin

formation in the hippocampus of the 22 days old PS rats (Xu *et al.* 2013). Miyata et al. found morphological changes in OLs in the corpus callosum of mice exposed to acute stress in form of chronic water-immersion and restraint stress (Miyata *et al.* 2011). Moreover, *in vitro* exposure of OLs to dexamethason led to an 1.5-fold increase in MBP-expressing OL cell diameter.

Our data leave a lot of room to speculations as to what those expression changes of myelin-associated genes in hippocampus and amygdala stand for on cellular level. Future experiments are required to get a more detailed picture, especially regarding OL numbers and myelin distribution. A myelin staining is necessary for example to clarify if the increased expression of the myelin-associated genes reflects increased myelination, or if it reflects a compensatory mechanism resulting from myelin damage or missformation. Next to this, instead of being the result of increased myelin-production of the same number of OLs, the increased expression of myelin-associated genes could also derive from an alteration of the OL/neuron ratio reflecting either increase in OL numbers or decreased neuronal numbers. Our data are not conclusive in this regard. Although we have detected *Sox10* expression changes in hippocampus and amygdala, and we found highly significant correlations of *Sox10* expression with the expression of *Mbp*, *Mag* and *Mog*, expression changes of *Sox10* and of myelin-associated genes are not proportional. It is thus not clear if this hints towards an increased OL number or an increased *Sox10* expression. Next to this, it would be highly interesting to know if we face *de novo* myelination of axons that would be blank in the other groups or if already myelinated axons show thicker myelin sheaths, and which neurons were targeted. Also, a third alternative cannot be excluded, which is a changed spacing of myelin sections along axons. Interestingly, myelination is a dynamic process, i.e. new OLs differentiate throughout adulthood and build up myelin (Young *et al.* 2013). Although the velocity of saltatory conduction is mainly determined by the thickness of the myelin sheath, other structural myelin properties such as dispersion of internodes could also play a role. In a recent study, Tomassi and colleagues have traced myelinated axons of pyramidal cells of different layers of the neocortex and found that the longitudinal myelin distribution pattern differs between individual axons (Tomassy *et al.* 2014). Neurons of the same layer displayed more similar myelin profiles, with layer V pyramidal cells showing dense myelination while layer II/III pyramidal cells were significantly less myelinated. Of note, a part of the sparsely myelinated axons was characterized by long unmyelinated stretches, where afferent and efferent synapses were located. This kind of analysis would be very interesting for myelinated neurons of the hippocampus or the amygdala. A possibly PS-induced altered connectivity in hippocampus and amygdala in opposing directions

might e.g. affect HPA-axis function, as those regions play opposing roles in HPA-axis function. Although highly speculative, changes in myelination could not only reflect increased signal transduction velocity and connectivity but could also be regarded as a form of plasticity. In this context it is interesting to note that myelinating OLs also participate in the metabolism of extracellular lecticans, which are components of the perineuronal net matrix and are also involved in synaptic plasticity (Levy *et al.* 2014).

2.4.4. On the (missing) relationship of DNA methylation and expression

One of the questions addressed by study presented here was whether the *5-Htt* genotype, PS, or their interaction would affect DNA methylation patterns in the hippocampus in a long-range fashion and whether those changes in DNA methylation would have be associated with changes in gene expression. The first question can be answered with yes, as 5-Htt genotype, PS, and their interaction did affect DNA methylation in a few hundred genomic regions. The second question turned out to be more difficult to answer than initially anticipated. Surprisingly, only a modest part of the DMRs that we identified matched to genes that were also differentially expressed. Next to this, for a considerable number of genes, DNA methylation and gene expression did not have an inverse relationship. Three major aspects that will be discussed more detailed contribute to this finding. First, the relationship of DNA methylation and gene expression is highly context-dependent and expression is regulated by many factors. Second, we analyzed changes in a cumulative signal originating from a mixture of cell types as we used the whole hippocampus. Third, technical aspects and a very conservative bioinformatic approach diminished the numbers of detected DMRs.

Although there are promoters, for which it has been shown that they are regulated by DNA methylation, these findings cannot be generalized without limitations. Genome-wide studies on the relation of DNA methylation, both in promoter regions and genome-wide, and gene expression let to the realization that this relationship is very complex, not linear and highly context dependent. Weber and coworkers have analyzed methylation, histone modifications and RNA polymerase occupancy at 16,000 promoters in human somatic and germline cells (Weber *et al.* 2007). They categorized their DMRs depending on the CpG density into low-, intermediate and high-CpG promoters (LCPs, ICPs and HCPs) and found that the promoters in these categories have different associations with gene expression. Although methylation of ICPs and HCPs was associated with inactive promoters, only a part of the inactive HCPs were methylated in the first place. This indicates that while methylation of a HPC might not allow expression, *lacking* methylation

does not necessarily indicate promoter activity. Remarkably, for LCPs, Weber and colleagues detected no correlation at all between the methylation status and promoter activity. Guo and colleagues analyzed genome-wide changes in the methylation levels of single CpG sites in murine dentate granule neurons after neural activity. Although only 1% of the CpG sites were analyzed due to the method employed, the sequencing approach yielded single CpG site signals, giving a precise picture of CpG sites near TSS. The correlation between CpG methylation near TSS and gene expression was, however, only modest (Guo *et al.* 2011). Another level of complexity is added by the multitude of other regulatory levels of gene expression, that is for example the chromatin accessibility, which is regulated by histone modifications, at a given genomic region, non-coding RNAs, interactions with enhancer, silencer and other remote regulatory regions and the availability of transcription factors in a given point in time.

Next to this, we examined the whole hippocampus and thus analyzed changes in a cumulative signal originating from a mixture of cell types. Although the DNA methylation patterns of neurons and glia are expected to resemble each other more than those of for example hepatocytes or myocytes, studies show that their DNA methylation pattern clearly diverge from each other (Iwamoto *et al.* 2011; Guintivano *et al.* 2013; Kozlenkov *et al.* 2014). This entanglement and overlap of different methylation and expression patterns decreases the odds of finding an association between DNA methylation and gene expression and emphasizes the future necessity of cell type specific epigenome analyses (also see 2.4.6. Conclusion and outlook).

And finally, technical and bioinformatical aspects have a part in this observation. The use of MeDIP on chip suffers from an improvable resolution as the DNA fragment size is around 200bp during immunoprecipitation and the promoter array itself offers an average resolution of 35bp. Furthermore, the algorithm applied identified DMRs only when the signal comprised at least five consecutive array probes, thereby potentially excluding smaller regions from the output. Also, the tiling array applied here covered only promoter regions, other regulatory regions that could potentially be regulated by DNA methylation, such as enhancer and silencer regions, were not assessed. Furthermore, in some occasions, individual DMRs were assigned to two neighboring or embedded genes, although possibly not playing a functional role for both genes. Next to this, expression profiles were assessed by 3'IVT arrays and thus did not impart splice form-specific information thereby possibly diluting and covering up the effects of *5-Htt* genotype and PS on expression on specific isoforms.

2.4.5. Study limitations

The following limitations should be considered when interpreting the data presented here. From weaning onwards, animals were single housed in individually ventilated cages (IVCs) in order to prevent the establishment of a hierarchy. Cages were enriched with a cardboard tube and paper tissues and placed in close proximity to each other thereby enabling visual contact between neighboring cages. The isolated housing might still have been an additional stressor for the animals. The differences between control and PS animals might also have been mitigated by the increased mortality and subsequent loss of the weakest PS pups. This notion is underlined by our finding in a previous study that showed a direct correlation between low birth weight (which was due to restricted fetal growth in response to PS) and, amongst others, adult depression-like behavior (van den Hove *et al.* 2010). Most likely, some PS pups in the present study were too small and weak to drink sufficient water from the IVC sipper tube (personal observation).

Furthermore, behavior was assessed in the same animals as CORT, hippocampal gene expression and DNA methylation enabling us to directly associate behavioral findings with physiological parameters and changes on molecular level. Evidently, the drawback of this approach is that effects of behavioral testing itself on CORT, gene expression and DNA methylation profiles cannot be excluded. Although all animals underwent the same testing battery, we cannot exclude an interaction of behavioral testing and genotype and/or PS. The same is true for CORT measurements. Moreover, we cannot exclude an effect of the estrous cycle on behavior, CORT or gene expression in the female mice as we did not control for it.

Next to this, a few technical limitations should be pointed out. Although currently still being the gold standard, pyrosequencing is a technique based on bisulfite-treated DNA, hence it yields a cumulative signal for both 5-mC and 5-hmC. The basis of MeDIP, however, is an immunoprecipitation with an antibody specific for 5-mC. Thus, data from MeDIP and pyrosequencing are not completely comparable by all means, especially in the brain, where remarkable levels of 5-hmC have been previously detected (Wen *et al.* 2014). Moreover, n-numbers for both the expression and the promoter array reflect 2-3 arrays per group and p-values represent nominal p-values. The lacking significance after multiple-testing correction of the array data might on the one hand be due to the low n-number per group, on the other the heterogeneity of cell types in the hippocampus might also have contributed to this (as discussed in the section "On the (missing) relationship of DNA methylation and expression"). Additionally, we cannot exclude that left-right asymmetries might have influenced our results as we used the left hippocampus

for the gene expression study and the right hippocampus for the DNA methylation analysis (Moskal *et al.* 2006).

Finally, the analysis of a single brain region, such as the hippocampus, obviously limits the explanatory power of the molecular finding on behavior, since other structures, such as the amygdala and the prefrontal cortex, are also involved in regulating stress and emotion response.

Taken together, these limitations should cause the reader to interpret the presented data with caution, until future research reveals the extent to which the molecular players identified here may provide useful targets for intervention strategies in the treatment of stress-related disorders of emotion regulation.

2.4.6. Conclusion and outlook

In conclusion, this study showed that the 5-Htt genotype, PS exposure and an interaction of both altered the DNA methylation profiles of numerous genes, a part of which was also differentially expressed. Furthermore, processes associated with myelination seemed to be affected by a GxE-interaction on mRNA expression level. We moreover found differences in DNA methylation level at two specific CpG sites in an intronic region of the *Mbp* gene, which correlated with anxiety-like behavior in the EPM. As discussed in the section "5-Htt genotype dependent changes in expression of myelin-associated genes and in Mbp methylation induced by PS", there are several possibilities to interpret our DNA methylation data. It is possible that DNA methylation was changed in cells of the oligodendrocyte lineage, which would fit to the small change in DNA methylation, or that the differences we measured reflect an altered proportion of specific cell types to each other, i.e. an altered number of oligodendrocytes or neurons. To clarify this issue, DNA methylation should be analyzed in OLs and neurons separately. The necessity for analyzing epigenetic patterns in a cell type-specific approach has been discussed in the section "On the (missing) relationship of DNA methylation and expression" and emphasized by recent studies showing for example that DNA methylation patterns differ greatly between neurons and glial cells. Analyzing a heterozygous tissue like the hippocampus as a whole can not only diminish and obscure epigenetic changes taken place in only a part of the analyzed cells, e.g. OLs, but more also impede attributing the detected changes to specific processes, as the cell type they stem from is unknown. The separation of cell types could be achieved for example by fluorescence-activated cell sorting (FACS) or fluorescence-activated sorting of fixed nuclei (FAST-FIN) (Marion-Poll *et al.* 2014). Considering the complex arborization of adult neurons and OLs, nuclei sorting

should be preferred in our case as it has the major advantage of using fixed tissue. Working with fixed tissue is not only less time-consuming in terms of processing the dissected brains than using fresh tissue but also avoids the risk of inducing cellular reactions by the dissociation and isolation procedure, which is very hard to control for and would very likely tamper with the data.

In order to disentangle the mechanisms by which 5-HT and PS exposure interact to alter myelination, it would be interesting to conduct a histological study to characterize myelin structure and distribution as well as the number and relative proportion of OLs and OPCs in different brain regions at different developmental stages. If myelination should be altered, this would raise the question to which degree connectivity between brain regions involved in emotion processing are altered and if this could be tied to the behavioral alterations observed. One could speculate that the opposing findings regarding myelin-associated genes in hippocampus and amygdala might have resulted as an adaptive reaction to PS exposure and differences in connectivity in these regions might impact the development and function of the HPA-axis, as those regions play opposing roles in HPA-axis regulation.

In addition to our data on 5' promoter DNA methylation, it would be helpful to assess the methylation levels of intragenic CGIs, as they often mark intragenic promoters regulating tissue-specific expression (Manaukea 2010). As the promoter array was based on MeDIP, it was specific for 5-mC. We used a bisulfite-DNA based approach (pyrosequencing) in order to validate the results from the promoter arrays and thus received a signal comprising disentangably both 5-mC and 5-hmC levels. Although 5-hmC is a less abundant modification than 5-mC, 5-hmC levels can reach significant levels for single CpG sites, especially in the brain. Wen and colleagues even found that 5-hmC is the main modification status of 13.4% of all analyzed CpGs in the adult brain and that some genomic regions such as poised enhancers show 5-hmC levels reaching 30% (Wen *et al.* 2014). Pyrosequencing, albeit being the gold standard for DNA methylation analysis, might not suffice to validate those data and should be supplemented by analyzing 5-hmC in a separate approach, e.g. oxidative bisulfite sequencing. We could furthermore investigate if SOX10 binds to its putative binding site near CpG site 14 using ChIP experiments and if this is dependent on the methylation status or chromatin conformation in this region. It would also be helpful to complete the DNA methylation data with data on other epigenetic marks, i.e. histone modifications associated with promoter activity and silencing and associated with enhancers, as this would give a more reliable picture of the chromatin conformation of the respective regions. Taken

together, our data indicate that DNA methylation, especially of *Mbp,* and processes associated with myelination might be interesting targets to be followed up in investigating the pathomechanisms of emotion disorders, but additional research will be necessary to validate those findings and elucidate the issues discussed in this section.

3. Project 2 – Resilience towards PS in 5-Htt deficient female mice

3.1. Introduction

In the second PS study, we followed up on the findings of the first study and raised the question of how variation in the *5-Htt* gene influences resilience to PS. Figure 3.1-1 shows an overview of the experimental setup. We applied the same prenatal restraint stress paradigm and tested this time only adult female offspring in a testing battery comprising the EPM for anxiety-like behavior, the sucrose preference test for anhedonia, the 3-chamber sociability test for sociability and the Porsolt swim test (PST) for behavioral despair. We furthermore assessed CORT levels at baseline and after acute restraint stress. As PS had the strongest effect on sociability, PS females were then split into a social, resilient and an unsocial, vulnerable group based on their performance in the 3-chamber-sociability test. We then created genome-wide hippocampal gene expression profiles using mRNA sequencing and identified pathways and gene ontology (GO) terms enriched due to genotype (G), PS (E for environment) and their interaction (GxE) as well as enriched in social, but not unsocial, PS offspring and *vice versa* using the enrichr online tool (Chen Tan 2013).

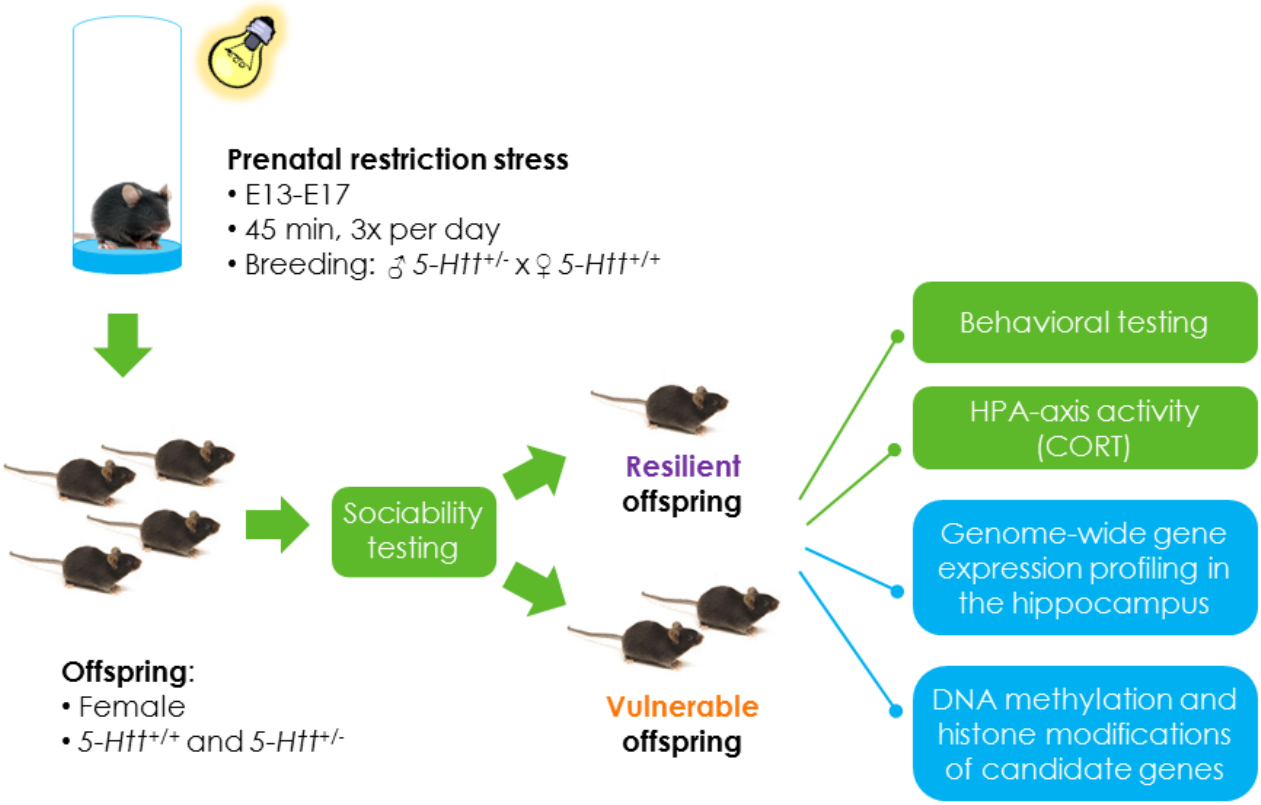

Figure 3.1-1 Experimental setup of the PS resilience study.

3.2. Methods and Materials

3.2.1. Animals and ethics

Breeding and behavioral studies were performed in collaboration with Nicole Leibold (University of Maastricht) at the Zentrum für experimentelle molekulare Medizin (ZEMM) in Würzburg. The study was approved by the Regierung von Unterfranken (Permit number: 55.2-2531.01-93/12), and all efforts were made to minimize suffering.

Breeding pairs. Male *5-Htt+/-* mice [B6.129(Cg)-Slc6a4tm1Kpl/J] and female C57BL/6J mice were used for breeding. Females were obtained from Charles River (Sulzfeld, Germany). Males were bred at the ZEMM animal facility. Temperature was set to 21±1°C, light-dark cycle was 12h/12h with lights on from 7 am. Standard rodent chow and water were available *ad libitum*. Two females were bred with one male. After determination of pregnancy by the observation of vaginal plugs, possibly pregnant females were housed separately.

PS. Pregnant females (n=22) were stressed as described above from E13 through E17. Control females (n=16) were left undisturbed in their home cages. Pregnant females were weight at E0, E13 and E17.

Pups. Pups were weaned at P25 weight at P5, P12, P21 and P60. Only female pups were used for behavioral testing. Male pups were housed in groups of 4 to 7. Female pups were housed from P28±1 onwards in groups of 3±1 at inverted day-night-cycle (12h:12h, lights on from 7 pm).

3.2.2. Behavioral testing

All behavioral tests were performed on female pups (n=20 for control groups, n=36-42 for PS groups) from P40 onwards under inverted day-night-cycle (12h:12h, lights on from 8 pm). Behavioral testing was performed together with Nicole Leibold (Maastricht University). Litters with less than 5 animals were excluded. First, anxiety-like behavior was tested in the EPM. Next, we assessed behavioral parameters reflecting different symptoms of depression. Behavioral despair was assessed using the PST, sociability in the 3-chamber-sociability test and anhedonia in the sucrose preference test. Finally, one week after behavioral testing, we measured the animals' CORT levels at baseline and after restraint stress. All tests were performed during the night-phase between 9 am and 6 pm, except for the sucrose preference test, where animals were tested between 8 am

and 8 pm. Animals were sacrificed one week after CORT measurement. Brains and adrenals were removed, immediately frozen in isopentane chilled on dry ice and frozen at -80C° for later use.

Elevated plus maze

Anxiety-like behavior was assessed in the EPM. As the name indicates, the maze is plus-shaped with two opposing closed arms (30 cm × 5 cm) that comprise 15 cm high walls and two opposing open arms without walls (30 cm × 5 cm, with 0.5 cm wide boundaries elevated 0.2 cm). It is worked from black opaque PERSPEX XT (TSE Systems, Inc., Bad Homburg, Germany), semi-permeable to infrared light. The four arms come together in the center (5 cm × 5 cm). The maze was placed 60 cm above floor level, illumination was low. Mice were tracked using infrared light from below the maze emitted by infrared LEDs. Each animal was placed in the center facing an open arm and allowed to explore the maze for 5 min. The area was cleaned with Terralin liquid (Schülke, Norderstedt, Germany) between trials. The trials were recorded using an infrared-sensitive camera. The VideoMot2 tracking software (TSE Systems, Bad Homburg, Germany) was used to analyze time spend and distance moved in the open arms, the closed arms and the center as well as the number of entries into the different arms. Two animals jumped from the EPM, these trials became void and animals were allowed to explore the maze another 5 min. This second exposure was not included as a trial but performed only for the need of having all mice being exposed at least 5 min to the EPM. Tests were performed during the night-phase between 9 am and 7 pm.

Porsolt swim test

The PST is used to assess behavioral despair in rodents (Borsini and Meli 1988; van Donkelaar et al. 2010). Mice were placed in a 40 cm tall persplex cylinder of 19 cm diameter filled up to 15 cm with water of 31±1°C and allowed to swim for 10 min. All mice of one cage were tested in separate cylinders in parallel. The setup was illuminated from below with a light-box. Behavior was recorded and mice tracked with the Ethovision Pro software (Noldus, The Netherlands). The calculated distance moved and latency to immobility are a correlate of mobility in mice in the PST. Tests were performed during the night-phase between 9 am and 7 pm. The cylinders were cleaned with Terralin and water was renewed between the trials. Temperature was verified using a thermometer.

Sucrose preference test

Anhedonic behavior can be investigated in the sucrose preference test by testing if mice prefer a sucrose solution over water when been given the choice. For this, animals were single housed for 12 h (dark phase, from 8 am to 8 pm) and given the free choice between regular tap water and 1% sucrose solution. Animals were not food- or water-deprived prior to testing. To exclude the influence a preferred site for drinking, the sugar bottle was positioned alternating on the right or left site. Bottles were weighed before and after testing. The bottles were prepared one day before the actual test in order to ensure that the solutions have the same temperature as the room, to avoid dripping of the solutions from the bottle. Sucrose preference was calculated as percent of volume of consumed sucrose solution of total volume consumed. A sucrose preference of less than 65% is considered anhedonic.

Sociability and locomotor activity in the 3-chamber sociability box

Sociability was analyzed in the 3-chamber sociability box. The transparent persplex setup was illuminated by the light box below and consisted of a neutral middle chamber, called in this work "center", and two side chambers of equal size that could be entered from the center. The side chambers contained each a smaller wire cage. In the first trial, the test subject ("test-mouse") was allowed to explore (only) the center for 5 min. In the second trial, a conspecific animal was introduced to one of the two wire cages and the test-mouse was allowed to explore all three chambers for 10 min. Both trials were recorded. Trial 1 was tracked with VideoMot2 in order to analyze the distance moved of the animals. Number of rearings and time spent in each chamber during trial 2 were assessed manually.

3.2.3. Physiological parameters

CORT at baseline and immediately after restraint stress

One week after the last behavioral test, we assessed hypothalamo-pituitary-adrenal axis function by measuring basic CORT levels and CORT levels immediately after acute stress. One day prior to measuring, we shaved the mice's legs. The next day, we fixated the mice using a cellulose face cloth and drew blood from the saphenous vein before the restraint stress (basal CORT) and immediately after 20 min of restriction stress. The stress procedure was performed as described for the PS. The lateral saphenous vein (Nr. 17 in Fig. 3.2-1) was punctured using Microlance needles (BD, 25 G 5/8", orange, 0,5 x 16 mm).

Blood samples were collected using heparinized capillary tubes (Microvette ® CB300, Sarstedt, Germany) and kept on ice. Samples were subsequently centrifuged for 5 min at 4°C at 3000g. Plasma was then stored at -80°C. Plasma CORT concentrations were determined using a radioactive immunoassay as described by van den Hove et al 2006. All samples were taken between 10 h and 13 h.

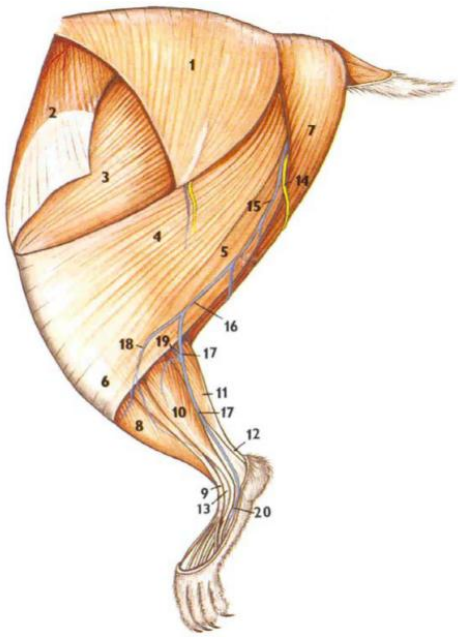

Figure 3.2-1 Scheme of the rodent leg with the saphenous vein. Picture from http://www.animalcare.ubc.ca/sop/ACS-2012-Tech02.pdf. Blood for CORT measurement was drawn from the saphenous vein.

Adrenal weight

Adrenals were dissected, placed on dry ice, stored at -80°C and weighed.

3.2.4. Processing of brain tissue

Frozen brains were semi-thawed on a 4°C cooling plate and rapidly dissected under the stereo microscope. The following brain regions were collected: prefrontal cortex, striatum, hippocampus, amygdala, hypothalamus, a part of the brain stem containing most of the raphe nuclei and cerebellum. The dissected tissues were immediately placed on dry ice and stored at -80°C. In order to avoid laterality effects in future data, we next crunched both frozen hippocampi of one animal using a metal cube filled with dry ice and piece of stainless steel cooled on dry ice (construction by Uwe Kiesel). The crunched and mixed tissue was then divided into two parts for further applications.

3.2.5. Gene expression analysis

RNA extraction

Total RNA including miRNA was extracted from half of the crunched hippocampus of the female mice using the miRNeasy Mini Kit (Qiagen). All centrifugation steps were performed at 12 000 g. Frozen samples were homogenized with one stainless steel bead (Qiagen) in 300 µl QIAzol Lysis reagent using the TissueLyzer (Qiagen, 20 Hz, 60 sec, 4°C). Homogenates were incubated at RT for 5 min, mixed with 60 µl of chloroform (Roth) and incubated for another 10 min on ice. After adding 50 µl of ddH2O, samples were transferred to 1.5-ml MaXtract High Density tubes (Qiagen) and centrifuged for 5 min at 17°C. The aqueous phase was transferred to a new tube, mixed with the 1.5 fold volume of ethanol (95-100%) and transferred to a RNeasy® Mini column. The column was then centrifuged for 15 sec, washed with 300 µl RWT buffer and again centrifuged for 15 sec. For DNA digestion, samples were incubated on the column with 10 µl of RNase-free DNase (Qiagen) and 70 µl RDD buffer for 15 min at RT. After another 15 s of centrifugation, samples were washed once with 350 µl of RWT buffer and twice with 500 µl of RPE buffer, followed by 2 min and 1 min of centrifugation in a new collection tube. Finally, columns were transferred to the final collection tubes, incubated with 50 µl of DNase/RNase free water for 1 min and then centrifuged for 1 min. RNA was stored at -80°C. RNA quality was checked on a 1.5% agarose gel with ethidium bromide and verified with the Experion (Biorad, München, Germany) according to the manufacturer's instructions. Experion RQI values were between 7.6 and 9.7 RNA concentrations were determined on the Nanodrop (Thermo Scientific, Wilmington, Delaware, USA).

Transcriptome analysis by mRNA sequencing

Library preparation. Library preparation and mRNA sequencing was performed by IGA Technologies (Udine, Italy). Only RNA samples with a RQI value of 8 or higher were chosen for RNAseq. In brief, poly-A containing mRNA was isolated from total RNA using poly-T oligo-attached magnetic beads. mRNA was then fragmented and transcribed into cDNA. After blunting the ends and adding an A overhang, adapters unique to each sample were ligated to the cDNA fragments so that reads could be associated to the right sample later on. The ligation product was then purified and amplified by PCR using primers targeting the adapters.

mRNA seq. mRNA sequencing was performed on an Illumina HiSeq2000 sequencer. Four barcoded samples were multi-plexed in one lane in order to obtain a minimum of 30 mio

reads per sample. The minimum uniquely aligned read number per analyzed sample was 26 mio. We analyzed a total of 48 animals (n=8/group).

Bioinformatics. Raw data were analyzed by Konrad Förstner at the Core Unit System Medicine (University of Würzburg) using Deseq2 and R. The gene lists with the differentially expressed genes are enclosed to this thesis (Appendix Table 3).

We were mainly interested in differentially expressed genes and pathways regarding the following comparisons:

Gene x environment (GxE) design:

- Genotype (G) effects: All *5-Htt*+/+ vs. all *5-Htt*+/- animals
- Environmental (E) effects: All control (C) vs. all PS animals
- GxE interaction: *5-Htt*+/+ control vs. *5-Htt*+/+ PS compared to *5-Htt*+/- control vs. *5-Htt*+/- PS

Resilience/sociability design:

- Social, resilient *5-Htt*+/+ PS vs. *5-Htt*+/+ control animals compared to unsocial, vulnerable *5-Htt*+/+ PS vs. *5-Htt*+/+ control animals
- Social, resilient *5-Htt*+/- PS vs. *5-Htt*+/- control animals compared to unsocial, vulnerable *5-Htt*+/- PS vs. *5-Htt*+/- control animals

Gene lists with a nonimal p-value of $p<0.01$ were used for performing several enrichment analyses using the online tool enrichr (Chen, Tan 2013). Single genes with an adjusted p-value of $p<0.05$ were discussed regardless of relevance in a pathway.

3.2.6. Statistics

Statistics on behavioral data were performed using IBM SPSS Statistics (IBM Deutschland GmbH, Ehningen, DE). Data were tested for normal distribution and homogeneity of variance. 2-factorial ANOVAs or Kruskal-Wallis tests were performed to test for overall main effects (genotype effects, PS effects, GxE interaction). Kruskal-Wallis tests were followed up with Mann-Whitney tests. Paired data were analyzed with the Wilcoxon-signed rank test. Correlations were either calculated with Spearman's or Pearson's correlation coefficient. P-values smaller than 0.05 were considered significant. P-values for the Mann-Whitney tests were Bonferroni-Holm corrected.

3.3. Results

3.3.1. Dam and pups weight

As shown in Table 3.3-1, control and PS dams had the same weight at E13, i.e. before the PS procedure. At E17, PS dams gained only 16% in weight, whereas C dams gained 23.9%. Litter size was the same in C and PS groups. Pups did not differ in weight at any time point (Table 3.3-2).

Table 3.3-1. Weight of dams, in g, and litter sizes.

Weight, g	E13	SEM	E17	SEM	Pups per litter
C	30.82	0.49	38.18	0.85	7.36
PS	30.82	0.32	35.75	0.42	7.64

Table 3.3-2 Weight of pups.

Weight, g	P5/6	SEM	P12/13	SEM	P21/22	SEM
C	2.66	0.12	5.54	0.18	7.62	0.54
PS	2.98	0.11	5.72	0.15	8.06	0.24

3.3.2. Offspring behavior

Female adult offspring underwent a battery of behavioral tests consisting of – in chronological order – the EPM, the PST and, performed in parallel, the 3-chamber-sociability test and sucrose preference test. Because the later grouping of the PS mice into social, resilient and unsocial, vulnerable groups is based on performance in the sociability test, the sociability data are presented first.

Sociability

Figure 3.3-1 displays the 3-chamber sociability setup (A). In the first trial, the test mouse was allowed to explore the middle chamber for 5 min. For the second trial, a conspecific target-mouse was alternately placed in one of the wire-cages in the right or left chamber. The test mouse was then allowed to explore all three chambers for 10 min. Figure 3.3-1 B) shows time spent in each of the chambers during the second trial, whereas C) displays the single measurements single values of time spent in the chamber with the target mouse (target chamber, TC).

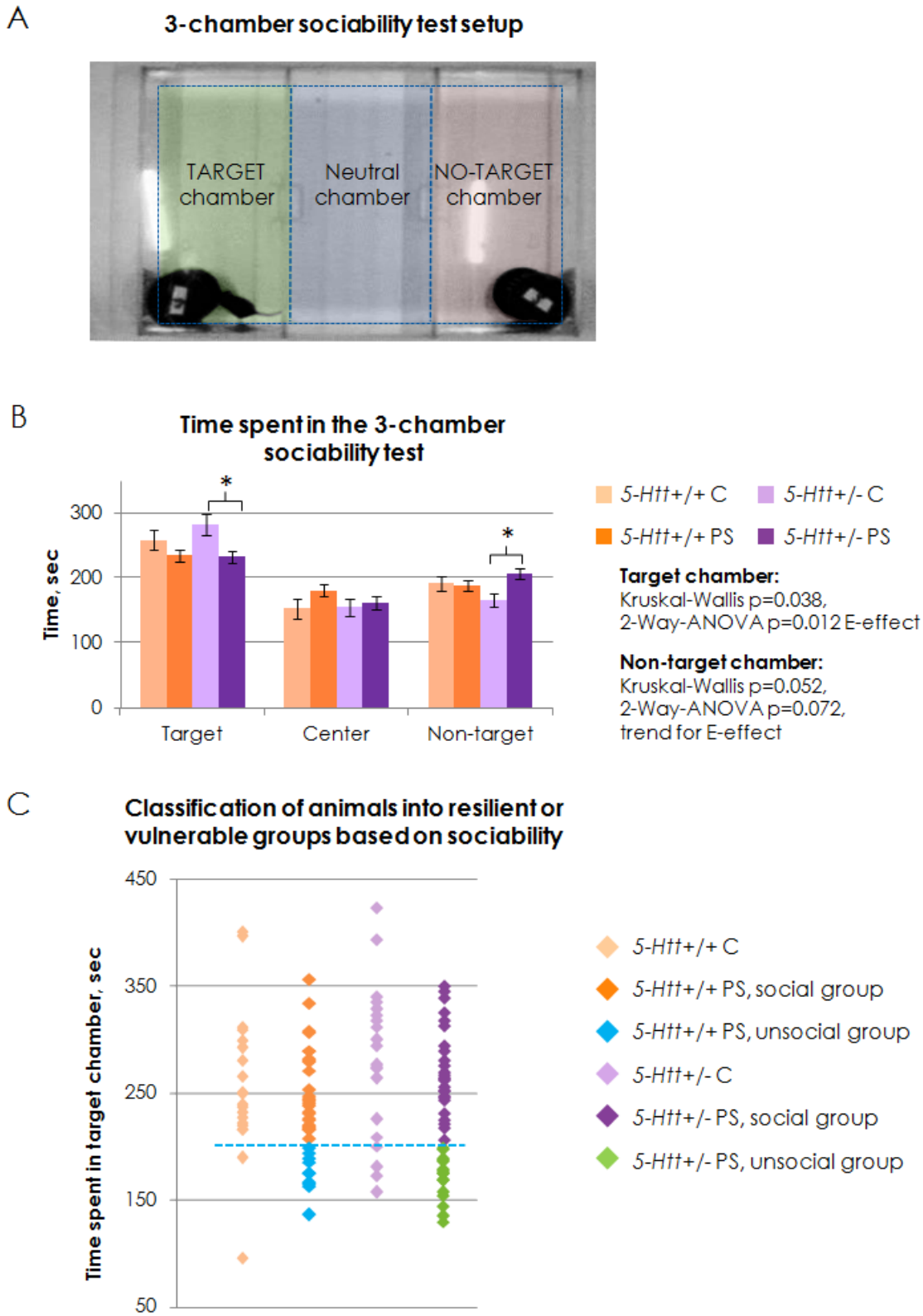

Figure 3.3-1 Sociability in the 3-chamber-sociability test in female *5-Htt+/+* and *5-Htt+/-* mice exposed to PS or not (control; C). A) Setup 3-chamber-sociability test. B) Time spent in each of the three chambers of the sociability test during a 10 min session. N=20 per group for C mice, N=36-40 per group for PS mice. Bars represent means, error bars SEM. Statistical testing as indicated. *p<0.05 in the Mann-Whitney Test. C) Classification of PS mice into social and unsocial groups based on time spent in target chamber. Social and unsocial mice were defined as mice that spent more/less than the 200 s expected by chance in the target chamber, respectively.

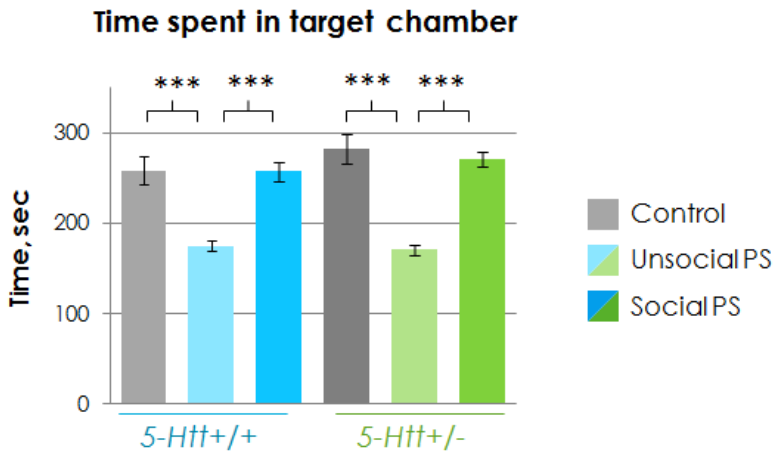

Figure 3.3-2 Time spent in the target chamber in the 3-chamber-sociability test during a 10 min session. Female *5-Htt+/+* and *5-Htt+/-* offspring exposed to PS or not (control; C). PS mice were grouped into social and unsocial groups as presented in Fig. 3.3-3. N=10-20. Kruskal-Wallis test followed by Man-Whithney test. ***p<0.0001. Bars represent means, error bars SEM.

As shown in Figure 3.3-1 B), overall, all groups spent more time in the chamber with the target mouse than expected by chance (t>200 s). However, animals exposed to PS spent less time in the target chamber (2-way-ANOVA, p=0.012). There is also a trend for those animals to spend more time in the chamber without the target (no-target-chamber, NTC, 2-way-ANOVA p=0.072), an effect which is particularly observed in *5-Htt+/-* animals.

Segregation of PS animals into social, resilient and unsocial, vulnerable groups. When looking at single values for time spent in the TC in Figure 3.3-1 C), we found that in every group a part of the animals spent less than 200s in the TC, hence showing no preference for the TC. For the PS animals, these animals were then categorized as "unsocial" /"vulnerable". PS animals that spent more than 200s in the TC were classified as "social" / "resilient". As the control animals were never exposed to PS, they were not divided into unsocial/social groups. When looking at time spent in TC after this classification (Fig. 3.3-2), we found that in both genotypes, PS-social animals spent the same amount of time in the TC as controls, whereas PS-unsocial animals spent significantly less time in the TC than the other two groups (KW p<0.0001, MWU p<0.0005 for all comparisons). The following behavioral data will be presented in this sociability-based setup.

Locomotor activity

The first trial of the sociability test was used to assess locomotor activity and rearing. As depicted in Figure 3.3-3, in the *5-Htt+/+* animals, locomotion was increased in the PS unsocial group compared to the social animals (K-W p=0.011, MWU p=0.009), whereas in the *5-Htt+/-* group, locomotor activity was decreased in unsocial PS animals when compared to the control animals (MWU p=0.036) during the first two minutes of the trial. After five minutes, the pattern was still the same, but less pronounced. No significant changes were found for the number of performed rearings.

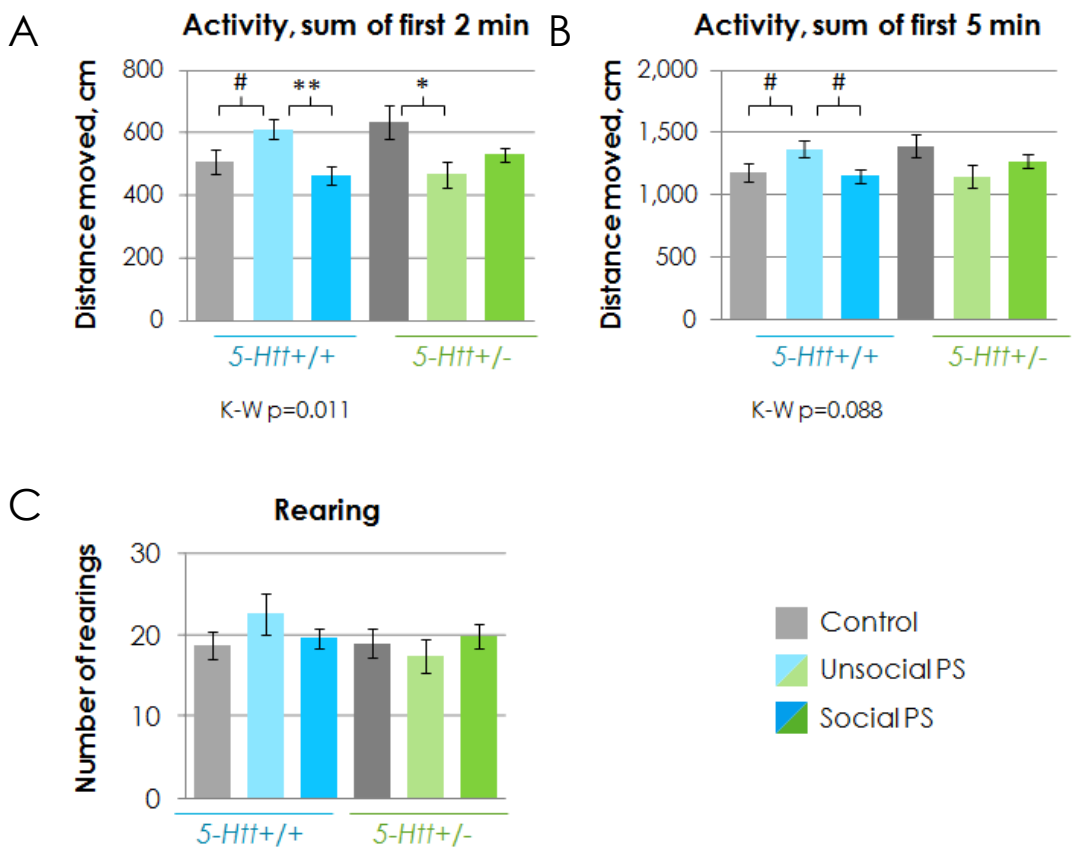

Figure 3.3-3 Locomoter activity as measured in form of distance moved and number of rearings in the first 5 min that mice spent exploring the neutral chamber of the 3-chamber-sociability setup. Female *5-Htt+/+* and *5-Htt+/-* offspring was exposed to PS or not (C). PS mice were grouped into social and unsocial groups as presented in Fig. 3.3-1. A) Distance moved in the first two minutes. B) Distance moved in the first five minutes. C) Number of rearings performed during the five minutes. N=10-20. Kruskal-Wallis test followed by Mann-Whithney test. *p<0.01, **p<0.001, #p<0.1. Bars represent means, error bars SEM.

Anxiety-like behavior in the elevated plus maze

Anxiety-like behavior was assessed using the EPM (Fig. 3.3.-4). Figure 3.3-4 A) shows time spent in the open and closed arms as well as the center of the EPM for all groups. Freezing on the open arms was not observed. In general, PS animals spent more time and covered a wider distance in the open arms of the EPM than control animals (MWU p=0.014 and p=0.010, respectively), indicating lower levels of anxiety in PS offspring. PS offspring did not, however, enter the open arms more often. While most groups showed a clear preference for the closed arms, the *5-Htt+/+* PS unsocial and *5-Htt+/-* PS social groups spent about the same amount of time in the closed and open arms. Thus, in the *5-Htt+/+* group the positive effect of PS on open arm exploration time is mainly observed in the vulnerable, unsocial PS offspring (K-W p=0.024, MWU p=0.016), while in the *5-Htt+/-* group, the social PS animals tended to spend more time in the open arms when compared to control animals (MWU p=0.056).

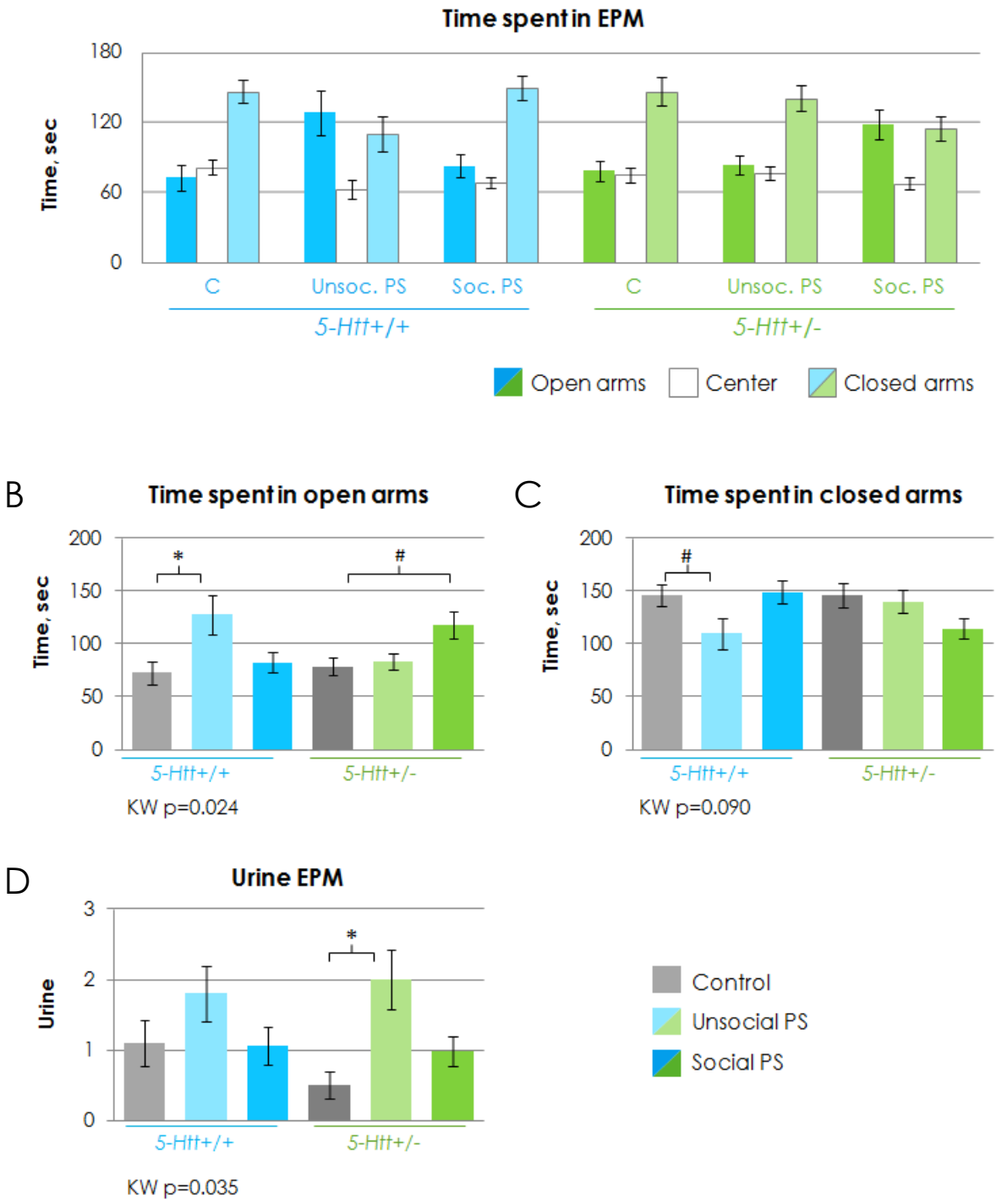

Figure 3.3-4 Anxiety-like behavior in the elevated plus maze (EPM). Female *5-Htt+/+* and *5-Htt+/-* offspring, exposed to PS or not (control, C), were tested for 5 min in the EPM. PS mice were furthermore grouped into social and unsocial groups as presented in Fig. 3.3-1. A) Time spent in the open (B) and closed arms (C) of the EPM. While most groups show a clear preference for the closed arms, the unsocial PS *5-Htt+/+* and the social *5-Htt+/-* mice do not. D) Urination in the EPM. N=10-20. Kruskal-Wallis test followed by Man-Whithney test. *p<0.01, **p<0.001, #p<0.1. Bars represent means, error bars SEM.

Behavioral despair in the PST

Distance moved in the PST did not differ between the groups (Fig. 3.3-5 A).

Anhedonia in the sucrose preference test

All groups showed a preference for the sucrose solution over water (ratio sugar solution/total volume > 65%), as shown in Figure 3.3-5 B). No differences between the groups were detected regarding sucrose preference. *5-Htt+/-* mice showed, however, a trend to drink less than *5-Htt+/+* mice (2-way-ANOVA, p=0.058).

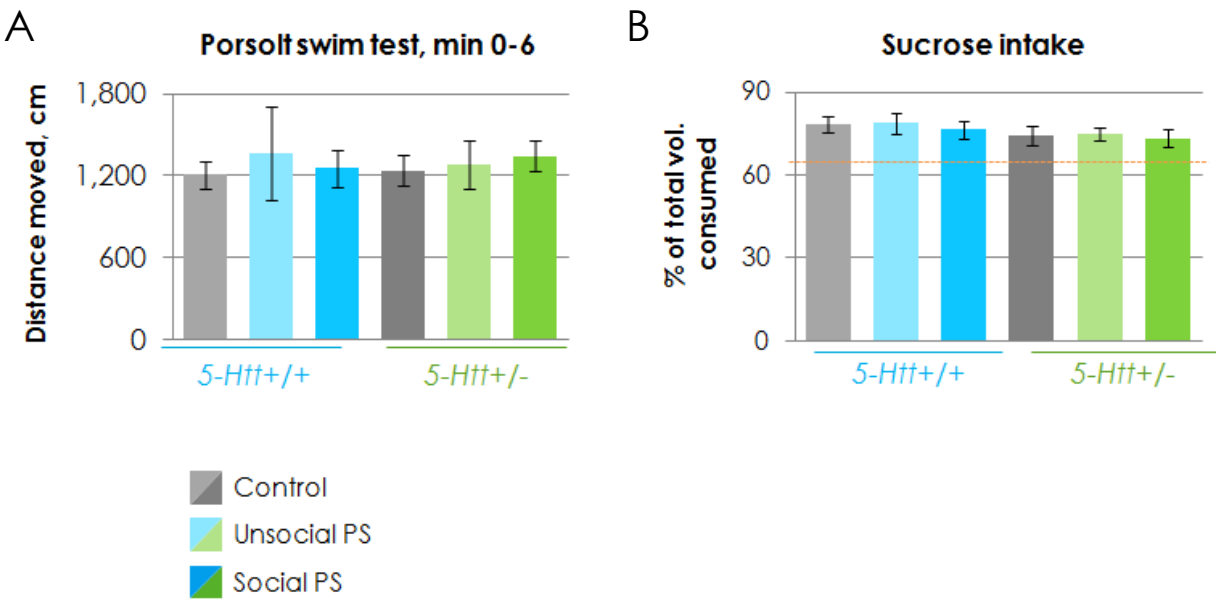

Figure 3.3-5 No effects of PS exposure on behavioral despair measured in the Porsolt swim test (PST) and the sucrose preference test in female *5-Htt+/-* mice. Female *5-Htt+/+* and *5-Htt+/-* offspring, exposed to PS or not (control, C). PS mice were furthermore grouped into social and unsocial groups as presented in Fig. 3.3-1. (A) Distance moved in the PST during the first 6 min. The animals were tested for 10 min in total. (B) Sucrose intake as calculated as the proportion of sucrose solution of total volume consumed.

3.3.3. Physiological parameters

CORT at baseline and immediately after restraint stress

Figure 3.3-6 depicts CORT levels at baseline and after 20 min of acute restraint stress. As to be expected, a significant increase of CORT after acute stress was detected. No difference in CORT levels between groups were detected in *5-Htt+/+* mice. *5-Htt+/-* PS unsocial animals showed a tendency for an increase in CORT when compared to controls (MWU, p=0.072).

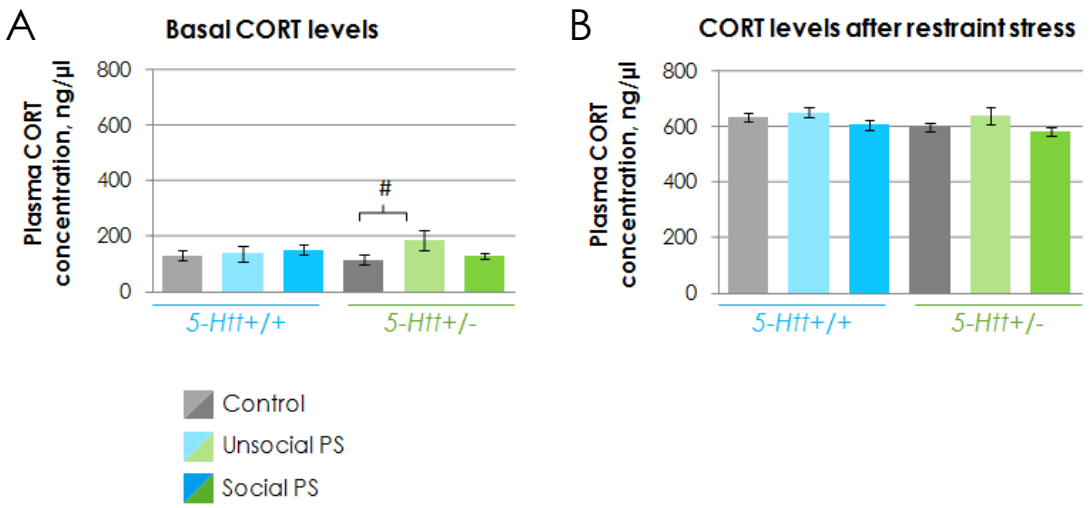

Figure 3.3-6 CORT levels at baseline and after acute stress. Female *5-Htt+/+* and *5-Htt+/-* offspring, exposed to PS or not (control, C). PS mice were grouped into social and unsocial groups as presented in Fig. 3.3-1. Plasma CORT concentration was assessed at baseline (A) and after 20 min of acute restraint stress (B).

Adrenal weight

Adrenal weight was normalized against body weight. No differences were detected (Fig. 3.3-7).

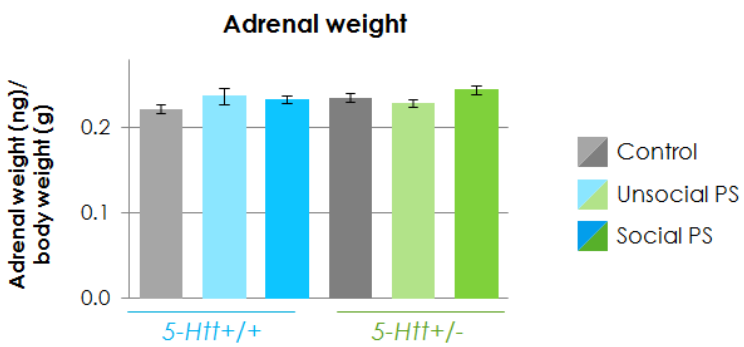

Figure 3.3-7 Adrenal weight. Female *5-Htt+/+* and *5-Htt+/-* offspring, exposed to PS or not (control, C). PS mice were grouped into social and unsocial groups as presented in Fig. 3.3-1. Adrenal weight was corrected for body weight.

3.3.4. Transcriptome analysis using mRNA sequencing

Gene expression screening using mRNA sequencing

We next conducted a transcriptome analysis with the aim to study the molecular mechanisms underlying the observed behavioral changes in the female PS offspring. Gene expression profiles of the hippocampus, a brain region not only involved in learning and memory but also in emotion and HPA axis regulation, were obtained by mRNA seq. First, we explored different comparisons: Genes differing between *5-Htt*+/+ and *5-Htt*+/- mice (genotype effects, G), genes changed between C and PS animals (environmental effect, E) and genes that were regulated by GxE interaction. We moreover investigated the genes differentially regulated in social and unsocial PS animals compared to controls in both genotypes. The transcriptome data will be discussed both in form of single differentially expressed genes (DEGs) as well as of enriched pathways and enriched functions determined using enrichr (Chen *et al.* 2013). An *adjusted* p<0.05 was applied for the discussion of single genes not involved in enriched pathways or terms, as it requires further validation using e.g. RT-qPCR or an enrichment analysis in order to

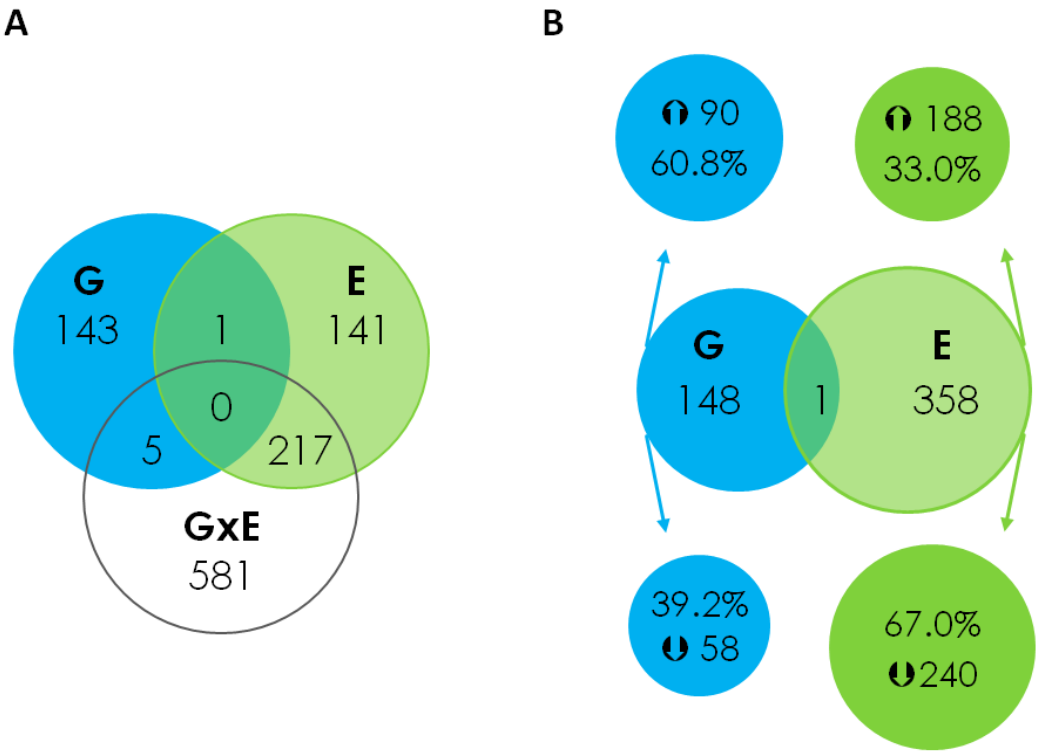

Figure 3.3-8 Number of differentially expressed genes (DEGs) in the hippocampus of female *5-Htt*+/- mice exposed to PS with p<0.01. Female *5-Htt*+/+ and *5-Htt*+/- offspring were exposed to PS or not (control, C). (A) Genes differentially expressed due to *5-Htt* genotype (G), PS exposure (E) or by their interaction (GxE). (B) DEGs up- and down-regulated due to a G- and E-effect. Transcriptome data were assessed using mRNAseq, n=8 for controls, n=16 for PS groups.

consider genes with a nominal p<0.01 as differentially expressed. When looking for enriched pathways and functions, gene lists with a nominal p<0.01 were used, as a significant enrichment can be regarded as supporting evidence for the validity of a candidate pathway. Furthermore, this increased gene numbers to an applicable magnitude as a gene list comprising only low numbers of genes cannot yield a proper enrichment analysis. For the overview of enrichment outputs, i.e. pathways, mammalian phenotype associated genes, terms that comprised less than three genes were excluded. VENN diagrams were furthermore also calculated with a nominal p<0.01. The complete enrichr output for every comparison, comprising mammalian phenotypes, KEGG pathways, GO terms of the categories biological processes, cellular component and molecular function, as well as ENCODE histone modifications and transcription factors, can be found in the Appendix Table 4. A part of these data is also presented in the results section.

As depicted in Figure 3.3-8, around 150 genes were affected by a G-effect and around 360 genes by PS, whereas the expression of a considerably higher number of genes, i.e. 803, was changed due to a GxE interaction (full gene lists in Appendix Table 3). Only few genes were regulated by both G and GxE, whereas the expression of 217 genes was affected both by PS (E) and in a GxE fashion. One gene*, mevalonate (diphospho) decarboxylase* (*Mvd*), was affected by G and E separately, but not by GxE. DEGs for social and unsocial mice will be discussed in the section "Genes regulated in social and unsocial female mice".

Changes in gene expression induced by the 5-Htt genotype

Table 3.3-3 A shows the most significantly DEGs affected by genotype (adjusted p<0.05). Strikingly, 14 out of those 18 DEGs were located on chromosome 11 (Chr 11), the top hit being *Slc6a4* aka *5-Htt*. As observed in our previous study, *5-Htt* expression was drastically increased, 132-fold, in *5-Htt*+/- mice when compared to *5-Htt*+/+ mice (Van den Hove and Jakob *et al.* 2011; Jakob 2012). Figure 3.3-9 illustrates the mapped mRNAseq reads at the *Slc6a4* locus. The reads of the *5-Htt*+/- animals cover the whole transcript except for exon 2, illustrating that it is not the wild-type but the truncated transcript that is overexpressed in the heterozygous animals. The most significant DEG after *5-Htt* was *Transient receptor potential cation channel, subfamily V, member 1 (Trpv1),* which was upregulated in *5-Htt*+/- mice with a log2FC of 2.25 when compared to *5-Htt*+/+ mice.

The Manhattan plot in Figure 3.3.-11 shows the p-values calculated for a G-effect plotted against the chromosomal location of all detected genes in our transcriptome data.

There seems to be a peak of G-affected DEGs in Chr 11. When applying a p-value for G-effect-DEGs of 0.01 (nominal) and then considering the chromosomal distribution of those genes, 21% of the DEGs were located on chr 11, which is significantly more than to be expected by chance, even after normalization for the number of genes per chromosome (one-dimensional Chi square test for chromosomal distribution, p<0.0001, residual chr11=32) (Fig. 3.3-10, lower graph, left). Interestingly, the majority of those DEGs were clustered in a 10 Mio kb DNA stretch just upstream of the *5-Htt*, as illustrated in Fig. 3.3-10 (upper graph, left), indicating a possible effect of the replacement of *5-Htt* exon 2 by a neo cassette on gene expression on Chr 11. In addition, the expression of the antisense *predicted gene 12343 (Gm12343)* that is transcribed from the opposite strand at the *5-Htt* locus and overlaps with the first exon and intron of *5-Htt* was increased in the *5-Htt+/-* animals as compared to the *5-Htt+/+* animals (p=4.20967E-13). We cannot exclude, however, that this effect is due to absent strand specifity of the sequencing results and only reflects the increased expression of the 5-Htt transcript. On the other hand, the manipulation at the *5-Htt* locus did not seem to have a high impact on the directly adjacent genes. Of the direct neighboring genes of *5-Htt*, *coiled-coil domain containing 55 (Ccdc55)* as well as the *predicted genes 22772* (*Gm22772*) and *22611 (Gm22611)* were not differentially expressed. The changes for *bleomycin hydrolase (Blmh)* (p=0.019) did not reach the cutoff of p<0.01.

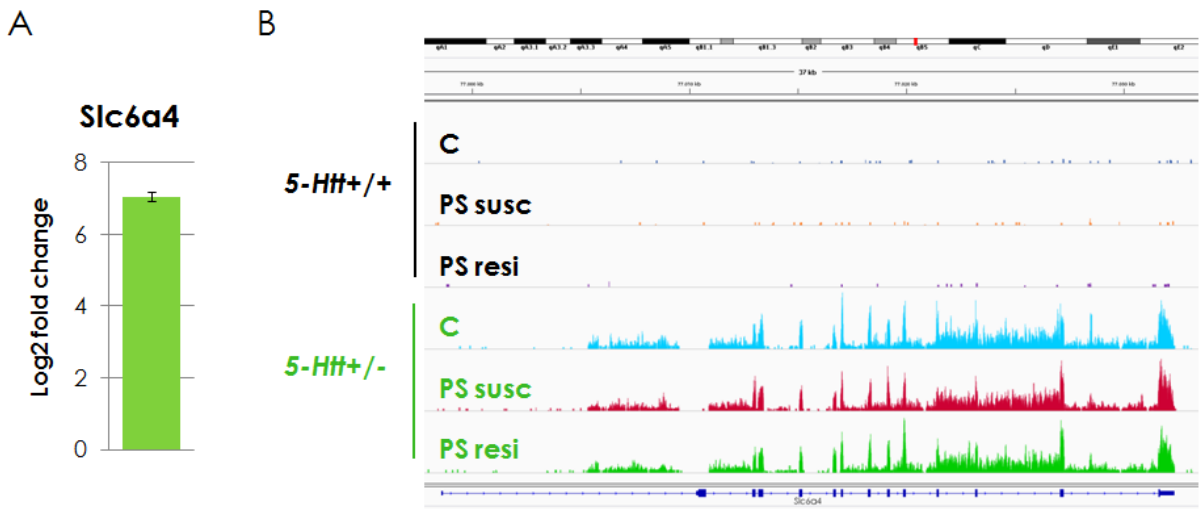

Figure 3.3-9 Expression the *5-Htt (Slc6a4)* gene in the hippocampus of female *5-Htt+/-* mice when compared to *5-Htt+/+* mice. Female *5-Htt+/+* and *5-Htt+/-* offspring were exposed to PS or not (control, C). PS animals were grouped into social and unsocial animals (see Fig. 3.3-1). Expression was assessed using mRNA sequencing. (A) Log2 fold change of *5-Htt* expression. N=24 per genotype. (B) Mapped reads at the *5-Htt* locus, note lacking reads of exon 2. N=8 per group.

Table 3.3-3 Differentially expressed genes (DEGs) in the hippocampus of female *5-Htt*+/- mice when compared to *5-Htt*+/+ mice (p<0.01), exposed to PS or not (control, C). Expression assessed using mRNA sequencing. N=24 per genotype. Chr = chromosome, Bm = Base mean of expression, log2FC = log2 fold change, Adj. p = adjusted p-value.

Symbol	Gene name	Chr	Bm	Log2FC	p	Adj. p
Slc6a4	solute carrier family 6 (neurotransmitter transporter, serotonin), member 4	11	330.3	7.05	0.0E+00	0.0E+00
Trpv1	transient receptor potential cation channel, subfamily V, member 1	11	28.3	2.25	1.9E-51	2.4E-47
Ctns	cystinosis, nephropathic	11	704.6	-0.19	4.9E-15	4.2E-11
Gm12343	predicted gene 12343	11	1.1	2.16	4.2E-13	2.5E-09
Shpk	sedoheptulokinase	11	225.9	0.30	4.8E-13	2.5E-09
Gm15772	predicted gene 15772	5	1245.0	0.38	1.8E-12	7.9E-09
Gm26665	predicted gene, 26665	1	19.9	-0.75	5.0E-12	1.9E-08
Nlrp1a	NLR family, pyrin domain containing 1A	11	13.9	0.85	4.1E-11	1.3E-07
Xaf1	XIAP associated factor 1	11	249.4	0.41	3.6E-09	1.0E-05
Rpl26	ribosomal protein L26	11	1160.2	-0.25	5.0E-09	1.3E-05
Gm15896	predicted gene 15896	9	14.3	-0.67	1.4E-08	3.3E-05
P2rx1	purinergic receptor P2X, ligand-gated ion channel, 1	11	18.6	0.67	2.2E-08	4.8E-05
Cyb5d2	cytochrome b5 domain containing 2	11	536.5	0.15	1.4E-07	2.8E-04
Nlrp1b	NLR family, pyrin domain containing 1B	11	28.8	-0.53	2.9E-07	5.4E-04
Nlrp1c-ps	NLR family, pyrin domain containing 1C, pseudogene	11	12.9	-0.70	5.2E-07	9.1E-04
Gucy2c	guanylate cyclase 2c	6	125.4	0.22	9.9E-07	1.6E-03
1200014J11Rik	RIKEN cDNA 1200014J11 gene	11	808.1	-0.11	1.6E-06	2.4E-03
P2rx5	purinergic receptor P2X, ligand-gated ion channel, 5	11	86.3	-0.43	3.4E-06	4.9E-03

Figure 3.3-10 Accumulation of differentially expressed genes (DEGs) on chr 11 in the hippocampus of female *5-Htt*+/- mice when compared to *5-Htt*+/+ mice in both PS studies. Female *5-Htt*+/+ and *5-Htt*+/- offspring were exposed to PS or not (control). Left side data from the present study (p<0.01), right side data from the old study (p<0.001presented in "2. Project 1"). In the present study, gene expression was assessed using mRNA sequencing, n=24 per genotype. In the old study, gene expression profiles were obtained using Affymetrix 430 2.0 GeneChip arrays, 2-4 hippocampi pooled per array, 5-6 arrays per genotyp. A) and C) show the DEGs on chr 11, including *Slc6a4* (*5-Htt*). Note the clustering of DEGs around 10 mio bp upstream of the *5-Htt*+/- locus. B) and D) show the number of DEGs per chromosome, normalized against the number of genes per chromosome. Note the unproportional high number of DEGs on chr 11.

►

Comparison of genotype effects in the two *5-Htt* PS studies - Differentially expressed genes on chr 11

Expression data 2nd PS study (mRNAseq p<0.01, 149 genes)

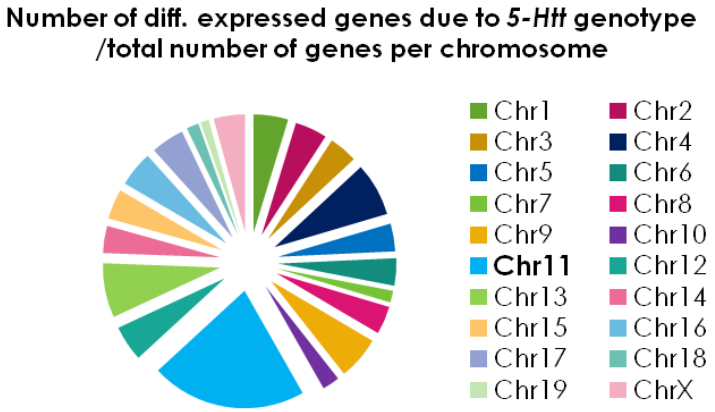

Expression data 1st PS study (MA p<0.001, 71 probesets)

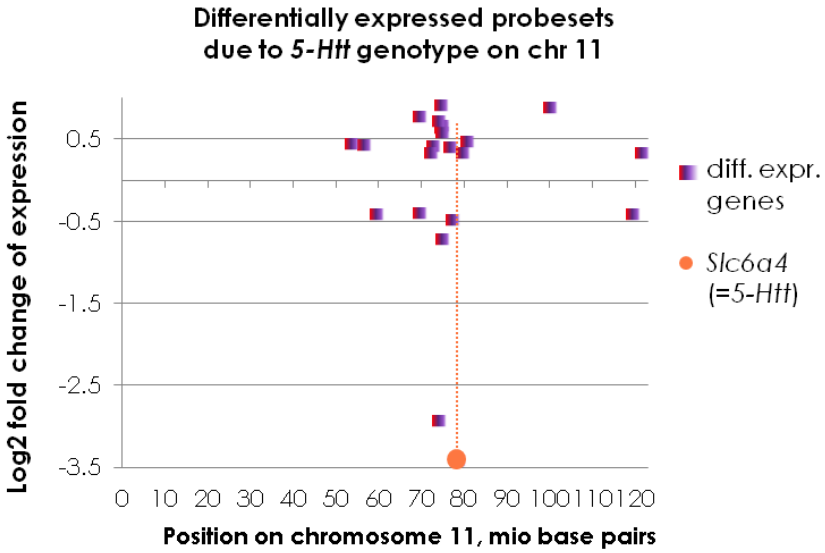

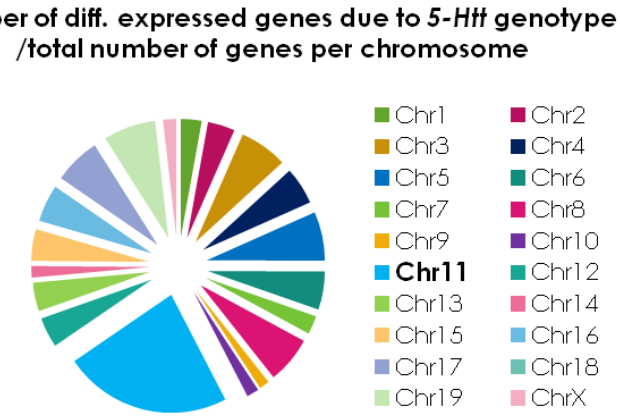

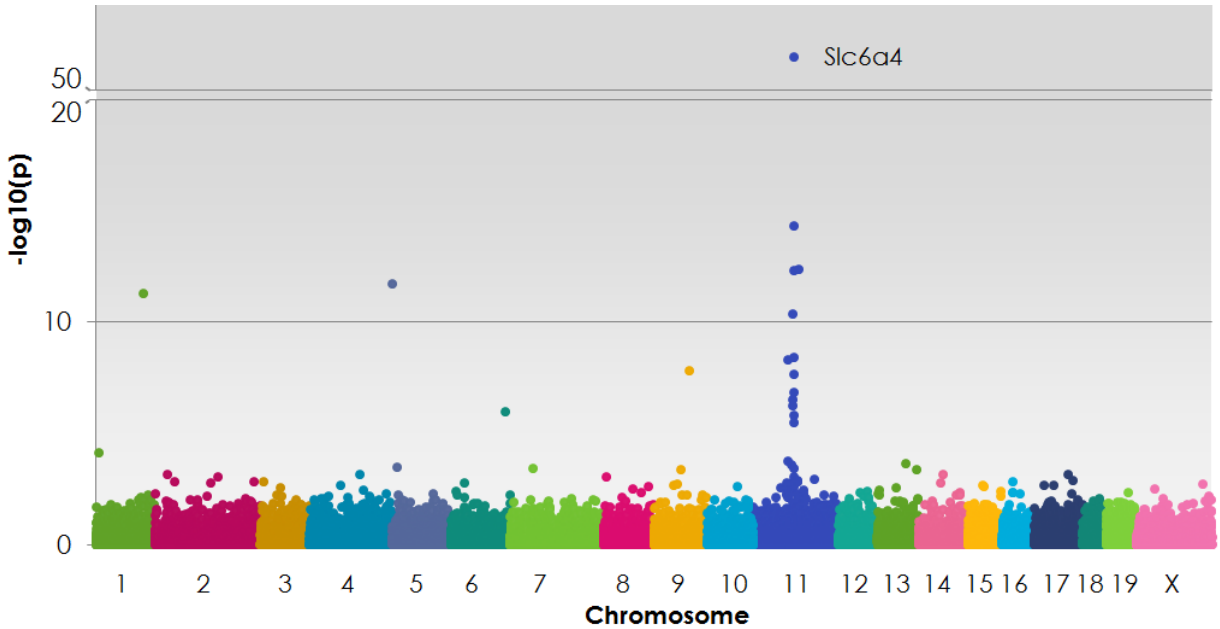

Figure 3.3-11 Manhatten plot showing an accumulation of differentially expressed genes on chr 11 in the hippocampus of female *5-Htt*+/- mice when compared to *5-Htt*+/+ mice, exposed to PS or not (control, C). Expression was assessed using mRNA sequencing. N= 24 per genotype.

Table 3.3-4 The most significant differentially expressed genes (DEGs) on chr 11 in the hippocampus of female *5-Htt*+/- mice when compared to *5-Htt*+/+ mice in the old PS study and the overlap with the new PS study. In the old study, gene expression profiles were obtaines using Affymetrix 430 2.0 GeneChip arrays, 2-4 hippocampi pooled per array, 5-6 arrays per genotyp. In the present study, gene expression was assessed using mRNA sequencing, n=24 per genotype. Log2FC = log2 fold change. Grey marks the overlapping genes in both studies.

Symbol	Gene name	Affy ID	Chr	Log2FC	p	adj. P	NCBI ID
Slc6a4	solute carrier family 6 (neurotransmitter transporter, serotonin), member 4	1417150_at	11	3.405	7.00E-15	3.16E-10	15567
Xaf1	XIAP associated factor 1	1443621_at	11	2.925	3.19E-09	7.20E-05	327959
Zzef1	zinc finger, ZZ-type with EF hand domain 1	1438691_at	11	-0.924	1.33E-08	0.00017	195018
NA	BG075643 (EST)	1441404_at	11	-0.866	1.47E-08	0.00017	NA
Ctns	cystinosis, nephropathic	1416274_at	11	-0.668	3.41E-07	0.00307	83429
12000-14J11Rik	RIKEN cDNA 1200014J11 gene	1439363_at	11	-0.635	4.86E-06	0.03653	66874

A similar picture emerges when comparing these findings to the results of the MA gene expression profiles of the hippocampus (see chapter 2). Table 3.3-4 shows the DEGs with an adjusted p<0.05 affected by genotype from the MA study. All six genes are located on Chr 11. Four of those six genes were also found in the mRNAseq study, with the same direction of the fold changes (adj. p<0.05, Table 3.3-3). In order to look at the distribution of DEGs affected by genotype over the different chromosome in the first study, the p-value was expanded to p<0.001 (71 annotated genes) for the DEGs, thereby providing a number of probesets similar to this analysis with the mRNAseq data (149 genes). The number of differentially expressed probesets (DEPSs) per chromosome was normalized for the different numbers of genes per chromosome. Similar to the mRNAseq results, an unproportioned part of the DEPSs, 23.1%, were located on Chr 11 (Fig. 3.3-11, right part) (one dimensional Chi square test, p<0.0001, residual chr11=16.7).

When analyzing *Xaf1* expression for single animals, the mapped reads exhibited a peculiar distribution. It seems that the calculated increase in *Xaf1* expression in 5-Htt+/- animals compared to 5-Htt+/+ animals was not so much based on the expression of the coding sequence but of the 3' UTR, indicating that, possibly, *Xaf1* is not overexpressed in *5-Htt+/-* mice. To be precise, all 5-Htt+/- animals expressed the 3' UTR, whereas only 2 out of 8 *5-Htt+/+* C and 3 out of 8 *5-Htt+/+* PS social animals expressed the 3' UTR at all. None of the *5-Htt+/+* PS unsocial animals expressed the *Xaf1* 3' UTR. Interestingly, the detected reads also do not map exactly to the 3' UTR. No other transcripts located in this genomic region are (yet) known.

Enrichment analyses using Enrichr yielded several enriched functions. Table 3.3-5 shows mammalian phenotypes (MP) enriched in the respective gene list. Amongst other, MPs with the terms "abnormal neuron physiology", "abnormal neuron morphology" and "abnormal nervous system" were found to be enriched in the G list. The DEGs associated with these terms show a high overlap, comprising nitric oxide synthase 3, endothelial cell (*Nos3*, *eNOS*), nuclear distribution gene E-like homolog 1 (*Ndel1*), distal-less homeobox 1 (*Dlx1*), reelin (*Reln*), and kinesin family member 1B (*Kif1b*). KEGG pathway analysis (Table 3.3-5, B) furthermore yielded one enriched pathway, i.e. "oxidative phosphorylation". NADH dehydrogenase (ubiquinone) Fe-S protein 5 (*Ndufs5*) and NADH dehydrogenase (ubiquinone) 1 alpha subcomplex, 5 (*Ndufa5*), both encoding subunits of complex I of the mitochondrial respiratory chain, as well as ATP synthase, H+ transporting, mitochondrial F0 complex, subunit C2 (subunit 9) (*Atp5g2*), which encodes a subunit of mitochondrial ATP synthase, were identified as DEGs within this pathway (Table 3.3-7, upper part, grey). The expression of all three genes was upregulated in *5-Htt+/-* animals.

As the number of DEGs used for analysis (149) was considerably lower than for the analysis of E and GxE effects (359 and 803 genes, respectively) and the identified pathway comprised only three genes, the enrichment analysis was repeated with a more adequate number of genes, using DEGs with $p<0.05$ (881 genes). Again, the top enriched pathway was the "oxidative phophorylation" pathway ($p=0.00005$) and it comprised, in addition to the three genes mentioned above, eight additional *Nduf* genes, ATP synthase, H+ transporting, mitochondrial F0 complex, subunit F2 (*Atp5j2*) and three cytochrome c oxidase subunits Vb (Cox5b), VIIa polypeptide 1 (*Cox7a1*) and VIIc (*Cox7c*) (Table 3.3-7). As illustrated in Figure 3.3-12, the affected *Nduf* genes all encode proteins of mitochondrial complex I, whereas the *ATP synthetase* genes belong to complexIV and the *cox* genes to complex V. Remarkably, all genes were again upregulated in *5-Htt+/-* mice, indicating small but significant effects of *5-Htt+/-* genotype on mitochondrial respiration. Next to this, mitochondrial ribosomal protein L14 (*Mrpl14*), a gene encoding a 39S subunit of the mitoribosome, was also upregulated in *5-Htt+/-* mice ($p<0.01$), although not being part of the KEGG pathway. Table 3.3-6 shows all Enrichr outputs related to mitochondria and ATP metabolism. Next to the KEGG pathway, several gene ontology (GO) terms associated with mitochondria and ATP metabolism were enriched, among them "ATP metabolic process", "mitochondrial respiratory chain complex I", and "oxidoreductase activity, acting on NAD(P)H". Interestingly, the above mentioned *Kif1b* encodes a motor protein concerned with the transport of mitochondria and synaptic vesicle precursors. Enrichr analysis furthermore identified several enriched GO terms in the category of Biological processes (3.3-5 C), two of them being rRNA related, showing a complete overlap, and two other being concerned with cell adhesion, showing a partial overlap.

Next to searching for enriched functions of the DEG, Enrichr also provides the possibility to search gene lists for enriched gene sets associated with specific histone modifications and transcription factors (TFs) using data from the ENCODE project. Appendix Table 4 shows the identified enriched gene sets and the corresponding histone modifications. Enrichr identified genes associated with H3K27ac (one hit) that marks active enhancers and H3K4me3 (three hits), which is associated with active and poised promoters, as shown in Table 3.3-5, D.

Table 3.3-5 Enrichment analysis of DEGs in the hippocampus of female *5-Htt*+/- offspring when compared to *5-Htt*+/+ offspring (p<0.05). Female *5-Htt*+/+ and *5-Htt*+/- offspring were exposed to PS or not (control). Expression was assessed using mRNA sequencing, n=24 per genotype. Enrichment analysis performed using the Enrichr online tool (Chan Tan 2013) with DEGs p<0.01. Overl. = the number of DEGs out of the total number of genes in this term.

Enriched term	Term ID	Overl.	P	Genes
A) Mammalian phenotypes				
Abnormal neuron physiology	MP0004811	7/310	8,24E-05	
Abnormal chemical nociception	MP0002735	3/35	0,00029	
Abnormal heart ventricle	MP0008775	3/41	0,00044	
Abnormal thermal nociception	MP0002733	4/102	0,00045	
Abnormal defecation	MP0003866	3/58	0,00115	
Abnormal neuron morphology	MP0002882	10/1007	0,00166	
Abnormal craniofacial develop	MP0003935	5/269	0,00224	
Abnormal mechanical nociception	MP0002734	3/79	0,00270	
Abnormal blastocyst morphology	MP0004957	3/101	0,00527	
Abnormal palate morphology	MP0003755	4/213	0,00616	
Abnormal nervous system	MP0003861	8/856	0,00759	
B) KEGG pathways				
Oxidative phosphorylation	HSA00190	3/128	0,04252	Ndufs5, Atp5g2, Ndufa5
C) GO: Biological processes				
Regulation of blood vessel size	GO:0050880	4/63	0,00046	Slc6a4, Nos3, Gclc, P2rx1
Regulation of tube size	GO:0035150	4/64	0,00048	Slc6a4, Nos3, Gclc, P2rx1
Rrna processing	GO:0006364	5/120	0,00056	Heatr1, Utp20, Exosc5, Gemin4, Rpl26
Rrna metabolic process	GO:0016072	5/126	0,00069	Heatr1, Utp20, Exosc5, Gemin4, Rpl26

ATP metabolic process	GO:0046034	8/377	0,00105	Stoml2, Myh8, Recql4, Ctns, Kif1b, Dnah9, Atp5g2, Chd8
Vascular process in circulatory system	GO:0003018	4/86	0,00138	Slc6a4, Nos3, Gclc, P2rx1
Purine ribonucleoside monophosphate metabolic process	GO:0009167	8/402	0,00157	Stoml2, Myh8, Recql4, Ctns, Kif1b, Atp5g2, Chd8, Dnah9
Purine nucleoside monophosphate metabolic process	GO:0009126	8/403	0,00159	Stoml2, Myh8, Recql4, Ctns, Kif1b, Atp5g2, Chd8, Dnah9
Ribonucleoside monophosphate metabolic process	GO:0009161	8/416	0,00193	Stoml2, Myh8, Recql4, Ctns, Kif1b, Atp5g2, Chd8, Dnah9
Ncrna processing	GO:0034470	6/241	0,00210	Utp20, Exosc5, Rpl26, Heatr1, Tarbp2, Gemin4
Attachment of spindle microtubules to kinetochore	GO:0008608	2/11	0,00214	Sgol1, Aurkb
Ncrna metabolic process	GO:0034660	7/332	0,00226	Utp20, Exosc5, Rpl26, Mael, Heatr1, Tarbp2, Gemin4
Nucleoside monophosphate metabolic process	GO:0009123	8/427	0,00227	Stoml2, Myh8, Recql4, Ctns, Kif1b, Atp5g2, Chd8, Dnah9
Organophosphate biosynthetic process	GO:0090407	8/436	0,00257	Stoml2, Gucy2c, Dpm3, Lpin3, Atp5g2, Pld2, Tsta3, Mvd
Positive regulation of TOR signaling	GO:0032008	2/16	0,00412	Lamtor2, Reln
D) Histone modifications				
H3K27ac	PANC1	18/1999	0,00670	
H3K4me3	HMF	9/874	0,02618	
H3K4me3	K562	25/3460	0,02049	
H3K4me3	NT2D1	16/1999	0,02976	

Table 3.3-6 Enriched terms associated with mitochondrial respiration in the hippocampus of female *5-Htt+/-* offspring when compared to *5-Htt+/+* offspring (p<0.05). Female *5-Htt+/+* and *5-Htt+/-* offspring were exposed to PS or not (control). Expression was assessed using mRNA sequencing, n=24 per genotype. Enrichment analysis performed using the Enrichr online tool (Chan Tan 2013) using DEGs with p<0.01. Overl. = the number of DEGs out of the total number of genes in this term.

Term	Term ID	Overl.	p	Genes
A) KEGG pathways				
OXIDATIVE PHOSPHORYLATION	HSA00190	3/128	0,0425	NDUFS5, ATP5G2, NDUFA5
B) GO: Biological processes				
ATP metabolic process	GO:0046034	8/377	0,0010	STOML2, MYH8, RECQL4, CTNS, KIF1B, DNAH9, ATP5G2, CHD8
Purine nucleoside monophosphate metabolic process	GO:0009126	8/403	0,0016	STOML2, MYH8, RECQL4, CTNS, KIF1B, ATP5G2, CHD8, DNAH9
C) GO: Cellular component				
Mitochondrial respiratory chain complex I	GO:0005747	2/47	0,0281	NDUFS5, NDUFA5
NADH dehydrogenase complex	GO:0030964	2/47	0,0281	NDUFS5, NDUFA5
Respiratory chain complex I	GO:0045271	2/47	0,0281	NDUFS5, NDUFA5
D) GO: Molecular function				
ATP binding	GO:0005524	15/1494	0,0047	MYH8, RECQL4, GUCY2C, UBE2G1, P2RX5, P2RX1, KIF1B, SHPK, AURKB, MVD, BLK, DNAH9, TRPV1, CHD8, GCLC
Oxidoreductase activity, acting on NAD(P)H	GO:0016651	3/104	0,0150	NDUFS5, NOS3, NDUFA5
NADH dehydrogenase (ubiquinone) activity	GO:0008137	2/46	0,0225	NDUFS5, NDUFA5
NADH dehydrogenase activity	GO:0003954	2/46	0,0225	NDUFS5, NDUFA5
NADH dehydrogenase (quinone) activity	GO:0050136	2/46	0,0225	NDUFS5, NDUFA5
Oxidoreductase activity, acting on NAD(P)H, quinone or similar compound as acceptor	GO:0016655	2/60	0,0362	NDUFS5, NDUFA5
ATPase activity	GO:0016887	5/395	0,0438	MYH8, RECQL4, KIF1B, CHD8, DNAH9

Table 3.3-7 DEGs in the pathway "oxidative phosphorylation", enriched in the hippocampus of female *5-Htt+/-* offspring when compared to *5-Htt+/+* offspring. Female *5-Htt+/+* and *5-Htt+/-* offspring were exposed to PS or not (control). Expression was assessed using mRNA sequencing, n=24 per genotype. Enrichment analysis performed using the Enrichr online tool (Chan Tan 2013). Log2FC = log 2 fold change, SE(lFC) = standard error of the mean of the log2 fold change, Dir. = direction. Grey background = DEGs p<0.01, white background DEGs p<0.05.

Symbol	Description	Log2FC	SE(lFC)	p	Dir.
Ndufa5	NADH dehydrogenase (ubiquinone) 1 alpha subcomplex, 5	0.122	0.042	0.004	↑
Ndufs5	NADH dehydrogenase (ubiquinone) Fe-S protein 5	0.097	0.033	0.004	↑
Atp5g2	ATP synthase, H+ transporting, mitochondrial F0 complex, subunit C2 (subunit 9)	0.079	0.027	0.004	↑
Ndufa12	NADH dehydrogenase (ubiquinone) 1 alpha subcomplex, 12	0.061	0.026	0.018	↑
Ndufa2	NADH dehydrogenase (ubiquinone) 1 alpha subcomplex, 2	0.137	0.058	0.019	↑
Ndufa4	NADH dehydrogenase (ubiquinone) 1 alpha subcomplex, 4	0.057	0.029	0.048	↑
Ndufa7	NADH dehydrogenase (ubiquinone) 1 alpha subcomplex, 7 (B14.5a)	0.074	0.033	0.025	↑
Ndufb7	NADH dehydrogenase (ubiquinone) 1 beta subcomplex, 7	0.103	0.045	0.023	↑
Ndufc2	NADH dehydrogenase (ubiquinone) 1, subcomplex unknown, 2	0.055	0.027	0.038	↑
Ndufs6	NADH dehydrogenase (ubiquinone) Fe-S protein 6	0.099	0.046	0.032	↑
Ndufs8	NADH dehydrogenase (ubiquinone) Fe-S protein 8	0.097	0.048	0.043	↑
Atp5j2	ATP synthase, H+ transporting, mitochondrial F0 complex, subunit F2	0.079	0.040	0.049	↑
Cox5b	cytochrome c oxidase subunit Vb	0.090	0.044	0.042	↑
Cox7a1	cytochrome c oxidase subunit VIIa 1	0.261	0.124	0.034	↑
Cox7c	cytochrome c oxidase subunit VIIc	0.073	0.033	0.025	↑

OXIDATIVE PHOSPHORYLATION

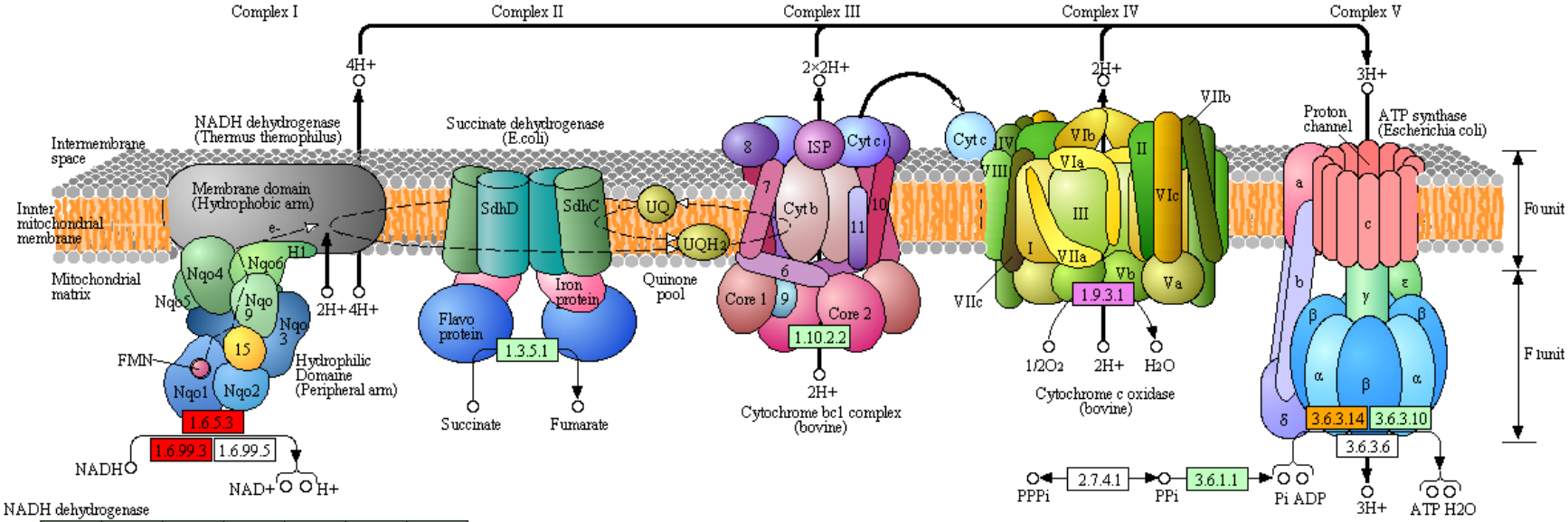

NADH dehydrogenase

E	ND1	ND2	ND3	ND4	ND4L	ND5	ND6										
E	Ndufs1	Ndufs2	Ndufs3	Ndufs4	Ndufs5	Ndufs6	Ndufs7	Ndufs8	Ndufv1	Ndufv2	Ndufv3						
B/A	NuoA	NuoB	NuoC	NuoD	NuoE	NuoF	NuoG	NuoH	NuoI	NuoJ	NuoK	NuoL	NuoM	NuoN			
B/A	NdhC	NdhK	NdhJ	NdhH	NdhA	NdhI	NdhG	NdhE	NdhF	NdhD	NdhB	NdhL	NdhM	NdhN	HoxE	HoxF	HoxU
E	Ndufa1	Ndufa2	Ndufa3	Ndufa4	Ndufa5	Ndufa6	Ndufa7	Ndufa8	Ndufa9	Ndufa10	Ndufab1	Ndufa11	Ndufa12	Ndufa13			
E	Ndufb1	Ndufb2	Ndufb3	Ndufb4	Ndufb5	Ndufb6	Ndufb7	Ndufb8	Ndufb9	Ndufb10	Ndufb11	Ndufc1	Ndufc2				

Succinate dehydrogenase / Fumarate reductase

E	SDHC	SDHD	SDHA	SDHB		
B/A	SdhC	SdhD	SdhA	SdhB		
			FrdA	FrdB	FrdC	FrdD

Cytochrome c reductase

E/B/A	ISP	Cyt b	Cyt 1					
E				COR1	QCR2	QCR6	QCR7	QCR8	QCR9	QCR10

Cytochrome c oxidase

E	COX10		COX3	COX1	COX2	COX4	COX5A	COX5B	COX6A	COX6B	COX6C	COX7A	COX7B	COX7C	COX8	E/B/A		
																COX11	COX15	COX17
B/A	CyoE	CyoD	CyoC	CyoB	CyoA													
		CoxD	CoxC	CoxA	CoxB													
		QoxD	QoxC	QoxB	QoxA													

Cytochrome c oxidase , cbb3-type

B	I	II	IV	III

Cytochrome bd complex

B/A	CydA	CydB

F-type ATPase (Bacteria)

alpha	beta	gamma	delta	epsilon
a	b	c		

F-type ATPase (Eukaryotes)

alpha	beta	gamma	delta	epsilon	
OSCP	a	b	c	d	e
f	g	f6/h	j	k	8

V/A-type ATPase (Bacteria, Archaeas)

A	B	C	D	E	F	G/H
I	K					

V-type ATPase (Eukaryotes)

A	B	C	D	E	F	G	H
a	c	d	e	S1			

00190 5/7/14

Effects of PS exposure on gene expression

Of the 359 genes affected by PS exposure, one third was up-regulated whereas two thirds were down-regulated in expression. Although the number of DEGs affected by PS with p<0.01 is considerably higher than those affected by genotype, only one gene remains significant after correction for multiple testing. The most significantly DEG (adjusted p<0.05) affected by PS was serum/glucocorticoid regulated kinase 1 (*Sgk1*), which was down-regulated in PS animals with a log2FC of 0.34 (FC1.27) compared to controls, especially in *5-Htt+/-* mice (Table 3.3-8). Enrichr identified several enriched MPs centering around survival and longevity, such as "premature death", "mortality/aging", "postnatal lethality" and "preweaning lethality" (Table 3.3-9, A). Next to this, several enriched MPs connected to the immune system were detected, i.e. "abnormal immune system", "abnormal innate immunity" and "abnormal inflammatory response". Table 3.39 B) shows enriched KEGG pathways, among them the p53 signaling pathway, which is depicted in Figure 3.3-13, and the glycine, serine and threonine metabolism pathway were identified to be enriched. Among the 14 most significantly enriched GO Biological processes terms (p<0.005) were the terms "L-serine metabolic process", "serine family amino acid biosynthetic process", "cellular amino acid metabolism" and "alpha-amino acid biosynthetic process".

Furthermore, the term "negative regulation of ERK1 and ERK2 cascade" was enriched. Enrichr analysis of gene sets associated with specific histone modifications yielded six hits on H3K4me3 and one on H3K27me3, indicating a profound PS-induced effect on histone methylation (Table 3.3-9, D).

Table 3.3-8 DEGs affected by PS exposure in the hippocampus of female *5-Htt+/-* and 5-Htt+/+ PS offspring when compared to control offspring (adjusted p<0.05). Female *5-Htt+/+* and *5-Htt+/-* offspring were exposed to PS or not (control). Expression was assessed using mRNA sequencing, n=16 for controls, n=32 for the PS group. Chr = chromosome, Bm = Base mean expression, Log2FC = log 2 fold change, Adj. p = adjusted p-value.

Symbol	Gene name	Chr	Bm	Log2FC	p	Adj. p
Sgk1	serum/glucocorticoid regulated kinase 1	10	2607.0	-0.34	4.3E-08	0.00077

Figure 3.3-12 DEGs in the KEGG pathway "oxidative phosphorylation", enriched in the hippocampus of female *5-Htt+/-* offspring when compared to *5-Htt+/+* offspring. Female *5-Htt+/+* and *5-Htt+/-* offspring were exposed to PS or not (control). Expression was assessed using mRNA sequencing, n=24 per genotype. Enrichment analysis performed using the enrichr online tool (Chan Tan 2013) with DEGs p<0.05. Pathway was created using KEGG (Kanehisa and Goto 2000).

Table 3.3-9 Enriched pathways and terms in the hippocampus of female *5-Htt*+/- and *5-Htt*+/+ PS offspring when compared to control offspring. Female *5-Htt*+/+ and *5-Htt*+/- offspring were exposed to PS or not (control). Expression was assessed using mRNA sequencing, n=16 for controls, n=32 for the PS group. Enrichment analysis performed using the Enrichr online tool (Chan Tan 2013) with DEGs p<0.01. Overl. = number of DEGs/total number of genes in this pathway or term.

Enriched term	Term ID	Overl.	P	Genes
A) Mammalian phenotype				
Premature death	MP0002083	29/969	0,00000	
Mortality/aging	MP0010768	32/1256	0,00000	
Abnormal survival	MP0010769	31/1230	0,00000	
Mammalian phenotype	MP0000001	62/3774	0,00001	
Increased sensitivity to induced morbidity/mortality	MP0009763	13/282	0,00001	
Abnormal body size	MP0003956	41/2129	0,00002	
Postnatal lethality	MP0002082	27/1115	0,00002	
Preweaning lethality	MP0010770	27/1116	0,00002	
Abnormal fat pad	MP0005334	11/235	0,00004	
Abnormal blood homeostasis	MP0009642	36/1835	0,00006	
Abnormal lung morphology	MP0001175	14/403	0,00008	
Abnormal immune system	MP0002722	19/749	0,00025	
Abnormal adipose tissue	MP0005452	14/457	0,00029	
Abnormal innate immunity	MP0002419	13/412	0,00037	
Abnormal blood vessel	MP0001614	19/779	0,00040	
Perinatal lethality	MP0002081	22/982	0,00042	
Abnormal skeleton morphology	MP0005508	7/128	0,00044	
Abnormal white adipose	MP0002970	9/221	0,00055	
Abnormal posterior eye	MP0005195	13/434	0,00059	
Muscle weakness	MP0000747	5/64	0,00067	
Abnormal anterior eye	MP0005193	11/339	0,00085	
Abnormal wound healing	MP0005023	6/104	0,00088	

Abnormal glucose homeostasis	MP0002078	16/637	0,00089
Abnormal female reproductive	MP0003699	14/518	0,00097
Abnormal inflammatory response	MP0001845	17/707	0,00098
Abnormal xenobiotic induced	MP0009765	6/108	0,00106
Abnormal neuron morphology	MP0002882	21/1007	0,00144
Abnormal fertility/fecundity	MP0002161	22/1089	0,00163
Abnormal hormone level	MP0003953	16/678	0,00169
Skeleton phenotype	MP0005390	9/266	0,00194
Abnormal liver physiology	MP0000609	12/442	0,00219
Altered response to	MP0003075	4/54	0,00283
Abnormal muscle physiology	MP0002106	7/179	0,00287
Eye inflammation	MP0001851	4/56	0,00320
Abnormal cell physiology	MP0005621	10/349	0,00355
Emphysema	MP0001958	3/28	0,00375
Abnormal urine homeostasis	MP0009643	9/297	0,00396
Abnormal fat cell	MP0009115	5/99	0,00413
Abnormal somatic nervous	MP0002752	15/676	0,00421
Muscle phenotype	MP0005369	8/248	0,00456
Abnormal brain morphology	MP0002152	22/1189	0,00476
Abnormal body te	MP0005535	6/154	0,00580
Abnormal skeleton development	MP0002113	11/443	0,00643
Abnormal lean body	MP0003959	4/71	0,00711
Abnormal motor capabilities/c	MP0002066	25/1483	0,00831
Abnormal kidney morphology	MP0002135	13/592	0,00834
Abnormal male reproductive	MP0003698	14/668	0,00916
Abnormal eye size	MP0002697	6/173	0,00985

B) KEGG pathways

Adipocytokine signaling pathway	6/72	0,00199	SLC2A1, IRS2, ADIPOR2, NFKBIA, TNFRSF1A, CPT1A
P53 signaling pathway	5/68	0,00783	SERPINE1, CCND3, GADD45G, CCNG2, CDKN1A

Renal cell carcinoma		4/69	0,03558	PGF, FLCN, SLC2A1, PIK3R5
Chronic myeloid leukemia		4/76	0,04732	STAT5B, NFKBIA, PIK3R5, CDKN1A
Glycine serine and threonine metabolism		3/45	0,04824	SHMT2, PHGDH, PSAT1

C) GO: Biological processes

Sulfur compound metabolic process	GO:0006790	14/314	0,00031	STAT5B, EIF2B4, MPST, TPST2, PHGDH, ELOVL1, GSTM4, MVK, MVD, BCAN, SDC4, SLC35B2, NUDT7, HS6ST1
L-serine metabolic process	GO:0006563	3/8	0,00046	SHMT2, PHGDH, PSAT1
Multi-organism reproductive process	GO:0044703	8/140	0,00143	PGF, STAT5B, MAFF, UCP2, VGF, AVP, ADIPOR2, ENDOU
Serine family amino acid biosynthetic process	GO:0009070	3/14	0,00176	SHMT2, PHGDH, PSAT1
Cellular amino acid metabolic process	GO:0006520	15/421	0,00177	DDAH2, YARS, PRODH, SHMT2, PSAT1, SLC7A5, ACMSD, DDC, PADI2, STAT5B, EIF2B4, DALRD3, PHGDH, GSTM4, ACY1
Negative regulation of ERK1 and ERK2 cascade	GO:0070373	4/35	0,00238	FLCN, SPRY1, CNKSR3, SLC9A3R1
Regulation of sodium ion transport	GO:0002028	5/60	0,00250	ACTN4, SLC9A3R1, PER1, SCN5A, CNKSR3
Multi-multicellular organism process	GO:0044706	7/121	0,00263	PGF, STAT5B, MAFF, UCP2, AVP, ADIPOR2, ENDOU
Regulation of sodium ion transmembrane transport	GO:1902305	4/38	0,00313	SCN5A, ACTN4, CNKSR3, SLC9A3R1
Acetyl-coa metabolic process	GO:0006084	3/19	0,00378	MVD, NUDT7, MVK
Positive regulation of lipid catabolic process	GO:0050996	3/20	0,00430	IRS2, PNPLA2, CPT1A
Negative regulation of myeloid cell differentiation	GO:0045638	5/69	0,00439	STAT5B, ZFP36, NFKBIA, WDR61, TOB2
Alpha-amino acid biosynthetic process	GO:1901607	5/69	0,00439	EIF2B4, PADI2, SHMT2, PHGDH, PSAT1
Mammary gland development	GO:0030879	3/21	0,00487	IRS2, GLI2, NOTCH4

D) Histone modifications	Cell line		
H3K4me3	AG04449	20/968	0,01079
H3K4me3	HL60	14/686	0,03355
H3K4me3	HVMF	16/838	0,04004
H3K4me3	GM12878	25/1447	0,03397
H3K4me3	GM12866	28/1618	0,02488
H3K4me3	AG10803	18/999	0,04853
H3K27me3	GM06990	6/205	0,03658

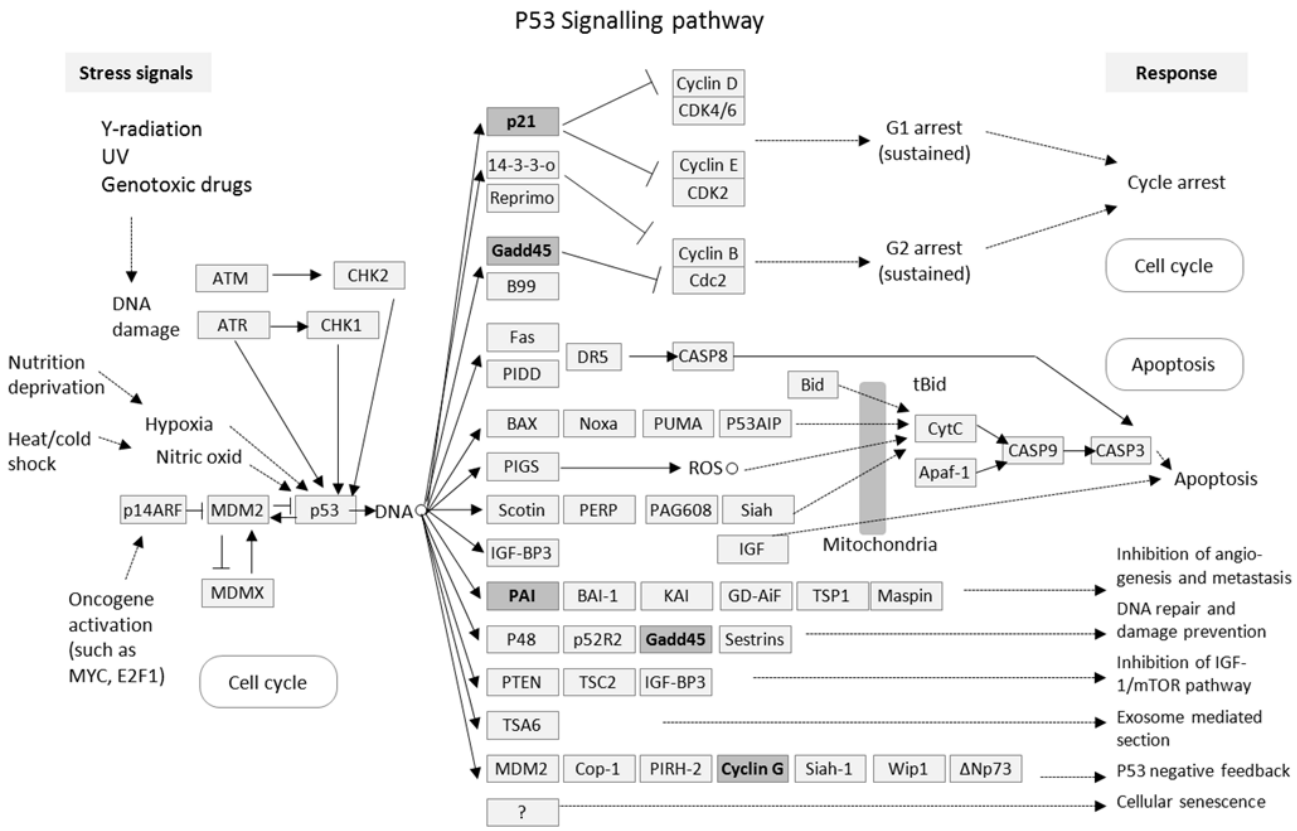

Figure 3.3-13 Genes in the KEGG P53 pathway affected by PS exposure(pink) (p<0.01), enriched in the hippocampus of female PS offspring when compared to control offspring. Female *5-Htt+/+* and *5-Htt+/-* offspring were exposed to PS or not (control). Expression was assessed using mRNA sequencing, n=16 for controls, n=32 for PS. The KEGG P53 pathway was identified as enriched by enrich analysis (Chen Tan 2013) using DEG with p<0.01.

Gene expression changes due to 5-Htt x PS interaction

The expression of 803 genes was regulated by an interaction of *5-Htt* genotype and PS, which is a considerably higher number of genes than found for the effects of the single factors (Fig. 3.3-8). Among the DEGs with an adjusted p<0.05 (Table 3.3-10) were *Sgk1* and *Sgk2*, the Wnt-signaling players frizzled (*Fzd*) 1 (*Fzd1*), *Fzd2* and *Fzd7* and the circadian clock gene period circadian clock 1 (Per1). Next to this, sirtuin 2 (*Sirt2*), a protein with HDAC activity, and two myelin-associated genes, *Mag* and *Cldn11,* were also differentially expressed.

Enrichr analysis indicates an enrichment of genes associated with myelin and OLs, as illustrated in Tables 3.3-11 and 3.3.-12. Two enriched MPs, "abnormal glial cell" and "abnormal myelination", were identified. Moreover, 11 of the 54 most significant enriched GO Biological processes (p<0.005) were associated with myelin and OLs, e.g. "axon ensheathment", "myelination", "regulation of gliogenesis" and "oligodendrocyte differentiation". Matching these findings, the GO Cellular component terms "paranode

region of axon", "myelin sheath", "glial cell projection" and "juxtaparanode region of axon" were also enriched ($p<0.05$). In addition to the 18 genes comprising the MP "abnormal myelination" term, (Fig. 3.3-15, gene names in blue), another seven genes associated with myelin were found to be differentially expressed in a GxE-interactive manner ($p<0.01$, Fig. 3.3-15, gene names in black). Almost all genes followed the same pattern, i.e. an increase in myelin gene expression in C *5-Htt+/-* animals compared to *5-Htt+/+* mice, followed by a decreased myelin gene expression after PS exposure in *5-Htt+/-* mice. As depicted in Figure 3.3-14, the identified genes comprise genes covering different aspects of OLs and myelin, i.e. genes encoding structural myelin proteins like *Mbp*, *Mobp* and *Mal*, proteins involved in fat metabolism like *Gal3st1* and *Fa2h*, proteins involved in cell-cell communication like *Mag*, *Mog* and *Cldn11*, OL TFs like *Olig1*, *Sox10* and *Myrf* and markers of the NG2+ oligodendrocyte progenitor cell (OLPs) population, i.e. *Pdgfra* and *Cspg4* (a.k.a. *Ng2*). Especially the increased expression of *Cspg4* indicates an increased number of NG2+ OLPs in the hippocampus C *5-Htt+/-* mice.

Table 3.3-11 A) shows the enriched MPs, of which many are associated with the nervous system, such as "abnormal neuron morphology", "abnormal brain morphology", "abnormal nervous system", "abnormal glial cell" and, interestingly, "abnormal myelination". Enriched KEGG pathways (Table 3.3-11 B) included the "one carbon pool by folate" pathway, a "basal cell carcinoma" pathway comprising fzd and wnt genes, two pathways centering on glycan degradation and the "notch signaling" pathway. All genes of the "basal cell carcinoma" pathway, i.e. frizzled homolog (Drosophila) (*Fzd) 1, Fzd2, Fzd7, bone morphogenetic protein 4 (Bmp4),* wingless-related MMTV integration site *(Wnt)* 3 and *Wnt5b*, showed the same expression pattern with slightly higher expression in *5-Htt+/-* controls than in *5-Htt+/+* animals, followed by a reduction in expression after PS exposure. The developmentally essential notch pathway comprised *Notch1*, *Notch4*, *Hdac2*, nuclear receptor corepressor 2 (*Ncor2*) and O-fucosylpeptide 3-beta-N-acetylglucosaminyltransferase (*Lfng*). Table 3.3-11 C shows the most significantly enriched GO Biological processes ($p<0.005$). Next to the myelin gene sets, several terms were associated with intracellular signaling cascades, especially the inositoltriphosphate signaling, such as "positive regulation of phosphatidylinositol 3-kinase signaling", "regulation of phosphatidylinositol 3-kinase signaling", "phosphatidylinositol-mediated signaling", "G-protein coupled receptor signaling pathway coupled to cGMP nucleotide second messenger", "response to cAMP" and "negative regulation of ERK1 and ERK2 cascade". Several other terms were related to the cytoskeleton, e.g. "cell projection assembly", "establishment or maintenance of apical/basal cell polarity", "actin filament

organization" and "actin cytoskeleton organization". Furthermore, the term "negative regulation of phosphorylation" was enriched.

When looking at enriched GO Molecular function terms (Appendix Table 4), many of them can be tied to chromatin and transcription regulation, e.g. "transcription factor binding", "chromatin DNA binding", "histone acetyltransferase binding", "RNA polymerase II regulatory region DNA binding" and "repressing transcription factor binding". The terms "chromatin", "heterochromatin" and "nuclear chromatin" was also enriched in the GO Cellular component category ($p<0.05$). The "chromatin" term comprised *Hdac2*, *Sirt2*, *Ncore2*, and the polycomb genes *Chromobox homolog 8* (*Cbx8*) and *Polyhomeotic-like 1 (Drosophila) (Phc1)*, amongst others. Of note, 16 out of the 19 identified genes in this term show the same expression pattern, e.i. increased expression in *5-Htt+/-* controls when compared to both groups of the *5-Htt+/+* genotype and decreased expression to *5-Htt+/+* level or below by PS exposure. Only *Hdac2*, WD repeat domain 61 *(Wdr61)* and *T* show the opposite expression pattern with the *5-Htt+/-* controls showing the lowest expession. The KEGG pathway "One carbon pool by folate" is also closely related to chromatin, as it constitutes the process providing methyl-donors and is thus involved in DNA methylation. Enrichr analysis regarding enriched gene sets associated with histone modifications yielded 15 hits, of which 14 pointed to genes associated with H3K4me3 and one to H3K4me1. Interestingly, expression of SET domain containing 1A (Setd1a), a gene encoding a part of a histone methyltransferase complex responsible for methylation of H3K4, is affected by a GxE interaction, although the expression change ($p= 0.030$) did not reach the statistical significance of $p<0.01$.

Analysis furthermore identified terms related to the wnt signaling pathway, such as the GO Molecular function terms "Wnt-activated receptor activity", "Wnt-protein binding" and "frizzled binding" and the GO Biological processes term "G-protein coupled receptor signaling pathway coupled to cGMP nucleotide second messenger" comprising *Fzd1, Fzd2* and *Fzd7*. The three *Fzd* genes showed the same expression pattern with slightly increased expression in *5-Htt+/-* controls when compared to *5-Htt+/+* animals, followed by a reduction in expression after PS exposure. Additionally, several GO Cellular component terms related to cell adherence, such as "cell-substrate junction", "adherence junction", "focal adhesion" and "anchoring junction", and the GO Molecular function term "PDZ domain binding" contained fzd genes.

Table 3.3-10 DEGs affected by a *5-Htt* x PS interaction in the hippocampus of female *5-Htt*+/- and 5-Htt+/+ PS and control offspring (adjusted p<0.05). Female *5-Htt*+/+ and *5-Htt*+/- offspring were exposed to PS or not (control). Expression was assessed using mRNA sequencing, n=8 for controls, n=16 for the PS groups for each genotype. Chr = chromosome, Bm = Base mean expression, Log2FC = log 2 fold change, Adj. p = adjusted p-value.

Symbol	Gene name	Chr	Bm	Log2FC	p	Adj. p
Sgk1	serum/glucocorticoid regulated kinase 1	10	2607.0	-0.52	1.2E-10	2.4E-06
Serpine1	serine (or cysteine) peptidase inhibitor, clade E, member 1	5	15.2	-0.97	4.3E-08	
Mt1	metallothionein 1	8	3255.1	-0.40	1.1E-06	8.6E-03
Tob2	transducer of ERBB2, 2	15	844.9	-0.28	1.7E-06	8.6E-03
Fzd2	frizzled homolog 2 (Drosophila)	11	202.6	-0.39	1.8E-06	8.6E-03
Cldn11	claudin 11	3	2837.1	-0.40	4.0E-06	1.0E-02
Ccdc153	coiled-coil domain containing 153	9	56.5	-0.98	4.1E-06	1.0E-02
Lfng	LFNG O-fucosylpeptide 3-beta-N-acetylglucosaminyltransferase	5	385.6	-0.40	4.2E-06	1.0E-02
Tprn	taperin	2	463.8	-0.29	4.6E-06	1.0E-02
Zfp36	zinc finger protein 36	7	70.4	-0.47	4.6E-06	1.0E-02
Ppp1r3g	protein phosphatase 1, regulatory (inhibitor) subunit 3G	13	183.5	-0.47	5.5E-06	1.0E-02
Pim3	proviral integration site 3	15	762.9	-0.31	5.8E-06	1.0E-02
Arl4d	ADP-ribosylation factor-like 4D	11	220.2	-0.43	8.5E-06	1.4E-02
Sgk2	serum/glucocorticoid regulated kinase 2	2	48.1	-0.61	9.1E-06	1.4E-02
Slc2a1	solute carrier family 2 (facilitated glucose transporter), member 1	4	1810.5	-0.42	1.6E-05	2.3E-02
Sall3	sal-like 3 (Drosophila)	18	192.7	-0.26	1.9E-05	2.4E-02
Zfp110	zinc finger protein 110	7	649.1	0.19	2.1E-05	2.4E-02
Trib1	tribbles homolog 1 (Drosophila)	15	334.6	-0.39	2.1E-05	2.4E-02
Hip1	huntingtin interacting protein 1	5	1993.6	-0.14	2.2E-05	2.4E-02
Gm12868	predicted gene 12868	4	668.7	-0.34	2.4E-05	2.5E-02
Mag	myelin-associated glycoprotein	7	2885.0	-0.40	2.9E-05	2.7E-02
Fzd7	frizzled homolog 7 (Drosophila)	1	327.6	-0.31	3.0E-05	2.7E-02
mmu-mir-6240	mmu-mir-6240	5	15.5	1.09	3.0E-05	
Zfp474	zinc finger protein 474	18	14.7	-1.04	3.1E-05	
Hepacam	hepatocyte cell adhesion molecule	9	2687.0	-0.20	3.1E-05	2.7E-02

Gm12693	predicted gene 12693	4	385.7	0.23	3.5E-05	2.7E-02
Pik3c2b	phosphoinositide-3-kinase, class 2, beta polypeptide	1	958.2	-0.22	3.5E-05	2.7E-02
Gm9791	predicted pseudogene 9791	3	150.1	-0.36	3.6E-05	2.7E-02
Nfkbia	nuclear factor of kappa light polypeptide gene enhancer in B cells inhibitor, alpha	12	442.5	-0.35	3.7E-05	2.7E-02
Afap1l1	actin filament associated protein 1-like 1	18	328.5	-0.27	3.9E-05	2.7E-02
Fam83d	family with sequence similarity 83, member D	2	75.4	-0.47	3.9E-05	2.7E-02
Cmtm3	CKLF-like MARVEL transmembrane domain containing 3	8	193.9	-0.31	3.9E-05	2.7E-02
Zbtb7c	zinc finger and BTB domain containing 7C	18	92.3	-0.40	4.2E-05	2.7E-02
Carhsp1	calcium regulated heat stable protein 1	16	1158.6	-0.25	4.8E-05	2.9E-02
Cpm	carboxypeptidase M	10	500.4	-0.25	4.8E-05	2.9E-02
Sdc4	syndecan 4	2	2208.3	-0.28	5.0E-05	2.9E-02
Kirrel2	kin of IRRE like 2 (Drosophila)	7	299.3	-0.32	6.5E-05	3.6E-02
5031439G07Rik	RIKEN cDNA 5031439G07 gene	15	4872.2	-0.14	6.8E-05	3.6E-02
Per1	period circadian clock 1	11	2256.3	-0.25	6.9E-05	3.6E-02
Gm4204	predicted gene 4204	1	3129.6	0.18	7.1E-05	3.6E-02
Mfsd2a	major facilitator superfamily domain containing 2A	4	669.8	-0.29	7.2E-05	3.6E-02
Sirt2	sirtuin 2	7	4041.3	-0.17	7.3E-05	3.6E-02
Agt	angiotensinogen (serpin peptidase inhibitor, clade A, member 8)	8	513.0	-0.34	7.6E-05	3.7E-02
Tsc22d3	TSC22 domain family, member 3	X	2137.7	-0.31	7.8E-05	3.7E-02
Ttyh2	tweety homolog 2 (Drosophila)	11	953.4	-0.29	8.2E-05	3.8E-02
Zfyve9	zinc finger, FYVE domain containing 9	4	3894.4	0.13	8.9E-05	4.0E-02
Prr5	proline rich 5 (renal)	15	209.9	-0.39	9.5E-05	4.2E-02
Tsc22d4	TSC22 domain family, member 4	5	1635.5	-0.20	1.0E-04	4.2E-02
l7Rn6	lethal, Chr 7, Rinchik 6	7	943.9	0.15	1.0E-04	4.2E-02
Bnc1	basonuclin 1	7	6.7	2.59	1.0E-04	
Fzd1	frizzled homolog 1 (Drosophila)	5	386.3	-0.22	1.0E-04	4.2E-02
Mt2	metallothionein 2	8	1651.1	-0.39	1.0E-04	4.2E-02
Pdlim2	PDZ and LIM domain 2	14	230.6	-0.43	1.1E-04	4.2E-02
Slc7a1	solute carrier family 7 (cationic amino acid transporter, y+ system), member 1	5	1617.4	-0.21	1.1E-04	4.4E-02
Plekhf1	pleckstrin homology domain containing, family F (with FYVE domain) member 1	7	77.4	-0.56	1.3E-04	4.8E-02
Ccnd3	cyclin D3	17	521.2	-0.23	1.3E-04	4.8E-02

Gpr34	G protein-coupled receptor 34	X	221.1	0.26	1.3E-04	4.8E-02
Sh3bp2	SH3-domain binding protein 2	5	145.3	-0.29	1.3E-04	4.8E-02

Table 3.3-11 Enriched pathways and terms due to a 5-Htt x PS-interaction in the hippocampus of female *5-Htt*+/- and *5-Htt*+/+ PS and control offspring (p<0.05). Female *5-Htt*+/+ and *5-Htt*+/- offspring were exposed to PS or not (control). Expression was assessed using mRNA sequencing, n=8 for control groups of each genotype, n=16 for the PS groups of each genotype. Enrichment analysis performed using the Enrichr online tool (Chan Tan 2013) with DEGs p<0.01. Overl. = number of DEGs/total number of genes in this pathway or term.

Enriched term	Term ID	Overl.	P	Genes
A) Mammalian phenotype term				
Abn. Neuron morphology	MP0002882	61/1007	3.81E-10	
Abn. Blood vessel	MP0001614	50/779	3.46E-09	
Abn. Brain morphology	MP0002152	65/1189	4.84E-09	
Mortality/aging	MP0010768	65/1256	3.77E-08	
Abn. Lung morphology	MP0001175	32/403	3.78E-08	
Abn. Survival	MP0010769	64/1230	4.09E-08	
Abn. Myelination	MP0000920	18/135	4.63E-08	
Abn. Motor capabilities/c	MP0002066	72/1483	6.78E-08	
Postnatal lethality	MP0002082	59/1115	9.26E-08	
Preweaning lethality	MP0010770	59/1116	9.54E-08	
Perinatal lethality	MP0002081	54/982	1.14E-07	
Abn. Nervous system	MP0003861	49/856	1.59E-07	
Abn. Glial cell	MP0003634	22/232	3.75E-07	
Abn. Somatic nervous	MP0002752	40/676	1.19E-06	
Abn. Blood vessel	MP0000249	22/255	1.63E-06	
Abn. Posterior eye	MP0005195	29/434	4.64E-06	
Abn. Cardiovascular devel	MP0002925	34/584	1.14E-05	
Premature death	MP0002083	47/969	2.27E-05	
Abn. Glial cell	MP0003690	8/44	3.97E-05	
Abn. Embryonic tissue	MP0002085	39/766	4.61E-05	

Normal phenotype	MP0002873	58/1376	0.00011	
Abn. Kidney physiology	MP0002136	24/397	0.00014	
Abn. Blood circulation	MP0002128	26/450	0.00015	
Abn. Cell physiology	MP0005621	22/349	0.00015	
Respiratory system phenotype	MP0005388	13/145	0.00016	
Abn. Respiratory system	MP0002133	13/145	0.00016	
Emphysema	MP0001958	46905	0.00017	
No abn. Phenotype	MP0002169	57/1371	0.00018	
Abn. Kidney morphology	MP0002135	31/592	0.00019	
Abn. Heart morphology	MP0000266	40/852	0.00020	
Abn. Hematopoietic stem	MP0004808	26908	0.00020	
Cellular phenotype	MP0005384	27/487	0.00021	
Abn. Fertility/fecundity	MP0002161	47/1089	0.00034	
Abn. Female reproductive	MP0003699	27/518	0.00052	
Abn. Immune system	MP0002722	35/749	0.00055	
Abn. Wound healing	MP0005023	10/104	0.00056	
Abn. Reproductive system	MP0003936	14/190	0.00060	
Abn. Skeleton morphology	MP0005508	11/128	0.00072	
Abn. Thymus morphology	MP0000703	22/393	0.00072	
Abn. Liver morphology	MP0000598	29/586	0.00072	
Prenatal lethality	MP0002080	64/1686	0.00078	
Decreased survivor rate	MP0008770	14/196	0.00080	
Abn. White adipose	MP0002970	15/221	0.00086	
Homeostasis/metabolism phenot	MP0005376	15/224	0.00097	

B) KEGG pathways

One carbon pool by folate	HSA00670	4/16	0.00579	SHMT2, ALDH1L1, GART, MTHFD2
Adipocytokine signaling pathway	HSA04920	8/72	0.00965	SLC2A1, IRS2, RELA, ADIPOR2, NFKBIA, TNFRSF1A, CPT1A, PTPN11
Basal cell carcinoma	HSA05217	6/56	0.02764	WNT3, WNT5B, BMP4, FZD1, FZD2, FZD7
N glycan degradation	HSA00511	3/16	0.03234	MAN2B2, MAN2B1, NEU4
Abc transporters general	HSA02010	5/44	0.03530	ABCA2, ABCA3, ABCA12, ABCG1, ABCG8
Glycan structures degradation	HSA01032	4/30	0.03694	MAN2B2, MAN2B1, GNS, NEU4
Renin angiotensin system	HSA04614	3/17	0.03702	MME, CTSA, AGT

Notch signaling pathway	HSA04330	5/47	0.04402	LFNG, NOTCH1, HDAC2, NOTCH4, NCOR2

C) Biological processes

Axon ensheathment	GO:0008366	14/62	0.0000	MBP, NKX6-2, EGR2, ARHGEF10, NAB2, CNTN2, MYRF, PLLP, FGFR3, CLDN11, GAL3ST1, NFASC, MAL, SIRT2
Ensheathment of neurons	GO:0007272	14/62	0.0000	MBP, NKX6-2, EGR2, ARHGEF10, NAB2, MYRF, CNTN2, PLLP, FGFR3, CLDN11, GAL3ST1, NFASC, MAL, SIRT2
Myelination	GO:0042552	13/59	0.0000	MBP, NKX6-2, EGR2, ARHGEF10, NAB2, CNTN2, MYRF, PLLP, FGFR3, GAL3ST1, NFASC, MAL, SIRT2
Brain development	GO:0007420	21/187	0.0000	IRS2, PLXNB2, DDIT4, RAB18, ARRB2, SPHK2, AK7, PTPN11, POU6F1, MEN1, SLC23A1, CXCR4, EGR2, FOXJ1, BDH1, AATK, MACROD2, FZD1, FZD2, FZD7, PHGDH
Epithelial cell development	GO:0002064	15/107	0.0000	PDGFB, RARA, RAPGEF3, SLC4A5, WNT5B, FGFR3, SOX8, LAMB2, BMP4, NOTCH1, FOXJ1, EZR, AGT, HAPLN2, HYDIN
Glial cell differentiation	GO:0010001	10/61	0.0001	CNP, EGR1, SOX10, EGR2, NAB2, MYRF, ERBB3, SOX8, KLF15, NOTCH1
Peripheral nervous system development	GO:0007422	7/28	0.0001	ERBB3, SOX8, SOX10, EGR2, NFASC, SERPINI1, PMP22
Regulation of gliogenesis	GO:0014013	10/67	0.0002	CXCR4, NKX6-2, SOX10, RELA, CNTN2, FGFR3, SOX8, SIRT2, NOTCH1, HDAC2
Negative regulation of phosphorylation	GO:0042326	25/325	0.0003	BMP4, CNKSR3, ERRFI1, NCK1, GADD45G, GADD45B, PER1, RPS6KA6, DUSP1, LRP5, FLCN, IRS2, PKIA, DDIT4, IGBP1, AKT1S1, PTPN1, ABL1, MEN1, SPRY1, KIRREL2, SLC9A3R1, PMEPA1, TRIB1, SIRT2
Tube formation	GO:0035148	13/114	0.0003	RARA, PLXNB2, BBS4, SOX8, SCRIB, FUZ, T, TCTN1, BMP4, PHACTR4, CELSR1, NOTCH1, EDAR
Positive regulation of gliogenesis	GO:0014015	7/35	0.0004	SOX8, CXCR4, NKX6-2, SOX10, RELA, NOTCH1, HDAC2
G-protein coupled receptor signaling pathway coupled to cgmp nucleotide second messenger	GO:0007199	4/8	0.0005	AGT, FZD1, FZD2, FZD7
Response to camp	GO:0051591	11/90	0.0005	VGF, RAPGEF3, EGR1, EGR2, RELA, JUNB, PPARGC1B, OXT, GPD1, CPS1, DUSP1
Response to peptide	GO:1901652	27/384	0.0006	NFKBIA, CACYBP, KLF15, PARP1, EEF2K, LRP5, IRS2, RELA, JUNB, RHOQ, VGF, PTPN11, NOTCH1, BCAR1, INPPL1, OXT, PDGFB, POR, FGFR3, KLB, CPS1, UCP2, PTPN1, EGR1, EGR2, EIF4G1, BDH1

Organ morphogenesis	GO:0009887	28/405	0.0006	T, LFNG, ERRFI1, TLE3, CSF1, GAMT, LRP5, RELA, VAX2, BBS4, IFT140, HDAC2, EDAR, GAA, IRX5, ID1, PDGFRA, ELN, FUZ, BMP4, SEMA6A, CSRNP1, NCOR2, DCHS1, GJB6, ITGB4, SOX8, MEN1
Axon ensheathment in CNS	GO:0032291	4/9	0.0007	FGFR3, NKX6-2, CNTN2, MYRF
CNS myelination	GO:0022010	4/9	0.0007	FGFR3, NKX6-2, CNTN2, MYRF
Angiogenesis	GO:0001525	19/236	0.0009	GPR124, PGF, SERPINE1, RAPGEF3, APOLD1, MYH9, BMP4, NOTCH1, CYR61, CLIC4, JMJD6, CSPG4, MFGE8, EPAS1, E2F8, TSPAN12, PLCD1, HS6ST1, ID1
Regulation of cell proliferation involved in kidney development	GO:1901722	4/10	0.0009	BMP4, EGR1, PDGFB, FLCN
Epithelium development	GO:0060429	20/256	0.0009	RARA, KRT15, FUZ, BMP4, CELSR1, NOTCH1, GJA4, ERRFI1, DCHS1, BNC1, PHGDH, PDGFB, WNT3, RELA, FGFR3, SDC4, SPRY1, FOXJ1, EDAR, AHI1
Platelet-derived growth factor receptor signaling pathway	GO:0048008	6/30	0.0011	PDGFB, BCAR1, CSRNP1, PDGFRA, PTPN1, ABL1
Alpha-amino acid biosynthetic process	GO:1901607	9/69	0.0011	MTHFD2, PADI2, CARNS1, SHMT2, CPS1, GART, PHGDH, GAMT, PSAT1
Positive regulation of lipid metabolic process	GO:0045834	11/103	0.0014	PDGFB, IRS2, PNPLA2, POR, PDGFRA, FGFR3, ABCG1, CYR61, AVP, AGT, CPT1A
Cell projection assembly	GO:0030031	17/213	0.0018	FUZ, TMEM107, INPPL1, BBS10, NCK1, FBF1, EZR, HYDIN, PDGFB, BBS4, ITGB4, TTYH1, IFT140, AK7, FOXJ1, SLC9A3R1, AHI1
Ameboidal-type cell migration	GO:0001667	12/123	0.0018	GPR124, TMEM201, MYH9, TNS1, SOX8, PHACTR4, NR4A1, CORO1B, CXCR4, SOX10, ID1, LRP5
Neural tube closure	GO:0001843	9/76	0.0020	RARA, PLXNB2, BBS4, SCRIB, FUZ, T, BMP4, PHACTR4, CELSR1
Renal system development	GO:0072001	4/13	0.0020	BMP4, ITGB4, PRKCSH, IFT140
Oligodendrocyte differentiation	GO:0048709	5/23	0.0021	EGR1, SOX10, CNP, SOX8, MYRF
Tube closure	GO:0060606	9/77	0.0022	RARA, PLXNB2, BBS4, SCRIB, FUZ, T, BMP4, PHACTR4, CELSR1
Negative regulation of ERK1 and ERK2	GO:0070373	6/35	0.0022	FLCN, SPRY1, CNKSR3, SLC9A3R1, RPS6KA6, PTPN1
Sprouting angiogenesis	GO:0002040	5/24	0.0024	GPR124, PGF, E2F8, NOTCH1, JMJD6
Response to peptide hormone	GO:0043434	24/364	0.0027	CACYBP, PTPN11, PARP1, BCAR1, EEF2K, INPPL1, OXT, LRP5, PDGFB, IRS2, RELA, JUNB, POR, FGFR3, KLB, CPS1, UCP2, PTPN1, RHOQ, VGF, EGR1, EGR2, EIF4G1, BDH1
Regulation of glial cell differentiation	GO:0045685	7/50	0.0027	CXCR4, NKX6-2, RELA, CNTN2, FGFR3, NOTCH1, HDAC2

Establishment or maintenance of apical/basal cell polarity	GO:0035088	5/25	0.0028	LLGL1, SCRIB, EZR, FOXJ1, CLIC4
Establishment or maintenance of bipolar cell polarity	GO:0061245	5/25	0.0028	LLGL1, SCRIB, EZR, FOXJ1, CLIC4
Response to wounding	GO:0009611	14/167	0.0029	PDGFB, PDGFRA, FGFR3, WNT5B, ERBB3, ITGB4, MDK, SCRIB, CELSR1, CORO1B, NOL3, PLLP, TNFRSF1A, BNC1
Positive regulation of phosphatidylinositol 3-kinase signaling	GO:0014068	7/51	0.0030	PDGFB, RARA, PLXNB1, PDGFRA, ERBB3, PRR5, AGT
Regulation of phosphatidylinositol 3-kinase signaling	GO:0014066	8/66	0.0031	PDGFB, RARA, PLXNB1, SLC9A3R1, PDGFRA, ERBB3, PRR5, AGT
Response to purine-containing compound	GO:0014074	12/132	0.0031	RAPGEF3, RELA, PPARGC1B, JUNB, GPD1, CPS1, VGF, EGR1, EGR2, CASQ2, OXT, DUSP1
Actin filament organization	GO:0007015	13/150	0.0031	ACTN4, PPARGC1B, ARPC1B, ELN, CORO1B, BCAR1, GSN, INPPL1, NCK1, SORBS3, EZR, FAT1, MSRB2
Lung alveolus development	GO:0048286	6/38	0.0031	HS6ST1, ERRFI1, ABCA12, BMP4, FZD1, TNS3
Response to insulin	GO:0032868	18/246	0.0032	PTPN11, PARP1, BCAR1, EEF2K, INPPL1, PDGFB, IRS2, RELA, FGFR3, KLB, UCP2, PTPN1, RHOQ, VGF, EGR1, EGR2, EIF4G1, BDH1
Positive regulation of glial cell differentiation	GO:0045687	5/26	0.0033	CXCR4, NKX6-2, RELA, NOTCH1, HDAC2
Cell fate commitment	GO:0045165	12/134	0.0035	GATA2, WNT3, RARA, OLIG1, WNT5B, FGFR3, SOX8, TCF3, BMP4, EPAS1, NOTCH1, MEN1
Cellular response to hormone stimulus	GO:0032870	28/462	0.0038	PGF, NPC1, PARP1, EEF2K, DUSP1, IRS2, RELA, JUNB, BBS4, NR4A1, RHOQ, RARA, BMP4, PTPN11, NOTCH1, BCAR1, POR, FGFR3, PAQR8, KLB, CPS1, UCP2, PTPN1, EGR1, EGR2, ADIPOR2, EIF4G1, TNFRSF1A
Response to organophosphorus	GO:0046683	11/118	0.0038	RAPGEF3, RELA, PPARGC1B, JUNB, GPD1, CPS1, VGF, EGR1, EGR2, OXT, DUSP1
Inositol lipid-mediated signaling	GO:0048017	12/136	0.0039	PDGFB, IRS2, PDGFRA, FGFR3, ERBB3, AKT1S1, KLB, NR4A1, PTPN11, GSN, PIK3C2B, SIRT2
Phosphatidylinositol-mediated signaling	GO:0048015	12/136	0.0039	PDGFB, IRS2, PDGFRA, FGFR3, ERBB3, AKT1S1, KLB, NR4A1, PTPN11, GSN, PIK3C2B, SIRT2
Actin cytoskeleton organization	GO:0030036	18/253	0.0042	MYH9, PDGFRA, DAAM2, WASF2, TRIOBP, PDGFB, KLHL1, LLGL1, PHACTR4, CORO1B, PTPN1, ABL1, RHOQ, RHOU, RHOG, FOXJ1, SLC9A3R1, INF2

Regulation of protein localization to nucleus	GO:1900180	13/156	0.0042	FLCN, PKIA, NFKBIA, OTUD7B, BMP4, PARP1, LZTS2, EDAR, TNFRSF1A, FZD1, LMNA, FZD7, OGG1
Morphogenesis of an epithelium	GO:0002009	20/296	0.0045	PGF, SCRIB, T, BMP4, CELSR1, NOTCH1, NOTCH4, CLIC4, CSF1, DCHS1, AGT, LRP5, PDGFB, BBS4, FGFR3, SOX8, PHACTR4, CXCR4, DDR1, AHI1
Apoptotic process involved in morphogenesis	GO:0060561	4/17	0.0046	SCRIB, NOTCH1, LRP5, CYR61
Cellular response to follicle-stimulating hormone stimulus	GO:0071372	3/8	0.0049	EGR1, NOTCH1, POR
L-serine metabolic process	GO:0006563	3/8	0.0049	SHMT2, PHGDH, PSAT1

D) Histone modifications	**Cell line**		
H3K4me3	SAEC	42/856	2.13E-04
H3K4me3	CACO2	40/808	2.54E-04
H3K4me3	HELAS3	30/587	9.34E-04
H3K4me3	GM12866	65/1618	0.0010
H3K4me3	HBMEC	49/1176	0.0021
H3K4me3	GM12878	56/1447	0.0048
H3K4me3	GM12875	64/1734	0.0072
H3K4me3	NHEK	30/724	0.0160
H3K4me3	BJ	33/818	0.0167
H3K4me3	HVMF	32/838	0.0348
H3K4me3	H7ES	84/2560	0.0339
H3K4me3	HUVEC	31/823	0.0434
H3K4me3	HCF	34/925	0.0469
H3K4me3	K562	109/3460	0.0429
H3K4me1	HCT116	15/341	0.0499

Table 3.3-12 Pathways and terms associated with myelination and oligodentrocytes, enriched due to a 5-Htt x PS-interaction in the hippocampus of female *5-Htt*+/- and *5-Htt*+/+ PS and control offspring (p<0.05). Female *5-Htt*+/+ and *5-Htt*+/- offspring were exposed to PS or not (control). Expression was assessed using mRNA sequencing, n=8 for control groups of each genotype, n=16 for the PS groups of each genotype. Enrichment analysis performed using the Enrichr online tool (Chan Tan 2013) with DEGs p<0.01. Overl. = number of DEGs/total number of genes in this pathway or term.

Enriched term	Term ID	Overl.	p	Genes
A) Mammalian phenotype term				
Abnormal myelination	MP0000920	18/135	4.63E-08	
Abnormal glial cell	MP0003634	22/232	3.75E-07	
B) GO: Biological processes				
Axon ensheathment	GO:0008366	14/62	1.71E-07	MBP, NKX6-2, EGR2, ARHGEF10, NAB2, CNTN2, MYRF, PLLP, FGFR3, CLDN11, GAL3ST1, NFASC, MAL, SIRT2
Ensheathment of neurons	GO:0007272	14/62	1.71E-07	MBP, NKX6-2, EGR2, ARHGEF10, NAB2, MYRF, CNTN2, PLLP, FGFR3, CLDN11, GAL3ST1, NFASC, MAL, SIRT2
Myelination	GO:0042552	13/59	6.03E-07	MBP, NKX6-2, EGR2, ARHGEF10, NAB2, CNTN2, MYRF, PLLP, FGFR3, GAL3ST1, NFASC, MAL, SIRT2
Glial cell differentiation	GO:0010001	10/61	1.12E-04	CNP, EGR1, SOX10, EGR2, NAB2, MYRF, ERBB3, SOX8, KLF15, NOTCH1
Regulation of gliogenesis	GO:0014013	10/67	2.22E-04	CXCR4, NKX6-2, SOX10, RELA, CNTN2, FGFR3, SOX8, SIRT2, NOTCH1, HDAC2
Positive regulation of gliogenesis	GO:0014015	7/35	4.20E-04	SOX8, CXCR4, NKX6-2, SOX10, RELA, NOTCH1, HDAC2
Axon ensheathment in central nervous system	GO:0032291	4/9	6.76E-04	FGFR3, NKX6-2, CNTN2, MYRF
Central nervous system myelination	GO:0022010	4/9	6.76E-04	FGFR3, NKX6-2, CNTN2, MYRF
Oligodendrocyte differentiation	GO:0048709	5/23	2.07E-03	EGR1, SOX10, CNP, SOX8, MYRF
Regulation of glial cell differentiation	GO:0045685	7/50	2.68E-03	CXCR4, NKX6-2, RELA, CNTN2, FGFR3, NOTCH1, HDAC2
Positive regulation of glial cell differentiation	GO:0045687	5/26	3.29E-03	CXCR4, NKX6-2, RELA, NOTCH1, HDAC2
C) GO: Cellular component				
Paranode region of axon	GO:0033270)	3/11	0.00975058	MAG, NFASC, SIRT2
Myelin sheath	GO:0043209)	3/17	0.02641262	ITPR3, SIRT2, CNTN2
Glial cell projection	GO:0097386)	2/9	0.0485649	EZR, SIRT2
Juxtaparanode region of axon	GO:0044224)	2/9	0.0485649	CNTN2, SIRT2

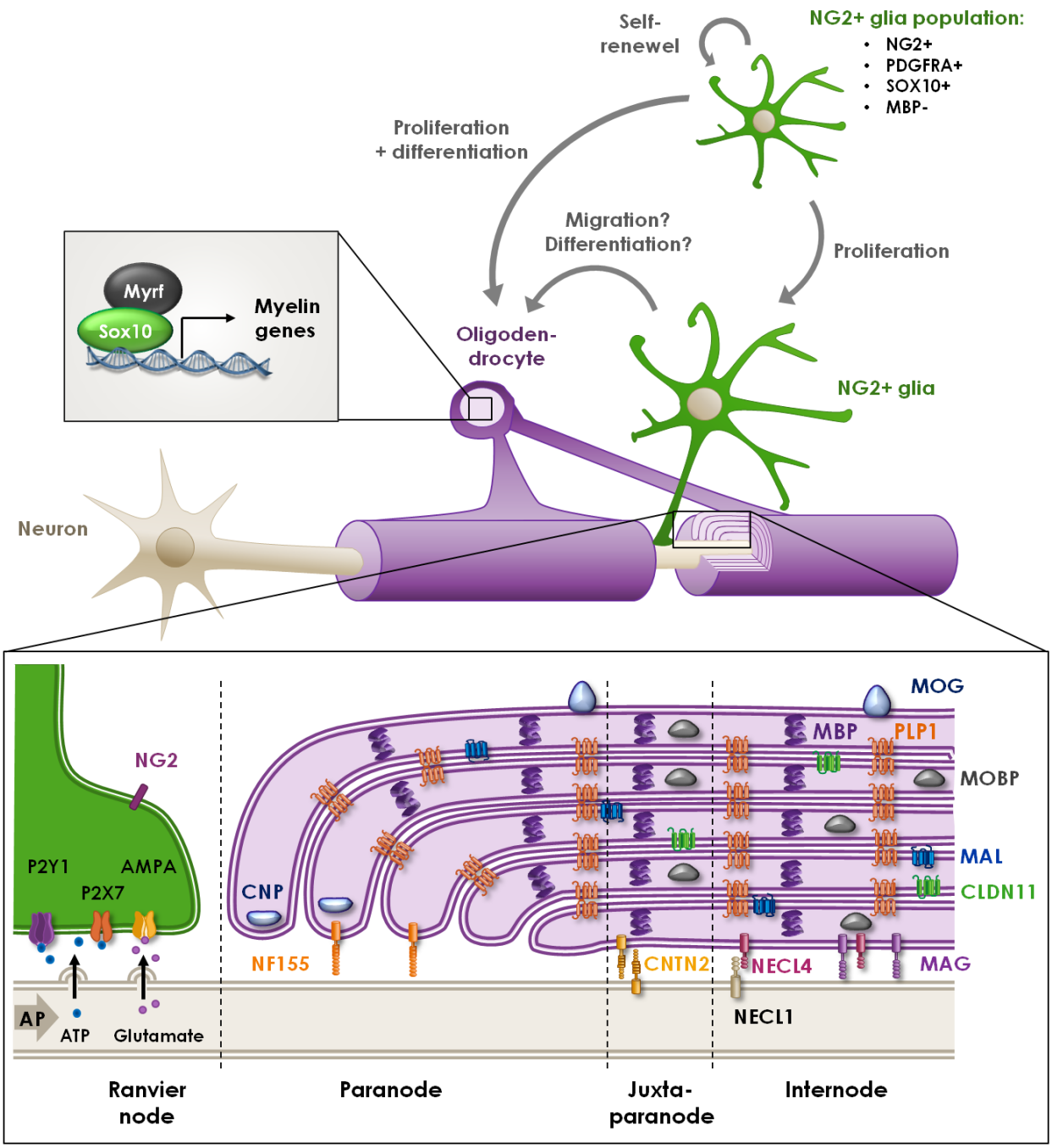

Figure 3.3-14 Genes encoding myelin proteins, oligodendrocyte-cell communication proteins and oligodendrocyte transcription factors affected by a GxE interaction in *5-Htt*+/+ and *5-Htt*+/- offspring exposed to PS or not (controls). All illustrated genes except proteolipid protein (myelin) 1 (*Plp1*), cell adhesion molecule 3 (*Cadm3*, also known as *Necl1*), purinergic receptor P2Y, G-protein coupled 1 (*P2ry1, a.k.a. P2y1*), purinergic receptor P2X, ligand-gated ion channel, 7 (P2rx7, a.k.a. P2x7) and genes encoding a-amino-3-hydroxy-5-methyl-4-isoxazolepropionic acid (AMPA) receptor proteins were differentially affected by a GxE interaction with p<0.01. *Mbp* = myelin basic protein, *Mobp* = myelin-associated oligodendrocytic basic protein, *Mal* = myelin and lymphocyte protein, *Cnp* = 2',3'-cyclic nucleotide 3' phosphodiesterase, *Mag* = myelin-associated glycoprotein, *Mog* = myelin oligodendrocyte glycoprotein, *Cldn11* = claudin 11, *Sox10* = SRY (sex determining region Y)-box 10, *Myrf* = myelin regulatory factor, chondroitin sulfate proteoglycan 4 (a.k.a. Ng2). See Fig. 3.3-15 for gene expression data of a subset of the illustrated genes. Lilac cell = myelinating oligodendrocyte, taupe cell = neuron, green cell = NG2-positive polydendrocyte.

Structural myelin proteins

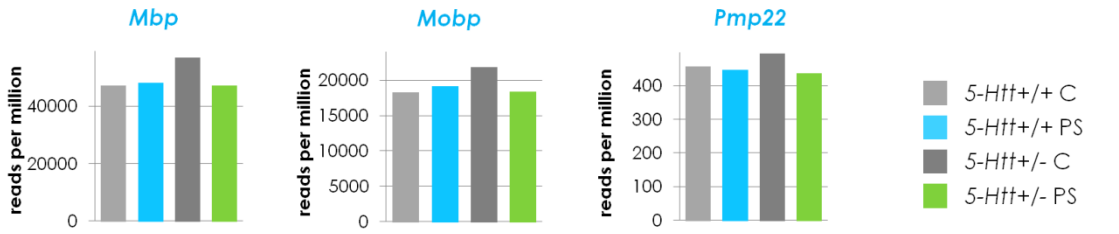

Enzymes ass. with myelin

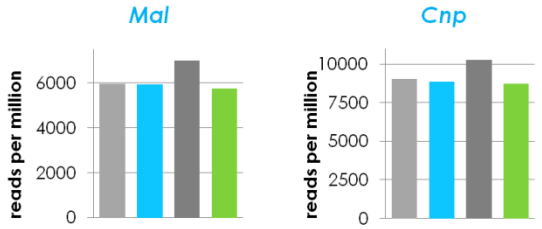

Lipid metabolism

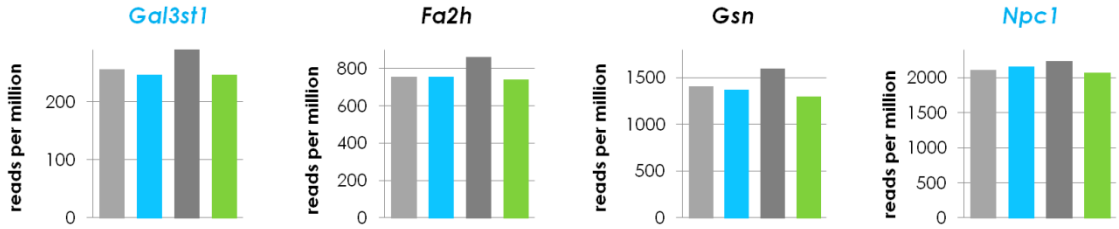

Cell-cell communication

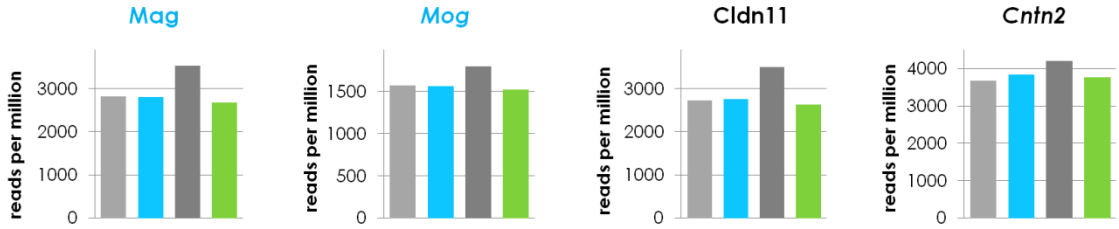

Transcription factors

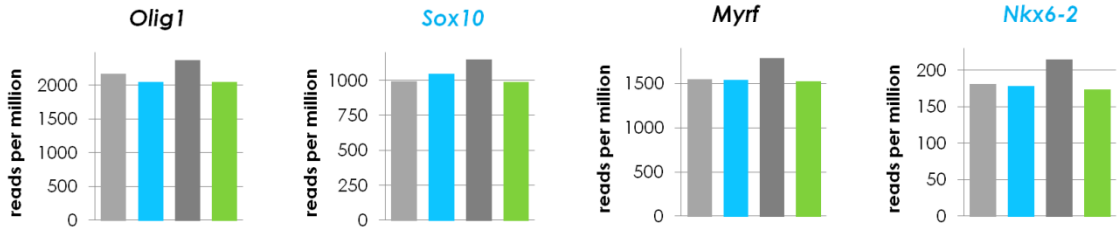

Markers of OLPs

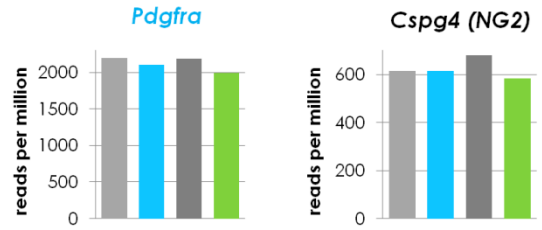

Figure 3.3-15 Expression of genes encoding myelin proteins, oligodendrocyte-cell communication proteins and oligodendrocyte transcription factors affected by a GxE interaction in *5-Htt*+/+ and *5-Htt*+/- offspring exposed to PS or not (controls).
Mbp = myelin basic protein, *Mobp* = myelin-associated oligodendrocytic basic protein, *Pmp22* = peripheral myelin protein 22, *Mal* = myelin and lymphocyte protein, *Cnp* = 2',3'-cyclic nucleotide 3' phosphodiesterase, *Gal3st1* = galactose-3-O-sulfotransferase 1, Fa2h = fatty acid 2-hydroxylase, *Gsn* = gelsolin, Npc1 = Niemann-Pick type C1, *Mag* = myelin-associated glycoprotein, *Mog* = myelin oligodendrocyte glycoprotein, *Cldn11* = claudin 11, *Olig1* = oligodendrocyte transcription factor 1, *Sox10* = SRY (sex determining region Y)-box 10, *Myrf* = myelin regulatory factor, *Nkx6-2* = NK6 homeobox 2, *Pdgfra* = platelet derived growth factor receptor, alpha polypeptide, *Cspg4* = chondroitin sulfate proteoglycan 4 (a.k.a. Ng2). Bars represent mean values, error bars SEM.

Genes regulated in social and unsocial female mice

As a last step, we aimed to identify the molecular mechanisms that specifically promote resilience or vulnerability to PS. For this purpose, for each genotype separately, we compared the social, resilient and the unsocial, vulnerable PS mice with the C mice (social PS vs. C, unsocial PS vs. C). Only genes that were differentially expressed in social <u>or</u> unsocial mice, but not in both, were used for Enrichr analysis, as genes present in both groups would rather be associated with a general PS reaction. The VENN diagrams in Figure 3.3-16 show that in PS *5-Htt*+/- animals, considerably more genes (413 and 865) were differentially expressed than in the *5-Htt*+/+ group (29 and 71), both in unsocial and social PS mice, which fits to the high number of genes affected by a GxE interaction. Furthermore, in both genotypes, double the number of genes was regulated in social PS vs. C mice when compared to unsocial PS vs. C mice. Tables 3.3-13 and 3.3-14 show the DEGs for the comparisons "exclusively differentially expressed in social vs. C mice" and "exclusively differentially expressed in unsocial vs. C mice" for both genotypes. As the number of genes with $p<0.001$ (the p-value used for all other DEG tables of this project) was 0 for unsocial and 1 for social *5-Htt*+/+ mice, Table 3.3-13 presents DEGs with $p<0.005$ instead of $p<0.001$. This exception was made to provide the reader with an overview of the top regulated genes in social and unsocial *5-Htt*+/+ mice, even though the DEGs did not reach the same p-values as for the same comparison in the other genotype.

While the number of DEGs in social and unsocial *5-Htt*+/+ animals was too low to perform a proper enrichment analysis, Enrichr analysis on unsocial and social *5-Htt*+/- mice identified several enriched KEGG pathways and terms, which are presented in Tables 3.3-15 and 3.3-16, respectively. Enrichment analysis revealed two main networks to be affected in social PS vs. C *5-Htt*+/- mice, but not in unsocial PS vs. C *5-Htt*+/- mice:

Mitochondrial respiration and myelination. The mitochondrial respiration pathway was also enriched due to G-effects, as reported in the section "Changes in gene expression induced by the 5-Htt genotype", whereas processes surrounding myelination were affected by a GxE-interaction, as described in "Gene expression changes due to 5-Htt x PS interaction". Table 3.3-17 shows the enriched terms associated with cellular respiration, such as the KEGG pathway "oxidative phosphorylation" and the GO Biological processes such as "cellular respiration" and "ATPase activity". As Figure 3.3-18 illustrates, the DEGs of the KEGG pathway "oxidative phosphorylation" encode components of complex I, III, IV and V of the mitochondrial respiration chain. The GO Cellular compartment terms "respiratory chain complex III" and "respiratory chain complex IV" as well as several GO Molecular function terms associated with ATPase activity and the term "wide pore channel activity" were also found to be enriched.

Figure 3.3-16 Number of differentially expressed genes (DEGs) in the hippocampus of female social and unsocial mice exposed to PS with p<0.01. Female *5-Htt+/+* and *5-Htt+/-* offspring were exposed to PS or not (control, C). Social, resilient and unsocial, vulnerable PS mice were each compared to control mice to assess differentially expressed genes (DEGs). Up- and down-regulated DEGs in social PS vs control and unsocial PS vs control *5-Htt+/+* mice on the left side, for *5-Htt+/-* mice on the left side. Transcriptome data were assessed using mRNAseq, n=8.

Table 3.3-28 and Figure 3.3-17 illustrate the log2FC in expression of the DEGs of the "oxidative phosphorylation" pathway and of several additional genes associated with mitochondria in *5-Htt+/-* mice. The expression of all those mitochondria-associated genes except one shows the same pattern, i.e. expression is significantly increased in the social PS *5-Htt+/-* mice compared to C *5-Htt+/-* mice, but not in unsocial PS *5-Htt+/-* mice compared to C *5-Htt+/-* mice. However, the direction of the change is the same in the latter comparison, indicating that this pathway is regulated more effectively in social PS *5-Htt+/-* mice than in unsocial. Interestingly, we also found genotype-dependent effects on mitochondrial respiration processes and the "oxidative phosphorylation" pathway (compare to Tables 3.3-5 and 3.3-6), mainly on genes encoding components of the NADH dehydrogenase (complex 1). This indicates that both genotype and – dependent on the sociability classification – PS affected mitochondrial function, however, by targeting different genes.

A similar picture emerges when looking at the myelin-associated genes: Their expression is significantly decreased in social PS *5-Htt+/-* mice compared to C *5-Htt+/-* mice, but not in unsocial PS *5-Htt+/-* mice compared to C *5-Htt+/-* mice. Although the direction of the change is the same in both comparisons, it did not reach statistical significance in the unsocial PS *5-Htt+/-* vs. C *5-Htt+/-* mice comparison. *Hdac2* and *Canx* expression was increased in both comparisons, however, more pronounced and only significantly ($p<0.01$) in social PS vs. C *5-Htt+/-* mice. Table 3.3-19 and Figure 3.3-19 illustrate the log2FC in expression of the DEGs involved in myelination. As the difference in expression of myelin-associated genes between social and unsocial PS *5-Htt+/-* animals is smaller than between *C 5-Htt+/-* mice and the respective PS group, we cannot exclude that the decrease in myelin-genes expression in unsocial PS *5-Htt+/-* mice would have reached statistical significance if the *n* per group would have been higher.

Table 3.3-13 Differentially expressed genes (DEGs) in the hippocampus of female social and unsocial *5-Htt*+/+ mice exposed to PS with p<0.005. Female *5-Htt*+/+ offspring were exposed to PS or not (control, C). Social, resilient and unsocial, vulnerable PS mice were each compared to control mice to assess differentially expressed genes (DEGs). Transcriptome data were assessed using mRNAseq, n=8. Chr = chromosome, Bm = Base mean, Log2FC = Log2 fold change, C = control. A) Regulated in unsocial vs. control, but not in social vs. control, *5-Htt*+/+ mice. B) Regulated in social vs. control, but not in unsocial vs. control, *5-Htt*+/+ mice.

Symbol	Gene name	Chr	Bm	Log2FC	p
A) Regulated in unsocial vs. C *5-Htt*+/+ mice, but not in social					
Crx	cone-rod homeobox containing gene	7	4,08	1,90	0,00011
A630091E08Rik	RIKEN cDNA A630091E08 gene	7	4,42	1,69	0,00038
Gm5386	predicted pseudogene 5386	X	7,58	1,51	0,00096
Gm12384	predicted gene 12384	4	17,10	-1,47	0,00136
Synpo2	synaptopodin 2	3	275,19	0,28	0,00152
Gm12895	predicted gene 12895	4	12,56	1,24	0,00265
Frrs1	ferric-chelate reductase 1	3	48,40	0,55	0,00395
Gm12523	predicted gene 12523	3	73,42	0,86	0,00407
Insl6	insulin-like 6	19	4,60	-1,22	0,00420
Gm12896	predicted gene 12896	4	12,86	1,18	0,00421
Gm3448	predicted gene 3448	17	537,04	0,33	0,00484
B) Regulated in social vs. C *5-Htt*+/+ mice, but not in unsocial					
Pld5	phospholipase D family, member 5	1	216,09	-0,26	3,27E-05
Gm23341	predicted gene, 23341	11	1,12	-1,86	0,00118
Rbm15	RNA binding motif protein 15	3	514,76	0,21	0,00123
Rsph3b	radial spoke 3B homolog (Chlamydomonas)	17	823,68	-0,15	0,00136
Lrrn4	leucine rich repeat neuronal 4	2	76,41	0,36	0,00151
Gpx7	glutathione peroxidase 7	4	75,10	-0,31	0,00189
Asf1b	ASF1 anti-silencing function 1 homolog B (S. cerevisiae)	8	38,97	0,43	0,00194
Rlbp1	retinaldehyde binding protein 1	7	559,18	-0,20	0,00196
Kcnj8	potassium inwardly-rectifying channel, subfamily J, member 8	6	78,74	-0,33	0,00199

Rasgrp2	RAS, guanyl releasing protein 2	19	324,83	-0,27	0,00212
Pisd	phosphatidylserine decarboxylase	5	1142,31	-0,18	0,00224
Gm15496	predicted gene 15496	3	135,65	0,21	0,00265
Peg12	paternally expressed 12	7	4,77	-1,16	0,00269
Acr	acrosin prepropeptide	15	42,67	-0,46	0,00304
Slco5a1	solute carrier organic anion transporter family, member 5A1	1	133,74	0,27	0,00306
Ddx41	DEAD (Asp-Glu-Ala-Asp) box polypeptide 41	13	1008,97	-0,19	0,00327
Gm14129	predicted gene 14129	2	0,57	1,71	0,00330
Il31ra	interleukin 31 receptor A	13	866,19	-0,47	0,00330
Atp12a	ATPase, H+/K+ transporting, nongastric, alpha polypeptide	14	3,36	-1,12	0,00373
Ypel2	yippee-like 2 (Drosophila)	11	1781,74	0,15	0,00377
Sfi1	Sfi1 homolog, spindle assembly associated (yeast)	11	1644,79	-0,26	0,00445
Gm23722	predicted gene, 23722	1	0,25	1,61	0,00482
Gm22157	predicted gene, 22157	13	0,10	-1,29	0,00486

Table 3.3-14 Differentially expressed genes (DEGs) in the hippocampus of female social and unsocial *5-Htt*+/- mice exposed to PS with p<0.001. Female *5-Htt*+/- offspring were exposed to PS or not (control, C). Social, resilient and unsocial, vulnerable PS mice were each compared to control mice to assess differentially expressed genes (DEGs). Transcriptome data were assessed using mRNAseq, n=8. Chr = chromosome, Bm = Base mean, Log2FC = Log2 fold change, C = control. A) Regulated in unsocial vs. control, but not in social vs. control, *5-Htt*+/- mice. B) Regulated in social vs. control, but not in unsocial vs. control, *5-Htt*+/- mice.

Symbol	Gene name	Chr	Bm	Log2FC	p
A) Regulated in unsocial vs. C *5-Htt*+/- mice, but not in social:					
Avp	arginine vasopressin	2	8.50138	-2.11	0.000015
Gstm4	glutathione S-transferase, mu 4	3	244.837	-0.27	0.000057
2410004P03Rik	RIKEN cDNA 2410004P03 gene	12	47.4138	-0.81	0.000061
Rassf10	Ras association (RalGDS/AF-6) domain family (N-terminal) member 10	7	23.1404	-0.75	0.000068
Pdgfra	platelet derived growth factor receptor, alpha polypeptide	5	2094.98	-0.18	0.000155
Rn7sk	RNA, 7SK, nuclear	9	13.763	1.19	0.000192

Psat1	phosphoserine aminotransferase 1	19	3091.67	-0.2	0.000246
Ak7	adenylate kinase 7	12	85.271	-0.81	0.000251
Oxt	oxytocin	2	3.61044	-1.75	0.000274
Tmem107	transmembrane protein 107	11	155.754	-0.27	0.000329
Cxcr4	chemokine (C-X-C motif) receptor 4	1	82.9284	-0.39	0.000355
Car9	carbonic anhydrase 9	4	9.4338	-1.03	0.000404
Gm11627	predicted gene 11627	11	46.6092	-0.48	0.000406
Gm24245	predicted gene, 24245	4	116.602	0.67	0.000513
Hspa2	heat shock protein 2	12	2019.06	-0.24	0.000527
Gm24270	predicted gene, 24270	9	87.82	0.62	0.000553
Psmc3ip	proteasome (prosome, macropain) 26S subunit, ATPase 3, interacting protein	11	106.233	-0.32	0.000570
Gas2l2	growth arrest-specific 2 like 2	11	55.1861	-0.39	0.000656
Gm15608	predicted gene 15608	10	239.697	0.52	0.000699
Rrp8	ribosomal RNA processing 8, methyltransferase, homolog (yeast)	7	383.628	-0.2	0.000747
9530080O11Rik	RIKEN cDNA 9530080O11 gene	4	103.742	0.32	0.000753
E030010N08Rik	RIKEN cDNA E030010N08 gene	1	15.4621	-1	0.000753
AI464131	expressed sequence AI464131	4	1144.4	-0.23	0.000813
Eva1a	eva-1 homolog A (C. elegans)	6	319.12	-0.29	0.000879
Unc5cl	unc-5 homolog C (C. elegans)-like	17	19.1487	-0.73	0.000930
Rhpn2	rhophilin, Rho GTPase binding protein 2	7	216.323	-0.32	0.000996

B) Regulated in social vs. C 5-*Htt*+/- mice, but not in unsocial:

5031439G07Rik	RIKEN cDNA 5031439G07 gene	15	4872.23	-0.18	0.000003
Chmp3	charged multivesicular body protein 3	6	3711.6	0.14	0.000004
Cct8	chaperonin containing Tcp1, subunit 8 (theta)	16	6415.26	0.14	0.000006
Gm13080	predicted gene 13080	4	303.753	0.26	0.000008
Gm12384	predicted gene 12384	4	11.7788	-2.24	0.000009
Ddx1	DEAD (Asp-Glu-Ala-Asp) box polypeptide 1	12	5084.55	0.13	0.000011
Wdr47	WD repeat domain 47	3	6983.25	0.12	0.000029
Plekhg3	pleckstrin homology domain containing, family G (with RhoGef domain) member 3	12	576.291	-0.37	0.000036

Cript	cysteine-rich PDZ-binding protein	17	1182.35	0.2	0.000036
Rtkn	rhotekin	6	899.601	-0.27	0.000042
Itgb4	integrin beta 4	11	198.398	-0.51	0.000042
Kif13a	kinesin family member 13A	13	1267.96	-0.18	0.000043
Amotl2	angiomotin-like 2	9	610.928	-0.26	0.000044
Igdcc3	immunoglobulin superfamily, DCC subclass, member 3	9	103.128	-0.38	0.000053
Zbtb7b	zinc finger and BTB domain containing 7B	3	429.219	-0.29	0.000075
Zfp551	zinc fingr protein 551	7	238.078	0.27	0.000078
0610009B22Rik	RIKEN cDNA 0610009B22 gene	11	423.734	0.21	0.000079
Rgs10	regulator of G-protein signalling 10	7	528.727	0.21	0.000089
Pgrmc1	progesterone receptor membrane component 1	X	9066.55	0.16	0.000106
Ankrd13a	ankyrin repeat domain 13a	5	1640.86	-0.17	0.000116
Phldb1	pleckstrin homology-like domain, family B, member 1	9	3552.88	-0.33	0.000119
Ddc	dopa decarboxylase	11	172.729	-0.35	0.000139
Kndc1	kinase non-catalytic C-lobe domain (KIND) containing 1	7	5200.19	-0.2	0.000141
Lamc1	laminin, gamma 1	1	1433.6	-0.18	0.000141
mt-Co3	mitochondrially encoded cytochrome c oxidase III	M	104326	0.23	0.000141
Gsn	gelsolin	2	1391.27	-0.37	0.000147
mt-Tc	mitochondrially encoded tRNA cysteine	M	510.828	0.42	0.000154
mt-Co2	mitochondrially encoded cytochrome c oxidase II	M	99318.7	0.2	0.000166
Gm6741	predicted gene 6741	17	304.783	0.21	0.000173
Hapln2	hyaluronan and proteoglycan link protein 2	3	406.99	-0.48	0.000174
Plekhh1	pleckstrin homology domain containing, family H (with MyTH4 domain) member 1	12	1205.74	-0.3	0.000175
Tmem63a	transmembrane protein 63a	1	848.134	-0.38	0.000185
Slco4a1	solute carrier organic anion transporter family, member 4a1	2	55.2467	-0.81	0.000185
Galnt6	UDP-N-acetyl-alpha-D-galactosamine:polypeptide N-acetylgalactosaminyltransferase 6	15	314.202	-0.39	0.000193
Fcrla	Fc receptor-like A	1	398.542	0.27	0.000197
Tcp1	t-complex protein 1	17	5375.66	0.15	0.000229
Cfdp1	craniofacial development protein 1	8	1852.84	0.17	0.000236
Fth-ps2	ferritin heavy chain, pseudogene 2	6	14.0827	1.99	0.000239
Fuk	fucokinase	8	376.465	-0.24	0.000249

Shmt2	serine hydroxymethyltransferase 2 (mitochondrial)	10	444.726	-0.24	0.000264
Gm13341	predicted gene 13341	2	12004.9	0.26	0.000265
Cilp2	cartilage intermediate layer protein 2	8	64.7631	-0.54	0.000270
Gm11512	predicted gene 11512	11	413.222	0.3	0.000271
Xrcc1	X-ray repair complementing defective repair in Chinese hamster cells 1	7	760.683	-0.18	0.000273
Rabep2	rabaptin, RAB GTPase binding effector protein 2	7	318.632	-0.21	0.000277
Gm14372	predicted gene 14372	7	315.478	-0.29	0.000286
BC029214	cDNA sequence BC029214	2	564.553	-0.18	0.000301
Lmna	lamin A	3	827.322	-0.26	0.000303
Gm2962	predicted pseudogene 2962	1	362.494	0.29	0.000316
Sox8	SRY-box containing gene 8	17	1222.84	-0.22	0.000335
1700040N02Rik	RIKEN cDNA 1700040N02 gene	2	294.966	-0.33	0.000363
Adamts4	a disintegrin-like and metallopeptidase (reprolysin type) with thrombospondin type 1 motif, 4	1	658.778	-0.33	0.000368
Gltp	glycolipid transfer protein	5	707.565	-0.25	0.000373
Myrf	myelin regulatory factor	19	1577.27	-0.3	0.000385
Psma1	proteasome (prosome, macropain) subunit, alpha type 1	7	2710.87	0.13	0.000395
Calm2	calmodulin 2	17	33684.3	0.15	0.000404
Gm7308	predicted pseudogene 7308	6	5581.79	0.21	0.000405
Dus3l	dihydrouridine synthase 3-like (S. cerevisiae)	17	1364.63	-0.25	0.000416
Wdr5b	WD repeat domain 5B	16	140.069	0.26	0.000426
Gm12543	predicted gene 12543	4	193.492	0.28	0.000430
Itpr3	inositol 1,4,5-triphosphate receptor 3	17	151.235	-0.41	0.000430
Pyroxd2	pyridine nucleotide-disulphide oxidoreductase domain 2	19	79.0938	-0.4	0.000449
6720427I07Rik	RIKEN cDNA 6720427I07 gene	13	168.585	0.47	0.000452
Wdr61	WD repeat domain 61	9	1987.97	0.08	0.000474
Tspan12	tetraspanin 12	6	736.335	0.2	0.000478
Nkx6-2	NK6 homeobox 2	7	182.998	-0.4	0.000482
Mbp	myelin basic protein	18	49001.9	-0.33	0.000494
Ube2e3	ubiquitin-conjugating enzyme E2E 3	2	2103.06	0.18	0.000494
Gm6206	predicted pseudogene 6206	X	1140.62	0.19	0.000509
mt-Cytb	mitochondrially encoded cytochrome b	M	192474	0.2	0.000520

Tuba3b	tubulin, alpha 3B	6	4.0043	2.01	0.000558
Gm13414	predicted gene 13414	2	881.92	0.16	0.000561
Pigo	phosphatidylinositol glycan anchor biosynthesis, class O	4	635.744	-0.23	0.000563
2010107E04Rik	RIKEN cDNA 2010107E04 gene	12	1663.72	0.23	0.000569
Exosc9	exosome component 9	3	1034.94	0.15	0.000573
Gm6335	predicted gene 6335	X	963.685	0.2	0.000574
Otud7b	OTU domain containing 7B	3	2512.45	-0.16	0.000591
Pcnt	pericentrin (kendrin)	10	1373.81	-0.16	0.000592
Gm12174	predicted gene 12174	11	1234.64	0.2	0.000598
Notch3	notch 3	17	387.567	-0.27	0.000606
4931403E22Rik	RIKEN cDNA 4931403E22 gene	19	1512.9	0.13	0.000614
Spin2c	spindlin family, member 2C	X	193.937	0.27	0.000620
Fam98c	family with sequence similarity 98, member C	7	401.846	-0.2	0.000627
Gm16515	predicted gene, Gm16515	11	411.443	-0.2	0.000630
Gm6563	predicted pseudogene 6563	19	728.498	0.21	0.000633
Vdac3	voltage-dependent anion channel 3	8	2042.16	0.13	0.000653
Zfp366	zinc finger protein 366	13	101.449	-0.5	0.000684
Slc5a6	solute carrier family 5 (sodium-dependent vitamin transporter), member 6	5	495.142	-0.19	0.000689
Mcm2	minichromosome maintenance deficient 2 mitotin (S. cerevisiae)	6	151.199	-0.33	0.000705
Pmepa1	prostate transmembrane protein, androgen induced 1	2	719.94	-0.22	0.000706
Zfp536	zinc finger protein 536	7	1341.32	-0.18	0.000733
Abca2	ATP-binding cassette, sub-family A (ABC1), member 2	2	8846.36	-0.23	0.000764
Rela	v-rel reticuloendotheliosis viral oncogene homolog A (avian)	19	572.38	-0.2	0.000766
Hdac2	histone deacetylase 2	10	3204.2	0.16	0.000778
4933428G20Rik	RIKEN cDNA 4933428G20 gene	11	359.875	-0.24	0.000798
Tnni1	troponin I, skeletal, slow 1	1	92.6681	-0.48	0.000803
Gal3st1	galactose-3-O-sulfotransferase 1	11	255.78	-0.3	0.000809
Rcc1	regulator of chromosome condensation 1	4	390.917	-0.18	0.000810
D8Ertd82e	DNA segment, Chr 8, ERATO Doi 82, expressed	8	957.184	-0.21	0.000813
Rpl7	ribosomal protein L7	1	2020.04	0.2	0.000817
Gm16339	predicted gene 16339	12	98.7139	-0.3	0.000842

Hr	hairless	14	379.033	-0.34	0.000855
Tcf3	transcription factor 3	10	772.608	-0.23	0.000863
Tmem88b	transmembrane protein 88B	4	963.277	-0.31	0.000878
Rpl15	ribosomal protein L15	14	2135.81	0.16	0.000899
Api5	apoptosis inhibitor 5	2	3595.05	0.16	0.000914
Micall1	microtubule associated monooxygenase, calponin and LIM domain containing -like 1	15	1858.91	-0.22	0.000919
Vps41	vacuolar protein sorting 41 (yeast)	13	7237.31	0.11	0.000939
Sema6a	sema domain, transmembrane domain (TM), and cytoplasmic domain, (semaphorin) 6A	18	675.575	-0.23	0.000944
Rpl5	ribosomal protein L5	5	1958.66	0.12	0.000945
Csrnp1	cysteine-serine-rich nuclear protein 1	9	118.732	-0.37	0.000995
Psmd13	proteasome (prosome, macropain) 26S subunit, non-ATPase, 13	7	4037.43	0.08	0.000997

Table 3.3-15 Enriched pathways and terms in the hippocampus of female unsocial, but not social, *5-Htt*+/- mice exposed to PS (p<0.05). Female *5-Htt*+/- offspring were exposed to PS or not (control, C). Social, resilient and unsocial, vulnerable PS mice were each compared to control mice to assess differentially expressed genes (DEGs). Transcriptome data were assessed using mRNAseq, n=8. Overlap = number of DEGs/total number of genes in this pathway or term. Enrichment analysis performed using Enrichr (Chen Tan 2013) using DEGs with p<0.01.

Enriched term	Term ID	Overlap	P	Genes
A) Mammalian phenotype term				
Abnormal brain morphology	MP0002152	23/1188	1.98E-05	NPC1, AVP, CDKN1A, FABP7, NDE1, PHGDH, GM2A, CXCR4, TSKU, FOXJ1, ADIPOR2, SLC9A3R1, AARS, PDGFRA, TRP53BP2, IL1RAPL1, LGALS1, HYDIN, CSPG4, ITPK1, EGR1, EGR2, SLC17A5
Abnormal skin development	MP0003941	3/10	0.00011	CDKN1A, PDGFRA, ABCA12
Abnormal gametogenesis	MP0001929	14/595	0.00017	NPC1, ACOX1, PSMC3IP, HSPA2, RSPH1, RARA, PDGFRA, TALDO1, DDX4, CXCR4, EGR1, EGR2, FOXJ1, ADIPOR2
Mammalian phenotype	MP0000001	45/3773	0.00018	ATF1, CDKN1A, E2F8, RHPN2, CAPN2, PDGFRA, MAPK13, ITPK1, TNS3, ACTB, GDF10, RSPH1, MAGED1, GPHN, CPT1A, SLC9A3R1, RARA, TALDO1, PTPN11, NOTCH4, CPS1, HPS6, SLC17A5, AVP, FMN1, ABCA12, GRIK1, GJB6, CD19, CXCR4, FOXJ1, EPAS1, TRPM8, LGALS1, CSPG4, IL21R, EGR1, EGR2, FKBP5, SLC35C1, CAR9, HTR5B, EZR, TRP53BP2, HYDIN

Abnormal lung morphology	MP0001175	10/402	0.00104	NPC1, ABCA12, CDKN1A, SLC35C1, RARA, PDGFRA, TNS3, CTSA, EGR1, NOL3
Other aberrant phenotype	MP0002168	4/62	0.00153	RARA, FOXJ1, CAPN2, CPT1A
Abnormal sex determination	MP0002210	10/425	0.00156	NPC1, ACOX1, PSMC3IP, HSPA2, STC2, PDGFRA, DDX4, EGR1, ADIPOR2, ACTB
Abnormal emotion/affect behavior	MP0002572	9/372	0.00225	SERPINI1, OXT, MYG1, GJB6, HYDIN, FABP7, GM2A, EGR1, SLC17A5
Abnormal lipid homeostasis	MP0002118	13/693	0.00231	NPC1, ABCA12, CPT1A, NEU4, CDKN1A, FABP7, ACOX1, PTPN11, OXT, IL21R, EGR1, ADIPOR2, ACTB
Abnormal muscle development	MP0000733	4/71	0.00246	CXCR4, PDGFRA, LGALS1, CDKN1A
Abnormal autonomic nervous	MP0006276	3/33	0.00249	OXT, MAGED1, PIRT
Abnormal fertility/fecundity	MP0002161	17/1088	0.00326	NPC1, FMN1, PSMC3IP, SLC35C1, RSPH1, DDX4, FOXJ1, ACOX1, SLC9A3R1, HSPA2, RARA, PDGFRA, TALDO1, PTPN11, HYDIN, EGR1, ACTB
Abnormal male reproductive	MP0001145	11/554	0.00336	NPC1, CDKN1A, ACOX1, PSMC3IP, HSPA2, RARA, STC2, PDGFRA, DDX4, EGR1, ADIPOR2
Abnormal fetal growth/weight/	MP0004197	6/199	0.00451	PDGFRA, PTPN11, ABCA12, CDKN1A, CXCR4, FOXJ1
Abnormal male reproductive	MP0003698	12/667	0.00479	NPC1, FMN1, ACOX1, HSPA2, SLC35C1, RSPH1, RARA, PDGFRA, TALDO1, DDX4, HYDIN, EGR1
Abnormal glial cell	MP0003690	3/43	0.00501	EGR1, PTPN11, NPC1
Abnormal nervous system	MP0003861	14/855	0.00524	CDKN1A, NDE1, PHGDH, CXCR4, FOXJ1, GPHN, SLC9A3R1, PDGFRA, TRP53BP2, PTPN11, HYDIN, ITPK1, EGR2, SLC17A5
Abnormal hormone level	MP0003953	12/677	0.00538	NPC1, AVP, MYG1, EPAS1, CDKN1A, PDGFRA, PTPN11, MAPK13, HPS6, EGR1, ADIPOR2, ACTB
Premature death	MP0002083	15/968	0.00631	NPC1, CDKN1A, OXT, CD19, FHIT, SLC9A3R1, RARA, PDGFRA, PTPN11, HYDIN, CTSA, EGR1, EGR2, ACTB, SLC17A5
Abnormal sex gland	MP0000653	11/629	0.00848	NPC1, CDKN1A, ACOX1, PSMC3IP, HSPA2, RARA, STC2, PDGFRA, DDX4, EGR1, ADIPOR2
Abnormal eating/drinking beha	MP0002069	10/543	0.00858	NPC1, AVP, GPHN, ABCA12, CDKN1A, OXT, CTSA, EGR2, ADIPOR2, ACTB
Abnormal neuron physiology	MP0004811	7/309	0.00982	MAGED1, TRP53BP2, PIRT, ATF1, NDE1, EGR2, TRPM8

B) Kegg pathways

Aminoacyl tRNA biosynthesis	HSA00970	3/38	0.00939	IARS, YARS, AARS
Leukocyte transendothelial migration	HSA04670	4/115	0.03813	PTPN11, CXCR4, EZR, MAPK13
Ppar signaling pathway	HSA03320	3/70	0.04316	ACOX1, CPT1A, FABP7
Adipocytokine signaling pathway	HSA04920	3/72	0.04617	ADIPOR2, CPT1A, PTPN11

C) GO Biological processes

Cell projection assembly	GO:0030031	10/213	6.04E-05	RSPH1, CAPZB, TMEM107, EZR, HYDIN, TTYH1, AK7, TMEM231, FOXJ1, SLC9A3R1
Fat cell differentiation	GO:0045444	7/96	6.14E-05	RARRES2, WNT5B, FBXO9, LRRC8C, EGR2, NUDT7, GDF10
Cellular response to acid chemical	GO:0071229	8/147	0.00013	WNT3, RARA, PDGFRA, WNT5B, CPS1, EGR1, CAPN2, CPT1A
Response to acid chemical	GO:0001101	10/275	0.00044	RARA, AARS, PDGFRA, OXT, CAPN2, CPT1A, WNT3, WNT5B, CPS1, EGR1
Microtubule bundle formation	GO:0001578	4/40	0.00084	TTLL6, RSPH1, AK7, GAS2L2
Cellular amino acid metabolic process	GO:0006520	12/421	0.00099	YARS, HPDL, MTHFD2, PSAT1, SLC7A5, ACMSD, IARS, GPT2, AARS, PHGDH, GSTM4, CPS1
Response to extracellular stimulus	GO:0009991	10/313	0.00116	RARA, STC2, OXT, SQSTM1, FADS1, RRP8, CPS1, CDKN1A, EGR1, ADIPOR2
Cellular response to lipid	GO:0071396	10/315	0.00122	RARA, NPC1, CPT1A, WNT3, SPON2, PAF1, WNT5B, PAQR8, CPS1, EGR1
Positive regulation of amine transport	GO:0051954	3/23	0.00194	AVP, GRIK1, OXT
Positive regulation of organic acid transport	GO:0032892	3/23	0.00194	AVP, GRIK1, OXT
Regulation of excretion	GO:0044062	3/25	0.00241	OXT, AVP, SLC9A3R1
Response to nutrient levels	GO:0031667	9/291	0.00253	RARA, STC2, OXT, SQSTM1, FADS1, RRP8, CPS1, EGR1, ADIPOR2
Cellular component assembly involved in morphogenesis	GO:0010927	7/186	0.00268	RSPH1, PDGFRA, AK7, TMEM231, TMEM107, FOXJ1, HYDIN

Positive regulation of glucose import	GO:0046326	3/30	0.00388	RARRES2, ADIPOR2, PTPN11
Cellular amino acid biosynthetic process	GO:0008652	5/106	0.00441	GPT2, CPS1, MTHFD2, PHGDH, PSAT1
Epithelial cell development	GO:0002064	5/107	0.00458	RARA, WNT5B, FOXJ1, EZR, HYDIN
Alpha-amino acid biosynthetic process	GO:1901607	4/69	0.00540	MTHFD2, CPS1, PHGDH, PSAT1
Female mating behavior	GO:0060180	2/10	0.00573	AVP, OXT
Positive regulation of glucose transport	GO:0010828	3/35	0.00580	RARRES2, ADIPOR2, PTPN11
Response to alcohol	GO:0097305	8/274	0.00605	RARA, STC2, AVP, OXT, CPS1, CDKN1A, EGR1, EIF4G1
Neurotrophin TRK receptor signaling pathway	GO:0048011	8/274	0.00605	MAGED1, PDGFRA, PTPN11, SQSTM1, CD19, MAPK13, ATF1, CDKN1A
Neurotrophin signaling pathway	GO:0038179	8/278	0.00657	MAGED1, PDGFRA, PTPN11, SQSTM1, CD19, MAPK13, ATF1, CDKN1A
Germ cell development	GO:0007281	5/121	0.00749	RARA, PAQR8, PAQR5, CXCR4, HSPA2
Social behavior	GO:0035176	3/39	0.00767	OXT, AVP, GNB1L
Intraspecies interaction between organisms	GO:0051703	3/39	0.00767	OXT, AVP, GNB1L
Response to amine	GO:0014075	3/40	0.00819	OXT, EGR1, CPS1
Platelet aggregation	GO:0070527	3/40	0.00819	ACTB, CSRP1, PDGFRA
Oligosaccharide metabolic process	GO:0009311	3/41	0.00873	GM2A, PRKCSH, NEU4
Multicellular organismal reproductive process	GO:0048609	11/491	0.00937	AVP, ACOX1, RARA, DDX4, PTPN11, OXT, WNT3, PAQR8, PAQR5, AK7, FOXJ1
Cellular response to camp	GO:0071320	3/43	0.00986	EGR1, EGR2, CPS1
Regulation of organic acid transport	GO:0032890	3/43	0.00986	GRIK1, OXT, AVP

D) Histone modifications

H3K4me3	LNCAP	13/920	0.04034

Table 3.3-16 Enriched pathways and terms in the hippocampus of female social, but not unsocial, *5-Htt*+/- mice exposed to PS (p<0.05). Female *5-Htt*+/- offspring were exposed to PS or not (control, C). Social, resilient and unsocial, vulnerable PS mice were each compared to control mice to assess differentially expressed genes (DEGs). Transcriptome data were assessed using mRNAseq, n=8. Overlap = number of DEGs/total number of genes in this pathway or term. Enrichment analysis performed using Enrichr (Chen Tan 2013) using DEGs with p<0.01.

Enriched term	Term ID	Overlap	P	Genes
A) Mammalian phenotype term				
Mammalian phenotype	MP0000001	115/3773	1.03E-08	
Abnormal brain morphology	MP0002152	50/1188	2.38E-07	
Abnormal neuron morphology	MP0002882	43/1006	1.40E-06	
Cellular phenotype	MP0005384	25/486	1.75E-05	
Prenatal lethality	MP0002080	57/1685	2.51E-05	
Abnormal blood circulation	MP0002128	23/449	4.13E-05	
Preweaning lethality	MP0010770	42/1115	3.88E-05	
Postnatal lethality	MP0002082	42/1114	3.80E-05	
Abnormal myelination	MP0000920	11/134	1.15E-04	
Abnormal cell content/	MP0000358	11/137	1.38E-04	
Abnormal motor capabilities/c	MP0002066	49/1482	1.95E-04	
Abnormal somatic nervous	MP0002752	28/675	2.05E-04	
Abnormal nervous system	MP0003861	33/855	1.96E-04	
Abnormal cell physiology	MP0005621	18/348	2.62E-04	
Normal phenotype	MP0002873	46/1375	2.49E-04	
Abnormal ureter morphology	MP0000534	7/60	2.98E-04	
Abnormal survival	MP0010769	42/1229	3.19E-04	
Abnormal vestibular system	MP0004742	6/45	4.25E-04	
Abnormal blood vessel	MP0001614	30/778	4.01E-04	
No abnormal phenotype	MP0002169	45/1370	4.39E-04	
Mortality/aging	MP0010768	42/1255	4.90E-04	
Abnormal cell differentiation	MP0005076	5/30	5.22E-04	
Abnormal respiratory system	MP0003115	8/93	7.43E-04	
Abnormal postnatal growth	MP0001731	28/732	7.17E-04	
Abnormal kidney morphology	MP0002135	24/591	8.00E-04	
Abnormal glial cell	MP0003634	13/231	9.13E-04	

Intracranial hemorrhage	MP0001915	7/74	9.49E-04	
Abnormal posterior eye	MP0005195	19/433	1.21E-03	
Abnormal lung morphology	MP0001175	18/402	1.31E-03	
Abnormal embryonic tissue	MP0002085	28/765	1.37E-03	
Abnormal heart morphology	MP0000266	30/851	1.62E-03	
Abnormal epidermal layer	MP0001216	13/251	1.86E-03	
Abnormal blood vessel	MP0000249	13/254	2.06E-03	
Decreased survivor rate	MP0008770	11/195	2.20E-03	
Abnormal inner ear	MP0000026	12/229	2.52E-03	
Abnormal antigen presenting	MP0002452	26/722	2.55E-03	
Aneurysm	MP0003279	4/26	2.51E-03	
Abnormal eye morphology	MP0002092	9/144	2.88E-03	
Abnormal urinary system	MP0003942	7/92	3.04E-03	
Abnormal cardiovascular devel	MP0002925	22/583	3.20E-03	
Abnormal hair follicle	MP0000377	9/149	3.57E-03	
Abnormal muscle physiology	MP0002106	10/178	3.56E-03	
Perinatal lethality	MP0002081	32/981	3.70E-03	
Abnormal fat cell	MP0009115	7/98	4.21E-03	
Abnormal pulmonary circulatio	MP0002295	5/54	5.54E-03	
Abnormal craniofacial bone	MP0002116	18/467	6.10E-03	
Abnormal nervous system	MP0002272	11/227	6.56E-03	
Abnormal embryo size	MP0001697	18/471	6.62E-03	
Abnormal respiration	MP0001943	17/438	7.15E-03	
Abnormal fluid regulation	MP0001784	18/475	7.19E-03	
Abnormal fetal growth/weight/	MP0004197	10/199	7.43E-03	
Vision/eye phenotype	MP0005391	11/235	8.33E-03	
Nervous system phenotype	MP0003631	11/240	9.61E-03	
abnormal adaptive immunity	MP0002420	33/1092	9.69E-03	

B) KEGG pathways

Proteasome	HSA03050	5/22	0.00164	PSMA2, PSMA1, PSMD13, PSMA4, PSMD6
Oxidative phosphorylation	HSA00190	11/128	0.00576	PPA2, COX3, COX2, COX1, UQCRC2, NDUFS1, ATP6V1C1, UQCRH, UQCRB, CYTB, ATP6V0A2
C5 branched dibasic acid metabolism	HSA00660	2/2	0.00622	ILVBL, SUCLA2

Notch signaling pathway	HSA04330	6/47	0.00746	DVL2, SNW1, NOTCH3, HDAC2, PSEN2, NCOR2
Focal adhesion	HSA04510	13/200	0.02255	PGF, LAMC1, LAMB2, BCAR1, COL11A2, PDGFB, PDGFA, ACTN4, PPP1CB, ITGB4, ITGA3, CDC42, COL5A3
Ecm receptor interaction	HSA04512	7/87	0.03465	COL11A2, LAMC1, ITGB4, LAMB2, HSPG2, ITGA3, COL5A3
C) Biological processes				
Organ morphogenesis	GO:0009887	31/405	5.93E-06	DVL2, PCNT, TLE3, CSF1, GAMT, LRP5, RELA, IFT140, HDAC2, EDAR, IRX5, ID3, ELN, EPHB1, BMP4, SEMA6A, TULP3, CSRNP1, NCOR2, MYO7A, COL11A2, PSEN2, DCHS1, STK40, HSPG2, PDGFA, ITGB4, SOX8, PRRX2, MEN1, NFIC
Cellular respiration	GO:0045333	8/38	5.27E-05	UQCRC2, FASTKD2, MT-CO1, NDUFS1, SLC25A14, UQCRH, MT-CO3, UQCRB
Antigen processing and presentation of exogenous peptide antigen via mhc class i	GO:0042590	11/79	6.68E-05	PDIA3, TAPBP, PSMD5, PSMD6, PSMA2, PSMA1, PSMA4, SEC61G, FCER1G, PSMD14, PSMD13
Viral life cycle	GO:0019058	13/118	1.33E-04	CHMP3, CHMP5, RPL15, RPLP2, RPLP1, CHMP2B, RPL7, RPL5, FURIN, PPIA, VPS37C, RPS4X, RPL39
Aerobic respiration	GO:0009060	6/22	1.39E-04	UQCRC2, MT-CO1, SLC25A14, UQCRH, MT-CO3, UQCRB
Antigen processing and presentation of peptide antigen via mhc class i	GO:0002474	12/104	1.62E-04	TAPBP, PSMA2, PSMA1, PSMA4, SEC61G, FCER1G, PDIA3, CANX, PSMD5, PSMD6, PSMD14, PSMD13
Myelination	GO:0042552	9/59	1.65E-04	TSPAN2, MBP, NKX6-2, NAB2, CNTN2, MYRF, PLLP, SERINC5, GAL3ST1
Antigen processing and presentation of exogenous peptide antigen via mhc class i, tap-dependent	GO:0002479	10/75	1.96E-04	PDIA3, TAPBP, PSMD5, PSMD6, PSMA2, PSMA1, PSMA4, SEC61G, PSMD14, PSMD13
Axon ensheathment	GO:0008366	9/62	2.31E-04	TSPAN2, MBP, NKX6-2, NAB2, CNTN2, MYRF, PLLP, SERINC5, GAL3ST1
Ensheathment of neurons	GO:0007272	9/62	2.31E-04	TSPAN2, MBP, NKX6-2, NAB2, MYRF, CNTN2, PLLP, SERINC5, GAL3ST1
Cellular component disassembly	GO:0022411	24/350	3.19E-04	RPL15, RPLP2, RPLP1, LAMC1, ADAMTS4, ELN, COL16A1, COL11A2, DEDD2, MICAL3, ADAM15, RPL39, PLEC, HSPG2, LMNA, DDIT4, RPL7, RPL5, FURIN, BCAN, GSN, RPS4X, COL5A3, GSPT2
Extracellular matrix organization	GO:0030198	24/359	4.50E-04	LTBP4, LAMC1, ADAMTS4, ELN, VIT, LAMB2, BMP4, COL16A1, COL11A2, ADAM15, CRISPLD2, PLEC, HAPLN2, HSPG2, FBLN1, PDGFB, PDGFA, ITGB4, EFEMP2, ITGA3, FURIN, BCAN, COL5A3, SULF2

Extracellular structure organization	GO:0043062	24/360	4.67E-04	LTBP4, LAMC1, ADAMTS4, ELN, VIT, LAMB2, BMP4, COL16A1, COL11A2, ADAM15, CRISPLD2, PLEC, HAPLN2, HSPG2, FBLN1, PDGFB, PDGFA, ITGB4, EFEMP2, ITGA3, FURIN, BCAN, COL5A3, SULF2
Signal transduction involved in dna integrity checkpoint	GO:0072401	9/71	5.69E-04	PSMD5, PSMD6, CDC5L, PSMA2, PSMA1, PSMA4, RBM38, PSMD14, PSMD13
Signal transduction involved in dna damage checkpoint	GO:0072422	9/71	5.69E-04	PSMD5, PSMD6, CDC5L, PSMA2, PSMA1, PSMA4, RBM38, PSMD14, PSMD13
Platelet-derived growth factor receptor signaling pathway	GO:0048008	6/30	5.88E-04	PDGFB, PDGFA, BCAR1, GAB1, CSRNP1, PTPN1
Signal transduction involved in cell cycle checkpoint	GO:0072395	9/72	6.24E-04	PSMD5, PSMD6, CDC5L, PSMA2, PSMA1, PSMA4, RBM38, PSMD14, PSMD13
Brain development	GO:0007420	15/187	9.88E-04	TSPAN2, IRS2, DDIT4, RAB18, ARRB2, NKX2-2, TULP3, POU6F1, MEN1, SLC23A1, BAG6, OXCT1, PAFAH1B2, AATK, HSPG2
Positive regulation of gliogenesis	GO:0014015	6/35	1.20E-03	SOX8, NKX6-2, NKX2-2, SOX10, RELA, HDAC2
Regulation of cellular response to growth factor stimulus	GO:0090287	14/176	1.55E-03	PDGFB, GPR124, LTBP4, TMEM204, PPP1CB, SNW1, ITGA3, PTPN1, MEN1, SPRY1, VASN, PRKD2, PMEPA1, SULF2
Dna damage response, signal transduction by p53 class mediator resulting in cell cycle arrest	GO:0006977	8/67	1.62E-03	PSMD5, PSMD6, PSMA2, PSMA1, PSMA4, RBM38, PSMD14, PSMD13
Oxidative phosphorylation	GO:0006119	4/14	1.65E-03	UQCRC2, MT-CO1, UQCRH, UQCRB
Mesodermal cell differentiation	GO:0048333	4/14	1.65E-03	BMP4, ITGB4, ITGA3, KDM6B
Signal transduction involved in mitotic g1 dna damage checkpoint	GO:0072431	8/68	1.76E-03	PSMD5, PSMD6, PSMA2, PSMA1, PSMA4, RBM38, PSMD14, PSMD13
Intracellular signal transduction involved in g1 dna damage checkpoint	GO:1902400	8/68	1.76E-03	PSMD5, PSMD6, PSMA2, PSMA1, PSMA4, RBM38, PSMD14, PSMD13
Signal transduction involved in mitotic dna damage checkpoint	GO:1902402	8/69	1.92E-03	PSMD5, PSMD6, PSMA2, PSMA1, PSMA4, RBM38, PSMD14, PSMD13
Signal transduction involved in mitotic dna integrity checkpoint	GO:1902403	8/69	1.92E-03	PSMD5, PSMD6, PSMA2, PSMA1, PSMA4, RBM38, PSMD14, PSMD13
Signal transduction involved in mitotic cell cycle checkpoint	GO:0072413	8/69	1.92E-03	PSMD5, PSMD6, PSMA2, PSMA1, PSMA4, RBM38, PSMD14, PSMD13
Actin filament organization	GO:0007015	12/150	3.14E-03	ACTN4, PPARGC1B, ARPC1B, ELN, BCAR1, CDC42, GSN, MICAL3, NCK1, SHROOM1, FAT1, MSRB2

Angiogenesis	GO:0001525	16/236	3.40E-03	GPR124, PGF, APOLD1, VASH1, EPHB1, BMP4, ECM1, ADAM15, HSPG2, JMJD6, PDGFA, CDC42, TSPAN12, PRKD2, PLCD1, HS6ST1
Signal transduction by p53 class mediator	GO:0072331	11/132	3.45E-03	DDIT4, PSMA2, PSMA1, PSMA4, SNW1, BAG6, PSMD5, PSMD6, RBM38, PSMD14, PSMD13
Cell cycle g1/s phase transition	GO:0044843	12/152	3.47E-03	ORC5, PSMA2, PSMA1, PSMA4, RCC1, RHOU, PSMD5, PSMD6, MCM2, NFATC1, PSMD14, PSMD13
G1/s transition of mitotic cell cycle	GO:0000082	12/152	3.47E-03	ORC5, PSMA2, PSMA1, PSMA4, RCC1, RHOU, PSMD5, PSMD6, MCM2, NFATC1, PSMD14, PSMD13
Fibroblast migration	GO:0010761	3/8	3.53E-03	SYNE2, TNS1, TMEM201
Atp metabolic process	GO:0046034	22/377	3.82E-03	KIF13A, DDX1, ABCG1, ABCG8, CCT8, MYO7A, LONP2, EIF4A2, SKIV2L, KIF21B, MYO3A, ABCA2, ABCA3, MYO1D, HSPD1, UQCRC2, MT-CO1, PSMD6, NDUFS1, KIF1C, UQCRH, UQCRB
Regulation of cellular amino acid metabolic process	GO:0006521	7/62	4.16E-03	PSMD5, PSMD6, PSMA2, PSMA1, PSMA4, PSMD14, PSMD13
Extracellular matrix disassembly	GO:0022617	10/116	4.16E-03	LAMC1, ADAMTS4, ELN, COL16A1, FURIN, BCAN, COL11A2, ADAM15, HSPG2, COL5A3
Positive regulation of endothelial cell proliferation	GO:0001938	7/63	4.50E-03	PDGFB, PGF, PLXNB3, PRKD2, BMP4, NR4A1, ECM1
Axon ensheathment in central nervous system	GO:0032291	3/9	4.61E-03	NKX6-2, CNTN2, MYRF
Central nervous system myelination	GO:0022010	3/9	4.61E-03	NKX6-2, CNTN2, MYRF
Regulation of cellular amine metabolic process	GO:0033238	8/82	5.08E-03	PSMD5, PSMD6, PSMA2, PSMA1, PSMA4, PSMD14, PSMD13, GPR37
Regulation of dna biosynthetic process	GO:2000278	5/34	5.52E-03	PDGFB, PDGFA, MEN1, PRKD2, ARRB2
Regulation of muscle cell differentiation	GO:0051147	10/122	5.77E-03	MORF4L2, PTBP1, SOX8, TCF3, BMP4, HDAC2, CDC42, BOC, RBM38, ID3
Regulation of cell proliferation involved in kidney development	GO:1901722	3/10	5.86E-03	BMP4, PDGFB, PDGFA
Establishment of protein localization to membrane	GO:0090150	15/229	6.03E-03	RAB3GAP2, RPL15, RPLP2, KIF13A, RPLP1, SYNE3, BAG6, RPL39, RAB11A, MICALL1, SEC61G, PACS2, RPL7, RPL5, RPS4X
Negative regulation of ubiquitin-protein ligase activity involved in mitotic cell cycle	GO:0051436	7/67	6.12E-03	PSMD5, PSMD6, PSMA2, PSMA1, PSMA4, PSMD14, PSMD13

Regulation of gliogenesis	GO:0014013	7/67	6.12E-03	NKX6-2, SOX10, RELA, CNTN2, SOX8, NKX2-2, HDAC2
Positive regulation of cell cycle arrest	GO:0071158	8/85	6.18E-03	PSMD5, PSMD6, PSMA2, PSMA1, PSMA4, RBM38, PSMD14, PSMD13
Protein localization to organelle	GO:0033365	22/396	6.54E-03	RPL15, RPLP2, RPLP1, MTX2, SYNE2, PDIA3, RPL39, LMNA, MCM3AP, RPL7, RPL5, IFT140, RPS4X, JAK3, CRIPT, BMP4, LONP2, CEP250, MICALL1, SEC61G, TOMM40, KLHL21
Mitotic cell cycle phase transition	GO:0044772	17/277	6.58E-03	CEP164, RCC1, PCNT, CEP250, CCNY, PSMD14, PSMD13, ORC5, PPP1CB, PSMA2, PSMA1, PSMA4, RHOU, PSMD5, PSMD6, MCM2, NFATC1
Heart development	GO:0007507	12/167	6.94E-03	PDGFB, GAB1, SCUBE1, DVL2, BMP4, ITGA3, POU6F1, TXNRD2, OXCT1, NFATC1, JMJD6, ID3
Signal transduction in response to dna damage	GO:0042770	9/106	7.01E-03	PSMA2, PSMA1, PSMA4, PSMD5, PSMD6, CDC5L, RBM38, PSMD14, PSMD13
Cell cycle phase transition	GO:0044770	17/280	7.25E-03	CEP164, RCC1, PCNT, CEP250, CCNY, PSMD14, PSMD13, ORC5, PPP1CB, PSMA2, PSMA1, PSMA4, RHOU, PSMD5, PSMD6, MCM2, NFATC1
Positive regulation of sodium ion transmembrane transporter activity	GO:2000651	3/11	7.30E-03	ACTN4, CNKSR3, WNK2
Establishment of nucleus localization	GO:0040023	3/11	7.30E-03	CDC42, SYNE2, TMEM201
Regulation of endothelial cell proliferation	GO:0001936	8/88	7.46E-03	PDGFB, PGF, PLXNB3, VASH1, PRKD2, BMP4, NR4A1, ECM1
Oligodendrocyte differentiation	GO:0048709	4/23	7.68E-03	SOX10, TSPAN2, SOX8, MYRF
Jak-stat cascade involved in growth hormone signaling pathway	GO:0060397	4/23	7.68E-03	IRS2, STAT5B, JAK3, PTPN1
Gpi anchor biosynthetic process	GO:0006506	4/23	7.68E-03	PIGZ, PIGU, PIGO, MPPE1
Purine ribonucleoside monophosphate metabolic process	GO:0009167	22/402	7.68E-03	EIF4A2, SKIV2L, MYO3A, ABCA2, ABCA3, MYO1D, HSPD1, MT-CO1, NDUFS1, KIF1C, UQCRH, UQCRB, KIF13A, DDX1, ABCG1, ABCG8, CCT8, MYO7A, LONP2, KIF21B, UQCRC2, PSMD6
Hydrogen ion transmembrane transport	GO:1902600	9/108	7.82E-03	COA6, SLC9A1, MT-CO1, ATP6V1C1, UQCRH, MT-CO2, MT-CO3, SLC47A1, ATP6V0A2
Purine nucleoside monophosphate metabolic process	GO:0009126	22/403	7.88E-03	EIF4A2, SKIV2L, MYO3A, ABCA2, ABCA3, MYO1D, HSPD1, MT-CO1, NDUFS1, KIF1C, UQCRH, UQCRB, KIF13A, DDX1, ABCG1, ABCG8, CCT8, MYO7A, LONP2, KIF21B, UQCRC2, PSMD6
Translational termination	GO:0006415	8/89	7.93E-03	RPL15, RPLP2, RPLP1, RPS4X, RPL39, RPL7, RPL5, GSPT2

Antigen processing and presentation of exogenous peptide antigen	GO:0002478	12/171	8.21E-03	TAPBP, PSMA2, PSMA1, PSMA4, SEC61G, FCER1G, PDIA3, CANX, PSMD5, PSMD6, PSMD14, PSMD13
Lung alveolus development	GO:0048286	5/38	8.39E-03	PDGFA, STK40, HS6ST1, BMP4, PSEN2
Hair follicle development	GO:0001942	5/38	8.39E-03	PDGFA, RELA, CELSR1, EDAR, PSEN2
Positive regulation of ubiquitin-protein ligase activity involved in mitotic cell cycle	GO:0051437	7/72	8.70E-03	PSMD5, PSMD6, PSMA2, PSMA1, PSMA4, PSMD14, PSMD13
Sprouting angiogenesis	GO:0002040	4/24	8.75E-03	GPR124, PGF, CDC42, JMJD6
Antigen processing and presentation of exogenous antigen	GO:0019884	12/173	8.92E-03	TAPBP, PSMA2, PSMA1, PSMA4, SEC61G, FCER1G, PDIA3, CANX, PSMD5, PSMD6, PSMD14, PSMD13
Regulation of glomerulus development	GO:0090192	3/12	8.93E-03	BMP4, PDGFB, PDGFA
Hemidesmosome assembly	GO:0031581	3/12	8.93E-03	ITGB4, LAMC1, PLEC
Dna damage response, signal transduction by p53 class mediator	GO:0030330	8/91	8.93E-03	PSMD5, PSMD6, PSMA2, PSMA1, PSMA4, RBM38, PSMD14, PSMD13
Regulation of cell cycle g1/s phase transition	GO:1902806	10/131	9.05E-03	PSMA2, PSMA1, PSMA4, TCF3, PSMD5, PSMD6, STXBP4, RBM38, PSMD14, PSMD13
Protein complex disassembly	GO:0043241	10/132	9.48E-03	RPL15, RPLP2, RPLP1, DDIT4, RPL7, RPL5, MICAL3, RPS4X, RPL39, GSPT2
Hematopoietic or lymphoid organ development	GO:0048534	12/175	9.67E-03	PDGFB, STAT5B, GATA2, TCF3, SPNS2, PPP2R3C, MEN1, PSEN2, TXNRD2, CSF1, CD248, LRP5
T cell homeostasis	GO:0043029	4/25	9.92E-03	STAT5B, SPNS2, JAK3, PPP2R3C
Retrograde vesicle-mediated transport, golgi to er	GO:0006890	4/25	9.92E-03	TAPBP, COPB1, TMED10, KIF1C
Negative regulation of ligase activity	GO:0051352	7/74	9.92E-03	PSMD5, PSMD6, PSMA2, PSMA1, PSMA4, PSMD14, PSMD13
Negative regulation of ubiquitin-protein transferase activity	GO:0051444	7/74	9.92E-03	PSMD5, PSMD6, PSMA2, PSMA1, PSMA4, PSMD14, PSMD13

D) Histone modifications	**Cell line**	**Overlap**	**P-value**
H3K4me3	HBMEC	46/1176	0.00128
H3K4me3	SAEC	36/856	0.00136
H3K4me3	GM12875	62/1734	0.00162
H3K4me3	CACO2	33/808	0.00333
H3K4me3	NHEK	29/724	0.00742
H3K4me3	SKNSHRA	32/831	0.00861

H3K4me3	H7ES	81/2560	0.00806
H3K4me3	GM12866	54/1618	0.01223
H3K27ac	MCF7	65/1999	0.01038
H3K4me3	HELAS3	23/587	0.02015
H3K4me3	CD20RO01778	34/977	0.02606
H3K4me3	NHLF	33/953	0.02981
H3K4me3	HAC	32/922	0.03127
H3K4me3	GM12864	18/470	0.04426
H3K4me3	SKMC	34/1030	0.04828
H3K4me3	BJ	28/818	0.04847
H3K27me3	HEPG2	8/150	0.03526

Table 3.3-17 Pathways and terms associated with mitochondrial respiration and ATP metabolism, enriched in the hippocampus of female social, but not unsocial, *5-Htt*+/- mice exposed to PS. Female *5-Htt*+/- offspring were exposed to PS or not (control, C). Social, resilient and unsocial, vulnerable PS mice were each compared to control mice to assess differentially expressed genes (DEGs). Transcriptome data were assessed using mRNAseq, Overlap = number of DEGs/total number of genes in this pathway or term. Enrichment analysis performed using Enrichr (Chen Tan 2013) using DEGs with p<0.001.

Term	Term ID	Overlap	p	Genes
A) KEGG pathways				
Oxidative phosphorylation	HSA00190	11/128	0,005762	PPA2, COX3, COX2, COX1, UQCRC2, NDUFS1, ATP6V1C1, UQCRH, UQCRB, CYTB, ATP6V0A2
B) GO: Biological processes				
Cellular respiration	GO:0045333	8/38	0,000053	UQCRC2, FASTKD2, MT-CO1, NDUFS1, SLC25A14, UQCRH, MT-CO3, UQCRB
Oxidative phosphorylation	GO:0006119	4/14	0,001650	UQCRC2, MT-CO1, UQCRH, UQCRB
Aerobic respiration	GO:0009060	6/22	0,000139	UQCRC2, MT-CO1, SLC25A14, UQCRH, MT-CO3, UQCRB
ATP metabolic process	GO:0046034	22/377	0,003818	KIF13A, DDX1, ABCG1, ABCG8, CCT8, MYO7A, LONP2, EIF4A2, SKIV2L, KIF21B, MYO3A, ABCA2, ABCA3, MYO1D, HSPD1, UQCRC2, MT-CO1, PSMD6, NDUFS1, KIF1C, UQCRH, UQCRB

C) GO: Cellular component

Cytochrome complex	GO:0070069	6/18	0,000049	UQCRC2, MT-CO1, UQCRH, MT-CO2, MT-CO3, UQCRB
Respiratory chain complex III	GO:0045275	3/8	0,003327	UQCRC2, UQCRH, UQCRB
Mitochondrial respiratory chain complex III	GO:0005750	3/8	0,003327	UQCRC2, UQCRH, UQCRB
Respiratory chain complex IV	GO:0045277	3/9	0,004342	MT-CO2, MT-CO3, MT-CO1

D) GO: Molecular function

Oxidoreductase activity, acting on a heme group of donors	GO:0016675	5/32	0,004017	MT-CO1, POR, COA6, MT-CO2, MT-CO3
Actin-dependent atpase activity	GO:0030898	3/11	0,006897	MYO3A, MYO7A, MYO1D
ATPase activity	GO:0016887	21/395	0,009679	ATP11A, EIF4A2, SKIV2L, MYO3A, ABCA2, ABCA3, MYO1D, HSPD1, KIF1C, KIF13A, ATP2C2, DDX1, ABCG1, ABCG8, CCT8, MYO7A, LONP2, ATP6V1C1, KIF21B, TAPBP, PSMD6
Cytochrome-c oxidase activity	GO:0004129	4/31	0,017800	MT-CO1, COA6, MT-CO2, MT-CO3
Heme-copper terminal oxidase activity	GO:0015002	4/31	0,017800	MT-CO1, COA6, MT-CO2, MT-CO3
Oxidoreductase activity, acting on a heme group of donors, oxygen as acceptor	GO:0016676	4/31	0,017800	MT-CO1, COA6, MT-CO2, MT-CO3
Electron carrier activity	GO:0009055	8/107	0,018448	POR, ALDH4A1, COA6, MT-CO1, NDUFS1, MT-CO2, MT-CO3, ETFDH
ATPase activity, coupled	GO:0042623	15/272	0,020038	ATP2C2, DDX1, ATP11A, ABCG1, CCT8, MYO7A, LONP2, ATP6V1C1, EIF4A2, SKIV2L, TAPBP, MYO3A, ABCA2, ABCA3, MYO1D
Wide pore channel activity	GO:0022829	3/23	0,038184	TOMM40, GJC2, VDAC3
ATPase activity, coupled to transmembrane movement of substances	GO:0042626	7/104	0,042115	TAPBP, ATP2C2, ABCA2, ABCA3, ATP11A, ABCG1, ATP6V1C1
ATPase activity, coupled to movement of substances	GO:0043492	7/105	0,043858	TAPBP, ATP2C2, ABCA2, ABCA3, ATP11A, ABCG1, ATP6V1C1

Table 3.3-18 Genes of the enriched KEGG pathway "Oxidataive phosphorylation" and other genes associated with mitochondrial respiration and ATP metabolism, differentially expressed in the hippocampus of female social, but not unsocial, *5-Htt*+/- mice exposed to PS. Female *5-Htt*+/- offspring were exposed to PS or not (control, C). Social, resilient and unsocial, vulnerable PS mice were each compared to control mice to assess differentially expressed genes (DEGs). Transcriptome data were assessed using mRNAseq, enrichment analysis was performed using Enrichr (Chen Tan 2013). Log2FC = log2 fold change, lfcSE = Log2FC standard error. Enrichment analysis performed using Enrichr (Chen Tan 2013) using DEGs with p<0.001.

		unsocial			social		
Symbol	**Gene name**	**Log2FC**	**lfcSE**	**p**	**Log2FC**	**lfcSE**	**p**
Ndufs1	NADH dehydrogenase (ubiquinone) Fe-S protein 1	-0.026	0.030	0.38	-0.094	0.030	0.0015
mt-Co1 (COX1)	mitochondrially encoded cytochrome c oxidase I	-0.070	0.060	0.24	-0.180	0.060	0.0026
mt-Co2 (COX2)	mitochondrially encoded cytochrome c oxidase II	-0.091	0.053	0.08	-0.199	0.053	0.0002
mt-Co3 (COX3)	mitochondrially encoded cytochrome c oxidase III	-0.083	0.061	0.17	-0.231	0.061	0.0001
mt-Cytb (CYTB)	mitochondrially encoded cytochrome b	-0.072	0.058	0.22	-0.203	0.058	0.0005
Uqcrb	ubiquinol-cytochrome c reductase binding protein	-0.073	0.072	0.31	-0.189	0.072	0.0088
Uqcrc2	ubiquinol cytochrome c reductase core protein 2	0.004	0.037	0.92	-0.097	0.037	0.0088
Uqcrh	ubiquinol-cytochrome c reductase hinge protein	-0.074	0.067	0.27	-0.209	0.067	0.0018
Ppa2	pyrophosphatase (inorganic) 2	-0.143	0.056	0.01	-0.167	0.056	0.0030
Atp6v1c1	ATPase, H+ transporting, lysosomal V1 subunit C1	-0.011	0.031	0.72	-0.087	0.031	0.0052
Atp6v0a2	ATPase, H+ transporting, lysosomal V0 subunit A2	0.027	0.041	0.51	0.116	0.041	0.0044
Additional mitochondria-associated genes not in the KEGG pathway:							
Mpc1-ps	mitochondrial pyruvate carrier 1, pseudogene	-0.048	0.051	0.34	-0.142	0.051	0.0053
Mrpl30	mitochondrial ribosomal protein L30	-0.046	0.050	0.36	-0.129	0.050	0.0093
Immt	inner membrane protein, mitochondrial	-0.020	0.035	0.56	-0.095	0.035	0.0065
Slc25a14	solute carrier family 25 (mitochondrial carrier, brain), member 14	-0.069	0.042	0.10	-0.137	0.042	0.0011
mt-Ty	mitochondrially encoded tRNA tyrosine	-0.180	0.134	0.18	-0.389	0.134	0.0037
Yars2	tyrosyl-tRNA synthetase 2 (mitochondrial)	-0.078	0.052	0.14	-0.144	0.052	0.0055
mt-Tc	mitochondrially encoded tRNA cysteine	-0.211	0.112	0.06	-0.422	0.112	0.0002

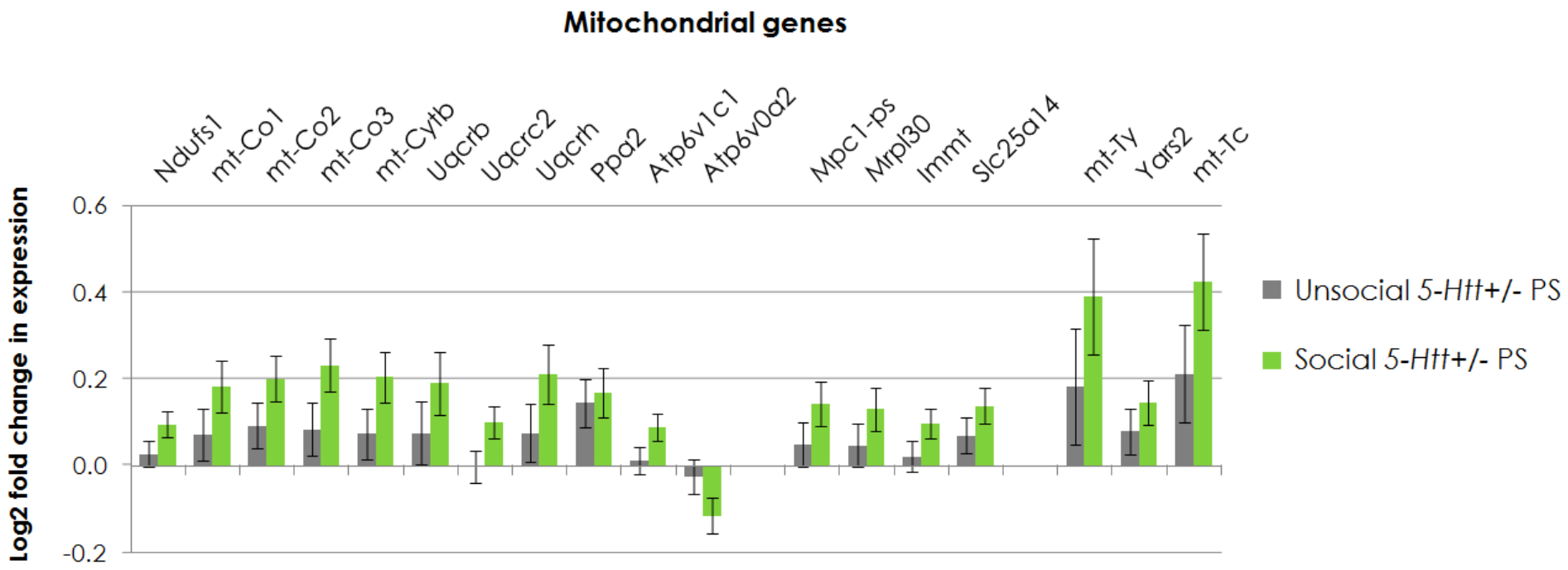

Figure 3.3-17 Expression changes of genes in the enriched KEGG pathway "Oxidataive phosphorylation" and other genes associated with mitochondrial respiration, differentially expressed in the hippocampus of female social, but not unsocial, *5-Htt+/-* mice exposed to PS. Female *5-Htt+/-* offspring were exposed to PS or not (control, C). Social, resilient and unsocial, vulnerable PS mice were each compared to control mice to assess differentially expressed genes (DEGs). Transcriptome data were assessed using mRNAseq, enrichment analysis was performed using enrichr (Chen Tan 2013). *Ndufs1* = NADH dehydrogenase (ubiquinone) Fe-S protein 1, *mt-Co* = cytochrome c oxidase, mitochondrial, *mt-Cytb* = cytochrome b, mitochondrial, *Uqcrc2* = ubiquinol cytochrome c reductase core protein 2, *Uqcrh* = ubiquinol-cytochrome c reductase hinge protein, *Ppa2* = pyrophosphatase (inorganic) 2, *Atp6v1c1* = ATPase, H+ transporting, lysosomal V1 subunit C1, *Atp6v0a2* = ATPase, H+ transporting, lysosomal V0 subunit A2, *Mpc1-ps* = mitochondrial pyruvate carrier 1, pseudogene, *Mrpl30* = mitochondrial ribosomal protein L30, *Immt* = inner membrane protein, mitochondrial, *Slc25a14* = solute carrier family 25 (mitochondrial carrier, brain), member 14, *mt-Ty* = tRNA tyrosine, mitochondrial, *Yars2* = tyrosyl-tRNA synthetase 2 (mitochondrial), *mt-Tc* = tRNA cysteine, mitochondrial.

OXIDATIVE PHOSPHORYLATION

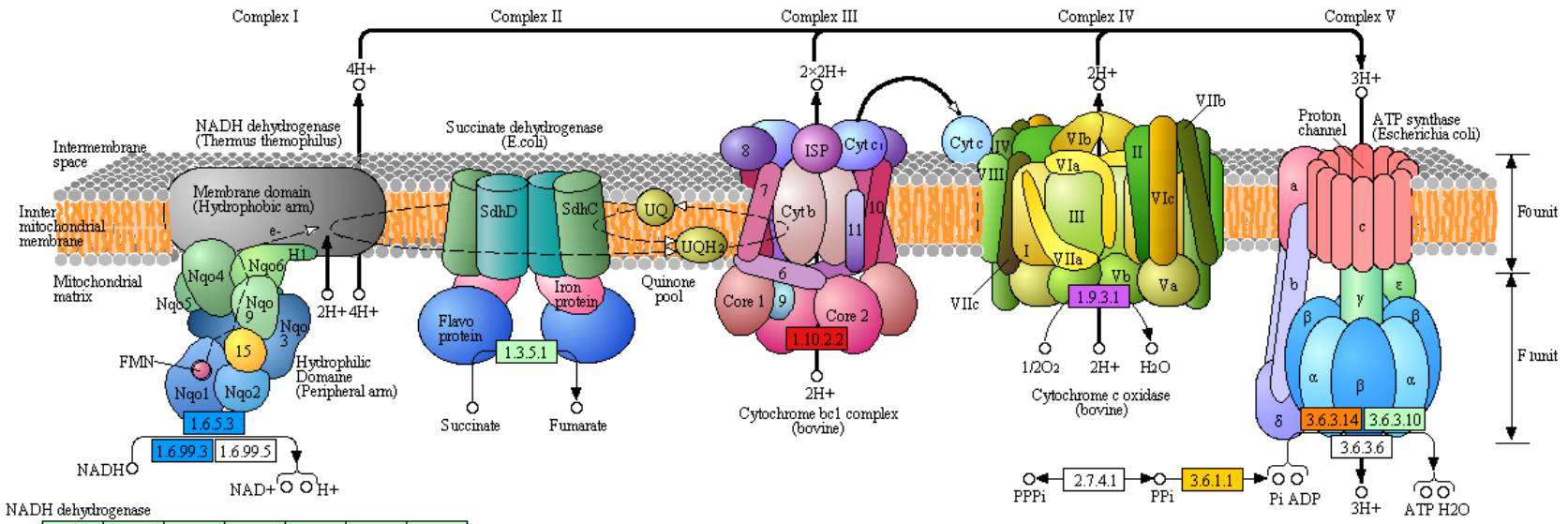

NADH dehydrogenase

E	ND1	ND2	ND3	ND4	ND4L	ND5	ND6										
E	Ndufs1	Ndufs2	Ndufs3	Ndufs4	Ndufs5	Ndufs6	Ndufs7	Ndufs8	Ndufv1	Ndufv2	Ndufv3						
B/A	NuoA	NuoB	NuoC	NuoD	NuoE	NuoF	NuoG	NuoH	NuoI	NuoJ	NuoK	NuoL	NuoM	NuoN			
B/A	NdhC	NdhK	NdhJ	NdhH	NdhA	NdhI	NdhG	NdhE	NdhF	NdhD	NdhB	NdhL	NdhM	NdhN	HoxE	HoxF	HoxU
E	Ndufa1	Ndufa2	Ndufa3	Ndufa4	Ndufa5	Ndufa6	Ndufa7	Ndufa8	Ndufa9	Ndufa10	Ndufab1	Ndufa11	Ndufa12	Ndufa13			
E	Ndufb1	Ndufb2	Ndufb3	Ndufb4	Ndufb5	Ndufb6	Ndufb7	Ndufb8	Ndufb9	Ndufb10	Ndufb11	Ndufc1	Ndufc2				

Succinate dehydrogenase / Fumarate reductase

E	SDHC	SDHD	SDHA	SDHB		
B/A	SdhC	SdhD	SdhA	SdhB		
			FrdA	FrdB	FrdC	FrdD

Cytochrome c reductase

E/B/A	ISP	Cyt b	Cyt 1							
E				COR1	QCR2	QCR6	QCR7	QCR8	QCR9	QCR10

Cytochrome c oxidase

E	COX10		COX3	COX1	COX2	COX4	COX5A	COX5B	COX6A	COX6B	COX6C	COX7A	COX7B	COX7C	COX8	E/B/A			
																COX11	COX15	COX17	
B/A	CyoE	CyoD	CyoC	CyoB	CyoA														
		CoxD	CoxC	CoxA	CoxB														
		QoxD	QoxC	QoxB	QoxA														

Cytochrome c oxidase , cbb3-type

B	I	II	IV	III

Cytochrome bd complex

B/A	CydA	CydB

F-type ATPase (Bacteria)

alpha	beta	gamma	delta	epsilon
a	b	c		

F-type ATPase (Eukaryotes)

alpha	beta	gamma	delta	epsilon	
OSCP	a	b	c	d	e
f	g	f6/h	j	k	8

V/A-type ATPase (Bacteria, Archaeas)

A	B	C	D	E	F	G/H
I	K					

V-type ATPase (Eukaryotes)

A	B	C	D	E	F	G	H
a	c	d	e	S1			

Figure 3.3-18 Genes in the enriched KEGG pathway "Oxidataive phosphorylation", differentially expressed in the hippocampus of female social, but not unsocial, *5-Htt*+/- mice exposed to PS. Female *5-Htt*+/- offspring were exposed to PS or not (control, C). Social, resilient and unsocial, vulnerable PS mice were each compared to control mice to assess differentially expressed genes (DEGs). Transcriptome data were assessed using mRNAseq, enrichment analysis was performed using enrichr (Chen Tan 2013) and DEGs with p<0.01. Pathway was created using KEGG (Kanehisa and Goto 2000).

◀

Table 3.3-19 Pathways and terms associated with myelination and oligodendrocytes, enriched in the hippocampus of female social, but not unsocial, *5-Htt*+/- mice exposed to PS. Female *5-Htt*+/- offspring were exposed to PS or not (control, C). Social, resilient and unsocial, vulnerable PS mice were each compared to control mice to assess differentially expressed genes (DEGs). Transcriptome data were assessed using mRNAseq, Overlap = number of DEGs/total number of genes in pathway or term. Enrichment analysis performed using Enrichr (Chen Tan 2013) using DEGs with p<0.001.

Term	Term ID	Overlap	p	Genes
A) Mammalian phenotypes				
Abnormal myelination	MP0000920	11/134	0,00011	MOG, NKX6-2, LAMC1, PMP22, GAL3ST1, CANX, MBP, SOX10, CSF1, GJC2, LMNA
Abnormal glial cell	MP0003634	13/231	0,00091	LAMC1, PMP22, ACP2, NKX2-2, MYO7A, CANX, CSF1, HSPG2, LRP5, PDGFB, OLIG1, MAN2B1, SOX10
B) GO: Biological processes				
Myelination	GO:0042552	9/59	0,00017	TSPAN2, MBP, NKX6-2, NAB2, CNTN2, MYRF, PLLP, SERINC5, GAL3ST1
Axon ensheathment	GO:0008366	9/62	0,00023	TSPAN2, MBP, NKX6-2, NAB2, CNTN2, MYRF, PLLP, SERINC5, GAL3ST1
Ensheathment of neurons	GO:0007272	9/62	0,00023	TSPAN2, MBP, NKX6-2, NAB2, MYRF, CNTN2, PLLP, SERINC5, GAL3ST1
Positive regulation of gliogenesis	GO:0014015	6/35	0,00120	SOX8, NKX6-2, NKX2-2, SOX10, RELA, HDAC2
Axon ensheathment in central nervous system	GO:0032291	3/9	0,00461	NKX6-2, CNTN2, MYRF
Central nervous system myelination	GO:0022010	3/9	0,00461	NKX6-2, CNTN2, MYRF
Regulation of gliogenesis	GO:0014013	7/67	0,00612	NKX6-2, SOX10, RELA, CNTN2, SOX8, NKX2-2, HDAC2
Oligodendrocyte differentiation	GO:0048709	4/23	0,00768	SOX10, TSPAN2, SOX8, MYRF
C) GO: Cellular Compartment				
Myelin sheath	GO:0043209	5/17	0,00035	TSPAN2, GJC2, ITPR3, SERINC5, CNTN2

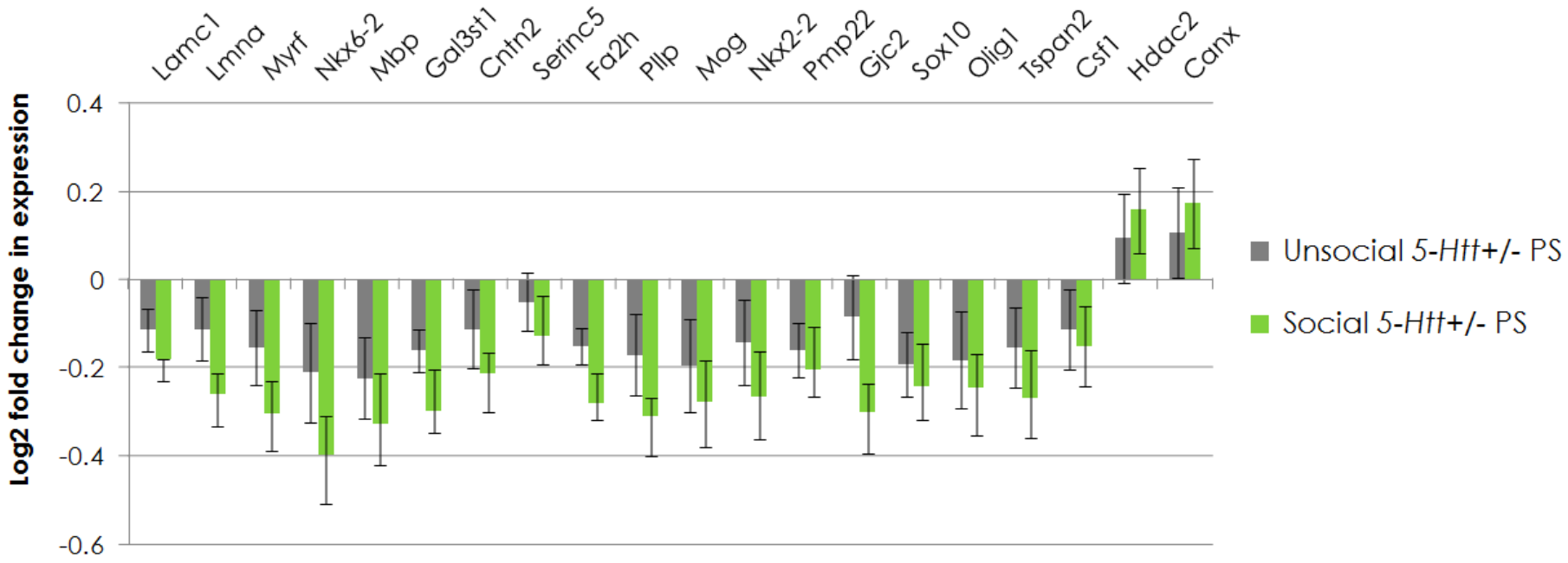

Figure 3.3-19 Expression changes of genes associated with myelination and oligodendrocytes and enriched in myelin-associated GO terms, differentially expressed in the hippocampus of female social, but not unsocial, *5-Htt+/-* mice exposed to PS. Female *5-Htt+/-* offspring were exposed to PS or not (control, C). Social, resilient and unsocial, vulnerable PS mice were each compared to control mice to assess differentially expressed genes (DEGs). Transcriptome data were assessed using mRNAseq, enrichment analysis was performed using enrichr (Chen Tan 2013) and DEGs with p<0.01. *Lamc1* = laminin, gamma 1, *Lmna* = lamin A, *Myrf* = myelin regulatory factor, *Nkx6-2* = NK6 homeobox 2, *Mbp* = myelin basic protein, *Gal3st1* = galactose-3-O-sulfotransferase 1, *Cntn2* = contactin 2, *Serinc5* = serine incorporator 5, *Fa2h* = fatty acid 2-hydroxylase, *Pllp* = plasmolipin, *Mog* = myelin oligodendrocyte glycoprotein, *Nkx2-2* = NK2 homeobox 2, *Pmp22* = peripheral myelin protein 22, *Gjc2* = gap junction protein, gamma 2, *Sox10* = SRY (sex determining region Y)-box 10, *Olig1* = oligodendrocyte transcription factor 1, *Tspan2* = tetraspanin 2, *Csf1* = colony stimulating factor 1 (macrophage), Hdac2 = histone deacetylase 2, Canx = calnexin.

3.4. Discussion

In the present study, we found that exposure of PS negatively affected sociability in female *5-Htt*+/+ and *5-Htt*+/- mice. Moreover, when dividing animals into unsocial (PS-vulnerable) and social (PS-resilient) groups, anxiety-like behavior was modulated by an interaction of *5-Htt*+/- genotype and PS. A transcriptome analysis using mRNAseq on the hippocampi of the tested animals revealed several enriched pathways affected by *5-Htt* genotype, PS and their interaction. While the expression of genes associated with myelination, OLs, and possibly NG2+ polydendrocytes was increased in C *5-Htt*+/- mice when compared to C *5-Htt*+/+ mice, PS exposure ablated this effect in *5-Htt*+/- mice. The *5-Htt* genotype furthermore affected mitochondrial respiration with *5-Htt*+/- mice showing increased expression of genes associated with oxidative phosphorylation when compared to *5-Htt*+/+ mice. In addition, transcriptome data and enrichment analysis indicated that myelination-associated processes were reduced in social, but not in unsocial, *5-Htt*+/- mice exposed to PS when compared to C *5-Htt*+/- mice. In contrast to that, gene expression associated with mitochondrial respiration was increased in social, but not or less in unsocial, *5-Htt*+/- mice exposed to PS when compared to C *5-Htt*+/- mice. Next to this, mRNAseq revealed broad effects of the modification in the *5-Htt* gene on gene expression of genes located in a 10 Mio kb region upstream of *5-Htt* on chromosome 11.

3.4.1. Behavioral effects of *5-Htt* x PS interaction

Female 5-Htt+/+ and *5-Htt*+/- mice were tested for anxiety- and depressive-like behavior as well as HPA-axis function. While PS exposure had an overall negative effect on sociability as assessed by the time spent in the target chamber during the 3-chamber sociability test, it had an anxiolytic effect on the animals as indicated by an increased time spent and distance moved in the open arms of the EPM when compared to controls. This is in line with a study by Jones and colleagues, where PS offspring of both *5-Htt*+/+ and *5-Htt*+/- mothers was less anxious in the EPM when compared to C offspring (Jones et al 2010), although the offspring's genotype was not accounted for in that study. Another study using a 5-Htt x PS paradigm showed no PS effect in the EPM and an anxiogenic PS effect in the dark-light-test (Heiming *et al.* 2009).

When grouping the PS animals based on their performance in the sociability test into vulnerable mice showing impaired sociability and resilient mice showing normal levels of social behavior, a different picture regarding anxiety-like behavior emerges. PS only had

an anxiolytic effect on the unsocial PS *5-Htt+/+* group, but not on the corresponding social group. In the *5-Htt+/-* group, on the other hand, we found the opposite pattern, with the social *5-Htt+/-* mice showing a tendency for an anxiolytic effect in the EPM, and the vulnerable mice not. We can conclude from this that reduced sociability in the *5-Htt+/+* group is most likely not a result of increased anxiety. This indicates that, despite being both modulated by an interaction of PS and *5-Htt* genotype, social anxiety and state-anxiety, which is assessed in the EPM, represent different concepts. Next to this, a similar interaction was observed for locomotor activity. Unsocial *5-Htt+/+* mice showed increased locomotion when compared to social ones, while in the *5-Htt+/-* group, unsocial mice showed decreased mobility when compared to the control mice. In this study, neither PS nor *5-Htt* genotype influenced basal or stress-induced CORT levels significantly. Unsocial PS *5-Htt+/-* mice, however, showed a tendency for an increase in basal CORT levels when compared to controls. No effects were found on anhedonic behavior in the sucrose preference test and the PST. Taken together, contrasting our expectations, we did not observe a clear-cut depressive- or anxiety-like phenotype, neither in the *5-Htt+/-* animals nor in the PS groups or due to an interaction. On the contrary, PS had an anxiolytic effect in the EPM in our study. This is in contrast to a study by Heiming and colleagues, where perinatal stress had no effect on anxiety-like behavior in the EPM (Heiming *et al.* 2009), and to our previous study. The observed PS effects on sociability in *5-Htt+/+* mice might rather fit an autistic phenotype. Further tests that would help elucidate a possible autism-like phenotype, e.g. assessing repetitive behavior or communication, were not performed, as this was not the initial aim of the study.

As indicated above, the behavioral effects observed in this study differ from those observed in the first study. For example, in the first study, the *5-Htt+/-* genotype but not PS had an anxiolytic effect in the EZM, whereas PS decreased the total distance moved in the EZM and in the FST. Neither of these effects were observed in the second study, where PS had an anxiolytic effect in the EPM and no effects were observed in the PST. Moreover, in general, only limited G-effects were observed in the second study. This discrepancy is most likely the result of differences in study designs. The first major change was using a different breeding design, with *5-Htt+/-* mothers in the first study and wt mothers obtained from a commercial breeder in the second. Consequently, there might have been differences in the stress reaction to the PS treatment and in maternal behavior due to a maternal G-effect, which in turn could have had consequences for the offspring's behavior. In support of this notion, Jones and colleagues found that offspring of mothers differing in the *5-Htt* genotype show differences in emotional behavior (Jones *et al.* 2010). Unfortunately, that study did not control for the offspring's

genotype, hence it cannot be excluded that the observed behavioral effects could result from differences in the offspring's genotype. They furthermore found that PS had an anxiolytic effect in the EPM, no matter the genotype of the dams, an effect that we also observed in the second study.

Next to this, we cannot exclude that mothers additionally differed in epigenetic patterns, as they were bred in different facilities, i.e. exposed to a different environment, and that this difference also affected the offspring directly or indirectly. Indeed, variation in the epigenome in one mouse line induced by conditions associated with the breeding facility might be an underestimated factor in behavioral experiments and it might be interesting to investigate to which extend such differences exist and influence behavior. The second major difference was in housing: While the offspring was single housed in individually ventilated (IV) cages in the first study in order to prevent the establishment of a hierarchy, we housed the offspring in groups of 3±1 animals per (regular non-IV) cage in the second study as recent studies had shown that isolation of female mice might represent an additional stressor and might thus influence behavior. On the other hand, we cannot exclude that a possible establishment of hierarchy influenced the behavioral data in the second study. Third, the differences in local conditions between the facilities and in handling might also have contributed to the differences in the studies outcome. Finally, both housing and conditions in the animal facilities could also have had an impact on the epigenome of both mothers and offspring.

3.4.2. Hippocampal gene expression profiles of *5-Htt*+/- mice exposed to PS

We conducted a transcriptome analysis with the aim to study the molecular mechanisms underlying the observed behavioral changes in female PS offspring. Gene expression profiles of the hippocampus, a brain region not only involved in learning and memory but also in emotion and HPA axis regulation, were obtained by mRNA sequencing. While genotype and PS exposure affected about 150 and 350 DEGs, respectively, the expression patterns of considerably more genes, 803 DEGs to be precise, displayed an interaction between 5-Htt and PS. This picture is similar to the behavioral findings, where E- and GxE-effects had a higher impact on emotional behavior than the 5-Htt genotype. Interestingly, the majority of the DEGs affected by PS (67.0 %) were downregulated in animals exposed to PS when compared to control animals. Moreover, while there was only a small overlap between G and GxE or G and E, a considerable degree, i.e. 217 genes, were affected both by E and GxE.

Enrichment analysis using Enrichr (Chen Tan 2013) identified several regulated pathways and GO terms affected by G, E and GxE. Two of these pathways were furthermore also differentially regulated in social, but not in unsocial, *5-Htt+/-* mice when compared to control *5-Htt+/-* mice, i.e. mitochondrial respiration and myelination. The KEGG pathway "oxidative phosphorylation" as well as several enriched GO terms associated with mitochondrial respiration were regulated by genotype. The majority of these genes showed a consistent increased expression in *5-Htt+/-* animals when compared to *5-Htt+/+* animals. Several genes encoded components of the mitochondrial respiratory complex I, as well as a few of complex IV and V. Mitochondria produce most of the brain ATP and reactive oxygen species (ROS) by the above mentioned oxidative phosphorylation pathway, and are moreover engaged in intracellular Ca2+ signalling by buffering cytosolic Ca2+ as well as in both the intrinsic and extrinsic apoptosis pathway (Manji *et al.* 2012, Morava and Kozicz 2013). While ATP is essential for neuronal function for the obvious reasons, ROS have also been shown to be critically involved in neuronal plasticity and memory formation (Massaad and Klann 2011). Mitochondria and the oxidative phosphorylation pathway are thus essential for proper neuronal function (Kann and Kovacs 2007). As such, mitochondrial dysfunction impacts on e.g. neuronal plasticity and neurogenesis (Jonas 2006, Li *et al.* 2010 , Jiao and Li 2011). Evidence for the negative impact of mitochondrial dysfunction on neuronal processes comes from studies analyzing patients with rare genetic defects of the mitochondrial metabolism. Patients suffering from mitochondrial diseases show a high comorbidity with psychiatric disorders (reviewed in Manji *et al.* 2012). For example in a study by Fattal and coworkers, patients with mitochondrial cytopathies had a life-time prevalence of 54% for MDD, 17% for BP and 11% for panic disorder (Fattal *et al.* 2007).

Nex to this, several GO biological processes involved with RNA were enriched due to genotype, such as "Rrna processing", "Ncrna metabolic process" and "Ribonucleoside monophosphate metabolic process", the latter including the gene Kif1b. Interestingly, Kif1b might present an interaction point for the main pathways identified in this screening, i.e. myelination and mitochondrial respiration. KIF1B is a motor protein concerned with the axonal transport of mitochondria and synaptic vesicle precursors (Nangaku *et al.* 1994, Zhao *et al.* 2001, Nakamura *et al.* 2002). Lyons and coworkers showed that KIF1B is essentially involved in the localization of *Mbp* mRNA to the myelinating processes in OLs and in the development of some very long axons in the PNS and CNS in the zebrafish (Lyons *et al.* 2009). Along this line, KIF1B has been suggested to play a role in MS and in neurodegenerative diseases (Aulchenko *et al.* 2008, Melo *et al.* 2013).

Sgk1, a serine/threonine protein kinase whose expression is induced by cortisol (Anacker *et al.* 2013), was down-regulated by a logFC of 0.34 in PS mice when compared to control mice. SGK1 is involved in the cellular response to acute and chronic stress, and promotes various molecular and cellular functions, amongst others the activity of transcription factors such as CREB and NF-kB, the regulation of ion channels and membrane transporters, cell metabolism, cell proliferation, neuroexcitability, apoptosis, inflammation, and hormone secretion (Lang *et al.* 2006, Anacker *et al.* 2013). SGK1 was shown to be involved in the CORT-induced reduction of neurogenesis by affecting Hedgehog signaling and by mediating cortisol-induced phosphorylation and nuclear translocation of the GR in a human hippocampal cell culture, an effect that was even present after 9 h of CORT-withdrawal (Anacker *et al.* 2013). Anacker and coworkers furthermore found increased SGK1 mRNA expression in the blood of MDD patients and in the hippocampus of male Sprague-Dawley rats submitted to unpredictable chronic mild stress (UCMS) and PS (Anacker *et al.* 2013). This is in contrast to our results, as we found decreased hippocampal *Sgk1* levels in PS animals when compared to control animals, an effect that was more pronounced in *5-Htt*+/- mice than in *5-Htt*+/+ mice. The sonic hedgehog pathway was not enriched in our study. Xydous and coworkers furthermore found that *Sgk1* induction by dexamethasone is accompanied by increased H3K4me3 and H3K9/14ac levels at its promoter in vitro (Xydous *et al.* 2014). Simultanous administration of nicotinamide, however, prevented both Sgk1 induction as well as the described epigenetic changes. Interestingly, Enrichr analysis suggested an enrichment of PS- and GxE-affected genes associated with H3K4me3. It would thus be interesting to investigate if our animals exhibit global or *Sgk1*-specific changes in H3K4me3 levels and if this could be a programming effect of PS. Moreover, nicotinamide exhibits benzodiazepine-like actions and has anxiolytic properties (Möhler *et al.* 1979, Akhundov *et al.* 1993), which raises the question if the decreased *Sgk1* expression – and possibly accompanying epigenetic changes - in our PS animals is associated with the decreased anxiety exhibited by the PS animals in the EPM when compared to controls.

Pathways enriched due to GxE-interaction were, amongst others, the "One carbon pool by folate" pathway, the "Adipocytokine signaling pathway", the "Basal cell carcinoma" pathway and the "Notch signaling pathway". The "One carbon pool by folate" pathway will be discussed in the following section, as it might be associated with epigenetic changes, particular DNA methylation. The "Adipocytokine signaling pathway" contained the genes *Rela* and *Irs2*. *Rela,* aka *p65*, is a component of the transcription factor NF-kappa-B, which is involved in synaptic plasticity, neurogenesis, and differentiation (Sarnico *et al.* 2009). Interestingly, p65 can be deacetylated by SIRT2 (Rothgiesser *et al.*

2010), the expression of which was also affected by a GxE-effect in our study. CNS-specific deletion of *Irs2*, a cellular mediator of insulin signaling, leads to deficits in NMDA receptor-dependent synaptic plasticity in the hippocampus of mice (Costello *et al.* 2012). Next to this, the "Basal cell carcinoma" pathway, was enriched. It comprised of *Fzd1, Fzd2, Fzd 7, Wnt3, Wnt5b* and *Bmp4*, i.e. mainly genes of the wnt/fzd pathway. Of note, all DEGs in the pathway showed the same expression pattern with slightly increased expression in *5-Htt+/-* controls when compared to *5-Htt+/+* animals, followed by a reduction in expression after PS exposure. Enrichr analysis additionally identified terms related to the wnt signalling pathway, such as the GO Molecular function terms "Wnt-activated receptor activity", "Wnt-protein binding" and "frizzled binding". The developmentally essential "Notch signaling pathway" comprised *Notch1, Notch4, Hdac2, Ncor2* and *Lfng*.

Next to this, Enrichr analysis associated epigenetic mechanisms with GxE-effects in our study, as indicated by the enriched GO terms related to chromatin and transcription regulation and the enriched KEGG pathway "One carbon pool by folate". The GO Molecular function terms "chromatin DNA binding", "histone acetyltransferase binding", "RNA polymerase II regulatory region DNA binding" and "repressing transcription factor binding" were enriched as well as the terms "chromatin", "heterochromatin" and "nuclear chromatin" in the GO Cellular component cathegory. The term "chromatin" comprised several important epigenetic players involved in chromatin remodeling, such as *Hdac2, Sirt2, Ncor2,* and the polycomb (Pc) genes *Cbx8* and polyhomeotic-like 1 (*Drosophila*) *(Phc1)*. Of note, 16 out of the 19 genes identified in this term show the same expression pattern, e.i. expression being increased in *5-Htt+/-* controls when compared to both groups of the *5-Htt+/+* genotype and expression being decreased to *5-Htt+/+* level or below by PS exposure. Only *Hdac2*, WD repeat domain 61 *(Wdr61)* and *T* show the opposite expression pattern with the *5-Htt+/-* controls showing the lowest expession. Both HDAC2 and SIRT2 are HDACs, which repress transcription by removing acetylgroups from histones and thus inducing a condensed chromatin state. HDAC2 was linked to physiological and pathological processes in the aging brain as well as cognition (Fischer *et al.* 2010, Chouliaras *et al.* 2013). Peleg and coworkers linked impaired memory consolidation in aged mice to alterations in hippocampal H4K12 acetylation levels, while Chouliaras and coworkers identified increased HDAC2 levels in aged mice (Chouliaras *et al.* 2013, Peleg *et al.* 2010). Overexpression of HDAC2 in WT mice impaired synaptic function and memory performance, whereas HDAC2 deficiency increased synaptic plasticity and enhanced fear memory formation (Guan *et al.* 2009). HDAC2 levels were furthermore found to be increased in the brains of AD-model mice and in AD patients

(Gräff *et al.* 2012). Treatment with HDAC inhibitors such as phenylbutyrate, valproate and vorinostat on the other hand restored memory formation in AD mouse models (Ricobaraza *et al.* 2009 Ricobaraza *et al.* 2012, Kilgore *et al.* 2010). The nuclear corepressor NCOR2 (aka SMRT) is a part of a chromatin modification complex and plays a role in regulating age-related changes in mitochondrial oxidative metabolism (Reilly *et al.* 2010). Both *Cbx8,* a homologue of the Drosophila *Pc* gene, and *Phc1* encode components of the polycomp repressive complex 1 (PRC1) (Spivakov and Fischer 2007, Ohtsubo *et al.* 2008). In general, PRC1 and 2 are epigenetic repressor complexes silencing various genes, e.g. homeobox (*Hox*) genes, and are crucially involved in antero-posterior neural patterning during embryogenesis (Qi *et al.* 2013). Both PRC1 and PCR2 are involved supressing developmental genes in stem-cells and in the epigenetic process inducing the switch from neurogenesis to astrogenesis in NPCs (Lee *et al.* 2006, Boyer *et al.* 2006, Hirabayashi *et al.* 2009). In addition to those enriched GO terms associated with chromatin remodeling, the enriched pathway "One carbon pool by folate", containing amoungst others the DEG *Shmt2,* can also be tied to changes in epigenetic mechanisms. This complex pathway describes the one-carbon metabolism, which centers around the vitamine folate, the main 1-carbon donor for protein and DNA methylation as well as DNA synthesis (reviewed in Crider *et al.* 2012). SHMT2 is a mitochondrial hydroxymethyltransferase responsible for *de novo* thymidylate biosynthesis, which is closely linked to the folate pathway and is essential for mitochondrial DNA integrity (Anderson *et al.* 2011). As described in the introduction, the establishment and maintainance of the proper DNA methylation patterns is crucial for development and disturbances of the folate pathway could interfere with DNA methylation processes. In this context, Enrichr analysis identified the enrichment of GxE-affected DEGs associated with H3K4me3. Insterestingly, expression of SET domain containing 1A (Setd1a), a gene encoding a part of a histone methyltransferase complex responsible for methylation of H3K4, is affected by a GxE interaction, although the expression change ($p=0.030$) did not reach the statistical significance of $p<0.01$.

3.4.3. Altered expression of genes associated with myelination and oligodendrocytes due to *5-Htt* x PS interaction

The present thesis comprises two major studies that both analyzed the effects of PS on mice deficient in 5-HTT. We found in both studies a GxE interaction affecting the expression of myelin associated genes in the hippocampus. In the first study, PS increased expression of myelin-associated genes in the *5-Htt*+/+ offspring when compared to controls, but not in *5-Htt*+/- offspring. This is in line with a study by Föcking and coworkers,

who found that PS increases MBP protein levels in the hippocampus of female WT mice (Focking *et al.* 2014). Our second study revealed a negative effect of PS exposure on myelin-associated gene expression in *5-Htt+/-* mice; an effect that was not apparent in *5-Htt+/+* mice. Moreover, C *5-Htt+/-* mice showed an increased expression of myelin-associated genes when compared to C *5-Htt+/+* mice, whereas in the first study we found increased expression in the hippocampus of *5-Htt+/+* animals when compared to *5-Htt+/-* animals. This discrepancy could be the result of differences in the experimental setup of the projects, which lied mainly in the breeding and the housing properties, as discussed in the previous section.

In the second study, Enrichr analysis (Chen *et al.* 2013) identified the Mammalian Phenotype term "abnormal myelination" as well as several GO terms associated with myelin or glia, such as "axon ensheathment", "myelination", "regulation of gliogenesis" and "oligodendrocyte differentiation", as enriched. The DEGs in these terms show a remarkably consistent expression pattern with increased expression in *5-Htt+/-* C mice when compared to *5-Htt+/+* and decreased expression in *5-Htt+/-* mice exposed to PS. The identified DEGs covered different aspects of myelin and OLs: structural myelin proteins, such MBP and MOBP, enzymes associated with myelin, i.e. MAL and CNP, proteins involved in lipid metabolism, such as GAL3ST1, FA2H and NPC1, proteins involved in OL-cell communication, such as MAG, MOG and CLDN11, and transcription factors, such as OLIG1, SOX10, MYRF, SOX8 and NKX6.2. In addition, we found changes in *Cspg4* (aka *NG2*) and *Pdgfra*, both markers of the NG2+ OL progenitor cell population.

SOX10 and MYRF are essential myelin transcription factors in the CNS as they induce terminal OL differentiation. While *Sox10* is expressed already in OPCs, *Myrf* expression starts only in promyelinating OLs, i.e. after cell-cycle exit. SOX10 directly induces *Myrf* expression in OLs, whereupon SOX10 and MYRF were reported to cooperate in inducing the expression of a myelin-gene network (Hornig *et al.* 2013). As *Sox10* is being expressed during all developmental OL stages, it was suggested that most likely other factors that are yet unknown are involved in *Myrf* induction. *Sox10* still plays a crucial role in OL maturation, as shown by *Sox10*-deficient mice, in which OPCs do not develop into mature myelinating OLs. Interestingly, we also found a change in *Egr2* (aka *Krox20*) expression. SOX10 and EGR2 are known to fulfill an analogous function to SOX10/MYRF in swan cells of the PNS (Marathe *et al.* 2013). It has reported that OLs do not express *Egr2*, thus the low *Egr2* expression we detected in the hippocampus is likely to reflect neuronal reflection. As the change of *Egr2* expression followed the same pattern as the myelin-genes and exceeded the FCs observed e.g. for *Mbp* and *Mag,* it is tempting to

speculate if *Egr2* might possibly be involved in CNS myelination in an indirect way, e.g. via a neuron-NG2 interaction. SOX8 is closely related to SOX10 and can partially take over SOX10 functions in myelin-associated gene expression (Stolt *et al.* 2004; Hornig *et al.* 2013).

Taken together, we can conclude from the combination of affected genes that the gene expression findings most likely reflect changes both in progenitor cells (*NG2, Pdgfra*), mature OLs (*Myrf, Mbp, Mag*) and myelin (*Mbp, Mag, Mog, Mobp*). The expression changes of the respective genes indicate increased OL number and/or myelination in C *5-Htt+/-* mice when compared to *5-Htt+/+* mice, which was reduced by PS exposure. On a structural level this could either mean that the myelin sheath thickness or the number of myelinated internodes was increased in C 5-Htt+/- mice compared to the ones of *5-Htt+/+* mice. As the expression of genes encoding proteins located only on the outer or on the inner myelin leaf (*Mog* and *Mag*), respectively, was changed in the same manner as e.g. *Mbp* and *Mal*, this favors the second explanation. As such, the *5-Htt+/-* genotype may be associated with an increase in OL numbers, which in turn could either be the result of increased oligodendrogenesis or changes in migration patterns of OPCs. Indeed, we found hints for increased numbers of NG2+ OPCs in the hippocampus of the C *5-Htt+/-* compared *5-Htt+/+* mice, as described in the following section. In conclusion, the expression changes in myelin-associated genes we detected in the hippocampus likely reflect changes of GM methylation. After WM tract methylation, the myelination within the GM is what affects signal transduction most. In addition, myelinating OLs of the hippocampus and neocortex exclusively produce the extracellular metallo protease ADAMTS4, which is involved in the metabolism of lecticans. Lecticans are part of perineuronal nets, which emerge late during postnatal brain development, and participate in regulating synaptic plasticity (Levy *et al.* 2014). In line with this function, we indeed found a GxE-effect on *Adamts4* expression matching the myelin-genes' expression pattern. Next to this, changes in perineuronal OL number could also contribute to the detected expression changes. Perineuronal OLs are non-myelinating OLs in close contact to neurons, on which they could have a trophic effect (Vostrikov *et al.* 2007; Szuchet *et al.* 2011). Although not producing myelin, they were described to harbor a reservoir of untranslated myelin-gene transcripts, which would be activated in case of need for (re-)myelination (Szuchet *et al.* 2011). As discussed two sections below, decreased numbers of perineuronal OLs have been detected in SC, BP and MDD patients when compared to controls (Vostrikov *et al.* 2007).

We found changes in expression of *Pdgfra* and the chondroitin sulphate proteoglycan *Ng2* (official name *Cspg4*), two markers of a NG2-+ glial population that one the one hand gives rise to OLs in the adult brain and on the other hand represents a functional glial population on its own. OPCs originate mostly from the ventricular zones of the developing rodent brain from about E12.5 onwards and subsequently migrate to various brain regions (Le Bras *et al.* 2005). In the first postnatal weeks, they produce mature OLs (P7-14) and myelination begins. In the adult brain, another progenitor cell population with the ability to produce OLs can be found, the migratory and mitotic NG2+ glia. NG2+ glial cells have been recognized as the fourth type of glia of the CNS, next to astrocytes, OLs and microglia. In contrast to the other adult progenitor cell populations of the CNS, NG2+ glia are uniformly distributed throughout the brain and display unique physiological properties. NG2+ glia comprise 2-3% of the total cell population in adult grey matter and 8-9% in adult white matter (5% in total Dawson 2000). *In vitro*, NG2+ cells have the potential to be differentiated into OLs, astrocytes and neurons (Stallcup and Beasley 1987; Kondo and Raff 2000; Diers-Fenger *et al.* 2001; Belachew *et al.* 2003). Whether this multipotency also occurs *in vivo* is still under heavy debate, as data from different transgenic mouse models are contradictory. Zhu and colleagues found that embryonic NG2+ glia cells produce astrocytes but no neurons (Zhu *et al.* 2008; Zhu *et al.* 2008; Zhu *et al.* 2011), whereas others found neurons in the piriform cortex derived from NG2+ glia (Doerflinger *et al.* 2003; Rivers *et al.* 2008; Guo *et al.* 2010). Huang and colleagues used a NG2-CreERT2 mouse line to follow the fate of NG2+ glia and found that NG2+ glia generate OLs across the lifespan and embryonic NG2+ glia also produce, to a smaller degree, astrocytes. All experiments confirm, however, that NG2+ glia mainly give rise to mature OLs (Rivers *et al.* 2008; Huang *et al.* 2014). NG2+ glia furthermore respond to various types of injuries by migrating to the site of action and repopulating depleted areas, if necessary (Keirstead *et al.* 1998; Reynolds *et al.* 2002; Watanabe *et al.* 2002; Liu and Shubayev 2011; Lee *et al.* 2013; Sypecka *et al.* 2013). Next to their role as progenitor cells, NG2+ glia cells seem to have also an independent role on their own in normal CNS physiology. Those cells are also called polydendrocytes and synantocytes as they are characterized by multiple cell processes that also extend to neurons, forming unique unidirectional neuron-NG2+-glia synapses with NG2+ cells building the postsynapse (reviewed (Sakry *et al.* 2011). Bergles and colleagues for example described NG2+ cells of the CA1 region of the hippocampus making synaptic contact with CA3 neurons (Bergles *et al.* 2000). NG2+ glia moreover express glutamatergic AMPA receptors and GABAA receptors, which can be activated by synaptic neuronal input triggering depolarization of NG2+ cells (Williamson *et al.* 1998; Bergles *et al.* 2000; Matthias *et al.*

2003; Lin and Bergles 2004; Jabs *et al.* 2005; Bergles *et al.* 2010; Hamilton *et al.* 2010). Next to this, ATP binding by P2Y1 and P2X7 purine receptors also triggers Ca2+ influx (Hamilton *et al.* 2010). NG2+ glia also contact areas of unmyelinated axons in the white matter, where glutamate is released from the axons, and it was estimated that one NG2+ cell could receive input from up to 70 synapses (Lin *et al.* 2005; Kukley *et al.* 2007; Ziskin *et al.* 2007). Although they have been suggested to play a role in regulating the availability, recruiting and differentiation of myelinating OLs (Sakry *et al.* 2011), the exact physiological role of these synaptic contacts remains to be elucidated. Altogether, NG2+ glia most likely play an important role in the neuron-glia-network exceeding their function as OPCs.

The expression of a set of myelin- and OL associated genes including *Ng2* was increased in C *5-Htt+/-* compared to both C and PS *5-Htt+/+* mice, but reduced to wild type-level in *5-Htt+/-* mice exposed to PS. This indicates that while the *5-Htt* genotype *per se* increased expression, the interaction of *5-Htt* and PS reduced or normalized expression. As discussed in section 2.4., myelination starts only around P10 in the murine hippocampus (Savaskan *et al.* 1999), but PS could have had an impact on OPC proliferation, migration or epigenetic programming. NG2+ OPCs express the GR and the GR-cofactors SRC1 and p300 in vivo (Matsusue *et al.* 2014), making them potential targets for stress effects. Moreover, several studies linked changes in stress exposure to altered myelination. Xu and colleagues for example exposed Sprague-Dawley rats to PS and found disturbed myelin formation in the hippocampus of the 22 days old PS rats (Xu *et al.* 2013). Miyata et al. found morphological changes in OLs in the corpus callosum of mice exposed to acute stress in form of chronic water-immersion and restraint stress (Miyata *et al.* 2011). The interaction of the serotonergic system with myelinating cells or NG2+ glia is not yet understood in detail, there is work, however, connecting the serotonergic system and its manipulation with myelin formation. Postnatal citalopram (SSRI) treatment of rat pups resulted in both hypo- and hypermyelination of axons of the corpus callosum and altered OL morphology in the adult brain (Simpson *et al.* 2011). Fan and colleagues recently showed that all developmental rat OL stages from NG2+ OPCs to mature MBP+ OLs express HTR1A and HTR2A, marking both NG2+ glia and OLs as possibly sensitive to alterations in 5-HT homeostasis (Fan *et al.* 2014). NG2+ OPCs derived from human embryonic stem cells also express HTR1A (Schaumburg *et al.* 2008). Immature OLs furthermore react with a steady increase in intracellular Ca^{2+} in response to 5-HT exposure, which is most likely due to released intracellular Ca^{2+} stores (Nagatomo *et al.* 2004; Fan *et al.* 2014). 5-HT exposure has detrimental effects on immature OLs in mono-culture, and to a smaller degree also on OPCs, as reflected by less and shorter processes

and a simpler morphology, as well a decrease in immature OL number, reduced MBP and PLP1 expression in immature OLs and immature OL cell death at high 5-HT concentrations. Exposure of a NG2+-OPC-neuron-coculture to 5-HT reduces the number of myelinated internodes and leads to abnormal clustering of CNTNAP1 at the nodes of Ranvier, albeit it does not lead to cell death (Fan *et al.* 2014). Notably, the number of OLs was not affected.

There is evidence associating changes in OL number and myelination with several psychiatric disorders, such as schizophrenia, bipolar disorder and major depressive disorder (Chambers and Perrone-Bizzozero 2004; Mathews *et al.* 2004; Le-Niculescu *et al.* 2007; Le-Niculescu *et al.* 2009; Parlapani *et al.* 2009; Sibille *et al.* 2009; Ayalew *et al.* 2012; Edgar and Sibille 2012; Mosebach *et al.* 2013; Hercher *et al.* 2014). Vostrikov and co-workers for example found a lack of the regular age-associated increase in OL number in the PFC and adjacent WM as well as decreased perineuronal OLs in the PFC in SC, BP and MDD patients when compared to healthy controls (Vostrikov *et al.* 2007; Vostrikov and Uranova 2011). Altered myelination likely causes changes in the functional connectivity of neuronal networks involved in emotional processing, as it would affect timing and synchronization, resulting in behavioral and cognitive changes (Salami *et al.* 2003; Buzsaki and Draguhn 2004; Pajevic *et al.* 2014). Several studies furthermore associated variance in the serotonergic system with white matter (WM) changes. A study by Frodl and coworkers found smaller WM volumes in the hippocampus of MDD patient carrying the La/La 5-HTTLPR than patients with the La/(Lg + S) or (Lg + S)/(Lg + S) genotypes, i.e. the L-allele in addition to the A-SNP, the A-SNP allele associated with increased 5-HTT expression (Frodl *et al.* 2008). Of note, myelin makes up 50% of WM in the human brain (Miller *et al.* 2012). Pacheco and colleagues used diffusion tensor imaging (TDI) in order to analyze the uncinate fasciculus (UF), a white matter tract that connects the amygdala to medial and orbital prefrontal cortex and is highly involved in emotional processing, in 37 healthy female participants (Pacheco *et al.* 2009). They found a negative correlation between the number of low-expressing 5-HTTLPR alleles and the fractional anisotropy (FA) of diffusion of the left frontal UF, indicating reduced connectivity between amygdala and PFC in low-expressing 5-HTTLPR allele carriers, and a positive correlation of FA and age. The FA is an unspecific measure of white-matter structure reflecting the number of axons and/or their degree of myelination as well as other fibers crossing the tract of interest in other directions (Jasinska and Perkins 2009). As shown by Pacheco and others, white matter tracks also change with age, with increased integrity in childhood and early adulthood, and a decrease of the same from middle adulthood into old age (Salat *et al.* 2005; Snook *et al.* 2005; Pacheco *et al.* 2009). A later

study by Wiggins and coworkers found a decreased connectivity between the right amygdala and PFC with age in adolescent low-expressing allele carriers, but not in high-expressing allele carriers, indicating an interaction of 5-HTT genotype and age (Wiggins *et al.* 2014). This underlines the complexity of GxE interactions, but also the importance to analyze GxE interactions in a developmental framework, as different windows of vulnerability likely exist. Our work indicates that the late prenatal development might be such a window in which cell populations that are programmed to become myelinating OLs and NG2 cells might be especially vulnerable to an interaction of stress exposure and variance in 5-HT homeostasis, possibly leading to altered connectivity in the adult brain and consequently behavioral alterations. As we analyzed only gene expression in the hippocampus in this study, our findings raise several questions, e.g. do these expression changes in myelin-genes translate to myelin with an intact structure or is it a sort of compensation, how are OL numbers, what type of OL is affected and how did the OL population develop in other brain regions. The last issue is especially interesting in the light of our former study, where we showed region-specific GxE-effects on myelin-associated gene expression patterns in the hippocampus and amygdala (see Fig. 2.3-3). This indicates that PS and *5-Htt* genotype do not exert their effects in the same (unspecific) way on all brain regions. One could rather expect increased myelination and thus connectivity between some regions, and decreased connectivity between others, leading to a shift in functions underlying specific processes involved e.g. in sociability, anxiety-like behavior etc. One could speculate that differences in connectivity in the hippocampus and amygdala might result from a developmental adaptation to PS, leading to altered stress responsibility as those regions have opposite regulatory functions on HPA-axis activity. An analysis of NG2+ glia and perineuronal OLs could additionally reveal a possible altered interaction with neurons and subsequently synaptic plasticity. Next to these points, getting an overview of the general myelination status of WM tracts connecting brain regions involved in emotional processing, such as amygdala, PFC, NAA, in *5-Htt*+/- mice exposed to stress would highly interesting.

3.4.4. Manipulation at the *5-Htt* locus affected expression of numerous genes on Chr 11

The transcriptome analysis using mRNAseq revealed a significant effect of the *5-Htt* genotype on the expression of genes on the same chromosome, i.e. Chr 11. Fourteen out of the 18 DEGs with an adjusted $p<0.05$ affected by a G-effect were located on Chr 11, albeit the observed expression FCs were not as high as for the *5-Htt*. When looking at nominal p-values ($p<0.01$), 21% of the DEGs were located on chr 11, which is significantly

more than to be expected by chance. Although the authors of the original study describing the *5-Htt-/-* mouse line for the first time "…*anticipated that a 5-HTT gene lacking exon 2 would result in an inactive or highly dysfunctional gene product without altering the expression of neighboring genes*" (Bengel *et al.* 1998), our data suggest otherwise. Noteworthy, most of the DEGs were not adjacent to *5-Htt*, but were clustered in a DNA stretch 10 Mio kb upstream of the *5-Htt* gene, indicating a specific effect of the manipulation of the *5-Htt* locus on this genomic region. 9 of the DEGs on Chr 11 belong to one synteny block, i.e. genomic fragments that are highly similar between species and comprise homologous genes on homologous chromosomes. As in the mouse, the synteny block, comprising the DEGs, and the *5-Htt* gene are located on the same (homologous) chromosome in the rat, rhesus macaque and human genome, respectively. As described by Bengel and coworkers, a genomic region comprising exon 2, the translation start site and a sequence encoding a part of the functionally essential first transmembrane domain was exchanged for a neo cassette (Bengel *et al.* 1998). In theory, both the deletion of the described region and/or the insertion of the neo cassette could have had long-range off-target effects. As reported by several groups, insertion of a neo-cassette into a gene can lead to reduced expression of genes located downstream of the target gene, both adjacent and as distant as 100 kb. The region where we observed changes in expression was, however, located upstream and substantially more distant. In a highly interesting study, Meier and colleagues compared the off-target effects of gene targeting using different methods, i.e. neo cassette vs. Cre/loxP- and Flp/FRT-mediated recombination (Meier *et al.* 2010). The target genes were *Tnr* and *Ncam*. In contrast to the authors expectations, both the *Tnr-/-* mice carrying the neo cassette and the $Tnr^{flox/flox}$ mice showed reduced expression of the 1.1 Mb upstream located gene *Gas5*, indicating that not so much the size of the inserted sequence caused this effect but more likely the disruption of a regulatory element in the highly conserved region of the *Tnr* intron. No off-target effects were detected for neither of the *Ncam* mouse lines, likely because this manipulation did not target a conserved region (Meier *et al.* 2010). The manipulation at the *5-Htt* locus could have similarly altered expression by disrupting a conserved regulatory element, thereby possibly interfering with enhancer-promoter or silencer-promoter interaction, for example by inducing or ablating the formation of chromatin loops or activating/silencing chromatin hubs. As activating chromatin hubs are thought to be held together by transcription factors and cohesion molecules (Razin *et al.* 2013), this might indicate that chromatin hub formation is regulated in a spatiotemporal manner. The effects of the genetic manipulation in *5-Htt* mice might thus have different effects on different tissues during different windows of

development, making an estimation of the *5-Htt* KO's off-target effects highly challenging. An analysis of the chr11-genes in different regions of the adult brain would be a start. It would furthermore be important to test if these expression changes are really completely independent of *5-Htt* expression, e.g. by analyzing those genes in a tissue not expressing *5-Htt*. It might also be possible that the expression of a non-coding RNA involved in expression regulation or chromatin conformation of the synteny block region was altered. If variation in the 5-HTTLPR or the VNTR in the 5-HTT intron 2 has a similar effect on the corresponding region of the human genome would be another very interesting question to address.

This finding raises several questions, both regarding *5-Htt* mice and KO models in general. We should consider the possibility that a part of the molecular and behavioral phenotypes observed in *5-Htt* mice could be - at least partially - attributed to off-target effects on genes located on Chr 11. In both studies, next to changes in *5-Htt*, we also found consistent increases in *Trpv1* and *Xaf1* expression in *5-Htt*+/- mice when compared to *5-Htt*+/+ mice. The 5-Htt transcript was upregulated in *5-Htt*+/- mice with a log2FC of 7.04 when compared to *5-Htt*+/+ mice, which seems counterintuitive, but was expected and can be explained when looking at the mapped reads. We did not detect an upregulation of the wild-type transcript, but, as indicated by the missing reads on *5-Htt* exon2, of the truncated transcript that does not produce a functional 5-HTT protein. We found the same effect in our previous study. An increase in the truncated transcript and 5-HTT protein was also reported previously by Ravary and coworkers (Ravary *et al.* 2001). Ravary and coworkers also analyzed apoptotic processes, which could have been induced by the misfolded 5-HTT protein, but found no signs of apoptosis in serotonergic cells induced by the accumulation of truncated 5-HTT protein.

Although *Trpv1* is best known as a capsaicin receptor of the dorsal root ganglia, additional functions of TRPV1 in the CNS have been revealed (Hu *et al.* 2012). *Trpv1* is expressed throughout the CNS including hippocampus, however at lower levels as compared to the dorsal root ganglia. In our study, *Trpv1* expression was very low, especially in the *5-Htt*+/+ animals. Activation of TRPV1 by capsaicin, heat, voltage, pH or lipoxygenase products leads to unselective cation gating, predominantly Ca^{2+}. TRPV1 was detected in neuronal cell bodies and synapses, as well as in astrocytes and microglia. Interestingly, TRPV1 is involved in anxiety-like behavior, conditioned fear and long-term depression (LTD) in the hippocampus and the nucleus accumbens (Marsch *et al.* 2007; Gibson *et al.* 2008; Chavez *et al.* 2010; Grueter *et al.* 2010; Hakimizadeh *et al.* 2012). Both knock out and blocking of TRPV1 leads to anxiolytic effects, whereas

treatment with an TRPV1 agonist leads to increased anxiety-like behavior in the EPM in rodents (Kasckow *et al.* 2004; Marsch *et al.* 2007; Aguiar *et al.* 2009). Although *Trpv1* was expressed only at low levels in the hippocampus of both genotypes in our study, expression was increased with a FC of 2.2 in *5-Htt+/-* mice when compared to *5-Htt+/+* mice. Furthermore, *Trpv1* expression changes might have been higher in other brain regions. We could continuatively speculate that increased *Trpv1* expression might contribute to the anxious phenotype observed in *5-Htt-/-* mice, especially if *Trpv1* expression is increased in a gene-dose-dependent manner in *5-Htt-/-* mice, which were not analyzed in the present study.

The proapoptotic *Xaf1* is a putative tumor-suppressor gene. It promotes cell death by inhibiting the anti-apoptotic XIAP and other inhibitors of apoptosis as survivin (Liston *et al.* 2001; Arora *et al.* 2007), and by a XIAP-independent mitochondrial apoptosis pathway involving TNF-a induced cytochrome c release from the mitochondria (Wang *et al.* 2006). Hypoxia-induced ischemia in neonatal rat brains increases *Xaf1* expression, thereby promoting apoptosis by translocating XIAP into the nucleus (Russell *et al.* 2008). Of note, the increase in *Xaf1* expression was higher in the first study, where MA targeting 3' UTRs were used to detect expression changes, than in the second study, where we applied mRNAseq to characterize the transcriptome. The finding of the first study was confirmed by RT-qPCR using primers targeting the 3' UTR. When looking at the mRNAseq data of *Xaf1*, it seems as if most of the differences in expression between *5-Htt+/-* and *5-Htt+/+* mice can be attributed to the differences in reads mapped to the 3' UTR. When using mRNAseq, the reads of the whole transcript were evaluated for the calculation of expression changes, explaining the difference to the MA study, where only the 3' UTR was recognized, and indicating an overestimation of the increase in *Xaf1* expression in the first study. When looking at *Xaf1* expression using mRNAseq of single animals, we found reads mapping to the 3' UTR of all *5-Htt+/-* animals, but only for 2 out of 8 *5-Htt+/+* C and 3 out of 8 *5-Htt+/+* PS social animals. None of the *5-Htt+/+* PS unsocial animals expressed the *Xaf1* 3' UTR. The fact that the 3' UTR seemed to be expressed in a different manner than the rest of the transcript and that the reads also did not exactly map to the 3' UTR but began a bit more downstream might hint to an yet unknown transcript, e.g. a non-coding RNA, transcribed from the 3' UTR of *Xaf1*.

Taken together, off-target effects should be carefully assessed when creating a knock-out model and possible off-target effects considered when interpreting behavioral and molecular data. It is very likely, however, that it is not possible to consider all the small,

possibly cumulative, effects introduced by genetic manipulation and the subsequently triggered processes, hence additional methods should be applied to validate a model.

3.4.5. Pathways affected in social, but not in unsocial, *5-Htt*+/- mice exposed to PS

Another aim of this study was to identify molecular players promoting resilience to PS. In general, resilience can be defined as the ability to cope with change and adversity. When facing advers conditions, a range of reactions can be observed. Only a part of the individuals exposed to a certain stressor develops a mental disorder, while most of the individiuals successfully adapt. Human studies found several psychosocial factors promoting resilience, such as active copying strategies, optimisms, high positive emotionality, openness to social support, cognitive flexibility, exploration and a broadened focus of attention (Fredrickson 2001; Tugade and Fredrickson 2004; Southwick *et al.* 2005; Ong *et al.* 2006). The neuronal correlates and molecular mechanisms underlying either resilience or susceptibility are, however, only poorly understood. In animal models different outcome measures have been used to determine resilience, considering that the experimenter usually has only a restricted number of possible measurements in the same individual. Krishnan and coworkers for example exposed male mice to a social defeat paradigm and tested if the animals afterwards would approach again the larger mouse that defeated them previously (Krishnan *et al.* 2007). In the current study, we used sociability as measured in the 3-chamber-sociability test as the outcome to group animals into social, resilient, and unsocial, vulnerable, animals, because in our testing battery, sociability was the behavior affected most by PS exposure. The sociablity rating indeed covered a wide range of reactions both in the control groups and the PS groups, with most PS animals being categorized as "social" and only about a third of them being categorized as "unsocial".

When comparing social and unsocial animals with the control group of the respective genotype, we found only a small number of genes to be differentially expressed in the *5-Htt*+/+ animals (71 in social, 28 in unsocial), whereas a huge number of genes was regulated in *5-Htt*+/- animals (865 in social, 413 in unsocial). This is not unexpected when considering the high number of DEGs affected by GxE and emphasizes the importance of such models. Interestingly, in both genotypes, at least double the number of genes was regulated in social vs control animals when compared to unsocial vs control animals, which might indicate that maintaining or acquiring normal sociability after PS exposure requires more active processes than the mere reaction to PS. When we investigated how

the social and the unsocial animals diverged from each other in regard to regulated pathways, two pathways that we already identified in our GxE-comparison emerged for the *5-Htt+/-* animals, i.e. myelination and mitochondrial respiration. While both processes seemed to be affected by PS in the *5-Htt+/-* animals, the regulation was stronger in the social group than in the unsocial group.

Mitochondrial respiration and ATP metabolism seemed to be affected in social, but not unsocial, 5-Htt+/- mice when compared to control *5-Htt+/-* mice, with social animals showing consistently increased expression of all but one DEG (*Atpv0a2*) in the enriched "oxidative phosphorylation" pathway. These processes were also up-regulated in *5-Htt+/-* mice when compared to *5-Htt+/+* mice, however in the sociability-context, the enriched pathway comprised different and a greater number of genes than those affected by genotype. This is reflected in the targeted complexes, as most of the proteins encoded by the DEGs belong to the mitochondrial respiratory chain complex III and IV, a notion which is supported by the enrichment of the GO terms "mitochondrial respiratory chain complex III" and "respiratory chain complex IV". Additional enriched GO term such as "cellular respiration" and "ATP metabolic process" (comprising 22 genes) can be tied to the process of mitochondrial respiration. As eleborated in section 3.4.2 "Hippocampal gene expression profiles of *5-Htt+/-* mice exposed to PS", mitochondria are essential for proper neuronal function as they are the main ATP and ROS provider in the brain and furthermore engaged in intrinsic and extrinsic apoptosis pathways (Kann and Kovács 2007). Mitochondrial dysfunction impacts fore example on neuronal plasticity and neurogenesis (Jonas 2006; Li *et al.* 2010; Jiao and Li 2011). Thus, unsocial mice with low mitochondrial capacity might have reacted differently to PS exposure than social mice with higher metabolic capacity, which migh have been able to raise the energy required for adaptive processes counteracting the effects of PS.

A similar picture emerges when looking at the myelination pathway. While PS seems to have generally down-regulated the expression of myelin-associated genes in *5-Htt+/-* animals, the degree of this effect was stronger in the social group. How this finding can be attributed to the observed behavioral phenotype is unclear, as we do not know what structural changes in myelination occured, i.e. which fibers and connections are concerned. As discussed in the section "Hippocampal gene expression profiles of *5-Htt+/-* mice exposed to PS", developmental changes in myelination could contribute to altered connectivity in brain regions involved in emotional processing, which could underly increased social behavior in the social *5-Htt+/-* group. Felix-Ortiz and Tye for example have shown that optogenetic activation of glutamatergic projections from the

basolateral amygdala to the ventral hippocampus affects social behavior in the 3-chamber-sociability test and the resident-juvenile intruder test in C57BL/6 mice (Felix-Ortiz and Tye 2014).

The variance we observed within geneticly homogenous groups with the same experimental conditions could result from diverse factors. Although experimental conditions were standardized as much as possible, some circumstances of development defy control and influence the offspring's development, amongst others the pups position in the placenta, differences in maternal care, different interactions with litter mates, transgenerational effects and possibly also stochastic events of mutagenesis. The pups' position in the placenta could have impacted on their supply with oxygen and nutritients, thereby affecting fetal growth and body weight at birth. In humans, low body weight has been associated with an increased risk for the development of several chronic diseases, such as cardiovascular diseases, diabetes, but also increased susceptibility to stress and risk for affective disorders (Curhan *et al.* 1996; Nilsson *et al.* 2001; Gale and Martyn 2004; Wiles *et al.* 2005; Costello *et al.* 2007). All of the mentioned factors could also have had an impact on the epigenome thereby influencing the pup's brain development and behavior. As some epigenetic marks can be transmitted from the parents, inter- and transgenerational effects might also play a role. However, when looking at the sociability measurement per litter, we could not detect any clear patterns.

In a previous study of our group (Jakob *et al.* 2014), we exposed *5-Htt+/-* mice to PS and grouped the offspring based on their performance in the FST into resilient and vulnerable animals. The candidate genes from this study, growth hormone (*Gh*), prolactin (*Prl*), calcium/calmodulin-dependent protein kinase II alpha (*Camk2a*), c-fos induced growth factor (*Figf)* and the galanin receptor 3 (*Galr3*) amongst others, were not differentially expressed in this study. *Gh* and *Prl*, however, showed as to be expected a high correlation and showed furthermore an increase in unsocial, but not social, *5-Htt+/+* animals. This change did not reach statistical significance as variation within the groups was exceptionally high. This was also observed in the previous study and could be due to the fact that we did not control for the females' estrogen cycle and these genes' expression is regulated by estrogens (Donahue *et al.* 2006; Nogami *et al.* 2007). Differences between the candidate genes from the previous study and the current study could be based an a several factors previously discussed (section "Altered expression of genes associated with myelination and oligodentrocytes due to *5-Htt* x PS interaction"), including breeding design and environmental conditions. Furthermore, two different

outcome measures were used for the grouping, hence very likely molecular substrates of different circuits and processes were analyzed in the two studies with regard to resilience.

In conclusion, different environmental factors including conditions of fetal growth, maternal care and (transgenerational?) epigenetic mechansisms might have interacted with PS exposure and *5-Htt* genotype, producing differences in sociability and on molecular level affecting myelination and mitochondrial respiration.

3.4.6. Study limitations and methodological issues

The following limitations should be considered when interpreting the data presented in this study. From weaning onwards, animals were housed in groups of 3±1 animals in order to avoid isolation stress. We cannot exclude, however, that hierarchies had been established that possibly influenced our data. Furthermore, behavior was assessed in the same animals as CORT and hippocampal gene expression profiles, enabling us to directly associate behavioral findings with physiological parameters and changes on molecular level. The evident drawback of this approach is that we cannot exclude effects of behavioral testing itself on CORT and gene expression profile. Moreover, despite all animals going through the same tests, we cannot exclude an interaction of behavioral testing and genotype and/or PS. The same is true for CORT measurements. In addition, we cannot exclude an effect of the estrous cycle on behavior, CORT or gene expression in the female mice as we did not control for it in order to protect the dams from additional, potentially confounding stress exposure.

Next to this, a few technical limitations should be pointed out. When looking at the number of DEGs affected by different factors, the numbers of genes passing multiple correction seems counterintuitive. *Sgk1* was the only DEG with an adjusted $p<0.05$ affected by PS, which is peculiar when considering that there were 359 genes affected by PS with a nominal $p<0.01$ and considering that we identified 18 DEGs with an adjusted $p<0.05$ due to genotype although only 149 genes were affected by genotype with a nominal $p<0.01$. A possible reason for this is the smaller sample size for the control groups when compared to the PS group (16 control animals vs 32 PS animals) as well as a broader reaction to PS than to genotype, e.g. PS groups containing social and unsocial animals, which might increase the SD.

Our study identified mitochondrial respiration, myelination and epigenetic mechanisms as the major processes affected by *5-Htt* genotype, PS or their interaction. In all three cases, the expression patterns were very consistent among the genes within a single

pathway and, additionally, very similar between myelination-associated genes and genes involved in chromatin remodelling. It might thus be possible that the enrichment of pathways and terms related to epigenetic mechanisms do not indicate a general alteration of epigenetic processes in the analyzed tissue, but could also result from changes in OL number and hence reflect OL-specific epigenetic machinery. This could be clarified by a cell-type specific analysis of epigenetic players and patterns, as discussed in 3.4.7 "Conclusion and outlook".

Finally, the analysis of a single brain region, such as the hippocampus, limits the explanatory power of the molecular findings on behavior, since other structures, such as the amygdala and the prefrontal cortex, are also involved in regulating stress and emotion response. Taken together, the presented data should be interpreted with caution, until future research reveals the extent to which the molecular players emerged from this study could provide useful targets for intervention strategies in the treatment of stress-related disorders of emotion regulation.

3.4.7. Conclusion and outlook

In conclusion, this study showed that variation in the *5-Htt* genotype, PS exposure or an interaction of both affects behavior as well as several molecular pathways, among them mitochondrial respiration, myelination and chromatin remodeling, in the hippocampus of female mice. Following up on the finding that myelination or at least gene expression of myelin-associated genes is affected by a GxE-interaction, a histological study aiming at characterizing myelin structure and distribution as well as the number and relative proportion of OLs, OPCs and NG2+ glia in different brain regions will be necessary. It will be of special interest to study these things at different developmental stages in order to disentangle the mechanisms by which 5-HT and PS exposure interact to alter myelination. If changes in myelination should be validated, it would be furthermore of interest to investigate to which degree connectivity between brain regions involved in emotion processing are altered and if this could be tied to the behavioral alterations observed.

Next to this, the results of the transcriptome analysis suggest that mechanisms of chromatin remodeling including *Sirt2*, *Hdac2* and components of the PRC1 were involved in mediating the observed GxE-interactions. Along this line, it would be interesting to analyze the related epigenetic changes, i.e. histone modifications and DNA methylation changes, at possible target genes of these chromatin modulators, e.g. by chromatin-immunoprecipitation (ChIP) followed by sequencing or target specific RT-qPCR. As SIRT2 deacetylases not only histones but also cytosolic proteins, SIRT2-target

proteins outside the nucleus should be analyzed. Additionally, both global and target-specific H3K4me3 levels could be investigated, as gene sets associated with this histone modification were enriched in several comparisons. When following up on this study and investigating epigenetic patterns in our samples, a cell-type specific approach will be necessary. Recent studies have underlined the importance of analyzing epigenetic patterns in a cell-type specific manner, as for example DNA methylation patterns differ greatly between neurons and glial cells. Analyzing a heterozygous tissue like the hippocampus as a whole might not only diminish and obscure epigenetic changes taken place in only a part of the analyzed cells, but attributing detected changes to specific processes will also be complicated as long as the cell type they stem from is unknown. This situation gets even more complex when the relative proportion of the various cell types is altered between conditions, as changes in epigenetic markers could then also "only" reflect an increase/decrease in a specific cell type. In this study, this could be the case, as judging from the hippocampal gene expression profiles we suspect altered OL/OPC numbers or an altered proportion of OL/OPCs, e.g. due to a reduced number of neurons. If the identified players involved in chromatin remodeling are associated with OL/OPC number is yet to be investigated. Therefore it will be crucial to separate cells or nuclei for epigenetic analyses such as DNA methylation and histone modifications (in particular H3K4me3), e.g. either by fluorescence-activated cell sorting (FACS) or fluorescence-activated sorting of fixed nuclei (FAST-FIN) (Marion-Poll *et al.* 2014). In light of the complex arborization of adult neurons and OLs, nuclei sorting is the more realistic option and furthermore has the major advantage that it can be performed on fixed tissue. Working with fixed tissue is highly preferable over using fresh tissue in this case as the latter is not only time-consuming in terms of processing the dissected brains but also carries the risk of inducing cellular reactions by the dissociation and isolation procedure, which is very hard to control for and can introduce flaws into the data.

Finally, we observed genomic effects of the manipulation at the *5-Htt* locus on the expression of genes clustered 10 Mio bp upstream on Chr 11. A possible explanation could be that the region disrupted by the *Neo* cassette is somehow involved in regulating the chromatin conformation in the affected region, e.g. by participating in a chromatin hub. As chromatin hubs also involve transcription factors, it would be interesting to analyze if the observed effect is aspecific, i.e. the same in all tissues, or if different genomic effects can be observed in different tissues/cell types at different points in time. It would be also interesting to disentangle to which degree the observed behavioral and molecular effects stem are influenced by those genomic effects, e.g. by a rescue experiment. Last but not least, it will be interesting to analyze human

transcriptome data from subjects carrying genomic polymorphisms in the 5-Htt gene, e.g. variation in the 5-HTTLPR or the VNTR in the 2nd exon.

Albeit the identified pathways might represent exciting new targets for the therapy of disorders of emotion dysregulation, additional research is needed to validate those findings and to disentangle exactly how 5-HT and PS are linked myelination, mitochondria and how they impact on epigenetic mechanisms.

4. Appendix

4.1. Appendix Tables (see enclosed DVD)

Project 1 – GxE

- **Appendix Table 1:** Differentially methylated regions due to *5-Htt* genotype, due to PS or due to interaction of *5-Htt* genotype and PS
- **Appendix Table 2:** Modulatory Modularity Clustering of myelin-associated genes

Project 2 – Resilience to PS

- **Appendix Table 3:** Differentially expressed genes due to *5-Htt* genotype, due to PS, due to interaction of *5-Htt* genotype and PS as well as differentially expressed genes in social and unsocial *5-Htt*+/+ and *5-Htt*+/- mice
- **Appendix Table 4:** Enrichment analysis of differentially expressed genes due to *5-Htt* genotype, due to PS, due to interaction of *5-Htt* genotype and PS as well as differentially expressed genes in social and unsocial *5-Htt*+/+ and *5-Htt*+/- mice

4.2. References

Abou Jamra, R., T. Becker, et al. (2008). "Genetic variation of the FAT gene at 4q35 is associated with bipolar affective disorder." Molecular Psychiatry **13**(3): 277-284.

Aggarwal, S., L. Yurlova, et al. (2011). "A size barrier limits protein diffusion at the cell surface to generate lipid-rich myelin-membrane sheets." Dev Cell **21**(3): 445-456.

Aguiar, D. C., A. L. Terzian, et al. (2009). "Anxiolytic-like effects induced by blockade of transient receptor potential vanilloid type 1 (TRPV1) channels in the medial prefrontal cortex of rats." Psychopharmacology **205**(2): 217-225.

Aguilera, G. and C. Rabadan-Diehl (2000). "Regulation of vasopressin V1b receptors in the anterior pituitary gland of the rat." Experimental physiology **85 Spec No**: 19S-26S.

Akhundov, R.A., A.A. Sultanov et al. (1993). "Psychoregulating role of nicotinamide". Biull Eksp Biol Med **115**(5):487-91.

Amir, R. E., I. B. Van den Veyver, et al. (1999). "Rett syndrome is caused by mutations in X-linked MECP2, encoding methyl-CpG-binding protein 2." Nature Genetics **23**(2): 185-188.

Anacker, C., A. Cattaneo, et al. (2013). "Role for the Kinase SGK1 in Stress, Depression, and Glucocorticoid Effects on Hippocampal Neurogenesis". Proceedings of the National Academy of Sciences **110** (21): 8708–13

Anderson, D.D., C.M. Quintero et al. (2011). "Identification of a de Novo Thymidylate Biosynthesis Pathway in Mammalian Mitochondria". Proceedings of the National Academy of Sciences **108** (37): 15163–68. doi:10.1073/pnas.1103623108.

Antequera, F. and A. Bird (1993). "Number of CpG islands and genes in human and mouse." Proceedings of the National Academy of Sciences of the United States of America **90**(24): 11995-11999.

Aran, D., G. Toperoff, et al. (2011). "Replication timing-related and gene body-specific methylation of active human genes." Human molecular genetics **20**(4): 670-680.

Araragi, N., B. Mlinar, et al. (2013). "Conservation of 5-HT1A receptor-mediated autoinhibition of serotonin (5-HT) neurons in mice with altered 5-HT homeostasis." Frontiers in Pharmacology **4**.

Arora, V., H. H. Cheung, et al. (2007). "Degradation of survivin by the X-linked inhibitor of apoptosis (XIAP)-XAF1 complex." The Journal of biological chemistry **282**(36): 26202-26209.

Arranz, B., K. Blennow, et al. (1997). "Serotonergic, noradrenergic, and dopaminergic measures in suicide brains." Biological Psychiatry **41**(10): 1000-1009.

Asberg, M. and L. Traskman (1981). "Studies of CSF 5-HIAA in depression and suicidal behaviour." Advances in experimental medicine and biology **133**: 739-752.

Aulchenko, Y.S., I.A. Hoppenbrouwer et al. (2008). "Genetic Variation in the KIF1B Locus Influences Susceptibility to Multiple Sclerosis". Nature Genetics **40** (12): 1402–3.

Ayalew, M., H. Le-Niculescu, et al. (2012). "Convergent functional genomics of schizophrenia: from comprehensive understanding to genetic risk prediction." Mol Psychiatry **17**(9): 887-905.

Baganz, N. L., R. E. Horton, et al. (2008). "Organic cation transporter 3: Keeping the brake on extracellular serotonin in serotonin-transporter-deficient mice." Proceedings of the National Academy of Sciences of the United States of America **105**(48): 18976-18981.

Balboa, M. A., J. Balsinde, et al. (1996). "Novel group V phospholipase A2 involved in arachidonic acid mobilization in murine P388D1 macrophages." J Biol Chem **271**(50): 32381-32384.

Ball, M. P., J. B. Li, et al. (2009). "Targeted and genome-scale strategies reveal gene-body methylation signatures in human cells." Nature biotechnology **27**(4): 361-368.

Bamm, V. V., M. De Avila, et al. (2011). "Structured functional domains of myelin basic protein: cross talk between actin polymerization and Ca(2+)-dependent calmodulin interaction." Biophys J **101**(5): 1248-1256.

Barker, D. J. (1997). "Maternal nutrition, fetal nutrition, and disease in later life." Nutrition **13**(9): 807-813.

Barros, V. G., M. Duhalde-Vega, et al. (2006). "Astrocyte-neuron vulnerability to prenatal stress in the adult rat brain." Journal of Neuroscience Research **83**(5): 787-800.
Barros, V. G., P. Rodriguez, et al. (2006). "Prenatal stress and early adoption effects on benzodiazepine receptors and anxiogenic behavior in the adult rat brain." Synapse **60**(8): 609-618.
Bartolomucci, A., V. Carola, et al. (2010). "Increased vulnerability to psychosocial stress in heterozygous serotonin transporter knockout mice." Disease Models & Mechanisms **3**: 459-470.
Behan, A. T., D. L. van den Hove, et al. (2011). "Evidence of female-specific glial deficits in the hippocampus in a mouse model of prenatal stress." European neuropsychopharmacology : the journal of the European College of Neuropsychopharmacology **21**(1): 71-79.
Belachew, S., R. Chittajallu, et al. (2003). "Postnatal NG2 proteoglycan-expressing progenitor cells are intrinsically multipotent and generate functional neurons." The Journal of cell biology **161**(1): 169-186.
Bengel, D., D. L. Murphy, et al. (1998). "Altered brain serotonin homeostasis and locomotor insensitivity to 3, 4-methylenedioxymethamphetamine ("Ecstasy") in serotonin transporter-deficient mice." Molecular pharmacology **53**: 649–655.
Berger, M., J. A. Gray, et al. (2009). "The expanded biology of serotonin." Annual review of medicine **60**: 355-366.
Bergles, D. E., R. Jabs, et al. (2010). "Neuron-glia synapses in the brain." Brain Research Reviews **63**(1-2): 130-137.
Bergles, D. E., J. D. Roberts, et al. (2000). "Glutamatergic synapses on oligodendrocyte precursor cells in the hippocampus." Nature **405**(6783): 187-191.
Beydoun, H. and A. F. Saftlas (2008). "Physical and mental health outcomes of prenatal maternal stress in human and animal studies: a review of recent evidence." Paediatric and perinatal epidemiology **22**(5): 438-466.
Bird, A. (2002). "DNA methylation patterns and epigenetic memory." Genes & Development **16**(1): 6-21.
Bird, A. P. (1980). "DNA methylation and the frequency of CpG in animal DNA." Nucleic Acids Research **8**(7): 1499-1504.
Blakely, R. D., L. J. De Felice, et al. (1994). "Molecular physiology of norepinephrine and serotonin transporters." The Journal of experimental biology **196**: 263-281.
Boggs, J. M., G. Rangaraj, et al. (2005). "Effect of arginine loss in myelin basic protein, as occurs in its deiminated charge isoform, on mediation of actin polymerization and actin binding to a lipid membrane in vitro." Biochemistry **44**(9): 3524-3534.
Bond, A. M., O. G. Bhalala, et al. (2012). "The dynamic role of bone morphogenetic proteins in neural stem cell fate and maturation." Developmental Neurobiology **72**: 1068-1084.
Borsini, F. and A. Meli (1988). "Is the forced swimming test a suitable model for revealing antidepressant activity?" Psychopharmacology **94**(2): 147-160.
Boyer, L.A., K. Plath et al. (2006). "Polycomb Complexes Repress Developmental Regulators in Murine Embryonic Stem Cells". Nature **441** (7091): 349–53.
Brenet, F., M. Moh, et al. (2011). "DNA methylation of the first exon is tightly linked to transcriptional silencing." PLoS ONE **6**(1): e14524.
Britsch, S., D. E. Goerich, et al. (2001). "The transcription factor Sox10 is a key regulator of peripheral glial development." Genes & Development **15**(1): 66-78.
Brown, G. L., M. H. Ebert, et al. (1982). "Aggression, suicide, and serotonin: relationships to CSF amine metabolites." The American journal of psychiatry **139**(6): 741-746.
Brown, R. W., R. Diaz, et al. (1996). "The ontogeny of 11 beta-hydroxysteroid dehydrogenase type 2 and mineralocorticoid receptor gene expression reveal intricate control of glucocorticoid action in development." Endocrinology **137**(2): 794-797.
Bruniquel, D. and R. H. Schwartz (2003). "Selective, stable demethylation of the interleukin-2 gene enhances transcription by an active process." Nature immunology **4**(3): 235-240.
Bryne, J. C., E. Valen, et al. (2008). "JASPAR, the open access database of transcription factor-binding profiles: new content and tools in the 2008 update." Nucleic Acids Res **36**(Database issue): D102-106.

Burlet, G., B. Fernette, et al. (2005). "Antenatal glucocorticoids blunt the functioning of the hypothalamic-pituitary-adrenal axis of neonates and disturb some behaviors in juveniles." Neuroscience **133**(1): 221-230.

Buss, C., E. P. Davis, et al. (2010). "High pregnancy anxiety during mid-gestation is associated with decreased gray matter density in 6-9-year-old children." Psychoneuroendocrinology **35**(1): 141-153.

Buzsaki, G. and A. Draguhn (2004). "Neuronal oscillations in cortical networks." Science **304**(5679): 1926-1929.

Cabrera, R. J., E. L. Rodriguez-Echandia, et al. (1999). "Effects of prenatal exposure to a mild chronic variable stress on body weight, preweaning mortality and rat behavior." Brazilian journal of medical and biological research = Revista brasileira de pesquisas medicas e biologicas / Sociedade Brasileira de Biofisica ... [et al.] **32**(10): 1229-1237.

Cadet, R., P. Pradier, et al. (1986). "Effects of prenatal maternal stress on the pituitary adrenocortical reactivity in guinea-pig pups." Journal of developmental physiology **8**(6): 467-475.

Candau, R., J. X. Zhou, et al. (1997). "Histone acetyltransferase activity and interaction with ADA2 are critical for GCN5 function in vivo." The EMBO journal **16**(3): 555-565.

Carola, V., G. Frazzetto, et al. (2008). "Identifying Molecular Substrates in a Mouse Model of the Serotonin Transporter × Environment Risk Factor for Anxiety and Depression." Biological Psychiatry **63**: 840-846.

Caronia, G., J. Wilcoxon, et al. (2010). "Bone morphogenetic protein signaling in the developing telencephalon controls formation of the hippocampal dentate gyrus and modifies fear-related behavior." The Journal of neuroscience : the official journal of the Society for Neuroscience **30**(18): 6291-6301.

Carroll, J. C., J. M. Boyce-Rustay, et al. (2007). "Effects of Mild Early Life Stress on Abnormal Emotion-related Behaviors in 5-HTT Knockout Mice." Behavior Genetics **37**: 214-222.

Caspi, A., K. Sugden, et al. (2003). "Influence of life stress on depression: moderation by a polymorphism in the 5-HTT gene." Science **301**(5631): 386-389.

Castets, F., T. Rakitina, et al. (2000). "Zinedin, SG2NA, and striatin are calmodulin-binding, WD repeat proteins principally expressed in the brain." The Journal of biological chemistry **275**(26): 19970-19977.

Chambers, J. S. and N. I. Perrone-Bizzozero (2004). "Altered myelination of the hippocampal formation in subjects with schizophrenia and bipolar disorder." Neurochem Res **29**(12): 2293-2302.

Chapman, R. H. and J. M. Stern (1979). "Failure of severe maternal stress or ACTH during pregnancy to affect emotionality of male rat offspring: implications of litter effects for prenatal studies." Developmental Psychobiology **12**(3): 255-267.

Chareyron, L. J., P. B. Lavenex, et al. (2012). "Postnatal development of the amygdala: a stereological study in rats." The Journal of Comparative Neurology **520**: 3745-3763.

Chatzittofis, A., P. Nordstrom, et al. (2013). "CSF 5-HIAA, cortisol and DHEAS levels in suicide attempters." European neuropsychopharmacology : the journal of the European College of Neuropsychopharmacology **23**(10): 1280-1287.

Chavez, A. E., C. Q. Chiu, et al. (2010). "TRPV1 activation by endogenous anandamide triggers postsynaptic long-term depression in dentate gyrus." Nature Neuroscience **13**(12): 1511-1518.

Chen, E. Y., C. M. Tan, et al. (2013). "Enrichr: interactive and collaborative HTML5 gene list enrichment analysis tool." BMC bioinformatics **14**: 128.

Cho, W. (2000). "Structure, function, and regulation of group V phospholipase A(2)." Biochim Biophys Acta **1488**(1-2): 48-58.

Choi, S., J. Ko, et al. (2006). "ARF6 and EFA6A regulate the development and maintenance of dendritic spines." J Neurosci **26**(18): 4811-4819.

Chouliaras, L., D.L.A. van den Hove et al. (2013). „Histone Deacetylase 2 in the Mouse Hippocampus: Attenuation of Age-Related Increase by Caloric Restriction". Current Alzheimer research **10** (8): 868–76.

Cintra, A., V. Solfrini, et al. (1993). "Prenatal development of glucocorticoid receptor gene expression and immunoreactivity in the rat brain and pituitary gland: a combined in

situ hybridization and immunocytochemical analysis." Neuroendocrinology **57**(6): 1133-1147.
Ciurciu, A., O. Komonyi, et al. (2006). "The Drosophila histone acetyltransferase Gcn5 and transcriptional adaptor Ada2a are involved in nucleosomal histone H4 acetylation." Mol Cell Biol **26**(24): 9413-9423.
Class, Q. A., K. M. Abel, et al. (2014). "Offspring psychopathology following preconception, prenatal and postnatal maternal bereavement stress." Psychological Medicine **44**(1): 71-84.
Coe, C. L., M. Kramer, et al. (2003). "Prenatal stress diminishes neurogenesis in the dentate gyrus of juvenile Rhesus monkeys." Biological Psychiatry **54**: 1025-1034.
Coe, C. L., M. Kramer, et al. (2002). "Prenatal stress diminishes the cytokine response of leukocytes to endotoxin stimulation in juvenile rhesus monkeys." The Journal of clinical endocrinology and metabolism **87**(2): 675-681.
Collier, D. A., G. Stober, et al. (1996). "A novel functional polymorphism within the promoter of the serotonin transporter gene: possible role in susceptibility to affective disorders." Molecular Psychiatry **1**(6): 453-460.
Coppen, A., A. J. Prange, Jr., et al. (1972). "Abnormalities of indoleamines in affective disorders." Archives of general psychiatry **26**(5): 474-478.
Copper, R. L., R. L. Goldenberg, et al. (1996). "The preterm prediction study: maternal stress is associated with spontaneous preterm birth at less than thirty-five weeks' gestation. National Institute of Child Health and Human Development Maternal-Fetal Medicine Units Network." American Journal of Obstetrics and Gynecology **175**(5): 1286-1292.
Cortellino, S., J. Xu, et al. (2011). "Thymine DNA glycosylase is essential for active DNA demethylation by linked deamination-base excision repair." Cell **146**(1): 67-79.
Costello, D. A., M. Claret et al. (2012). "Brain Deletion of Insulin Receptor Substrate 2 Disrupts Hippocampal Synaptic Plasticity and Metaplasticity". PLoS ONE **7** (2): e31124.
Costello, E. J., C. Worthman, et al. (2007). "Prediction from low birth weight to female adolescent depression: a test of competing hypotheses." Archives of general psychiatry **64**(3): 338-344.
Cox, B., A. K. Hadjantonakis, et al. (2000). "Cloning and expression throughout mouse development of mfat1, a homologue of the Drosophila tumour suppressor gene fat." Developmental dynamics : an official publication of the American Association of Anatomists **217**(3): 233-240.
Crider, K.S., T. P. Yang et al. (2012). "Folate and DNA Methylation: A Review of Molecular Mechanisms and the Evidence for Folate's Role". Advances in Nutrition: An International Review Journal **3** (1): 21–38.
Curhan, G. C., W. C. Willett, et al. (1996). "Birth weight and adult hypertension, diabetes mellitus, and obesity in US men." Circulation **94**(12): 3246-3250.
Dagliyan, O., E. A. Proctor, et al. (2011). "Structural and dynamic determinants of protein-peptide recognition." Structure **19**(12): 1837-1845.
Dallman, M. F., S. F. Akana, et al. (1994). "Corticosteroids and the control of function in the hypothalamo-pituitary-adrenal (HPA) axis." Annals of the New York Academy of Sciences **746**: 22-31; discussion 31-22, 64-27.
Daskalakis, N. P., R. C. Bagot, et al. (2013). "The three-hit concept of vulnerability and resilience: Toward understanding adaptation to early-life adversity outcome." Psychoneuroendocrinology **38**: 1858-1873.
Dauprat, P., G. Monin, et al. (1984). "The effects of psychosomatic stress at the end of pregnancy on maternal and fetal plasma cortisol levels and liver glycogen in guinea-pigs." Reproduction, nutrition, development **24**(1): 45-51.
de Weerth, C. and J. K. Buitelaar (2005). "Physiological stress reactivity in human pregnancy—a review." Neuroscience & Biobehavioral Reviews **29**: 295-312.
Delaney, K. A., M. M. Murph, et al. (2002). "Transfer of M2 muscarinic acetylcholine receptors to clathrin-derived early endosomes following clathrin-independent endocytosis." J Biol Chem **277**(36): 33439-33446.

Delgado, P. L., D. S. Charney, et al. (1990). "Serotonin function and the mechanism of antidepressant action. Reversal of antidepressant-induced remission by rapid depletion of plasma tryptophan." Archives of general psychiatry **47**(5): 411-418.

Diaz, R., R. W. Brown, et al. (1998). "Distinct ontogeny of glucocorticoid and mineralocorticoid receptor and 11beta-hydroxysteroid dehydrogenase types I and II mRNAs in the fetal rat brain suggest a complex control of glucocorticoid actions." The Journal of neuroscience : the official journal of the Society for Neuroscience **18**(7): 2570-2580.

Diers-Fenger, M., F. Kirchhoff, et al. (2001). "AN2/NG2 protein-expressing glial progenitor cells in the murine CNS: isolation, differentiation, and association with radial glia." Glia **34**(3): 213-228.

Doerflinger, N. H., W. B. Macklin, et al. (2003). "Inducible site-specific recombination in myelinating cells." Genesis **35**(1): 63-72.

Dogan, J., T. Schmidt, et al. (2012). "Fast association and slow transitions in the interaction between two intrinsically disordered protein domains." J Biol Chem **287**(41): 34316-34324.

Donahue, C. P., K. S. Kosik, et al. (2006). "Growth hormone is produced within the hippocampus where it responds to age, sex, and stress." Proceedings of the National Academy of Sciences of the United States of America **103**(15): 6031-6036.

Dorner, G. (1973). "[Possible significance of prenatal and-or perinatal nutrition for the pathogenesis of obesity]." Acta biologica et medica Germanica **30**(5): K19-22.

Dorner, G., H. Thoelke, et al. (1985). "High food supply in perinatal life appears to favour the development of insulin-treated diabetes mellitus (ITDM) in later life." Experimental and clinical endocrinology **85**(1): 1-6.

Dulac, C. (2010). "Brain function and chromatin plasticity." Nature **465**(7299): 728-735.

Dupouey, P., C. Jacque, et al. (1979). "Immunochemical studies of myelin basic protein in shiverer mouse devoid of major dense line of myelin." Neurosci Lett **12**(1): 113-118.

Eckhardt, F., J. Lewin, et al. (2006). "DNA methylation profiling of human chromosomes 6, 20 and 22." Nature Genetics **38**(12): 1378-1385.

Edgar, N. and E. Sibille (2012). "A putative functional role for oligodendrocytes in mood regulation." Translational Psychiatry **2**: e109.

Ehrlich, M., N. E. Hopkins, et al. (2003). "Satellite DNA hypomethylation in karyotyped Wilms tumors." Cancer genetics and cytogenetics **141**(2): 97-105.

Estanislau, C. and S. Morato (2005). "Prenatal stress produces more behavioral alterations than maternal separation in the elevated plus-maze and in the elevated T-maze." Behavioural Brain Research **163**(1): 70-77.

Fabre, V., C. Beaufour, et al. (2000). "Altered expression and functions of serotonin 5-HT1A and 5-HT1B receptors in knock-out mice lacking the 5-HT transporter." European Journal of Neuroscience **12**: 2299–2310.

Fan, G., K. Martinowich, et al. (2005). "DNA methylation controls the timing of astrogliogenesis through regulation of JAK-STAT signaling." Development **132**: 3345-3356.

Fan, L.-W., A. Bhatt, et al. (2014). "Exposure to serotonin adversely affects oligodendrocyte development and myelination in vitro." Journal of Neurochemistry: n/a-n/a.

Fattal, O., J. Link et al. (2007) "Psychiatric comorbidity in 36 adults with mitochondrial cytopathies." CNS Spectr. **12**(6):429-38.

Felix-Ortiz, A. C. and K. M. Tye (2014). "Amygdala inputs to the ventral hippocampus bidirectionally modulate social behavior." The Journal of neuroscience : the official journal of the Society for Neuroscience **34**(2): 586-595.

Feng, J., Y. Zhou, et al. (2010). "Dnmt1 and Dnmt3a maintain DNA methylation and regulate synaptic function in adult forebrain neurons." Nature Neuroscience **13**(4): 423-430.

Filion, G. J., S. Zhenilo, et al. (2006). "A family of human zinc finger proteins that bind methylated DNA and repress transcription." Molecular and cellular biology **26**(1): 169-181.

Fischer, A., F. Sananbenesi et al. (2010). "Targeting the Correct HDAC(s) to Treat Cognitive Disorders". Trends in Pharmacological Sciences **31** (12): 605–17.

Focking, M., R. Opstelten, et al. (2014). "Proteomic investigation of the hippocampus in prenatally stressed mice implicates changes in membrane trafficking, cytoskeletal, and metabolic function." Developmental Neuroscience **36**(5): 432-442.

Franklin, T. B., H. Russig, et al. (2010). "Epigenetic transmission of the impact of early stress across generations." Biological Psychiatry **68**(5): 408-415.
Fredrickson, B. L. (2001). "The role of positive emotions in positive psychology. The broaden-and-build theory of positive emotions." The American psychologist **56**(3): 218-226.
Frodl, T., P. Zill, et al. (2008). "Reduced hippocampal volumes associated with the long variant of the tri- and diallelic serotonin transporter polymorphism in major depression." American Journal of Medical Genetics Part B: Neuropsychiatric Genetics **147B**: 1003-1007.
Fuks, F., W. A. Burgers, et al. (2000). "DNA methyltransferase Dnmt1 associates with histone deacetylase activity." Nature Genetics **24**(1): 88-91.
Fuks, F., P. J. Hurd, et al. (2003). "The DNA methyltransferases associate with HP1 and the SUV39H1 histone methyltransferase." Nucleic Acids Research **31**(9): 2305-2312.
Fuks, F., P. J. Hurd, et al. (2003). "The methyl-CpG-binding protein MeCP2 links DNA methylation to histone methylation." The Journal of biological chemistry **278**(6): 4035-4040.
Galas, M. C., J. B. Helms, et al. (1997). "Regulated exocytosis in chromaffin cells. A potential role for a secretory granule-associated ARF6 protein." J Biol Chem **272**(5): 2788-2793.
Gale, C. R. and C. N. Martyn (2004). "Birth weight and later risk of depression in a national birth cohort." The British journal of psychiatry : the journal of mental science **184**: 28-33.
Ganguly, D., S. Otieno, et al. (2012). "Electrostatically accelerated coupled binding and folding of intrinsically disordered proteins." J Mol Biol **422**(5): 674-684.
Gartner, U., W. Hartig, et al. (2001). "Immunofluorescence and immunoelectron microscopic evidence for differences in myelination of GABAergic and cholinergic septohippocampal fibres." Int J Dev Neurosci **19**(3): 347-352.
Gaudet, F., J. G. Hodgson, et al. (2003). "Induction of tumors in mice by genomic hypomethylation." Science **300**(5618): 489-492.
Geiman, T. M., U. T. Sankpal, et al. (2004). "DNMT3B interacts with hSNF2H chromatin remodeling enzyme, HDACs 1 and 2, and components of the histone methylation system." Biochemical and biophysical research communications **318**(2): 544-555.
Gibson, H. E., J. G. Edwards, et al. (2008). "TRPV1 channels mediate long-term depression at synapses on hippocampal interneurons." Neuron **57**(5): 746-759.
Giedd, J. N., A. C. Vaituzis, et al. (1996). "Quantitative MRI of the temporal lobe, amygdala, and hippocampus in normal human development: ages 4-18 years." The Journal of Comparative Neurology **366**(2): 223-230.
Gitau, R., A. Cameron, et al. (1998). "Fetal exposure to maternal cortisol." Lancet **352**(9129): 707-708.
Globisch, D., M. Munzel, et al. (2010). "Tissue distribution of 5-hydroxymethylcytosine and search for active demethylation intermediates." PLoS ONE **5**(12): e15367.
Gluckman, P. D. and M. A. Hanson (2004). "Developmental origins of disease paradigm: a mechanistic and evolutionary perspective." Pediatric research **56**(3): 311-317.
Gobbi, G. (2005). "Serotonin firing activity as a marker for mood disorders: lessons from knockout mice." International review of neurobiology **65**: 249-272.
Goto, K., M. Numata, et al. (1994). "Expression of DNA methyltransferase gene in mature and immature neurons as well as proliferating cells in mice." Differentiation; research in biological diversity **56**(1-2): 39-44.
Gräff, J., D. Rei et al. (2012). „An Epigenetic Blockade of Cognitive Functions in the Neurodegenerating Brain". Nature **483** (7388): 222–26.
Grant, P. A., L. Duggan, et al. (1997). "Yeast Gcn5 functions in two multisubunit complexes to acetylate nucleosomal histones: characterization of an Ada complex and the SAGA (Spt/Ada) complex." Genes & Development **11**(13): 1640-1650.
Grueter, B. A., G. Brasnjo, et al. (2010). "Postsynaptic TRPV1 triggers cell type-specific long-term depression in the nucleus accumbens." Nature Neuroscience **13**(12): 1519-1525.
Guan, J.-S., S.J. Haggarty et al. (2009). "HDAC2 Negatively Regulates Memory Formation and Synaptic Plasticity". Nature **459** (7243): 55–60.
Gué, M., A. Bravard, et al. (2004). "Sex differences in learning deficits induced by prenatal stress in juvenile rats." Behavioural Brain Research **150**: 149-157.

Guintivano, J., M. J. Aryee, et al. (2013). "A cell epigenotype specific model for the correction of brain cellular heterogeneity bias and its application to age, brain region and major depression." Epigenetics : official journal of the DNA Methylation Society **8**(3): 290-302.
Gunnar, M. and K. Quevedo (2007). "The Neurobiology of Stress and Development." Annual Review of Psychology **58**: 145-173.
Guo, F., Y. Maeda, et al. (2010). "Pyramidal neurons are generated from oligodendroglial progenitor cells in adult piriform cortex." The Journal of neuroscience : the official journal of the Society for Neuroscience **30**(36): 12036-12049.
Guo, J. U., D. K. Ma, et al. (2011). "Neuronal activity modifies the DNA methylation landscape in the adult brain." Nature Neuroscience **14**: 1345-1351.
Guo, J. U., Y. Su, et al. (2013). "Distribution, recognition and regulation of non-CpG methylation in the adult mammalian brain." Nature Neuroscience **17**: 215-222.
Guo, J. U., Y. Su, et al. (2011). "Hydroxylation of 5-methylcytosine by TET1 promotes active DNA demethylation in the adult brain." Cell **145**(3): 423-434.
Gutknecht, L., C. Kriegebaum, et al. (2009). "Spatio-temporal expression of tryptophan hydroxylase isoforms in murine and human brain: convergent data from Tph2 knockout mice." European neuropsychopharmacology : the journal of the European College of Neuropsychopharmacology **19**(4): 266-282.
Gutteling, B. M., C. de Weerth, et al. (2005). "Prenatal stress and children's cortisol reaction to the first day of school." Psychoneuroendocrinology **30**(6): 541-549.
Gutteling, B. M., C. de Weerth, et al. (2006). "Does maternal prenatal stress adversely affect the child's learning and memory at age six?" Journal of abnormal child psychology **34**(6): 789-798.
Hakimizadeh, E., S. Oryan, et al. (2012). "Endocannabinoid System and TRPV1 Receptors in the Dorsal Hippocampus of the Rats Modulate Anxiety-like Behaviors." Iranian Journal of Basic Medical Sciences **15**: 795-802.
Hamilton, N., S. Vayro, et al. (2010). "Axons and astrocytes release ATP and glutamate to evoke calcium signals in NG2-glia." Glia **58**: 66-79.
Harauz, G. and J. M. Boggs (2013). "Myelin management by the 18.5-kDa and 21.5-kDa classic myelin basic protein isoforms." Journal of Neurochemistry **125**(3): 334-361.
Harauz, G. and J. M. Boggs (2013). "Myelin management by the 18.5-kDa and 21.5-kDa classic myelin basic protein isoforms." J Neurochem **125**(3): 334-361.
Harauz, G., N. Ishiyama, et al. (2004). "Myelin basic protein-diverse conformational states of an intrinsically unstructured protein and its roles in myelin assembly and multiple sclerosis." Micron **35**(7): 503-542.
Harris, A. and J. Seckl (2011). "Glucocorticoids, prenatal stress and the programming of disease." Hormones and Behavior **59**: 279-289.
Hashimoto, H., J. R. Horton, et al. (2008). "The SRA domain of UHRF1 flips 5-methylcytosine out of the DNA helix." Nature **455**(7214): 826-829.
Hashimoto, H., J. R. Horton, et al. (2009). "UHRF1, a modular multi-domain protein, regulates replication-coupled crosstalk between DNA methylation and histone modifications." Epigenetics : official journal of the DNA Methylation Society **4**(1): 8-14.
Hayashi, A., M. Nagaoka, et al. (1998). "Maternal stress induces synaptic loss and developmental disabilities of offspring." International journal of developmental neuroscience : the official journal of the International Society for Developmental Neuroscience **16**(3-4): 209-216.
He, Y. F., B. Z. Li, et al. (2011). "Tet-mediated formation of 5-carboxylcytosine and its excision by TDG in mammalian DNA." Science **333**(6047): 1303-1307.
Hedegaard, M., T. B. Henriksen, et al. (1993). "Psychological distress in pregnancy and preterm delivery." BMJ **307**(6898): 234-239.
Heiming, R. S., F. Jansen, et al. (2009). "Living in a dangerous world: the shaping of behavioral profile by early environment and 5-HTT genotype." Frontiers in Behavioral Neuroscience **3**: 26.
Hellman, A. and A. Chess (2007). "Gene body-specific methylation on the active X chromosome." Science **315**(5815): 1141-1143.

Hercher, C., V. Chopra, et al. (2014). "Evidence for morphological alterations in prefrontal white matter glia in schizophrenia and bipolar disorder." Journal of psychiatry & neuroscience : JPN **39**(6): 376-385.
Hernandez-Deviez, D. J., J. E. Casanova, et al. (2002). "Regulation of dendritic development by the ARF exchange factor ARNO." Nat Neurosci **5**(7): 623-624.
Hernandez-Deviez, D. J., M. G. Roth, et al. (2004). "ARNO and ARF6 regulate axonal elongation and branching through downstream activation of phosphatidylinositol 4-phosphate 5-kinase alpha." Mol Biol Cell **15**(1): 111-120.
Heron, J., T. G. O'Connor, et al. (2004). "The course of anxiety and depression through pregnancy and the postpartum in a community sample." Journal of Affective Disorders **80**(1): 65-73.
Hill, C. M., I. R. Bates, et al. (2002). "Effects of the osmolyte trimethylamine-N-oxide on conformation, self-association, and two-dimensional crystallization of myelin basic protein." J Struct Biol **139**(1): 13-26.
Hintsch, G., A. Zurlinden, et al. (2002). "The calsyntenins--a family of postsynaptic membrane proteins with distinct neuronal expression patterns." Molecular and cellular neurosciences **21**(3): 393-409.
Hirabayashi, Y., N. Suzki et al. (2009). "Polycomb Limits the Neurogenic Competence of Neural Precursor Cells to Promote Astrogenic Fate Transition". Neuron **63** (5): 600–613.
Hobel, C. J., C. Dunkel-Schetter, et al. (1999). "Maternal plasma corticotropin-releasing hormone associated with stress at 20 weeks' gestation in pregnancies ending in preterm delivery." American Journal of Obstetrics and Gynecology **180**(1 Pt 3): S257-263.
Holmes, A., D. L. Murphy, et al. (2002). "Reduced aggression in mice lacking the serotonin transporter." Psychopharmacology **161**(2): 160-167.
Holmes, A., R. J. Yang, et al. (2003). "Mice lacking the serotonin transporter exhibit 5-HT(1A) receptor-mediated abnormalities in tests for anxiety-like behavior." Neuropsychopharmacology : official publication of the American College of Neuropsychopharmacology **28**(12): 2077-2088.
Homberg, J. R. and K.-P. Lesch (2011). "Looking on the Bright Side of Serotonin Transporter Gene Variation." Biological Psychiatry **69**: 513-519.
Homberg, J. R. and D. L. van den Hove (2012). "The serotonin transporter gene and functional and pathological adaptation to environmental variation across the life span." Progress in Neurobiology **99**(2): 117-127.
Hornig, J., F. Fröb, et al. (2013). "The Transcription Factors Sox10 and Myrf Define an Essential Regulatory Network Module in Differentiating Oligodendrocytes." PLoS Genet **9**: e1003907.
Hu, F., S. Yang, et al. (2012). "Moderate extracellular acidification inhibits capsaicin-induced cell death through regulating calcium mobilization, NF-kappaB translocation and ROS production in synoviocytes." Biochemical and biophysical research communications **424**(1): 196-200.
Hu, J.-L., B. O. Zhou, et al. (2009). "The N-terminus of histone H3 is required for de novo DNA methylation in chromatin." Proceedings of the National Academy of Sciences of the United States of America **106**: 22187-22192.
Hu, X. Z., R. H. Lipsky, et al. (2006). "Serotonin transporter promoter gain-of-function genotypes are linked to obsessive-compulsive disorder." American Journal of Human Genetics **78**(5): 815-826.
Huang, D. W., B. T. Sherman, et al. (2007). "The DAVID Gene Functional Classification Tool: a novel biological module-centric algorithm to functionally analyze large gene lists." Genome biology **8**(9): R183.
Huang, D. W., B. T. Sherman, et al. (2007). "DAVID Bioinformatics Resources: expanded annotation database and novel algorithms to better extract biology from large gene lists." Nucleic Acids Research **35**(Web Server issue): W169-175.
Huang, W., N. Zhao, et al. (2014). "Novel NG2-CreERT2 knock-in mice demonstrate heterogeneous differentiation potential of NG2 glia during development." Glia **62**: 896-913.

Huizink, A. C., E. J. Mulder, et al. (2004). "Prenatal stress and risk for psychopathology: specific effects or induction of general susceptibility?" Psychological Bulletin **130**(1): 115-142.
Huttunen, M. O. and P. Niskanen (1978). "Prenatal loss of father and psychiatric disorders." Archives of general psychiatry **35**(4): 429-431.
Igosheva, N., O. Klimova, et al. (2004). "Prenatal stress alters cardiovascular responses in adult rats." The Journal of Physiology **557**(Pt 1): 273-285.
Illingworth, R., A. Kerr, et al. (2008). "A novel CpG island set identifies tissue-specific methylation at developmental gene loci." PLoS biology **6**(1): e22.
Illingworth, R. S., U. Gruenewald-Schneider, et al. (2010). "Orphan CpG islands identify numerous conserved promoters in the mammalian genome." PLoS genetics **6**(9): e1001134.
Inano, K., I. Suetake, et al. (2000). "Maintenance-type DNA methyltransferase is highly expressed in post-mitotic neurons and localized in the cytoplasmic compartment." Journal of Biochemistry **128**(2): 315-321.
Irizarry, R. A., C. Ladd-Acosta, et al. (2009). "The human colon cancer methylome shows similar hypo- and hypermethylation at conserved tissue-specific CpG island shores." Nature Genetics **41**(2): 178-186.
Irvin, D. K., S. D. Zurcher, et al. (2001). "Expression patterns of Notch1, Notch2, and Notch3 suggest multiple functional roles for the Notch-DSL signaling system during brain development." The Journal of Comparative Neurology **436**(2): 167-181.
Ito, S., A. C. D'Alessio, et al. (2010). "Role of Tet proteins in 5mC to 5hmC conversion, ES-cell self-renewal and inner cell mass specification." Nature **466**(7310): 1129-1133.
Iwamoto, K., M. Bundo, et al. (2011). "Neurons show distinctive DNA methylation profile and higher interindividual variations compared with non-neurons." Genome Research **21**(5): 688-696.
Jabs, R., T. Pivneva, et al. (2005). "Synaptic transmission onto hippocampal glial cells with hGFAP promoter activity." J Cell Sci **118**(Pt 16): 3791-3803.
Jakob, S. (2012). Molecular mechanisms of early-life stress in 5-Htt deficient mice:

Gene x environment interactions and epigenetic programming Ph.D., Wuerzburg.
Jakob, S., K. G. Schraut, et al. (2014). "Differential effects of prenatal stress in female 5-HTT-deficient mice: towards molecular mechanisms of resilience." Developmental Neuroscience **36**(6): 454-464.
Jansen, F., R. S. Heiming, et al. (2010). "Modulation of behavioural profile and stress response by 5-HTT genotype and social experience in adulthood." Behavioural Brain Research **207**: 21-29.
Jasinska, A. J. and S. C. Perkins (2009). "Impact of the Tri-Allelic Serotonin Transporter Polymorphism on the White-Matter Tract Connecting the Amygdala and the Prefrontal Cortex." The Journal of Neuroscience **29**: 10461-10462.
Jenkins, S. M. and V. Bennett (2001). "Ankyrin-G coordinates assembly of the spectrin-based membrane skeleton, voltage-gated sodium channels, and L1 CAMs at Purkinje neuron initial segments." J Cell Biol **155**(5): 739-746.
Jiao, S. and Z. Li (2011). "Nonapoptotic function of BAD and BAX in long-term depression of synaptic transmission." Neuron **70**(4): 758-772.
Jonas, E. (2006). "BCL-xL regulates synaptic plasticity." Molecular interventions **6**(4): 208-222.
Jones, K. L., R. M. Smith, et al. (2010). "Combined effect of maternal serotonin transporter genotype and prenatal stress in modulating offspring social interaction in mice." International Journal of Developmental Neuroscience **28**: 529-536.
Jones, P. A. (2012). "Functions of DNA methylation: islands, start sites, gene bodies and beyond." Nature Reviews Genetics **13**: 484-492.
Jones, P. L., G. J. Veenstra, et al. (1998). "Methylated DNA and MeCP2 recruit histone deacetylase to repress transcription." Nature Genetics **19**(2): 187-191.
Kann, O. and R. Kovács (2007). "Mitochondria and neuronal activity." American Journal of Physiology - Cell Physiology **292**: C641-C657.
Kasckow, J. W., J. J. Mulchahey, et al. (2004). "Effects of the vanilloid agonist olvanil and antagonist capsazepine on rat behaviors." Progress in Neuro-Psychopharmacology and Biological Psychiatry **28**: 291-295.

Keirstead, H. S., J. M. Levine, et al. (1998). "Response of the oligodendrocyte progenitor cell population (defined by NG2 labelling) to demyelination of the adult spinal cord." Glia **22**(2): 161-170.
Kenneth, N. S., B. A. Ramsbottom, et al. (2007). "TRRAP and GCN5 are used by c-Myc to activate RNA polymerase III transcription." Proceedings of the National Academy of Sciences of the United States of America **104**(38): 14917-14922.
Kikusui, T., Y. Kiyokawa, et al. (2007). "Deprivation of mother-pup interaction by early weaning alters myelin formation in male, but not female, ICR mice." Brain Res **1133**(1): 115-122.
Kilgore, M., C.A. Miller et al. (2010). "Inhibitors of Class 1 Histone Deacetylases Reverse Contextual Memory Deficits in a Mouse Model of Alzheimer's Disease". Neuropsychopharmacology **35** (4): 870–80.
Kim, D.-K., T. J. Tolliver, et al. (2005). "Altered serotonin synthesis, turnover and dynamic regulation in multiple brain regions of mice lacking the serotonin transporter." Neuropharmacology **49**: 798-810.
Kim, D. K., T. J. Tolliver, et al. (2005). "Altered serotonin synthesis, turnover and dynamic regulation in multiple brain regions of mice lacking the serotonin transporter." Neuropharmacology **49**(6): 798-810.
Kimura, H. and K. Shiota (2003). "Methyl-CpG-binding protein, MeCP2, is a target molecule for maintenance DNA methyltransferase, Dnmt1." The Journal of biological chemistry **278**(7): 4806-4812.
Kitraki, E., M. N. Alexis, et al. (1996). "Glucocorticoid receptor gene expression in the embryonic rat brain." Neuroendocrinology **63**(4): 305-317.
Kloke, V., R. S. Heiming, et al. (2013). "Unexpected effects of early-life adversity and social enrichment on the anxiety profile of mice varying in serotonin transporter genotype." Behavioural Brain Research **247**: 248-258.
Kloke, V., R. S. Heiming, et al. (2013). "Unexpected effects of early-life adversity and social enrichment on the anxiety profile of mice varying in serotonin transporter genotype." Behavioural Brain Research **247**: 248-258.
Kodama, Y., T. Kikusui, et al. (2008). "Effects of early weaning on anxiety and prefrontal cortical and hippocampal myelination in male and female Wistar rats." Dev Psychobiol **50**(4): 332-342.
Koldso, H., A. B. Christiansen, et al. (2013). "Comparative modeling of the human monoamine transporters: similarities in substrate binding." ACS chemical neuroscience **4**(2): 295-309.
Kondo, T. and M. Raff (2000). "Oligodendrocyte precursor cells reprogrammed to become multipotential CNS stem cells." Science **289**(5485): 1754-1757.
Kordeli, E., S. Lambert, et al. (1995). "AnkyrinG. A new ankyrin gene with neural-specific isoforms localized at the axonal initial segment and node of Ranvier." J Biol Chem **270**(5): 2352-2359.
Koressaar, T. and M. Remm (2007). "Enhancements and modifications of primer design program Primer3." Bioinformatics **23**(10): 1289-1291.
Kozlenkov, A., P. Roussos, et al. (2014). "Differences in DNA methylation between human neuronal and glial cells are concentrated in enhancers and non-CpG sites." Nucleic Acids Research **42**(1): 109-127.
Kraszpulski, M., P. A. Dickerson, et al. (2006). "Prenatal stress affects the developmental trajectory of the rat amygdala." Stress **9**: 85-95.
Krauss, M., M. Kinuta, et al. (2003). "ARF6 stimulates clathrin/AP-2 recruitment to synaptic membranes by activating phosphatidylinositol phosphate kinase type Igamma." J Cell Biol **162**(1): 113-124.
Kriaucionis, S. and N. Heintz (2009). "The nuclear DNA base 5-hydroxymethylcytosine is present in Purkinje neurons and the brain." Science **324**(5929): 929-930.
Kriegebaum, C., L. Gutknecht, et al. (2010). "[Serotonin now: Part 1. Neurobiology and developmental genetics]." Fortschritte der Neurologie-Psychiatrie **78**(6): 319-331.
Kriegebaum, C., L. Gutknecht, et al. (2010). "[Serotonin now: Part 2. Behavioral genetics and psychopathology]." Fortschritte der Neurologie-Psychiatrie **78**(6): 332-342.
Krishnan, V., M. H. Han, et al. (2007). "Molecular adaptations underlying susceptibility and resistance to social defeat in brain reward regions." Cell **131**(2): 391-404.

Kuan, P. F., H. Chun, et al. (2008). "CMARRT: a tool for the analysis of ChIP-chip data from tiling arrays by incorporating the correlation structure." Pacific Symposium on Biocomputing. Pacific Symposium on Biocomputing: 515-526.
Kukley, M., E. Capetillo-Zarate, et al. (2007). "Vesicular glutamate release from axons in white matter." Nature Neuroscience **10**(3): 311-320.
Laloux, C., J. Mairesse, et al. (2012). "Anxiety-like behaviour and associated neurochemical and endocrinological alterations in male pups exposed to prenatal stress." Psychoneuroendocrinology **37**: 1646-1658.
Landry, C. F., J. Ellison, et al. (1997). "Golli-MBP proteins mark the earliest stages of fiber extension and terminal arboration in the mouse peripheral nervous system." J Neurosci Res **50**(2): 265-271.
Landry, C. F., J. A. Ellison, et al. (1996). "Myelin basic protein gene expression in neurons: developmental and regional changes in protein targeting within neuronal nuclei, cell bodies, and processes." J Neurosci **16**(8): 2452-2462.
Landry, C. F., T. M. Pribyl, et al. (1998). "Embryonic expression of the myelin basic protein gene: identification of a promoter region that targets transgene expression to pioneer neurons." J Neurosci **18**(18): 7315-7327.
Lanfumey, L., C. Mannoury La Cour, et al. (2000). "5-HT-HPA interactions in two models of transgenic mice relevant to major depression." Neurochemical Research **25**(9-10): 1199-1206.
Lang, F., C. Böhmer et al. (2006). "(Patho)physiological significance of the serum- and glucocorticoid-inducible kinase isoforms". Physiological review. **86**(4):1151-78.
Lang, S. E., S. B. McMahon, et al. (2001). "E2F transcriptional activation requires TRRAP and GCN5 cofactors." The Journal of biological chemistry **276**(35): 32627-32634.
Le-Niculescu, H., Y. Balaraman, et al. (2007). "Towards understanding the schizophrenia code: an expanded convergent functional genomics approach." Am J Med Genet B Neuropsychiatr Genet **144B**(2): 129-158.
Le-Niculescu, H., S. M. Kurian, et al. (2009). "Identifying blood biomarkers for mood disorders using convergent functional genomics." Mol Psychiatry **14**(2): 156-174.
Le Bras, B., E. Chatzopoulou, et al. (2005). "Oligodendrocyte development in the embryonic brain: the contribution of the plp lineage." The International journal of developmental biology **49**(2-3): 209-220.
Lee, H. J., J. Wu, et al. (2013). "SOX2 expression is upregulated in adult spinal cord after contusion injury in both oligodendrocyte lineage and ependymal cells." Journal of Neuroscience Research **91**(2): 196-210.
Lee, T.I., R.G. Jenner et al. (2006). "Control of Developmental Regulators by Polycomb in Human Embryonic Stem Cells". Cell 125 (2): 301–13. doi:10.1016/j.cell.2006.02.043.
Lemaire, V., M. Koehl, et al. (2000). "Prenatal stress produces learning deficits associated with an inhibition of neurogenesis in the hippocampus." Proceedings of the National Academy of Sciences **97**: 11032-11037.
Lesage, J., F. Del-Favero, et al. (2004). "Prenatal stress induces intrauterine growth restriction and programmes glucose intolerance and feeding behaviour disturbances in the aged rat." The Journal of Endocrinology **181**: 291-296.
Lesch, K. P., D. Bengel, et al. (1996). "Association of anxiety-related traits with a polymorphism in the serotonin transporter gene regulatory region." Science **274**(5292): 1527-1531.
Lester, D. (1995). "The concentration of neurotransmitter metabolites in the cerebrospinal fluid of suicidal individuals: a meta-analysis." Pharmacopsychiatry **28**(2): 45-50.
Levine, S. (2001). "Primary social relationships influence the development of the hypothalamic--pituitary--adrenal axis in the rat." Physiology & Behavior **73**(3): 255-260.
Levy, C., J. m. Brooks, et al. (2014). "Cell-specific and developmental expression of lectican-cleaving proteases in mouse hippocampus and neocortex." Journal of Comparative Neurology: n/a-n/a.
Lewejohann, L., V. Kloke, et al. (2010). "Social status and day-to-day behaviour of male serotonin transporter knockout mice." Behavioural Brain Research **211**: 220-228.
Li, J., J. Olsen, et al. (2010). "Attention-deficit/hyperactivity disorder in the offspring following prenatal maternal bereavement: a nationwide follow-up study in Denmark." European child & adolescent psychiatry **19**(10): 747-753.

Li, Q., C. Wichems, et al. (2000). "Reduction in the density and expression, but not G-protein coupling, of serotonin receptors (5-HT1A) in 5-HT transporter knock-out mice: gender and brain region differences." The Journal of Neuroscience **20**: 7888–7895.
Li, Z., J. Jo, et al. (2010). "Caspase-3 activation via mitochondria is required for long-term depression and AMPA receptor internalization." Cell **141**(5): 859-871.
Light, K. J., A. L. Miller, et al. (2007). "FAT and bipolar affective disorder." Molecular Psychiatry **12**(10): 899-900.
Lin, S. C. and D. E. Bergles (2004). "Synaptic signaling between GABAergic interneurons and oligodendrocyte precursor cells in the hippocampus." Nature Neuroscience **7**(1): 24-32.
Lin, S. C., J. H. Huck, et al. (2005). "Climbing fiber innervation of NG2-expressing glia in the mammalian cerebellum." Neuron **46**(5): 773-785.
Liston, P., W. G. Fong, et al. (2001). "Identification of XAF1 as an antagonist of XIAP anti-Caspase activity." Nature cell biology **3**(2): 128-133.
Liu, H. and V. I. Shubayev (2011). "Matrix metalloproteinase-9 controls proliferation of NG2+ progenitor cells immediately after spinal cord injury." Experimental Neurology **231**(2): 236-246.
Llorente, E., M. L. Brito, et al. (2002). "Effect of prenatal stress on the hormonal response to acute and chronic stress and on immune parameters in the offspring." Journal of physiology and biochemistry **58**(3): 143-149.
Lock, L. F., N. Takagi, et al. (1987). "Methylation of the Hprt gene on the inactive X occurs after chromosome inactivation." Cell **48**(1): 39-46.
Loomans, E. M., O. van der Stelt, et al. (2011). "Antenatal maternal anxiety is associated with problem behaviour at age five." Early human development **87**(8): 565-570.
Lu, Z., L. Ku, et al. (2005). "Developmental abnormalities of myelin basic protein expression in fyn knock-out brain reveal a role of Fyn in posttranscriptional regulation." J Biol Chem **280**(1): 389-395.
Lubin, F. D., T. L. Roth, et al. (2008). "Epigenetic Regulation of bdnf Gene Transcription in the Consolidation of Fear Memory." The Journal of Neuroscience **28**: 10576-10586.
Lupien, S. J., B. S. McEwen, et al. (2009). "Effects of stress throughout the lifespan on the brain, behaviour and cognition." Nature reviews. Neuroscience **10**(6): 434-445.
Lyko, F., S. Foret, et al. (2010). "The honey bee epigenomes: differential methylation of brain DNA in queens and workers." PLoS biology **8**(11): e1000506.
Lyons, D.A., S.G. Naylor et al. (2009). „Kif1b is essential for mRNA localization in oligodendrocytes and development of myelinated axons". Nature genetics **41** (7): 854–58.
Lyons-Ruth, K., R. Wolfe, et al. (2000). "Depression and the parenting of young children: making the case for early preventive mental health services." Harvard review of psychiatry **8**(3): 148-153.
Malaspina, D., C. Corcoran, et al. (2008). "Acute maternal stress in pregnancy and schizophrenia in offspring: a cohort prospective study." BMC psychiatry **8**: 71.
Manji, H., T. Kato et al. (2012). "Impaired mitochondrial function in psychiatric disorders". Nature Reviews Neuroscience **5**:293-307.
Marathe, H. G., G. Mehta, et al. (2013). "SWI/SNF Enzymes Promote SOX10- Mediated Activation of Myelin Gene Expression." PLoS One **8**(7): e69037.
Marcus, S. M. (2009). "Depression during pregnancy: rates, risks and consequences--Motherisk Update 2008." The Canadian journal of clinical pharmacology = Journal canadien de pharmacologie clinique **16**(1): e15-22.
Marion-Poll, L., E. Montalban, et al. (2014). "Fluorescence-activated sorting of fixed nuclei: a general method for studying nuclei from specific cell populations that preserves post-translational modifications." European Journal of Neuroscience **39**: 1234-1244.
Marsch, R., E. Foeller, et al. (2007). "Reduced Anxiety, Conditioned Fear, and Hippocampal Long-Term Potentiation in Transient Receptor Potential Vanilloid Type 1 Receptor-Deficient Mice." The Journal of Neuroscience **27**: 832-839.
Martinez-Cerdeno, V., J. M. Lemen, et al. (2012). "N-Myc and GCN5 regulate significantly overlapping transcriptional programs in neural stem cells." PLoS One **7**(6): e39456.

Martinowich, K., D. Hattori, et al. (2003). "DNA Methylation-Related Chromatin Remodeling in Activity-Dependent Bdnf Gene Regulation." Science **302**: 890-893.

Massaad, C.A., and Klann, E. (2011). "Reactive oxygen species in the regulation of synaptic plasticity and memory." Antioxid Redox Signal. **14**(10):2013-54

Mathews, T. A., D. E. Fedele, et al. (2004). "Gene dose-dependent alterations in extraneuronal serotonin but not dopamine in mice with reduced serotonin transporter expression." Journal of Neuroscience Methods **140**: 169-181.

Matsusue, Y., N. Horii-Hayashi, et al. (2014). "Distribution of corticosteroid receptors in mature oligodendrocytes and oligodendrocyte progenitors of the adult mouse brain." The journal of histochemistry and cytochemistry : official journal of the Histochemistry Society **62**(3): 211-226.

Matthews, P. R., S. L. Eastwood, et al. (2012). "Reduced myelin basic protein and actin-related gene expression in visual cortex in schizophrenia." PLoS One **7**(6): e38211.

Matthias, K., F. Kirchhoff, et al. (2003). "Segregated expression of AMPA-type glutamate receptors and glutamate transporters defines distinct astrocyte populations in the mouse hippocampus." The Journal of neuroscience : the official journal of the Society for Neuroscience **23**(5): 1750-1758.

Maunakea, A. K., R. P. Nagarajan, et al. (2010). "Conserved role of intragenic DNA methylation in regulating alternative promoters." Nature **466**(7303): 253-257.

Mayer, W., A. Niveleau, et al. (2000). "Demethylation of the zygotic paternal genome." Nature **403**(6769): 501-502.

McEown, K. and D. Treit (2013). "Alpha2 GABAA receptor sub-units in the ventral hippocampus and alpha5 GABAA receptor sub-units in the dorsal hippocampus mediate anxiety and fear memory." Neuroscience **252**: 169-177.

McEwen, B. S. (2000). "Allostasis and allostatic load: implications for neuropsychopharmacology." Neuropsychopharmacology : official publication of the American College of Neuropsychopharmacology **22**(2): 108-124.

McGowan, P. O., A. Sasaki, et al. (2009). "Epigenetic regulation of the glucocorticoid receptor in human brain associates with childhood abuse." Nature Neuroscience **12**(3): 342-348.

McLean, M., A. Bisits, et al. (1995). "A placental clock controlling the length of human pregnancy." Nature Medicine **1**: 460-463.

McLean, M. and R. Smith (1999). "Corticotropin-releasing Hormone in Human Pregnancy and Parturition." Trends in endocrinology and metabolism: TEM **10**(5): 174-178.

McMahon, S. B., M. A. Wood, et al. (2000). "The essential cofactor TRRAP recruits the histone acetyltransferase hGCN5 to c-Myc." Molecular and cellular biology **20**(2): 556-562.

Meier, I. D., C. Bernreuther, et al. (2010). "Short DNA sequences inserted for gene targeting can accidentally interfere with off-target gene expression." The FASEB Journal **24**: 1714-1724.

Meijer, A. (1985). "Child psychiatric sequelae of maternal war stress." Acta psychiatrica Scandinavica **72**(6): 505-511.

Meissner, A., T. S. Mikkelsen, et al. (2008). "Genome-scale DNA methylation maps of pluripotent and differentiated cells." Nature **454**: 766-770.

Melo, T.Q., A.M. D'unhao et al. (2013). "Rotenone-Dependent Changes of Anterograde Motor Protein Expression and Mitochondrial Mobility in Brain Areas Related to Neurodegenerative Diseases". Cellular and Molecular Neurobiology **33** (3): 327–35.

Meltzer, H. Y. (1990). "Role of serotonin in depression." Annals of the New York Academy of Sciences **600**: 486-499; discussion 499-500.

Merens, W. and W. van der Does (2007). "Low-dose tryptophan depletion." Biological Psychiatry **62**(5): 542-543; author reply 543-544.

Miller, P., D. Coope, et al. (2012). "Quantitative evaluation of white matter tract DTI parameter changes in gliomas using nonlinear registration." NeuroImage **60**(4): 2309-2315.

Miyakawa, T., T. Yagi, et al. (1996). "Susceptibility to drug-induced seizures of Fyn tyrosine kinase-deficient mice." Neuroreport **7**(15-17): 2723-2726.

Miyata, S., Y. Koyama, et al. (2011). "Plasma corticosterone activates SGK1 and induces morphological changes in oligodendrocytes in corpus callosum." PLoS ONE **6**(5): e19859.

Miyazaki, H., M. Yamazaki, et al. (2005). "The small GTPase ADP-ribosylation factor 6 negatively regulates dendritic spine formation." FEBS Lett **579**(30): 6834-6838.
Möhler, H., P. Polc et al. (1979). "Nicotinamide Is a Brain Constituent with Benzodiazepine-like Actions". Nature **278** (5704): 563–65.
Moore, L. D., T. Le, et al. (2013). "DNA methylation and its basic function." Neuropsychopharmacology **38**(1): 23-38.
Morley-Fletcher, S., M. Darnaudery, et al. (2003). "Prenatal stress in rats predicts immobility behavior in the forced swim test. Effects of a chronic treatment with tianeptine." Brain research **989**(2): 246-251.
Morava, E., and Kozics, T. (2013). "Mitochondria and the economy of stress (mal)adaptation". Neuroscience and Biobehavioral Reviews **37**:668–680
Mosebach, J., G. Keilhoff, et al. (2013). "Increased nuclear Olig1-expression in the pregenual anterior cingulate white matter of patients with major depression: a regenerative attempt to compensate oligodendrocyte loss?" Journal of Psychiatric Research **47**(8): 1069-1079.
Moskal, J. R., R. A. Kroes, et al. (2006). "Distinct patterns of gene expression in the left and right hippocampal formation of developing rats." Hippocampus **16**(8): 629-634.
Mueller, B. R. and T. L. Bale (2006). "Impact of prenatal stress on long term body weight is dependent on timing and maternal sensitivity." Physiology & Behavior **88**(4-5): 605-614.
Mueller, B. R. and T. L. Bale (2008). "Sex-Specific Programming of Offspring Emotionality after Stress Early in Pregnancy." The Journal of Neuroscience **28**: 9055-9065.
Muhammad, A., C. Carroll, et al. (2012). "Stress during development alters dendritic morphology in the nucleus accumbens and prefrontal cortex." Neuroscience **216**: 103-109.
Murmu, M. S., S. Salomon, et al. (2006). "Changes of spine density and dendritic complexity in the prefrontal cortex in offspring of mothers exposed to stress during pregnancy." European Journal of Neuroscience **24**: 1477-1487.
Murphy, D. L. and K. P. Lesch (2008). "Targeting the murine serotonin transporter: insights into human neurobiology." Nature reviews. Neuroscience **9**(2): 85-96.
Nagatomo, T., M. Rashid, et al. (2004). "Functions of 5-HT2A receptor and its antagonists in the cardiovascular system." Pharmacology & therapeutics **104**(1): 59-81.
Nakamura, N., Y. Miyake et al. (2002). "KIF1Bbeta2, Capable of Interacting with CHP, Is Localized to Synaptic Vesicles". Journal of Biochemistry **132** (3): 483–91.
Nan, X., H. H. Ng, et al. (1998). "Transcriptional repression by the methyl-CpG-binding protein MeCP2 involves a histone deacetylase complex." Nature **393**(6683): 386-389.
Nangaku, M., R. Sato-Yoshitake et al. (1994). "KIF1B, a Novel Microtubule plus End-Directed Monomeric Motor Protein for Transport of Mitochondria". Cell **79** (7): 1209–20.
Nikolova, Y. S., K. C. Koenen, et al. (2014). "Beyond genotype: serotonin transporter epigenetic modification predicts human brain function." Nature Neuroscience **17**(9): 1153-1155.
Nilsson, P. M., P. Nyberg, et al. (2001). "Increased susceptibility to stress at a psychological assessment of stress tolerance is associated with impaired fetal growth." International Journal of Epidemiology **30**: 75-80.
Nogami, H., R. Hoshino, et al. (2007). "Region-specific expression and hormonal regulation of the first exon variants of rat prolactin receptor mRNA in rat brain and anterior pituitary gland." Journal of neuroendocrinology **19**(8): 583-593.
Noorlander, C. w., P. n. e. De Graan, et al. (2006). "Ontogeny of hippocampal corticosteroid receptors: Effects of antenatal glucocorticoids in human and mouse." The Journal of Comparative Neurology **499**: 924-932.
O'Connor, T. G., Y. Ben-Shlomo, et al. (2005). "Prenatal anxiety predicts individual differences in cortisol in pre-adolescent children." Biological Psychiatry **58**(3): 211-217.
O'Connor, T. G., K. Bergman, et al. (2013). "Prenatal cortisol exposure predicts infant cortisol response to acute stress." Developmental Psychobiology **55**(2): 145-155.
O'Donnell, K. J., A. Bugge Jensen, et al. (2012). "Maternal prenatal anxiety and downregulation of placental 11β-HSD2." Psychoneuroendocrinology **37**: 818-826.

Ohtsubo, M., S. Yasunaga et al. (2008). "Polycomb-Group Complex 1 Acts as an E3 Ubiquitin Ligase for Geminin to Sustain Hematopoietic Stem Cell Activity". Proceedings of the National Academy of Sciences of the United States of America **105** (30): 10396–401.

Okimoto, D. K., A. Blaus, et al. (2002). "Differential expression of c-fos and tyrosine hydroxylase mRNA in the adrenal gland of the infant rat: evidence for an adrenal hyporesponsive period." Endocrinology **143**(5): 1717-1725.

Ong, A. D., C. S. Bergeman, et al. (2006). "Psychological resilience, positive emotions, and successful adaptation to stress in later life." Journal of personality and social psychology **91**(4): 730-749.

Ooi, S. K., C. Qiu, et al. (2007). "DNMT3L connects unmethylated lysine 4 of histone H3 to de novo methylation of DNA." Nature **448**(7154): 714-717.

Oyarzo, C., P. Bertoglia, et al. (2012). "Adverse perinatal outcomes after the February 27th 2010 Chilean earthquake." The journal of maternal-fetal & neonatal medicine : the official journal of the European Association of Perinatal Medicine, the Federation of Asia and Oceania Perinatal Societies, the International Society of Perinatal Obstetricians **25**(10): 1868-1873.

Ozgen, H., N. Kahya, et al. (2014). "Regulation of cell proliferation by nucleocytoplasmic dynamics of postnatal and embryonic exon-II-containing MBP isoforms." Biochimica et biophysica acta **1843**(3): 517-530.

Pacheco, J., C. G. Beevers, et al. (2009). "Frontal-Limbic White Matter Pathway Associations with the Serotonin Transporter Gene Promoter Region (5-HTTLPR) Polymorphism." The Journal of Neuroscience **29**: 6229-6233.

Paez, P. M., D. Fulton, et al. (2011). "Modulation of canonical transient receptor potential channel 1 in the proliferation of oligodendrocyte precursor cells by the golli products of the myelin basic protein gene." J Neurosci **31**(10): 3625-3637.

Paez, P. M., D. J. Fulton, et al. (2009). "Regulation of store-operated and voltage-operated Ca2+ channels in the proliferation and death of oligodendrocyte precursor cells by golli proteins." ASN Neuro **1**(1).

Paez, P. M., D. J. Fulton, et al. (2009). "Golli myelin basic proteins regulate oligodendroglial progenitor cell migration through voltage-gated Ca2+ influx." J Neurosci **29**(20): 6663-6676.

Pajevic, S., P. J. Basser, et al. (2014). "Role of myelin plasticity in oscillations and synchrony of neuronal activity." Neuroscience **276**: 135-147.

Pan, Z., T. Kao, et al. (2006). "A common ankyrin-G-based mechanism retains KCNQ and NaV channels at electrically active domains of the axon." J Neurosci **26**(10): 2599-2613.

Parlapani, E., A. Schmitt, et al. (2009). "Association between myelin basic protein expression and left entorhinal cortex pre-alpha cell layer disorganization in schizophrenia." Brain research **1301**: 126-134.

Patin, V., A. Vincent, et al. (2004). "Does prenatal stress affect the motoric development of rat pups?" Brain research. Developmental brain research **149**(2): 85-92.

Pedraza, L., J. K. Huang, et al. (2001). "Organizing principles of the axoglial apparatus." Neuron **30**(2): 335-344.

Peleg, S., F. Sananbenesi et al. (2010). "Altered Histone Acetylation Is Associated with Age-Dependent Memory Impairment in Mice". Science (New York, N.Y.) **328** (5979): 753–56.

Petraglia, F., P. Florio, et al. (1996). "Human placenta and fetal membranes express human urocortin mRNA and peptide." The Journal of clinical endocrinology and metabolism **81**(10): 3807-3810.

Privat, A., C. Jacque, et al. (1979). "Absence of the major dense line in myelin of the mutant mouse "shiverer"." Neurosci Lett **12**(1): 107-112.

Prokhortchouk, A., B. Hendrich, et al. (2001). "The p120 catenin partner Kaiso is a DNA methylation-dependent transcriptional repressor." Genes & Development **15**(13): 1613-1618.

Qi, L., J.-L. Cao et al. (2013). "The Dynamics of Polycomb Group Proteins in Early Embryonic Nervous System in Mouse and Human". International Journal of Developmental Neuroscience: **31** (7): 487–95.

Rakyan, V. K., T. Hildmann, et al. (2004). "DNA methylation profiling of the human major histocompatibility complex: a pilot study for the human epigenome project." PLoS biology **2**(12): e405.
Ravary, A., A. Muzerelle, et al. (2001). "Abnormal trafficking and subcellular localization of an N-terminally truncated serotonin transporter protein." European Journal of Neuroscience **13**: 1349–1362.
Razin, S. V., A. A. Gavrilov, et al. (2013). "Communication of genome regulatory elements in a folded chromosome." FEBS Letters **587**: 1840-1847.
Readhead, C. and L. Hood (1990). "The dysmyelinating mouse mutations shiverer (shi) and myelin deficient (shimld)." Behav Genet **20**(2): 213-234.
Reilly, S.M., P. Bhargava et al. (2010). "Nuclear Receptor Corepressor SMRT Regulates Mitochondrial Oxidative Metabolism and Mediates Aging-Related Metabolic Deterioration". Cell Metabolism **12** (6): 643–53.
Reul, J. M. and E. R. de Kloet (1985). "Two receptor systems for corticosterone in rat brain: microdistribution and differential occupation." Endocrinology **117**(6): 2505-2511.
Reynolds, R., M. Dawson, et al. (2002). "The response of NG2-expressing oligodendrocyte progenitors to demyelination in MOG-EAE and MS." Journal of neurocytology **31**(6-7): 523-536.
Reynolds, R. M., G. H. Jacobsen, et al. (2013). "What is the evidence in humans that DNA methylation changes link events in utero and later life disease?" Clinical Endocrinology **78**: 814-822.
Ricobaraza, A., M. Cuadrado-Tejedor et al. (2009). "Phenylbutyrate Ameliorates Cognitive Deficit and Reduces Tau Pathology in an Alzheimer's Disease Mouse Model". Neuropsychopharmacology **34** (7): 1721–32.
Ricobaraza, A., M. Cuadrado-Tejedor et al. (2012). "Phenylbutyrate Rescues Dendritic Spine Loss Associated with Memory Deficits in a Mouse Model of Alzheimer Disease". Hippocampus **22** (5): 1040–50.
Rivers, L. E., K. M. Young, et al. (2008). "PDGFRA/NG2 glia generate myelinating oligodendrocytes and piriform projection neurons in adult mice." Nature Neuroscience **11**: 1392-1401.
Roseboom, T., S. de Rooij, et al. (2006). "The Dutch famine and its long-term consequences for adult health." Early human development **82**(8): 485-491.
Rosenfeld, P., Y. A. Gutierrez, et al. (1991). "Maternal regulation of the adrenocortical response in preweanling rats." Physiology & Behavior **50**(4): 661-671.
Rothgiesser, K.M., S. Erener et al. (2010). "SIRT2 Regulates NF-κB Dependent Gene Expression through Deacetylation of p65 Lys310". Journal of Cell Science **123** (Pt 24): 4251–58.
Rubertsson, C., J. Hellstrom, et al. (2014). "Anxiety in early pregnancy: prevalence and contributing factors." Archives of women's mental health **17**(3): 221-228.
Rudnick, G. (2011). "Cytoplasmic permeation pathway of neurotransmitter transporters." Biochemistry **50**(35): 7462-7475.
Rueckert, E. H., D. Barker, et al. (2013). "Cis-acting regulation of brain-specific ANK3 gene expression by a genetic variant associated with bipolar disorder." Mol Psychiatry **18**(8): 922-929.
Ruijter, J. M., C. Ramakers, et al. (2009). "Amplification efficiency: linking baseline and bias in the analysis of quantitative PCR data." Nucleic Acids Research **37**(6): e45.
Russell, J. C., H. Whiting, et al. (2008). "Nuclear translocation of X-linked inhibitor of apoptosis (XIAP) determines cell fate after hypoxia ischemia in neonatal brain." Journal of Neurochemistry **106**(3): 1357-1370.
Sakagami, H., H. Suzuki, et al. (2006). "Distinct spatiotemporal expression of EFA6D, a guanine nucleotide exchange factor for ARF6, among the EFA6 family in mouse brain." Brain Res **1093**(1): 1-11.
Sakry, D., K. Karram, et al. (2011). "Synapses between NG2 glia and neurons." Journal of Anatomy **219**: 2-7.
Salami, M., C. Itami, et al. (2003). "Change of conduction velocity by regional myelination yields constant latency irrespective of distance between thalamus and cortex." Proceedings of the National Academy of Sciences of the United States of America **100**(10): 6174-6179.

Salat, D. H., D. S. Tuch, et al. (2005). "Age-related changes in prefrontal white matter measured by diffusion tensor imaging." Annals of the New York Academy of Sciences **1064**: 37-49.

Sapolsky, R. M. and M. J. Meaney (1986). "Maturation of the adrenocortical stress response: neuroendocrine control mechanisms and the stress hyporesponsive period." Brain research **396**(1): 64-76.

Sarnico, I., A. Lanzillotta et al. (2009). "NF-kappaB Dimers in the Regulation of Neuronal Survival". International Review of Neurobiology **85**: 351–62.

Sarraf, S. A. and I. Stancheva (2004). "Methyl-CpG binding protein MBD1 couples histone H3 methylation at lysine 9 by SETDB1 to DNA replication and chromatin assembly." Molecular cell **15**(4): 595-605.

Savaskan, N. E., M. Plaschke, et al. (1999). "Myelin does not influence the choice behaviour of entorhinal axons but strongly inhibits their outgrowth length in vitro." The European journal of neuroscience **11**(1): 316-326.

Saxonov, S., P. Berg, et al. (2006). "A genome-wide analysis of CpG dinucleotides in the human genome distinguishes two distinct classes of promoters." Proceedings of the National Academy of Sciences of the United States of America **103**(5): 1412-1417.

Schapiro, S. (1962). "Pituitary ACTH and compensatory adrenal hypertrophy in stress-non-responsive infant rats." Endocrinology **71**: 986-989.

Schaumburg, C., B. A. O'Hara, et al. (2008). "Human Embryonic Stem Cell-Derived Oligodendrocyte Progenitor Cells Express the Serotonin Receptor and Are Susceptible to JC Virus Infection." Journal of Virology **82**: 8896-8899.

Schildkraut, J. J. and S. S. Kety (1967). "Biogenic amines and emotion." Science **156**(3771): 21-37.

Schmitt, A., R. Mössner, et al. (2003). "Organic cation transporter capable of transporting serotonin is up-regulated in serotonin transporter-deficient mice." Journal of neuroscience research **71**: 701–709.

Schneiderman, N., G. Ironson, et al. (2005). "Stress and health: psychological, behavioral, and biological determinants." Annual review of clinical psychology **1**: 607-628.

Schraut, K. G., S. B. Jakob, et al. (2014). "Prenatal stress-induced programming of genome-wide promoter DNA methylation in 5-HTT-deficient mice." Translational Psychiatry **4**: e473.

Schulze, T. G., S. D. Detera-Wadleigh, et al. (2009). "Two variants in Ankyrin 3 (ANK3) are independent genetic risk factors for bipolar disorder." Mol Psychiatry **14**(5): 487-491.

Schuurmans, C. and D. M. Kurrasch (2013). "Neurodevelopmental consequences of maternal distress: what do we really know?" Clinical Genetics **83**(2): 108-117.

Schwarze, C. E., A. Mobascher, et al. (2013). "Prenatal adversity: a risk factor in borderline personality disorder?" Psychological Medicine **43**(6): 1279-1291.

Secoli, S. R. and N. A. Teixeira (1998). "Chronic prenatal stress affects development and behavioral depression in rats." Stress (Amsterdam, Netherlands) **2**: 273-280.

Shepherd, J. K., S. S. Grewal, et al. (1994). "Behavioural and pharmacological characterisation of the elevated "zero-maze" as an animal model of anxiety." Psychopharmacology **116**(1): 56-64.

Shinohara, H., M. A. Balboa, et al. (1999). "Regulation of delayed prostaglandin production in activated P388D1 macrophages by group IV cytosolic and group V secretory phospholipase A2s." J Biol Chem **274**(18): 12263-12268.

Shukla, S., E. Kavak, et al. (2011). "CTCF-promoted RNA polymerase II pausing links DNA methylation to splicing." Nature **479**(7371): 74-79.

Sibille, E., Y. Wang, et al. (2009). "A molecular signature of depression in the amygdala." The American journal of psychiatry **166**(9): 1011-1024.

Sik, A., P. van Nieuwehuyzen, et al. (2003). "Performance of different mouse strains in an object recognition task." Behavioural Brain Research **147**(1-2): 49-54.

Simpson, K. L., K. J. Weaver, et al. (2011). "Perinatal antidepressant exposure alters cortical network function in rodents." Proceedings of the National Academy of Sciences **108**: 18465-18470.

Smith, E. N., C. S. Bloss, et al. (2009). "Genome-wide association study of bipolar disorder in European American and African American individuals." Mol Psychiatry **14**(8): 755-763.

Smith, G. S., L. Homchaudhuri, et al. (2012). "Classic 18.5- and 21.5-kDa myelin basic protein isoforms associate with cytoskeletal and SH3-domain proteins in the immortalized N19-oligodendroglial cell line stimulated by phorbol ester and IGF-1." Neurochem Res **37**(6): 1277-1295.

Smith, G. S., P. M. Paez, et al. (2011). "Classical 18.5-and 21.5-kDa isoforms of myelin basic protein inhibit calcium influx into oligodendroglial cells, in contrast to golli isoforms." J Neurosci Res **89**(4): 467-480.

Smith, G. S., B. Samborska, et al. (2013). "Nucleus-localized 21.5-kDa myelin basic protein promotes oligodendrocyte proliferation and enhances neurite outgrowth in coculture, unlike the plasma membrane-associated 18.5-kDa isoform." J Neurosci Res **91**(3): 349-362.

Snook, L., L. A. Paulson, et al. (2005). "Diffusion tensor imaging of neurodevelopment in children and young adults." NeuroImage **26**(4): 1164-1173.

Southwick, S. M., M. Vythilingam, et al. (2005). "The psychobiology of depression and resilience to stress: implications for prevention and treatment." Annual review of clinical psychology **1**: 255-291.

Speirs, H. J., Seckl, et al. (2004). "Ontogeny of glucocorticoid receptor and 11beta-hydroxysteroid dehydrogenase type-1 gene expression identifies potential critical periods of glucocorticoid susceptibility during development." Journal of Endocrinology **181**: 105-116.

Spivakov, M., and A. G. Fisher. 2007. "Epigenetic Signatures of Stem-Cell Identity". Nature Reviews. Genetics **8** (4): 263–71.

Stallcup, W. B. and L. Beasley (1987). "Bipotential glial precursor cells of the optic nerve express the NG2 proteoglycan." The Journal of neuroscience : the official journal of the Society for Neuroscience **7**(9): 2737-2744.

Stanley, M., J. J. Mann, et al. (1986). "Serotonin and serotonergic receptors in suicide." Annals of the New York Academy of Sciences **487**: 122-127.

Stefanski, V., C. Raabe, et al. (2005). "Pregnancy and social stress in female rats: influences on blood leukocytes and corticosterone concentrations." Journal of neuroimmunology **162**(1-2): 81-88.

Stilling, R. M., R. Ronicke, et al. (2014). "K-Lysine acetyltransferase 2a regulates a hippocampal gene expression network linked to memory formation." The EMBO journal **33**(17): 1912-1927.

Stolt, C. C., P. Lommes, et al. (2004). "Transcription factors Sox8 and Sox10 perform non-equivalent roles during oligodendrocyte development despite functional redundancy." Development **131**(10): 2349-2358.

Stolt, C. C., S. Rehberg, et al. (2002). "Terminal differentiation of myelin-forming oligodendrocytes depends on the transcription factor Sox10." Genes Dev **16**(2): 165-170.

Stone, E. A. and J. F. Ayroles (2009). "Modulated modularity clustering as an exploratory tool for functional genomic inference." PLoS genetics **5**(5): e1000479.

Stott, D. H. (1973). "Follow-up study from birth of the effects of prenatal stresses." Developmental medicine and child neurology **15**(6): 770-787.

Sun, G. Y., P. B. Shelat, et al. (2010). "Phospholipases A2 and inflammatory responses in the central nervous system." Neuromolecular Med **12**(2): 133-148.

Sypecka, J., A. Sarnowska, et al. (2013). "Differentiation of glia-committed NG2 cells: the role of factors released from hippocampus and spinal cord." Acta Neurobiologiae Experimentalis **73**(1): 116-129.

Szuchet, S., J. A. Nielsen, et al. (2011). "The genetic signature of perineuronal oligodendrocytes reveals their unique phenotype." European Journal of Neuroscience **34**: 1906-1922.

Tahiliani, M., K. P. Koh, et al. (2009). "Conversion of 5-methylcytosine to 5-hydroxymethylcytosine in mammalian DNA by MLL partner TET1." Science **324**(5929): 930-935.

Teixeira, J. M., N. M. Fisk, et al. (1999). "Association between maternal anxiety in pregnancy and increased uterine artery resistance index: cohort based study." BMJ **318**(7177): 153-157.

Teter, B., I. Rozovsky, et al. (1996). "Methylation of the glial fibrillary acidic protein gene shows novel biphasic changes during brain development." Glia **17**(3): 195-205.
Tomassy, G. S., D. R. Berger, et al. (2014). "Distinct profiles of myelin distribution along single axons of pyramidal neurons in the neocortex." Science **344**(6181): 319-324.
Torche, F. (2011). "The effect of maternal stress on birth outcomes: exploiting a natural experiment." Demography **48**(4): 1473-1491.
Torres, G. E., R. R. Gainetdinov, et al. (2003). "Plasma membrane monoamine transporters: structure, regulation and function." Nature reviews. Neuroscience **4**(1): 13-25.
Trent, N. L. and J. L. Menard (2010). "The ventral hippocampus and the lateral septum work in tandem to regulate rats' open-arm exploration in the elevated plus-maze." Physiology & Behavior **101**(1): 141-152.
Tsankova, N., W. Renthal, et al. (2007). "Epigenetic regulation in psychiatric disorders." Nature reviews. Neuroscience **8**(5): 355-367.
Tugade, M. M. and B. L. Fredrickson (2004). "Resilient individuals use positive emotions to bounce back from negative emotional experiences." Journal of personality and social psychology **86**(2): 320-333.
Untergasser, A., I. Cutcutache, et al. (2012). "Primer3--new capabilities and interfaces." Nucleic Acids Research **40**(15): e115.
Vale, W., J. Spiess, et al. (1981). "Characterization of a 41-residue ovine hypothalamic peptide that stimulates secretion of corticotropin and beta-endorphin." Science **213**(4514): 1394-1397.
Valinluck, V., H. H. Tsai, et al. (2004). "Oxidative damage to methyl-CpG sequences inhibits the binding of the methyl-CpG binding domain (MBD) of methyl-CpG binding protein 2 (MeCP2)." Nucleic Acids Research **32**(14): 4100-4108.
Van den Bergh, B. R. and A. Marcoen (2004). "High antenatal maternal anxiety is related to ADHD symptoms, externalizing problems, and anxiety in 8- and 9-year-olds." Child development **75**(4): 1085-1097.
Van den Bergh, B. R., M. Mennes, et al. (2005). "High antenatal maternal anxiety is related to impulsivity during performance on cognitive tasks in 14- and 15-year-olds." Neuroscience and biobehavioral reviews **29**(2): 259-269.
Van den Bergh, B. R. H., B. Van Calster, et al. (2007). "Antenatal Maternal Anxiety is Related to HPA-Axis Dysregulation and Self-Reported Depressive Symptoms in Adolescence: A Prospective Study on the Fetal Origins of Depressed Mood." Neuropsychopharmacology **33**: 536-545.
Van den Hove, D., S. B. Jakob, et al. (2011). "Differential Effects of Prenatal Stress in 5-Htt Deficient Mice: Towards Molecular Mechanisms of Gene × Environment Interactions." PLoS ONE **6**: e22715.
van den Hove, D. L., G. Kenis, et al. (2010). "Maternal stress-induced reduction in birth weight as a marker for adult affective state." Frontiers in bioscience **2**: 43-46.
Van den Hove, D. L. A., H. W. M. Steinbusch, et al. (2006). "Prenatal stress and neonatal rat brain development." Neuroscience **137**: 145-155.
van Donkelaar, E. L., A. Blokland, et al. (2010). "Acute tryptophan depletion in C57BL/6 mice does not induce central serotonin reduction or affective behavioural changes." Neurochemistry International **56**(1): 21-34.
van Os, J. and J. P. Selten (1998). "Prenatal exposure to maternal stress and subsequent schizophrenia. The May 1940 invasion of The Netherlands." The British journal of psychiatry : the journal of mental science **172**: 324-326.
Vincent, M. Y. and L. Jacobson (2014). "Glucocorticoid receptor deletion from the dorsal raphe nucleus of mice reduces dysphoria-like behavior and impairs hypothalamic-pituitary-adrenocortical axis feedback inhibition." The European journal of neuroscience **39**(10): 1671-1681.
Viola, H., C. B. Marta, et al. (2001). "Anxiolytic-like behavior in rats is induced by the neonatal intracranial injection of apotransferrin." J Neurosci Res **63**(2): 196-199.
Vostrikov, V. and N. Uranova (2011). "Age-related increase in the number of oligodendrocytes is dysregulated in schizophrenia and mood disorders." Schizophrenia research and treatment **2011**: 174689.

Vostrikov, V. M., N. A. Uranova, et al. (2007). "Deficit of perineuronal oligodendrocytes in the prefrontal cortex in schizophrenia and mood disorders." Schizophrenia Research **94**: 273-280.
Wadhwa, P. D., C. Dunkel-Schetter, et al. (1996). "Prenatal psychosocial factors and the neuroendocrine axis in human pregnancy." Psychosomatic medicine **58**(5): 432-446.
Wadhwa, P. D., T. J. Garite, et al. (2004). "Placental corticotropin-releasing hormone (CRH), spontaneous preterm birth, and fetal growth restriction: A prospective investigation." American Journal of Obstetrics and Gynecology **191**: 1063-1069.
Walker, J. J., F. Spiga, et al. (2012). "The origin of glucocorticoid hormone oscillations." PLoS biology **10**(6): e1001341.
Wang, J., H. He, et al. (2006). "HSF1 down-regulates XAF1 through transcriptional regulation." The Journal of biological chemistry **281**(5): 2451-2459.
Wankerl, M., R. Miller, et al. (2014). "Effects of genetic and early environmental risk factors for depression on serotonin transporter expression and methylation profiles." Translational Psychiatry **4**: e402.
Watanabe, M., Y. Toyama, et al. (2002). "Differentiation of proliferated NG2-positive glial progenitor cells in a remyelinating lesion." Journal of Neuroscience Research **69**(6): 826-836.
Watson, J. B., S. A. Mednick, et al. (1999). "Prenatal teratogens and the development of adult mental illness." Development and psychopathology **11**(3): 457-466.
Weaver, I. C., A. C. D'Alessio, et al. (2007). "The transcription factor nerve growth factor-inducible protein a mediates epigenetic programming: altering epigenetic marks by immediate-early genes." The Journal of neuroscience : the official journal of the Society for Neuroscience **27**(7): 1756-1768.
Weber, M., I. Hellmann, et al. (2007). "Distribution, silencing potential and evolutionary impact of promoter DNA methylation in the human genome." Nat Genet **39**(4): 457-466.
Weinstock, M. (2005). "The potential influence of maternal stress hormones on development and mental health of the offspring." Brain, Behavior, and Immunity **19**: 296-308.
Weinstock, M. (2008). "The long-term behavioural consequences of prenatal stress." Neuroscience and biobehavioral reviews **32**(6): 1073-1086.
Wellman, C. L., A. Izquierdo, et al. (2007). "Impaired stress-coping and fear extinction and abnormal corticolimbic morphology in serotonin transporter knock-out mice." The Journal of neuroscience : the official journal of the Society for Neuroscience **27**(3): 684-691.
Wen, L., X. Lie, et. Al. (2014). "Whole-genome analysis of 5-hydroxymethylcytosine and 5-methylcytosine at base resolution in the human brain." Genome Biology. **15**(3):R49
White, P. C., T. Mune, et al. (1997). "11 beta-Hydroxysteroid dehydrogenase and the syndrome of apparent mineralocorticoid excess." Endocrine reviews **18**(1): 135-156.
Whitnall, M. H. (1989). "Stress selectively activates the vasopressin-containing subset of corticotropin-releasing hormone neurons." Neuroendocrinology **50**(6): 702-707.
Wiggins, J. L., J. K. Bedoyan, et al. (2014). "Age-related effect of serotonin transporter genotype on amygdala and prefrontal cortex function in adolescence." Human brain mapping **35**: 646-658.
Wiles, N. J., T. J. Peters, et al. (2005). "Birth weight and psychological distress at age 45-51 years: results from the Aberdeen Children of the 1950s cohort study." The British journal of psychiatry : the journal of mental science **187**: 21-28.
Williamson, A. V., J. R. Mellor, et al. (1998). "Properties of GABA(A) receptors in cultured rat oligodendrocyte progenitor cells." Neuropharmacology **37**(7): 859-873.
Winsper, C., D. Wolke, et al. (2015). "Prospective associations between prenatal adversities and borderline personality disorder at 11-12 years." Psychological Medicine **45**(5): 1025-1037.
Wolf, S. F., D. J. Jolly, et al. (1984). "Methylation of the hypoxanthine phosphoribosyltransferase locus on the human X chromosome: implications for X-chromosome inactivation." Proceedings of the National Academy of Sciences of the United States of America **81**(9): 2806-2810.
Xie, W., C. L. Barr, et al. (2012). "Base-resolution analyses of sequence and parent-of-origin dependent DNA methylation in the mouse genome." Cell **148**(4): 816-831.

Xiong, F. and L. Zhang (2013). "Role of the hypothalamic-pituitary-adrenal axis in developmental programming of health and disease." Frontiers in Neuroendocrinology **34**(1): 27-46.

Xu, J., B. Yang, et al. (2013). "Effects of duration and timing of prenatal stress on hippocampal myelination and synaptophysin expression." Brain research **1527**: 57-66.

Xu, W., D. G. Edmondson, et al. (2000). "Loss of Gcn5l2 leads to increased apoptosis and mesodermal defects during mouse development." Nat Genet **26**(2): 229-232.

Xydous, M., A. Prombona et al. 2014. "The role of H3K4me3 and H3K9/14ac in the induction by dexamethasone of Per1 and Sgk1, two glucococorticoid early response genes that mediate the effects of acute stress in mammals". Biochimica et Biophysica Acta (BBA) - Gene Regulatory Mechanisms **1839** (9): 866–72.

Young, Kaylene M., K. Psachoulia, et al. (2013). "Oligodendrocyte Dynamics in the Healthy Adult CNS: Evidence for Myelin Remodeling." Neuron **77**: 873-885.

Young, S. N., S. E. Smith, et al. (1985). "Tryptophan depletion causes a rapid lowering of mood in normal males." Psychopharmacology **87**(2): 173-177.

Yu, W., Z. Qiu, et al. (2011). "PAK1IP1, a ribosomal stress-induced nucleolar protein, regulates cell proliferation via the p53-MDM2 loop." Nucleic Acids Research **39**(6): 2234-2248.

Zacher, B., P. F. Kuan, et al. (2010). "Starr: Simple Tiling ARRay analysis of Affymetrix ChIP-chip data." BMC bioinformatics **11**: 194.

Zagron, G. and M. Weinstock (2006). "Maternal adrenal hormone secretion mediates behavioural alterations induced by prenatal stress in male and female rats." Behavioural Brain Research **175**(2): 323-328.

Zaucker, A., S. Mercurio, et al. (2013). "notch3 is essential for oligodendrocyte development and vascular integrity in zebrafish." Disease Models & Mechanisms **6**: 1246-1259.

Zhang, W. N., T. Bast, et al. (2014). "Temporary inhibition of dorsal or ventral hippocampus by muscimol: distinct effects on measures of innate anxiety on the elevated plus maze, but similar disruption of contextual fear conditioning." Behavioural Brain Research **262**: 47-56.

Zhang, Y., R. Jurkowska, et al. (2010). "Chromatin methylation activity of Dnmt3a and Dnmt3a/3L is guided by interaction of the ADD domain with the histone H3 tail." Nucleic Acids Research **38**(13): 4246-4253.

Zhao, C., J. Takita et al. (2001). "Charcot-Marie-Tooth Disease Type 2A Caused by Mutation in a Microtubule Motor KIF1Bβ". Cell **105** (5): 587–97.

Zhou, F. C., J. H. Tao-Cheng, et al. (1998). "Serotonin transporters are located on the axons beyond the synaptic junctions: anatomical and functional evidence." Brain research **805**(1-2): 241-254.

Zhu, L. J., C. Gazin, et al. (2010). "ChIPpeakAnno: a Bioconductor package to annotate ChIP-seq and ChIP-chip data." BMC bioinformatics **11**: 237.

Zhu, X., D. E. Bergles, et al. (2008). "NG2 cells generate both oligodendrocytes and gray matter astrocytes." Development **135**(1): 145-157.

Zhu, X., R. A. Hill, et al. (2011). "Age-dependent fate and lineage restriction of single NG2 cells." Development **138**(4): 745-753.

Zhu, X., R. A. Hill, et al. (2008). "NG2 cells generate oligodendrocytes and gray matter astrocytes in the spinal cord." Neuron glia biology **4**(1): 19-26.

Ziskin, J. L., A. Nishiyama, et al. (2007). "Vesicular release of glutamate from unmyelinated axons in white matter." Nature Neuroscience **10**(3): 321-330.

4.3. List of figures

4.4. List of tables

4.5. Curriculum vitae

4.6. Publications

- **Schraut KG**, Jakob SB, Weidner MT, Schmitt AG, Scholz CJ, Strekalova T, El Hajj N, Eijssen LM, Domschke K, Reif A, Haaf T, Ortega G, Steinbusch HW, Lesch KP, Van den Hove DL. Prenatal stress-induced programming of genome-wide promoter DNA methylation in 5-HTT-deficient mice. Transl Psychiatry. 2014 Oct 21;4:e473. doi: 10.1038/tp.2014.107.

- Jakob S, **Schraut KG**, Schmitt AG, Scholz CJ, Ortega G, Steinbusch HW, Lesch KP, van den Hove DL. Differential effects of prenatal stress in female 5-Htt-deficient mice: towards molecular mechanisms of resilience. Dev Neurosci. 2014;36(6):454-64. doi: 10.1159/000363695. Epub 2014 Sep 4.

- Van den Hove DL, Jakob SB, **Schraut KG**, Kenis G, Schmitt AG, Kneitz S, Scholz CJ, Wiescholleck V, Ortega G, Prickaerts J, Steinbusch H, Lesch KP. Differential effects of prenatal stress in 5-Htt deficient mice: towards molecular mechanisms of gene × environment interactions. PLoS One. 2011;6(8):e22715. doi: 10.1371/journal.pone.0022715. Epub 2011 Aug 12.

- Eschbach C, Cano C, Haberkern H, **Schraut K**, Guan C, Triphan T, Gerber B. Associative learning between odorants and mechanosensory punishment in larval Drosophila. J Exp Biol. 2011 Dec 1;214(Pt 23):3897-905. doi: 10.1242/jeb.060533.

4.7. Acknowledgements

Ich möchte mich an dieser Stelle bei all den Menschen bedanken, die mich während meiner Doktorarbeit begleitet und unterstützt haben und diese Arbeit somit erst möglich gemacht haben!

Professor Dr. Klaus-Peter Lesch danke ich für Möglichkeit an diesem spannenden Projekt zu arbeiten, die hervorragende Betreuung dabei sowie für die Finanzierung nachdem mein Stipendium ausgelaufen war. Er hatte immer ein offenes Ohr für Vorschläge und Ideen (selbst wenn es um blasslila quadratische Poster ging). Des Weiteren möchte ich mich bei Frau Dr. Silke Groß-Lesch für das leckere Essen, das es zu diversen Anlässen gab, und die superleckere heiße Schokolade bedanken.

Professor Dr. Charlotte Förster danke ich herzlich für die Erstellung des Zweitgutachtens sowie für die unkomplizierten und hilfreichen Progress Reports.

Ich möchte mich ganz herzlich bei Dr. Daniel van den Hove für seine Unterstützung, seine Beratung und seinen Einsatz für meine Projekte bedanken. Danke für die Korrektur und kritische Auseinandersetzung mit zahlreichen Abstracts, Poster und Arbeiten sowie für die vielen produktiven und motivierenden wissenschaftlichen Diskussionen. Er hatte immer ein offenes Ohr und einen kühlen Kopf, egal worum es ging. Und Spaß hatten wir auch noch dabei. Science is fun ☺.

Bei Dr. Angelika (G.) Schmitt möchte ich mich vielmals für ihre Unterstützung rund um die Tierversuche und das ZEMM bedanken, u.a. das Erstellen des Tierversuchsantrags, die Organisation der Tiere und die tolle Einführung in die Dissektion von Gehirnen, und dafür, dass du immer ein offenes Ohr hast!

Bei der Graduate School of Life Sciences bedanke ich mich für die mehrjährige Finanzierung sowie für die vielen tollen Kurse. Mein Dank geht auch an das GK Emotions, sowohl für den interdisziplinären Austausch als auch für die Organisation der tollen Summer und Spring Schools inklusive toller Weinproben.

Von ganzem Herzen möchte ich mich bei unserem kleinen Epigenetik-Team bedanken, wir waren ein tolles Team ☺! Allen voran danke ich Gabi Ortega, der besten TA der Welt, für die tolle Zusammenarbeit im Labor, dafür dass wir durch Dick und Dünn gegangen sind, für dein nicht nachlassendes Engagement und deine kritische Denkweise! Danke für viele tolle Gespräche, für deinen Optimismus, einfach Danke für die tolle Zeit ☺! An dieser Stelle möchte ich mich auch bei Uwe Kiesel für den Entwurf und die Konstruktion diverser Laborgeräte bedanken! Bei Sissi Jakob möchte ich mich dafür bedanken, dass sie damals durch ihren tollen Vortrag den Funken der Epigenetik bei mir entzündet hat. Danke auch für die tolle Zusammenarbeit und die vielen Diskussionen und allgemein für die Einführung ins Doktoranden-Dasein ☺. Magdalena Weidner möchte ich für die intensiven wissenschaftlichen Diskussionen und natürlich für ihre engagierte Hilfe am Epigenetikprojekt bedanken. Ich hoffe, dass sie die Flamme weiterträgt ;). Mein Dank geht auch an Lisi Findeiss für ihre Hilfe am miRNA-Projekt.

Vielen Dank auch an Nicole Leibold, die mit mir die Tierversuche für das Resilienz-Projekt durchgeführt hat und ohne deren Expertise diese Experimente nie geklappt hätten. Danke auch für das oft lustige Überbrücken der viiieeelen langen Stunden im ZEMM.

Bei Dr. Claus-Jürgen Scholz und Dr. Konrad Förster bedanke ich mich vielmals für die bioinformatische Auswertung der Array- bzw. mRNA-Daten sowie für die geduldige Beantwortung meiner vielen unqualifizierten Fragen.

Vielen Dank an Professor Dr. Haaf und Dr. Nady El Hajj für die Bereitstellung des Pyrosequencers sowie die gute Betreuung und Unterstützung bei dessen Benutzung.

Sandy Popp und Antonia Post danke ich vielmals für die Hilfe in allen ZEMM-Angelegenheiten und für die wertvollen Inputs für die Verhaltensversuche. Danke auch an Olga Rivero und Jonas Waider für die Unterstützung im ZEMM sowie an Tobias Ruff für die Vertretung während des ECNP-Workshops.

Danke auch an Nicole Steigerwald für ihre Hilfe beim Präparieren.

Ein großes fettes Dankeschön geht an die tolle Labor- und Großraumbüro-Mannschaft, die stets unglaublich hilfsbereit waren und dieses Labor zu etwas Besonderem machen! Ihr habt dafür gesorgt, dass ich die Psychiatrie stets mit einem Lächeln betreten habe. Allen voran danke ich den charming Ladies Sarah und Julia für die vielen großartigen Stunden, die wir zusammen verbracht haben, an unserer super Tisch-Insel als auch privat. Danke für die zahlreichen Gespräche und eure Beratung in diversen Angelegenheiten, für die vielen lustigen und albernen Momente, für die Unterstützung in den nicht ganz so lustigen. Ihr seid toll Mädels! Vielen Dank auch an Julia für die statistische Beratung, die ich allzu häufig in Anspruch genommen habe, hust, und für die sie immer Zeit hatte. Danke auch an Inge, deren Liebe für Sushi uns viele leckere Abende beschert hat. Danke auch dafür, dass wir deine Küche verwüsten dürfen ;). Danke an Maggie für diverse Einladungen zum Kaffee. Danke auch an Andrea, die unsere 4er-Insel leider zu früh verlassen hat, und ihrer Nachfolgerin Miriam, deren boshafter Banter einfach nur herrlich ist.

Von ganzen Herzen möchte ich mich auch bei meinen langjährigen Freundinnen Mona und Madi bedanken! Einfach dafür, dass ihr da seid. Egal wie weit weg, es ist immer noch wie früher. Hab ich die Schafe schon erwähnt.

Herzlichen Dank auch an Miri mit einem j für ihren unendlichen Optimismus und die vielen und regelmäßigen Verabredungen zum Essen. Wir haben es bald geschafft.

Mein ganz besonderer Dank geht an meine Familie und an David, dem Mann an meiner Seite. Danke an meine Eltern Karl und Maria Schraut, die mich immer sowohl emotional als auch finanziell unterstützt haben, egal wohin der Weg mich geführt hat, und an meine Großmutter Lena, die mich die Liebe zum Detail gelehrt hat. David, du bist mein Stein in der Brandung und das Salz in der Suppe. Danke für all deine Geduld und Unterstützung und zahlreichen Tips für die Thesis (von denen ich den einen mehr hätte befolgen sollen…). Ohne euch wäre ich nicht da, wo ich heute bin.

D A N K E !

4.8. Affidavit

I hereby confirm that my thesis entitled "Epigenetic programming by prenatal stress in female serotonin transporter deficient mice" is the result of my own work. I did not receive any help or support from commercial consultants. All sources and / or materials applied are listed and specified in the thesis.

Furthermore, I confirm that this thesis has not yet been submitted as part of another examination process neither in identical nor in similar form.

Würzburg, _____ _____

Place, Date Signature

4.9. Eidesstattliche Erklärung

Hiermit erkläre ich an Eides statt, die Dissertation " Epigenetische Programmierung durch Pränatalstress in weiblichen Serotonintransporter-defizienten Mäusen" eigenhändig, d.h. insbesondere selbständig und ohne Hilfe eines kommerziellen Promotionsberaters, angefertigt und keine anderen als die von mir angegebenen Quellen und Hilfsmittel verwendet zu haben.

Ich erkläre außerdem, dass die Dissertation weder in der gleichen noch in ähnlicher Form bereits in einem anderen Prüfungsverfahren vorgelegen hat.

Würzburg, _____ _____

Ort, Datum Unterschrift